Amphiphilic and thermoresponsive block copolymers based on hydroxypropyl methyl cellulose as nano-carrier of hydrophobic drugs

Aijing Lu

THÈSE

Pour obtenir le grade de Docteur

Délivré par Université de Montpellier

Préparée au sein de l'école doctorale Sciences Chimiques Balard ED 459
Et de l'unité de recherche Institut Européen des Membranes (UMR 5635)

Spécialité : Chimie et Physicochimie des Matériaux

Présentée par Aijing LU

Copolymères à blocs amphiphiles et thermosensibles à base d'hydroxypropyl méthyl cellulose comme nano-vecteurs de principes actifs hydrophobes

Amphiphilic and thermoresponsive block copolymers based on hydroxypropyl methyl cellulose as nano-carrier of hydrophobic drugs

Soutenue le 2 avril, 2020 devant le jury composé de

M. André DERATANI, DR, IEM UMR 5635	Invité
M. Christophe MINGOTAUD, DR, IMRCP UMR 5623	Rapporteur
M. Luc PICTON, Prof., PBS, UMR 6270	Rapporteur
M. Mihai BARBOIU, DR, IEM UMR 5635	Président du jury
M. Suming LI, DR, IEM UMR 5635	Directeur de Thèse

Table of contents

Résumé

Les micelles à base de copolymères à blocs amphiphiles ont été largement étudiées en tant que matrice de principes actifs en raison de leurs propriétés intéressantes telles que la longue circulation, la charge de principes actifs et l'effet thérapeutique améliorés, et la biocompatibilité. Ainsi, des polyesters aliphatiques biocompatibles et biorésorbables tels que le polylactide (PLA) et la poly (ε-caprolactone) (PCL) ont été couramment utilisés comme bloc hydrophobe des copolymères à blocs amphiphiles, qui s'agrège dans le cœur pour encapsuler le principe actif hydrophobe. Le PLA et la PCL sont généralement obtenus par polymérisation par ouverture de cycle (POC) du lactide ou de l'ε-caprolactone. L'acide lactique étant une molécule chirale qui a deux énantiomères, les acides L-lactique et D-lactique, divers polymères PLA sont disponibles, y compris le poly(D-lactide) (PDLA) et le poly(L-lactide) (PLLA) isotactiques, le poly(DL-lactide) optiquement inactif (PDLLA) et les stéréocopolymères poly(D-lactide-co-L-lactide). En tant que dérivé de cellulose, l'hydroxypropyl méthyl cellulose (HPMC) est largement utilisée dans les systèmes d'administration contrôlée de principes actifs par voie orale en raison de sa biocompatibilité, son hydrophilie s, et ses propriétés thermosensibles. Les polymères amphiphiles à base de cellulose exploitaient en général les groupements hydroxyle sur les motifs glucose pour préparer des copolymères greffés. Mais de telles réactions sont difficilement contrôlables en raison de la présence de nombreux groupements hydroxyle le long des chaînes polymère. D'un autre côté, chaque chaîne de cellulose a un groupement terminal hémiacétal qui se transforme facilement en aldéhyde. L'amination réductrice entre l'aldéhyde et les groupes amino est bien établie, mais est rarement utilisée pour synthétiser des copolymères à base de cellulose en raison de la disponibilité limitée de l'extrémité réductrice, de la difficulté de trouver un solvant commun pour les deux blocs et de la nécessité éventuelle de protéger le groupements hydroxyle latéraux. Parallèlement, les oligomères HPMC ayant des masses molaires comprises entre 5K et 20K ont rarement été utilisés comme segment hydrophile pour

synthétiser des copolymères à blocs amphiphiles.

Dans ce travail de thèse, des copolymères à blocs $(HPMC)_2$-PLA amphiphiles et thermosensibles du type AB_2 ont été synthétisés à partir de HPMC à terminaison thiol et de PLLA à terminaison alcynyle par réaction clic thiol-yne. Deux autres types de copolymères à blocs amphiphiles linéaires de HPMC-PLA et HPMC-PCL ont été synthétisés à partir de HPMC avec un groupement terminal hémiacétal et de PLA ou PCL à terminaison amino par amination réductrice. Enfin, des copolymères HPMC-JEF diblocs, triblocs et à trois bras ont été synthétisés par amination réductrice entre le groupement terminal aldéhyde de l'HPMC hydrophile et le groupement amine de JEF. Ces copolymères amphiphiles et thermosensibles sont capables de s'auto-assembler en micelles qui peuvent servir de nanovecteur de principes actifs hydrophobes. Les comportements d'auto-assemblage, de chargement de principes actifs et de libération de principes actifs, et la biocompatibilité des copolymères ont été étudiés pour évaluer leur potentiel dans l'administration contrôlée de principes actifs antitumoraux hydrophobes. Le contenu principal de la thèse est présenté comme suit:

(1) Des copolymères $(HPMC)_2$-PLA amphiphiles et thermosensibles du type AB_2 avec différentes longueurs de blocs hydrophiles ont été synthétisés par une réaction clic thiol-yne initiée par UV entre l'HPMC à terminaison thiol et le PLLA à terminaison alcynyle. Le PLLA à terminaison alkynyle est obtenu par polymérisation par ouverture de cycle du L-lactide initiée par du propynol. L'HPMC à terminaison thiol est obtenue en deux étapes, réduction de l'amination du groupement d'extrémité aldéhyde de l'HPMC avec de la cystéamine, et puis réduction en utilisant du DTT. Les copolymères à blocs résultants ont été caractérisés par RMN, DOSY-RMN, SEC et FT-IR. La masse molaire des copolymères $(HPMC)_2$-PLA varie de 12000 à 22000 g/mol et la dispersité de 1,13 à 1,26.

Les micelles nanométriques sont formées par auto-assemblage de copolymères amphiphiles $(HPMC)_2$-PLA en milieu aqueux à température ambiante. La CMC a été déterminée par des changements d'intensité de diffusion d'une solution de copolymère à différentes concentrations. La valeur CMC augmente légèrement avec la diminution de la longueur du bloc HPMC. Les micelles sont de forme sphérique selon les images TEM. Le

diamètre moyen des micelles $(HPMC5K)_2$-PLA2K, $(HPMC7K)_2$-PLA2K, $(HPMC10K)_2$-PLA2K était de 66, 90 et 120, comme déterminé par la DLS. La taille augmente avec l'augmentation de la longueur du bloc HPMC hydrophile. Le point de trouble (CP) déterminé par la spectroscopy UV-Vis est d'environ 64 °C pour les trois copolymères, ce qui est inférieur à celui de l'homopolymère HPMC. Ces résultats montrent que la longueur de bloc HPMC a peu d'effet sur le Cp des copolymères. Par rapport à nos travaux antérieurs qui ont étudié les copolymères linéaires HPMC-PLA avec des composants similaires, les copolymères du type AB_2 $(HPMC)_2$-PLA présentaient des valeurs de CMC et de taille de micelles similaires, mais un CP beaucoup plus faible. Cela indique que la topologie des copolymères amphiphiles a une influence sur le CP et les propriétés d'auto-assemblage.

(2) Dans la deuxième partie, des copolymères diblocs amphiphiles ont été synthétisés à partir d'HPMC et de PLLA à terminaison amino (NH_2-PLLA) ou poly(L-lactide-co-DL-lactide) à terminaison amino (NH_2-PLA) par amination réductrice. Le NH_2-PLLA ou NH_2-PLA a été obtenu par polymérisation par ouverture du cycle du L-lactide ou d'un mélange de L-lactide et DL-lactide initiée par le 3-(Boc-amino)-1-propanol, suivie de déprotection des groupements amine en éliminant les groupements Boc. Les copolymères HPMC-PLLA et HPMC-PLA ont été finalement synthétisés par amination réductrice entre le groupement terminal hémiacétal d'HPMC hydrophile et le groupement amino de PLLA ou PLA hydrophobe. Ces copolymères PLLA-HPMC et PLA-HPMC obtenus avec diverses longueurs de blocs hydrophobes ont été caractérisés par RMN, DOSY-RMN et FT-IR.

Les micelles ont été obtenues par auto-assemblage de copolymères HPMC-PLLA ou HPMC-PLA en milieu aqueux. La morphologie, la taille et la distribution des tailles des micelles ont été déterminées par la DLS et la TEM. Les résultats ont révélé que les micelles étaient de forme sphérique et que la taille des micelles se situait entre 150 et 180 nm avec une distribution étroite. Le potentiel zêta des micelles est proche de zéro, en accord avec la charge de surface presque neutre des micelles HPMC-PLA. La concentration micellaire critique (CMC) a été déterminée par spectroscopie de fluorescence en utilisant le pyrène comme sonde. La valeur CMC diminue avec l'augmentation de la longueur du bloc PLA dans la zone de

0,009 à 0,15. De plus, la stéréochimie du bloc PLA ne semble pas affecter le CMC.

Le paclitaxel (PTX) est un principe actif anticancéreux hydrophobe qui a une bonne compatibilité avec le PLA. En fait, le PTX contient des groupements OH et NH qui sont capables d'interagir avec le groupement carbonyle du PLA. Ainsi, le PTX a été chargé au cœur des micelles pour évaluer le comportement de libération du principe actif. Une teneur en principe actif et une efficacité d'encapsulation améliorées des micelles sont obtenues avec l'augmentation de la longueur du bloc de PLA. Un profil de libération biphasique est observé avec une libération très rapide de c.a. 40% dans les 6 premières heures, suivie d'une libération plus lente jusqu'à 80% après 120 heures. Les tests MTT et SRB indiquent la bonne cytocompatibilité des micelles PLA-HPMC. Par ailleurs, le test SRB montre une cytotoxicité significative des micelles chargées de PTX sur les cellules SK-BR-3.

(3) Dans la troisième partie, les copolymères diblocs amphiphiles ont été synthétisés à partir dHPMC et de ppoly(ε-caprolactone) àterminaison amino (NH_2-PCL) ont été synthétisés de la même manière que dans la deuxième partie. La NH_2-PCL a été obtenue par la polymérisation par ouverture de cycle de l'ε-caprolactone, suivie d'une déprotection des groupements amine. Finalement les copolymères HPMC-PCL avec diverses longueurs de blocs hydrophiles et hydrophobes ont étéobtenus par amination réductrice entre le groupement terminal hémiacétal d'HPMC et le groupement amino de PCL, et ont été caractérisés par RMN, DOSY-RMN et FT-IR.

Les micelles ont étéobtenues par auto-assemblage de copolymères HPMC-PCL en milieu aqueux. La morphologie, la taille et la distribution des tailles des micelles ont été déterminées par la DLS et la TEM. La TEM montre que les micelles étaient de forme sphérique. La taille des micelles HPMC18K-PCL est plus grande que celle des micelles HPMC7K-PCL avec la même longueur de bloc PCL. D'autre part, le bloc PCL hydrophobe a une petite influence sur la taille des micelles. Le potentiel zêta des micelles est légèrement négatif, ce qui est dû à la nature neutre du bloc externe HPMC. La CMC des copolymères a été déterminée par spectroscopie de fluorescence en utilisant le pyrène comme sonde. La valeur de CMC des copolymères HPMC7K-PCL se situe dans la zone de 0,012 à 0,0009 g/L, tandis que celle de

HPMC18K-PCL se situe dans la zone de 0,003 à 0,009 g/L. La valeur de CMC diminue avec l'augmentation de la longueur du bloc hydrophobe.

Un autre principe actif anticancéreux hydrophobe, la curcumine a été encapsulée dans le coeur de la micelle pour évaluer le comportement de libération du principe actif. La teneur en principe actif et l'efficacité d'encapsulation des micelles de copolymères augmentent avec l'augmentation de la longueur du bloc PCL. La libération de la curcumine a été réalisée dans les conditions in vitro avec un système de dialyse. La vitesse de libération diminue avec l'augmentation de la longueur du bloc PCL. Les profils de libération de la curcumine à partir des différentes micelles ont montré un schéma biphasique similaire, y compris une libération initiale rapide dans les 6 premières heures et une libération plus lente jusqu'à 120 heures. Les micelles HPMC-PCL présentent une bonne biocompatibilité, comme le montre les tests MTT sur les cellules fibroblasts L2929.

(4) Dans la dernière partie, des copolymères amphiphiles et thermosensibles avec différentes topologies et différents rapports hydrophile/hydrophobe ont été synthétisés par amination réductrice entre le groupement terminal hémiacétal d'HPMC hydrophile et le groupement amine de JEFFAMINE. Des copolymères HPMC-JEF dibloc, tribloc et à trois bras ont été obtenus en faisant réagir l'HPMC avec la monoamine, la diamine ou la triamine JEFFAMINE. Les copolymères résultants présentent une structure de chaîne bien définie, la Mw variant de 6500 à 56000.

Le point de trouble des copolymères a été déterminé à 5 mg/mL. Pour les homopolymères HPMC, le point de trouble diminue avec l'augmentation de la masse molaire. Le point de trouble des copolymères HPMC-JEF est inférieur à celui des homopolymères HPMC dans tous les cas. La topologie et le rapport hydrophile/hydrophobe ont une influence significative sur le point de trouble des copolymères. Le point de trouble de HPMC-JEF linéaire augmente avec l'augmentation du rapport hydrophile/hydrophobe. En revanche, le HPMC7K-JEF T5K à trois bras présente un point de trouble plus élevé que les HPMC7K-JEF linéaires malgré sa fraction JEFFAMINE plus élevée. Il est également intéressant de noter que les copolymères diblocs HPMC-JEF M2K présentent deux points de trouble étant donné que les deux

composants sont thermosensibles.

Les copolymères HPMC-JEF s'auto-assemblent en micelles en milieu aqueux par dissolution directe. La structure cœur-couronne de la micelle a été confirmée par les spectres RMN dans un solvant sélectif et un bon solvant des deux blocs. Les valeurs de CMC des copolymères linéaires se situent dans la plage de 0,13 à 0,24 g/L. En revanche, les trois copolymères à trois bras présentent une CMC beaucoup plus faible car la structure en forme d'étoile facilitent la micellisation. Toutes les micelles sont de forme sphérique et leur taille est comprise entre 180 et 320 nm. La topologie et le rapport hydrophile/hydrophobe ont également une influence sur la taille des micelles des copolymères. La taille des copolymères augmente avec l'augmentation de la masse molaire des HPMC hydrophiles. Les copolymères HPMC-JEF à trois bras présentent la plus petite taille de micelles et les triblocs présentent la plus grande. Le potentiel zêta de toutes les micelles est légèrement négatif en raison de la nature neutre du bloc couronne HPMC. Étant donné que le HPMC-JEF M2K contient JEFFAMINE M2K qui a un point de trouble d'environ 22 °C, la taille des micelles change considérablement avec l'augmentation de la température en raison de l'extension de la chaîne et/ou de la déshydratation. Le test MTT a mis en évidence la cytocompatibilité des copolymères HPMC-JEF.

Abstract

Micelles based on amphiphilic block copolymers have been extensively investigated as drug carrier due to their favorable advantages in molecular design, long circulation, enhanced drug loading and therapeutic effect, and biocompatibility. Thus, biocompatible and bioresorbable aliphatic polyesters such as polylactide (PLA) and poly(ε-caprolactone) (PCL) have been commonly used as the hydrophobic block of copolymers, which aggregates into the core to encapsulate hydrophobic drugs. PLA and PCL are generally obtained by ring-opening polymerization (ROP) of lactide and caprolactone. As lactic acid is a chiral molecule which has two enantiomers, L- and D-lactic acids, various PLA polymers are available, including isotactic poly(D-lactide) (PDLA) and poly(L-lactide) (PLLA), optically inactive poly(DL-lactide) (PDLLA), and poly(D-lactide-co-L-lactide) stereocopolymers. As a hydrophilic cellulose derivative, hydroxypropyl methyl cellulose (HPMC) is widely used in controlled drug delivery due to its biocompatibility, hydrophilicity, and thermo-responsiveness. Cellulose-based amphiphilic graft copolymers are usually prepared by exploiting the hydroxyl groups on the glucose moieties. But such reactions are hardly controllable because of the presence of numerous hydroxyl groups along polymer chains. On the other hand, each cellulose chain has a hemiacetal end group which is easily transformed to aldehyde. Reductive amination between aldehyde and amino groups is well established, but is rarely used to synthesize cellulose-based copolymers because of the limited availability of the reducing-end, the difficulty of finding a common solvent for both blocks, and the eventual necessity to protect the lateral hydroxyl groups. Meanwhile, HPMC oligomers with molar masses between 5K and 20K have been rarely employed as hydrophilic segment to synthesize amphiphilic block copolymers.

In this work, amphiphilic and thermo-responsive AB_2-type $(HPMC)_2$-PLA block copolymers were synthesized from thiol terminated HPMC and alkynyl terminated PLLA by thiol-yne click reaction. On the other hand, linear amphiphilic HPMC-PLA and HPMC-PCL block copolymers - were synthesized from HPMC with hemiacetal end group and amino-

terminated PLA or PCL by reductive amination. And diblock, triblock and three-armed HPMC-JEF copolymers were synthesized by reductive amination between the aldehyde end group of hydrophilic HPMC and the amine group of JEFFAMINE. These amphiphilic and thermo-responsive copolymers are able to self-assemble in micelles which can serve as nano-carrier of hydrophobic drugs. The self-assembly, drug loading and drug release behaviors, and the biocompatibility of copolymers were investigated to evaluate their potential in controlled delivery of hydrophobic antitumor drugs. The main contents of thesis are shown in the following:

(1) AB_2-type thermo-responsive amphiphilic $(HPMC)_2$-PLA copolymers with various hydrophilic block lengths were synthesized by UV-initiated thiol-yne click reaction between thiol terminated HPMC and alkynyl terminated PLLA. The latter was obtained by ring-opening polymerization of L-lactide initiated by propynol. Thiol terminated HPMC was obtained in two steps, amination reduction of the aldehyde end group of HPMC with cysteamine and then reduction using DTT. The resulted block copolymers were characterized by NMR, DOSY-NMR, SEC and FT-IR. The molar mass of $(HPMC)_2$-PLA copolymers ranges from 12000 to 22000 g/mol, and the dispersity from 1.13 to 1.26.

Nano-scaled micelles are formed by self-assembly of AB_2-type amphiphilic $(HPMC)_2$-PLA copolymers in aqueous medium at room temperature. The CMC was determined by scattering intensity changes of copolymer solutions at different concentrations. The CMC value increases slightly with decreasing HPMC block length. The micelles are spherical in shape as evidenced by TEM. The average diameter of $(HPMC5K)_2$-PLA2K, $(HPMC7K)_2$-PLA2K, and $(HPMC10K)_2$-PLA2K micelles was 66, 90 and 120, as determined by DLS. The size increases with the increase of hydrophilic HPMC block length. The cloud point (CP) determined by UV–Vis spectroscopy is around 64 ℃ for the three copolymers which is lower than that of HPMC homopolymers, showing that the HPMC block length has little effect on the Cp of the copolymers. Compared to linear HPMC-PLA copolymers with similar components prepared in our previous work, the AB_2-type copolymers $(HPMC)_2$-PLA exhibited similar CMC and micelle size, but much lower CP. These findings indicates that the

topology of amphiphilic copolymers has influence on the CP and self-assembled properties.

(2) In the second part, amphiphilic diblock copolymers were synthesized from hydroxypropyl methyl cellulose (HPMC) and amino-terminated poly(L-lactide) (PLLA) or poly(L-lactide-co-DL-lactide) (PLA) by reductive amination. Amino-terminated PLA was obtained by ring-opening polymerization of L-lactide initiated by 3-(Boc-amino)-1-propanol, and deprotection of amine groups by removing the Boc group. Reductive amination then proceeded between the hemiacetal end group of hydrophilic HPMC and the amino group of hydrophobic PLA. The resulting PLLA-HPMC and PLA-HPMC copolymers with various hydrophobic block lengths were characterized by NMR, DOSY-NMR and FT-IR.

Micelles were obtained by self-assembly of HPMC-PLLA or HPMC-PLA copolymers in aqueous medium. The morphology, size and size distribution of micelles were determined by dynamic light scattering and transmission electron microscopy. Data revealed that the micelles were spherical in shape, and the micelle size was in the range from 150 to 180 nm with narrow distribution. The zeta potential of micelles is close to zero, in agreement with neutral surface charge of HPMC-PLA micelles. The critical micelle concentration (CMC) was determined by fluorescence spectroscopy using pyrene as probe. The CMC value decreases with increasing PLA block length in the range from 0.009 to 0.15. Moreover, the stereochemistry of the PLA block seems not to affect the CMC.

Paclitaxel is a hydrophobic anti-cancer chemotherapeutic agent which has good compatibility with PLA since PTX contains OH and NH groups which can interact with the carbonyl group of PLA. PTX was loaded in micelles to evaluate the drug release behavior. Enhanced drug loading content and encapsulation efficiency of micelles are obtained with the increase of PLA block length. A biphasic release profile is observed with a burst of c.a. 40% in the first 6 h, followed by slower release up to 80% after 120 h. MTT and SRB assays indicate the good cytocompatibility of HPMC-PLA micelles. Meanwhile, SRB assay shows a significant cytotoxicity of paclitaxel-loaded micelles to SK-BR-3 cells.

(3) In the third part, amphiphilic diblock copolymers were synthesized from HPMC and amino-terminated poly(ε-caprolactone) (PCL) using the same method. Amino-terminated

PCL was obtained by ring-opening polymerization of ε-caprolactone, and deprotection of amine groups. Finally reductive amination proceeds between the hemiacetal end group of HPMC and the amino group of PCL. The resulting HPMC-PCL copolymers with various hydrophilic and hydrophobic block lengths were characterized by NMR, DOSY-NMR and FT-IR.

Micelles were obtained by self-assembly of HPMC-PCL copolymers in aqueous medium. The morphology, size and size distribution of micelles were determined by dynamic light scattering and transmission electron microscopy. Micelles were spherical in shape as evidenced by TEM. The size of HPMC18K-PCL micelles is larger than that of HPMC7K-PCL with the same PCL block length. Meanwhile, the hydrophobic PCL block also has slight influence on the micelles size. The zeta potential of micelles is slightly negative due to the neutral nature of the shell block HPMC. The critical micelle concentration (CMC) was determined by fluorescence spectroscopy using pyrene as probe. The CMC value of HPMC7K-PCL copolymers is in the range of 0.012 to 0.0009 g/L, while that of HPMC18K-PCL is in the range of 0.003 to 0.009 g/L. The CMC value decreases with increase of the hydrophobic block length.

Another hydrophobic anti-cancer drug, curcumin was encapsulated into the core of micelles to evaluate the drug release behavior. The DLC and DLE of copolymers increase with the increase of PCL block length, and the drug release rate decreases with the increase of PCL block length. The drug release profiles showed a similar biphasic pattern including a rapid initial release within the first 6 hours and a slower release in the following 114 hours. HPMC-PCL micelles presented good biocompatibility as demonstrated by MTT test.

(4) In the last part, amphiphilic and thermo-responsive copolymers with different topologies and hydrophilic/hydrophobic ratios were synthesized by reductive amination between the hemiacetal endgroup of hydrophilic HPMC and the amine group of JEFFAMINE. Diblock, triblock and three-armed HPMC-JEF copolymers were obtained by reaction of HPMC with monoamine, diamine, or triamine JEFFAMINE. The resulting copolymers present well defined chain structure with the Mw varying from 6500 to 56000.

The cloud point (CP) of copolymers was determined at 5 mg/mL. For the HPMC homopolymers, the CP decreases with the increase of molar mass. The CP of HPMC-JEF copolymers is lower than that of HPMC homopolymers in all cases. Both topology and hydrophilic/hydrophobic ratio have significant influence on the CP of copolymers. Three-armed $(HPMC7K)_3$-JEF T5K presents a higher CP compared to HPMC7K-JEF copolymers in spite of its higher JEFFAMINE fraction. The CP of linear HPMC-JEF increases with increase of hydrophilic/hydrophobic ratio. Interestingly, HPMC-JEF M2K diblock copolymers present two CPs since both components are thermo-responsive.

HPMC-JEF copolymers self-assemble into micelles in aqueous media by direct dissolution method. The core-shell structure of micelles was confirmed by NMR spectra in selective solvent and good solvent of the two blocks. The CMC values of linear copolymers are in the range of 0.13 to 0.24 g/L. In contrast, the three armed copolymers exhibit a much lower CMC since star-shaped copolymers facilitate micellization. All micelles are spherical in shape and the size is in the range from 180 to 320 nm. Both topology and hydrophilic/hydrophobic ratio also have influence on micelle size of copolymers. The size of copolymers increases with the increase hydrophilic HPMC molar mass. The three-armed HPMC-JEF copolymers present the smallest micelle size and the triblock ones present the largest. The zeta potential of all micelles is slight negative due to the neutral nature of shell block HPMC. Since HPMC-JEF M2K contains JEFFAMINE M2K which has a CP around 22 °C, the micelle size significantly changes with increasing temperature due to chain extension and/or dehydration. MTT assay evidenced the cytocompatibility of HPMC-JEF copolymers.

List of Tables

List of Schemes

List of Figures

List of abbreviations

A

AFM atomic force microscopy

ATRP atom transfer radical polymerization

ATR attenuated total reflectance

C

CA cellulose acetate

CDs cyclodextrins

CMC critical micelle concentration

CMC carboxy methyl cellulose

CP cloud point

D

DEAM N,N-diethylacrylamide

DLC drug loading content

DLE drug loading efficiency

DLS dynamic light scattering

DMAc dimethylacetamid

DMF dimethylformamide

DMPA 2,2-dimethoxy-2-phenylacetophenone

DMSO dimethyl sulfoxide

DOSY diffusion ordered spectroscopy

DP polymerization degree

DTT 1,4-dithiothreitol

DS degree of substitution

E

EC ethyl cellulose

EM electron microscopy

EPR permeability and retention

F

FBS fetal bovine serum

FT-IR Fourier transform infrared

G

GSH glutathione

H

HA hyaluronic acid

HEC hydroxyethyl cellulose

HEMC hydroxymethyl cellulose

HPLC high performance liquid chromatography

HPMC hydroxypropyl methyl cellulose

L

LCST lower critical solution temperature

M

MADIX macromolecular design via the interchange of xanthates

MALLS multi-angle laser light scattering

MC methyl cellulose

MS molar substitution

MWCO molecular weight cut off

N

NADPH nicotinamide adenine dinucleotide phosphate

NMP nitroxide-mediated polymerization

NMR nuclear magnetic resonance

O

OD optical density

P

PBS phosphate buffered saline

PCL poly(ε-caprolactone)

PDI polydispersity index

PDLLA poly(DL-lactide)

PEG poly(ethylene glycol)

PEO poly(ethylene oxide)

PEOz poly(2-ethyl-2-oxazoline)

PGA polyglycolide

PLA polylactide

PLGA lactide/glycolide copolymers

PLLA poly(L-lactide)

PNIPAAm poly(N-isopropyl acrylamide)

PPO poly(propylene oxide)

PTFE polytetrafluoroethylene

PTX paclitaxel

PVCL poly(*N*-vinyl caprolactam)

R

RAFT reversible addition-fragmentation chain transfer polymerization

RI refractive index

ROP ring-opening polymerization

S

SEC size exclusion chromatography

SLS static light scattering

SEM scanning electron microscopy

T

TEM transmission electron microscopy

TFA trifluoroacetic acid

THF tetrahydrofuran

U

UCST upper critical solution temperature

UV ultraviolet

Number

2D two-dimensional

Symbol

Đ dispersity

Mn number average molar mass

Mw weight average molar mass

N_{agg} average molar mass M_w and the aggregation number

R_g radius of gyration

R_h hydrodynamic radius

Tg glass transition temperature

Tm melting temperature

Chapter 1 Introduction

1.1 Nano-sized drug delivery systems

Nanotechnology is helping to considerably improve, even revolutionize, many technology and industry sectors, including medicine, pharmacology, information technology, energy, food safety, and environmental science. With the development of nanotechnology, nano-carriers have been extensively investigated for biomedical applications in medical imaging, in disease diagnosis, and in particular in drug delivery due to their outstanding properties such as high stability, high carrier capacity, feasibility of incorporation of both hydrophilic and hydrophobic substances, feasibility of variable administration routes (oral, parenteral injection, or inhalation), and controlled or sustained drug release from the matrix [1]. Thus nano-carriers enable to improve the drug bioavailability, to reduce the dosing frequency and side effects, and may resolve the problem of nonadherence to prescribed therapy.

Cancer is the second leading cause of death globally according to the World Health Organization, and is responsible for an estimated 17.0 million new cases and 9.5 million deaths in 2018 [2]. About 1 in 6 deaths is due to cancer. Usual cancer treatments include surgery, chemotherapy and radiotherapy. As is well known, many usual chemotherapeutic drugs are highly hydrophobic, which greatly restrains their potential applications in cancer treatment. In fact, poor water solubility of anticancer drugs in the physiological environment is the first obstacle for their therapeutic efficiency. Well defined nano-carriers with encapsulated or conjugated drugs present great interest as they allow to increase the solubility of drugs, to improve the therapeutic efficiency and to reduce the side effects. At the same time, nano-carriers also protect the drugs from biodegradation or excretion.

Chemotherapeutic drugs have toxic effects not only on tumor tissue but also on normal tissue. Thus, biodistribution is of major importance for the therapeutic

efficiency of drugs which could be improved by passive targeting and active targeting. In general, both strategies improve the accumulation of drug delivery system in the targeted tissue, which requires long circulation time in the bloodstream. And prolonged circulation time can be achieved if the surface of nano-carriers allows to prevent non-specific protein adsorption, thus avoiding glomerular excretion in the kidney and recognition by the reticuloendothelial system (RES) located in liver, spleen and lung.

Passive targeting is based on the pathophysiological difference between tumor and normal tissues, as shown in Fig. 1.1. In tumor tissue, the endothelium of intratumoral blood vessels is destroyed by the rapid growth of tumor cells. And thus intratumoral blood vessels are leaky and highly permeable. This phenomenon is called the enhanced permeability and retention (EPR) effect, which promotes the accumulation of nanoparticles with sizes between 100 nm and 780 nm in tumor tissue without any special requirement [3].

Active targeting is based on the overexpression of receptors on tumor cells. With the rapid proliferation of tumor cells, the expression of some specific antigens or receptors is enhanced. Therefore, nano-carrier with high-affinity ligand on the surface could accumulate in tumor tissue by selecting the specific receptor on cancer cells. The commonly used antigens and receptors are as follows: (1) vascular receptors, such as integrin, aminopeptidase, vascular endothelial growth factor, etc.; (2) plasma protein receptors, such as transferrin and low-density lipoprotein; (3) growth factor receptors, such as folate, epidermal growth factor, transforming growth factor and fibroblast growth factor; (4) carbohydrate receptors, such as hyaluronic acid, sialic acid glycoprotein, interferon, etc. The ligand should allow binding to tumor cells while minimizing binding to normal cells. What is more, the density of ligand also needs to be optimized to make sure that the carriers are not cleared by the reticuloendothelial system. In addition, nano-carriers with active targeting not only promote accumulation but also improve cell uptake.

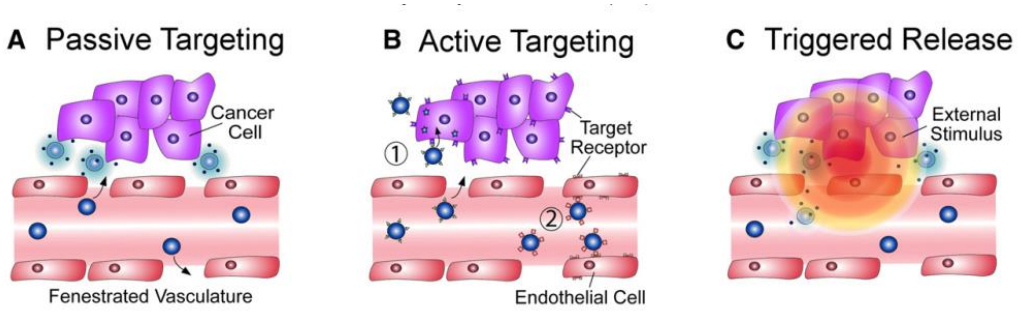

Fig. 1. 1 Schematic illustration of drug targeting strategies [3]

Another method to improve the therapeutic efficiency is triggered release, also named stimuli-responsive drug release. The commonly used triggers include internal stimuli, such as pH and redox, and external stimuli such as temperature, light, ultrasound, and magnetic force. Stimuli-responsive drug delivery systems are susceptible to respond to changes by disintegration, destabilization, isomerization, polymerization or aggregation of the nanocarriers, and subsequently release the drug. By combining targeting and controlled release, the drug concentration in target tissue can reach the optimum concentration range so as to improve the therapeutic efficiency and to prevent drug resistance.

1.2 Polymers in drug delivery systems

Polymeric drug delivery systems have attracted much attention due to their potential advantages since their size, geometry, surface properties and structures could be tailored by varying the chemical composition and topology of polymers which compose the systems. Several types of polymers have demonstrated high potential for clinical applications, including natural polymers and synthetic polymers. Fig.1.2 summarizes the commonly used synthetic polymers and linkages for building nano-carriers.

The main building blocks of nano-carriers include core-forming polymers which are generally hydrophobic or charged (Fig. 1.2a), shell-forming polymers which are generally neutral, hydrophilic and flexible to endow nano-carriers with stealth properties (Fig. 1.2b), targeting ligands for selective cellular uptake and accumulation

at target sites (Fig. 1.2c), and linkages between the shell and core and/or targeting moieties (Fig. 1.2d). Stimuli-responsiveness (pH, temperature, enzyme, redox, etc.) can be imparted into the core, shell and/or the linkages. Shell or core-crosslinking can be also utilized to enhance the stability of nano-carriers (Fig. 1.2e).

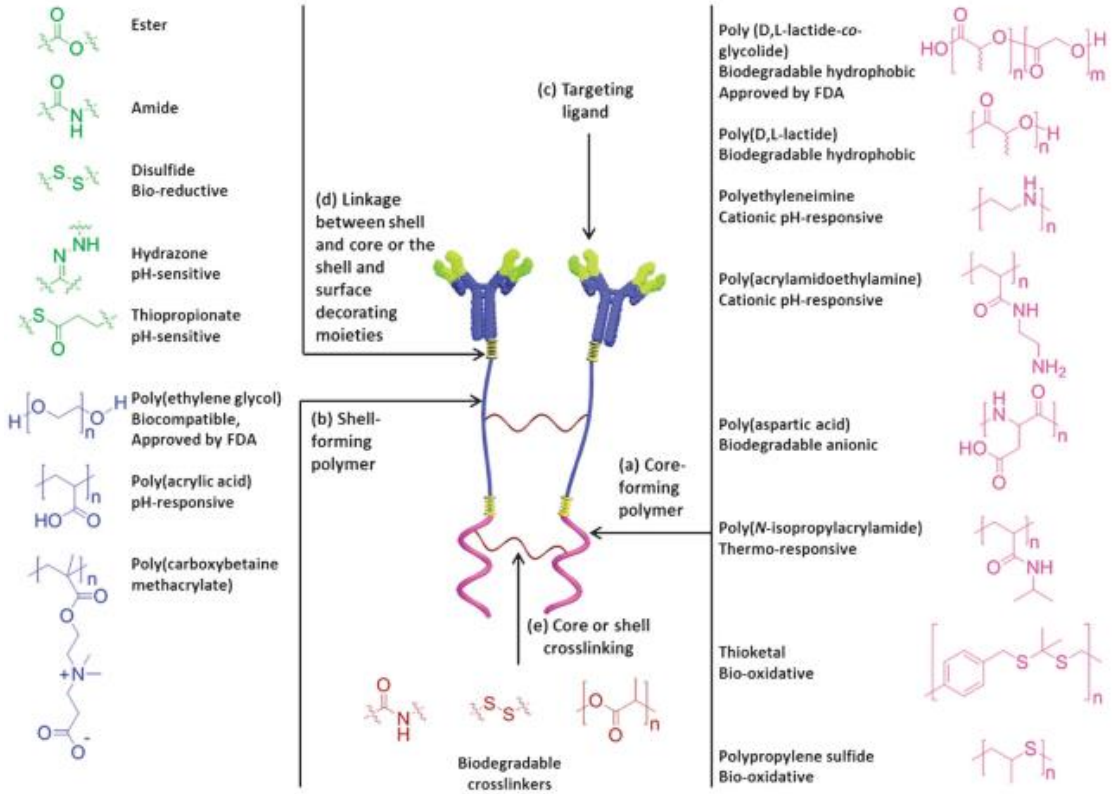

Fig. 1. 2 Building blocks of various types of polymeric nano-carriers with examples of some commonly used core-forming and shell-forming polymers, linkages between shell and core or shell and surface decorating moieties, and biodegradable crosslinkers [4]

As a hydrophilic block, natural biopolymers have been attracting more and more attention because they are biodegradable, biocompatible and bio-based. Biopolymers are macromolecules that are synthesized by living organisms such as plants, animals and microorganisms. They represent a diverse range of compositions and chemical functionality, and can be broadly classified as polysaccharides, polypeptides, and polyphenols (Fig. 1.3). Polysaccharides, including neutral polysaccharides such as

cellulose, cationic polysaccharides such as chitin or chitosan, and anionic polysaccharides such as alginate, are the most abundant biopolymer. And they display many beneficial biological activities such as anticoagulant, antiviral, antioxidant, anticancer and immunomodulating activities [5].

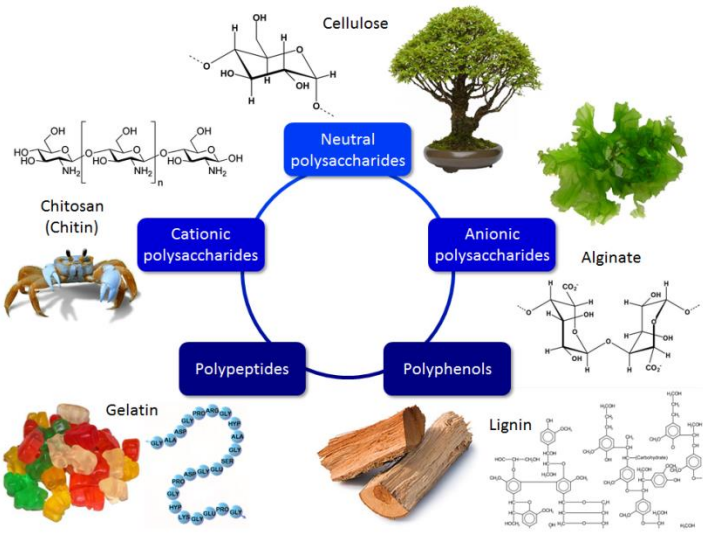

Fig. 1. 3 Origins and structures of natural biopolymers synthesized by living organisms (https://schneppgroup.wordpress.com/research/biopolymers/).

1.2.1 Polysaccharides

Polysaccharides have been widely used in drug delivery in the form of micelles, nanoparticles, hydrogels, nanogels, drug conjugates, *etc*. due to their outstanding properties such as biodegradability, biocompatibility, non-toxicity, easy chemical modification and targeting capacity [4-7]. Polysaccharides are biopolymers composed of a great deal of monosaccharides which are linked by O-glycosidic linkages [6]. The most extensively investigated polysaccharides include cellulose, chitosan, alginate, dextran, cyclodextrin, *etc*. Importantly, polysaccharides can be chemically modified through various reactions such as esterification, etherification, oxidation of hydroxyl groups, formation of ester or amide linkages of the carboxyl groups with hydroxyl or amine groups, and formation of amide linkages of the amine groups with carboxyl

groups. Chemical modification has been widely used to improve the physico-chemical properties of polysaccharides, in particular the solubility. The commonly used reactions to connect polysaccharides with crosslinkers and linkages are summarized in Table 1.1.

Table 1. 1 Covalent linkages to polysaccharides [6]

Functional group	Chemical modifications used	
–OH	Esterification with acylating agents	
	Etherification with alkylating agents	
	Oxidation of primary alcohol to COOH	Ester linkage to –OH
		Amide linkage to $–NH_2$
	Oxidation of vicinal secondary –OH to aldehydes	Hydrazone linkage to $–NHNH_2$
		Schiff base linkage to $–NH_2$
–COOH	Ester linkage to –OH	
	Amide linkage to $–NH_2$	
$–NH_2$	Amide linkage to –COOH	

1.2.1.1 Cellulose

Cellulose is the major component of many plants. It is a linear β-1,4-glucan molecule with a covalent acetal linkage between C4 and C1 carbon atoms, as shown in Fig 1.4 [7]. A cellulose chain has one non-reducing end terminated with the original C4-OH group and a reducing end terminated with an original C1-OH group. The reducing end is a hemiacetal structure which is in equilibrium with an aldehyde structure [8]. Cellulose is insoluble in water and common organic solvents due to strong intermolecular and intramolecular hydrogen bonding. Degradation of molecular chains or modification of the backbone could help to destruct the network of hydrogen bonds, and consequently, yielding cellulose derivatives with improved solubility.

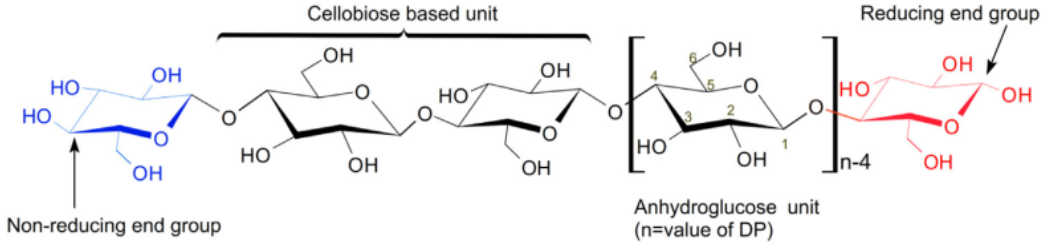

Fig. 1. 4 Molecular structure of cellulose (n=DP, degree of polymerization) [8]

Cellulose can be quantitatively degraded by acid treatment [9], or by cellulase catalyzed hydrolysis [10]. A great deal of hydroxyl groups can be esterified or etherified on the cellulose backbone chains. Thus cellulose acetate (CA), hydroxypropyl methyl cellulose (HPMC), methyl cellulose (MC), hydroxyethyl cellulose (HEC), ethyl cellulose (EC), carboxy methyl cellulose (CMC), hydroxymethyl cellulose (HEMC) are the commonly used soluble cellulose derivatives. These derivatives, and in particular EC, HPC [11], HPMC [11], and HEC [12] have been explored as a hydrophilic block to synthesize amphiphilic copolymers which are able to self-assemble into micelles.

1.2.1.2 Hydroxypropyl methyl cellulose (HPMC) and other cellulose derivative

HPMC is a cellulose derivative resulting from the substitution of hydroxyl groups by hydroxypropyl and methyl groups. The chemical structure of HPMC is illustrated in Fig. 1.5. The substituent R represents either a $–CH_3$ group, or a $–CH_2CH(CH_3)OH$ group, or simply a hydrogen atom. The physicochemical properties of HPMC are strongly affected by the degree of substitution, molar degree of substitution and degree of polymerization [13, 14]. The degree of substitution refers to the average number of substituted hydroxyl groups, and the molar degree of substitution refers to the number of substituents introduced into the anhydroglucose unit [14, 15].

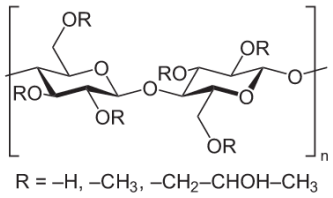

Fig. 1. 5 Chemical structure of HPMC

HPMC is one of the most important hydrophilic biopolymers used for the preparation of oral controlled drug delivery devices due to its high swellability which is the key characteristic determining release kinetics. Upon contact with water or biological fluid, the latter diffuses into the HPMC based devices, leading to polymer chain relaxation with volume expansion [16]. Subsequently, the incorporated drug will

be released by diffusion out of the system. HPMC based hydrogels have been used as carrier for several drugs such as yahom, naproxen, tramadol and ibuprofen. The factors influencing the release behavior have been studied, as documented in a review by Kamel et al. [17]. Composite of HPMC with indomethacin, an anti-inflammatory drug, was formulated by supercritical fluid (e.g., sc-CO_2) assisted impregnation method [18]. Data show that drug release obeys a power law. This strategy is very promising since it allows preparation of natural drug carriers in a 'green' way. HPMC is also used to form thermos-sensitive reversible hydrogels based on hydrophobic interactions [14].

Our group prepared amphiphilic diblock copolymers of HPMC with poly(L-lactide) (PLLA) by UV-initiated thiol-ene click reaction. Thiol-terminated HPMC (HPMC-SH) was obtained by coupling the reducing aldehyde endgroup of HPMC with the amine group of cysteamine, followed by reductive scission of the central disulfide bond of the resulting HPMC-S-S-HPMC by using excessive DL-1,4-dithiothreitol (DTT). And allyl-terminated PLLA was prepared by ring-opening polymerization of L-lactide in the presence of allyl alcohol. Subsequently UV-initiated thiol-ene click reaction was performed to couple HPMC-SH with allyl-terminated PLLA to yield a HPMC-PLLA block copolymer. The amphiphilic copolymers are water soluble and able to self-assemble in micelles in aqueous medium. The micelle size increases with increasing molar mass of the HPMC hydrophilic block. The HPMC block length also affects the critical micelle concentration (CMC) and lower critical solution temperature (LCST) of copolymers. Both the CMC and LCST increase with increasing HPMC block length. Spherical micelles are obtained by self-assembly of copolymers in aqueous solution. The micelle size increases with increasing HPMC block length. These results highlight the importance of the hydrophilic block or hydrophilic/hydrophobic balance on the self-assembly behavior of HPMC-PLA block copolymers which could be very promising as nano-carrier of hydrophobic drugs.

Other cellulose derivatives have also been considered as potential drug carrier, especially cellulose acetate (CA) and carboxymethyl cellulose (CMC). CA is a class of derivatives with substitution of hydroxyl groups by acetate ester. Studies mainly

focuse on CA beads and electrospun fibers for encapsulation of dyes and drugs. Electrospinning has attracted great interest for biomedical usages in recent years. Electrospun nanofibers provide many advantages for drug delivery applications such as high flexibility, enhanced control over drug release kinetics, simultaneous delivery of different drugs and enhanced local therapeutic effects [19]. Moreover, various drug loading methods can be employed by using different electrospinning methods with high encapsulation efficiency and loading capacity [20]. For example, multiaxial electrospinning is used for entrapment of therapeutic agents into core-shell nanofibers or multilayered fibers. These structures allow a premature release to prevent barrier and prolonged drug release [21, 22]. CA electrospun nanofibers are widely applied for encapsulation of therapeutic agents such as antimicrobial, antibacterial, antioxidant, and anti-inflammatory agents. Recently, research focused on uses of electrospun CA nanofibers in topical/transdermal drug delivery systems. CA-based stimuli-responsive drug delivery systems also have been developed [23].

Carboxymethyl cellulose (CMC) is a class of derivatives with negative charges on the polymer chains. Therefore, CMC is able to self-assemble together with positively charged polymers or proteins to yield coacervates as drug nano-carrier [23]. In fact, CMC has been used in a number of drug delivery and tissue engineering purposes. Apomorphine, a drug clinically used to regulate motor response in Parkinson's disease, was successfully loaded in a CMC powder formulation. A sustained nasal release was observed [24]. Sodium CMC has been applied in gastrointestinal drug delivery [25]. Thus, CMC is considered as a promising drug carrier for release in mucosal tissue [26]. On the other hand, research also focused on uses of CMC as tissue engineering scaffold. CMC based hydrogels exhibit pH-dependent swelling properties, and are able to release entrapped drug at appropriate pH, thus showing great potential for uses in wound dressing [27]. CMC based hydrogels are also used for encapsulating cells of nucleus pulposus, and hence could be used as a potential replacement for intervertebral disk degeneration [28]. Composites have also been prepared by combination of CMC with chitosan [29] and hydroxyapatite [30] for applications in bone and dental regeneration.

1.2.1.3 Modification routes of cellulose-based amphiphilic copolymers

Modification by grafting from hydroxyl groups has been investigated to synthesize cellulose-based copolymers for uses in drug delivery systems [31, 32]. Other modification routes have also been explored, including ring-opening polymerization of lactones initiated by the hydroxyl groups [33], living radical polymerization such as nitroxide-mediated polymerization (NMP) [34] , atom transfer radical polymerization (ATRP) [35] and reversible addition-fragmentation chain transfer polymerization (RAFT) [36].

Thanks to the presence of the reducing end of cellulose chains, cellulose-based block copolymers can be obtained via three different routes: enzymatic polymerization, polymerization of a synthetic block from an end-functionalized polysaccharide block, and end-to-end coupling of polysaccharide block with preformed synthetic block. All these methods involve the use of the reducing end. Among them, reductive amination of the hemiacetal group (reducing end) with amino groups is the most commonly used reaction, as illustrated in Fig.1.6. Reductive amination proceeds in two steps: nucleophilic addition of amine on the carbonyl group to form iminium which is the rate-determining step, followed by reduction of the iminium group in the presence of a reducing agent [37].

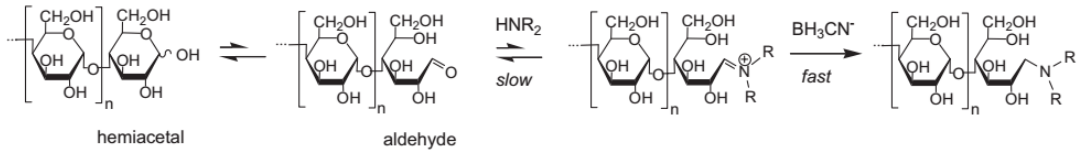

Fig. 1. 6 Reductive amination with cyanoborohydride at the reducing end of polysaccharide chain [37]

Polymerization of a synthetic block from an end-functionalized polysaccharide block means introducing an active end on the reducing end of polysaccharide chain which can serve as initiator for polymerization, including ring-opening polymerization (summarized in Fig 1.7), and radical polymerization (summarized in Fig 1.8). Cyclic monomers such as lactones, lactams or cyclic ethers are widely used to synthesize

polysaccharide-based block copolymers. In ring-opening polymerization, the molecular weight of polymers can be tailored by varying the monomer/initiator ratio and/or the conversion ratio. Controlled/living radical polymerization such as ATRP, NMP, RAFT and macromolecular design by interchange of xanthates (MADIX) has also been widely applied to synthesize well defined polysaccharide-based block copolymers [37, 38].

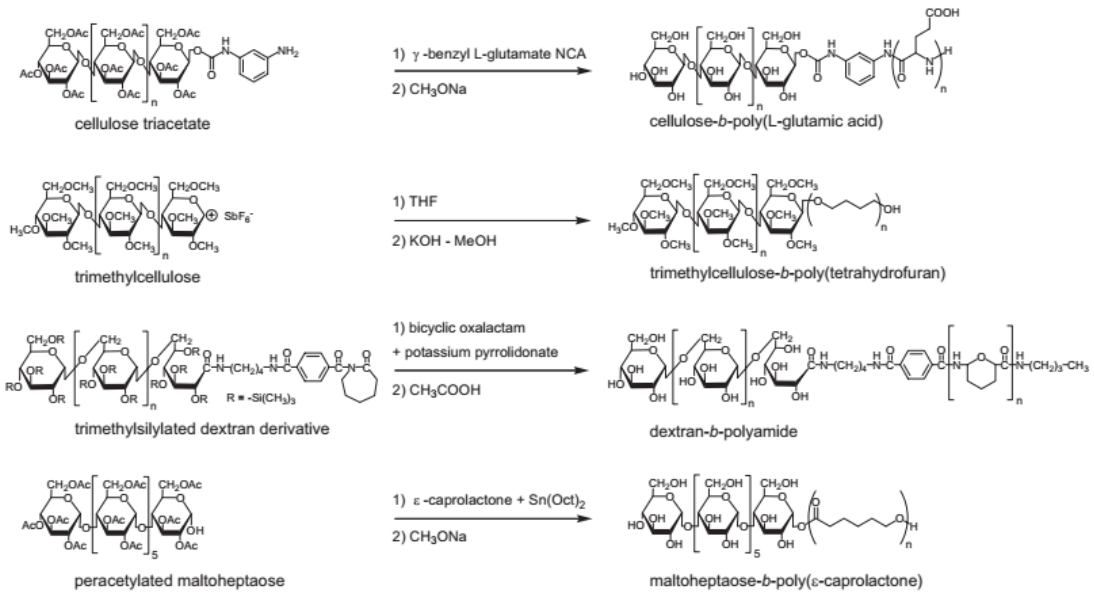

Fig. 1. 7 Ring-opening polymerization of polypeptide, polyether, polyamide and polyester from polysaccharides with suitably modified end groups [37]

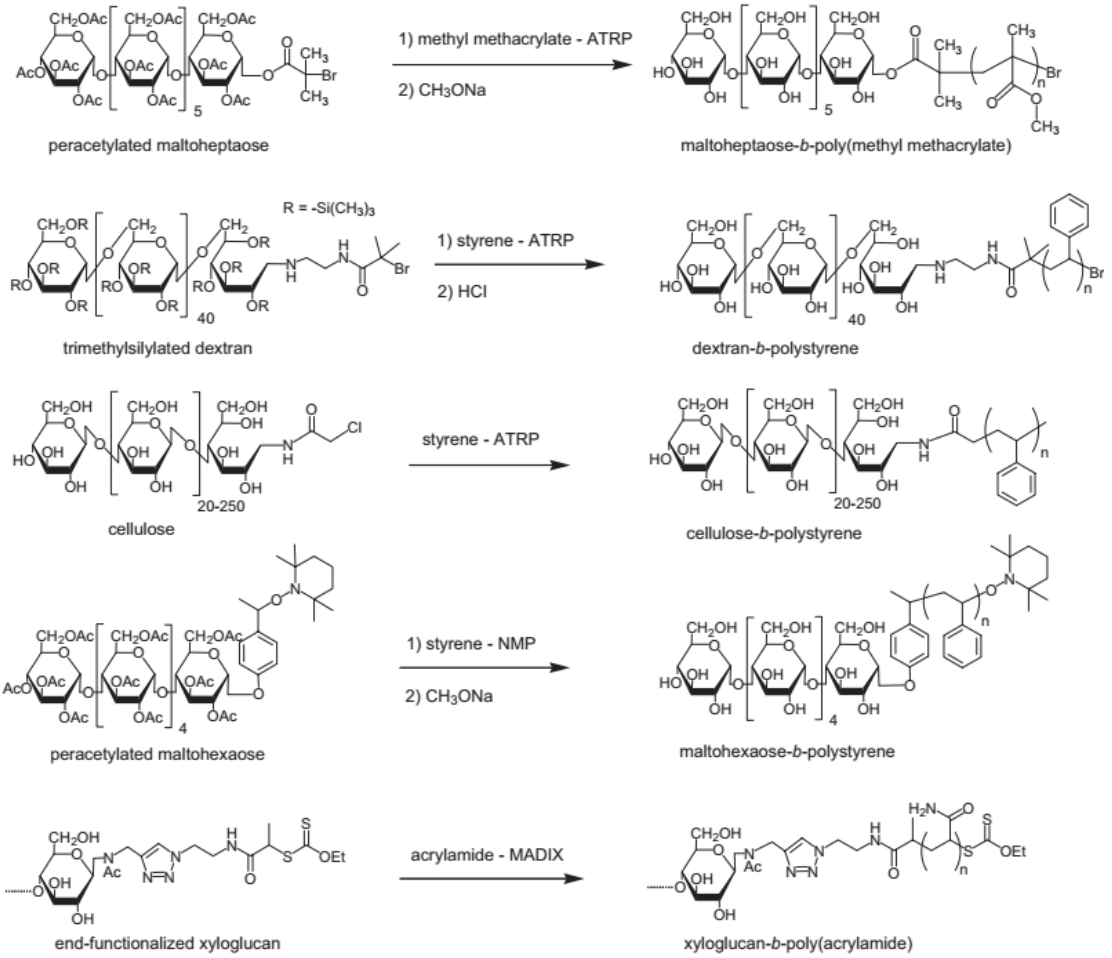

Fig. 1. 8 Controlled/'living' polymerization of vinyl blocks from poly- or oligosaccharides with suitably modified end groups. Note that hydroxyl groups are not protected in the third and the last methods [37]

End-to-end coupling of polysaccharide blocks with preformed synthetic blocks refers to couple a functional end group of the polymer on the reducing end of polysaccharide as summarized in Fig 1.9. Normally, this polymer should have low to intermediate molar mass, and have common solvent with the polysaccharide block. No side-reactions should occur during the coupling. The combination of two polymers usually requires long reaction time, *i.e.* a few days to achieve higher yield. Purification is generally realized by selective precipitation or dialysis [37].

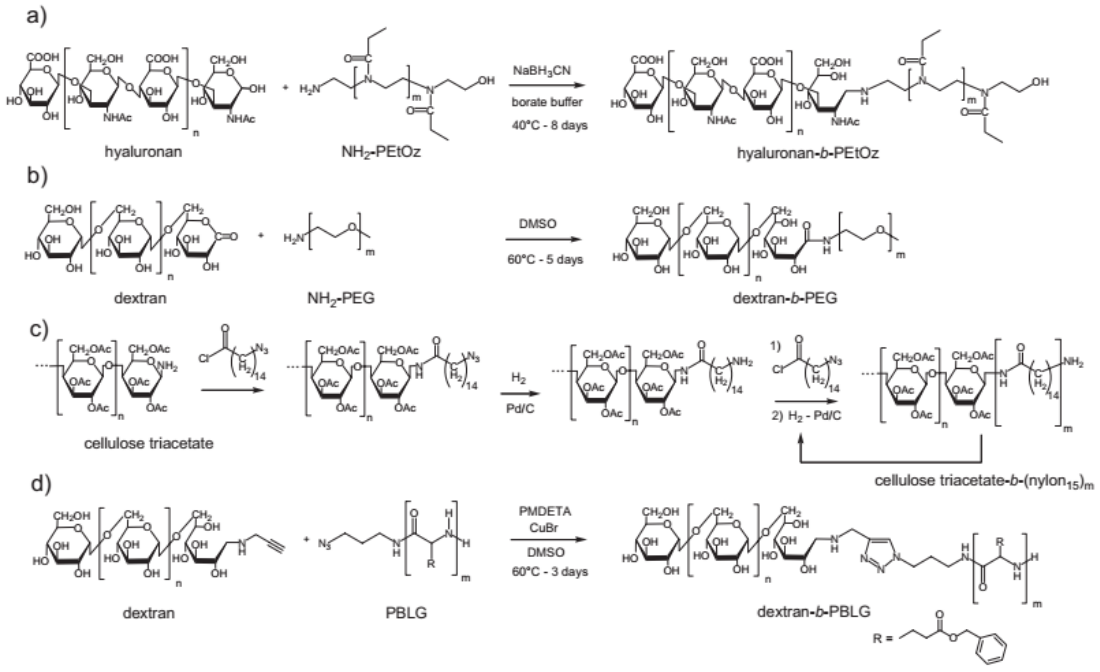

Fig. 1. 9 Coupling reactions between a polysaccharide block and a synthetic one: (a) common reductive amination, (b) aminolysis of a dextran lactone-end group, (c) stepwise elongation of a nylon block, and (d) copper(I)-catalyzed azide-alkyne cycloadditi [37]

1.2.1.4 Other polysaccharides

Chitosan, officially named as (1-4)-2-amino-2-deoxy-β-D-glucan, is a N-deacetylated product of chitin, as shown in Fig 1.10 [39]. On the chitosan chain, there are amounts of amino and hydroxyl groups as reaction point for combination with crosslinkers, target ligands or drugs. Chitosan is soluble in mildly acidic media due to the presence of amino groups, and is pH responsive as the amino groups can be converted to ammonium ones [40]. As a natural cationic polymer, chitosan is a low immunogenic, biocompatible and hydrophilic biopolymer which can be explored to construct drug delivery systems [41, 42]. In addition, chitosan is readily biodegradable in vivo by several enzymes [43]. Nevertheless, like other biopolymers, chitosan has poor water solubility for uses in drug delivery systems. Thus water solubility of chitosan can be enhanced by introducing hydrophilic groups [44, 45] or by degradation into short chains [46].

Chitosan particles prepared via coacervation method were used to encapsulate genetic material for applications in gene therapy. The system could efficiently protect the genetic material from nuclease attack. The transfection efficiency is dependent on the molar mass of chitosan, concentration of nucleotide and type of cells [47, 48]. Hydrogels based on chitosan have been used as drug carrier in the field of cancer treatment, using various methods of preparation and crosslinking agents. Entrapped drugs included paclitaxel, doxorubicin and camptothecin [49].

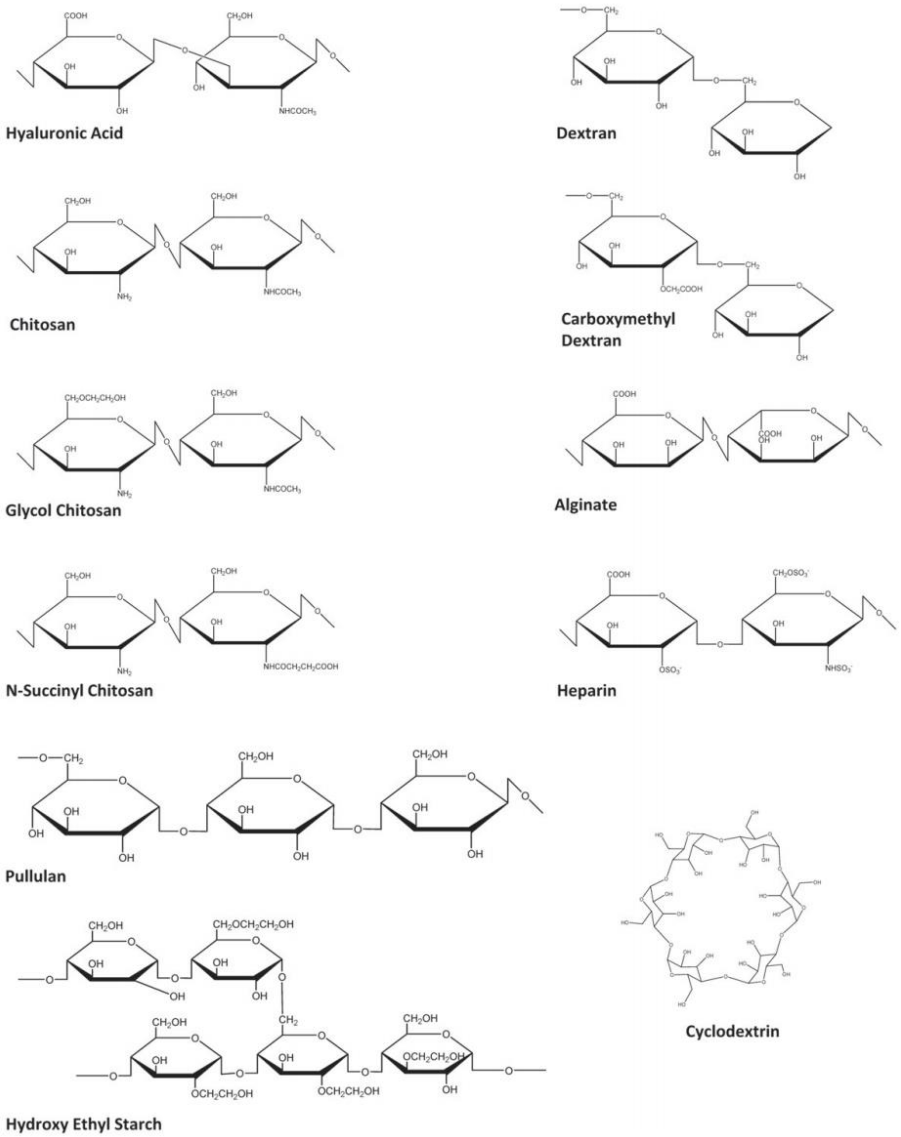

Fig. 1. 10 Chemical structures of polysaccharides [50]

Hyaluronic acid (HA) is the most popular glycosaminoglycan which is naturally highly charged. HA is a linear molecule with D-glucuronic and N-acetyl-D-glucosamine alternating on the backbone connected by β-1,4 and β-1,3 glycosidic linkages. HA is biocompatible, non-toxic, non-immunogenic, non-inflammatory, and degradable by native enzymes [51]. Thus it has been used for various medical applications including arthritis treatment, wound dressing, ocular surgery, and tissue regeneration. HA also has received much attention as a biopolymer for drug delivery system development because of its mucoadhesive property and biocompatibility. It has been used as a drug carrier in both non-parenteral and parenteral administrations. The former includes ocular and nasal delivery systems, and the latter includes sustained release formulations of protein drugs through subcutaneous injection. Many studies focused on particles and hydrogels prepared from HA and HA derivatives as drug carrier. Furthermore, the affinity of HA to the CD44 receptor which is overexpressed in various tumor cells makes HA an important biopolymer in cancer targeted drug delivery.

Starch chains consist of α-D-glucose connected by glycosidic bonds. While native starch is insoluble and semi-crystalline, starch derivatives such as dextrin, cyclodextrin and cycloamylose have been largely studied to prepare drug delivery systems. Cyclodextrins (CDs) consist of 6, 7 and 8 glucopyranoses linked by α-1,4 glycosidic into a cyclic oligomer. The cyclic structure provides CDs with a cavity which can encapsulate hydrophobic drugs and also form complex with specific molecules [23]. CDs have mainly been used to improve the water solubility of molecules by forming complexes, thus allowing to attenuate or prevent gastrointestinal or ocular irritation by lowering the local drug concentration below the irritation threshold. CDs can also increase percutaneous or rectal absorption of drugs, and their derivatives can increase the guest molecule bioavailability [52]. Enhanced bioavailability has been reported for quercetin, curcumin, arteminsinin, resveratrol and naringenin due to the inclusion complexes with CDs [53]. Recently, CDs and their derivatives have been used in dispersed vehicle systems such as emulsions, microcapsules, microspheres,

nanospheres, nanocapsules, liposomes, and beads [54]. Additionally, the host-guest property allows CDs to be used as building blocks in supramolecular chemistry [55].

1.2.2 Polyesters

Most synthetic and degradable polymers identified during the past decades contain hydrolyzable linkages along the backbone, namely ester, orthoester, anhydride, carbonate, amide, urea and urethane bonds. Ester bond-containing aliphatic polyesters such as polylactide (PLA), polyglycolide (PGA), and poly(ε-caprolactone) (PCL) are the most attractive degradable polymers because of their outstanding biocompatibility and versatility regarding physical, chemical and biological properties [56]. A number of products are currently used in clinics, mainly in the form of sutures, dental devices for guided tissue regeneration, orthopedic fixation devices, and drug delivery devices in the form of microspheres, implants, micelles and hydrogels.

The synthesis of high molar mass aliphatic polyesters is generally realized by ring-opening polymerization of heterocyclic monomers bearing at least one ester bond in the ring. The main members of the aliphatic polyester family are presented in Table 1.2. Only a few of them, namely PLA, PGA, PCL and some of their copolymers have reached the stage of clinical applications as bioresorbable devices. This is primarily due to the fact that being degradable or biodegradable is not sufficient. Many other prerequisites must be fulfilled for clinical uses: (1) biocompatibility, involving polymer, leachable oligomers, residual monomers and degradation products, shape and surface properties; (2) biofunctionality, including physical, mechanical and biological properties; (3) stability during processing, sterilization and storage; (4) bioresorption, including degradability, controlled degradation rate and resorption of degradation products.

Table 1. 2 Biodegradable aliphatic polyesters

Polymer and acronym	Structure
Polyglycolide (PGA)	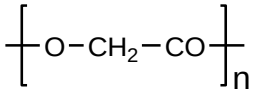

Polylactide (PLA)	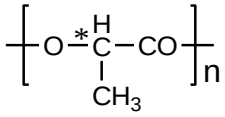
Poly(ε-caprolactone) (PCL)	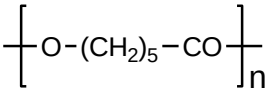
Poly(valerolactone) (PVL)	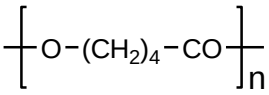
Poly(ε-decalactone) (PDL)	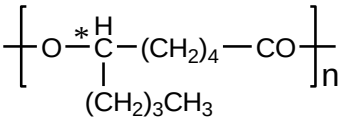
Poly(1,3-dioxane-2-one)	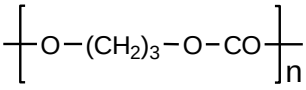
Poly(hydroxybutyrate) (PHB)	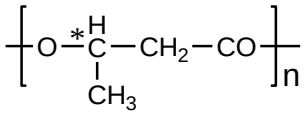
Poly(hydroxyvalerate) (PHV)	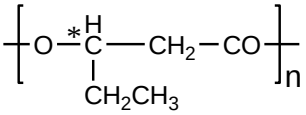
Poly(β-malic acid) (PMLA)	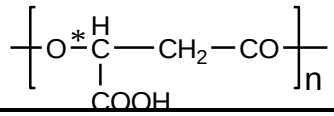

1.2.2.1 Polylactide (PLA)

In the aliphatic polyester family, polymers derived from lactic acid enantiomers have been most widely investigated for biomedical and pharmaceutical applications. Due to the presence of a chiral carbon atom, lactic acid exists in the form of L- and D-lactic acid enantiomers. Similarly, the cyclic diester of lactic acid, lactide has three diastereoisomers, i.e. L-lactide, D-lactide and meso-lactide. The latter contains one L-lactic unit and one D-lactic unit in the cycle. The chirality of LA units provides a worthwhile means to adjust bioresorption rates as well as physical and mechanical characteristics of LA-containing polymers. The chemical structure of lactic acid enantiomers and lactide diastereoisomers are shown in Fig. 1.11.

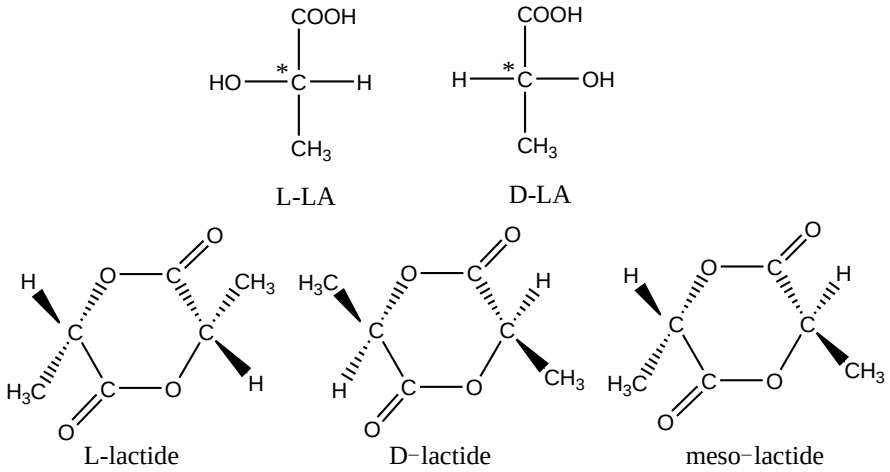

Fig. 1. 11 Chemical structures of L- and D-lactic acid enantiomers, and L-lactide, D-lactide and meso-lactide diastereoisomers

PLA is a FDA-approved polymer which has been extensively studied for drug delivery and tissue engineering applications due to its versatile properties [57]. Poly(L-lactide) (PLLA) or poly(D-lactide) (PDLA) has a glass transition temperature (Tg) of 60–65 ℃ and a melting temperature (Tm) of approximately 175-180 ℃ [58]. PLA stereocopolymers with 0-10% D-LA units in PLLA chains or with 0-10% L-LA units in PDLA chains are also semi-crystalline, but the degree of crystallinity decreases with decreasing optical purity. Thus, the degree of crystallinity can be tailored by polymerization of appropriate mixture of D- and L-lactides, which determines the physico-mechanical properties and degradability [59]. In addition, stereocomplexation between PLLA and PDLA blocks has been studied to construct functional colloidal systems for therapeutic applications such as membrane and injectable nanogel or hydrogel [60-62]. PLA is wildly used as a hydrophobic block to construct amphiphilic copolymers such as poly(ethylene glycol)-polylactide (PEG-PLA) block copolymers which can self-assemble into micelles. PEG-PLA copolymer micelles have been extensively studied as nano-carrier of hydrophobic chemotherapeutics [63]. The topology of copolymers has significant effect on the self-assembly properties [64]. Compared to linear block copolymers, star-shaped PEG/PLA copolymer micelles

present faster and more complete release of paclitaxel (PTX). In vivo drug release showed that the tolerability was increased four-fold by using PTX-loaded poly(N-vinylpyrrolidone)-block-poly(DL-lactide) micelles [65]. Multidrug PTX/LAP-loaded PEG-PLA micelles exhibited therapeutic effect to both HER-2-positive and HER-2-negative breast cancers [66]. Platinum (IV) complex was encapsulated into PEG-PLA micelles by covalent linking, and prolonged release up to two months was observed [67].

1.2.2.2 Poly(ε-caprolactone) (PCL)

PCL is a hydrophobic polyester with good biocompatibility, degradability and permeability to drugs. It has been approved by the US FDA for biomedical applications. PCL is a semi-crystalline polymer with a low Tg of -60 ℃ and a Tm of 65 ℃, and is readily soluble in various organic solvents [68]. Research recently focused on PCL as a tissue engineering scaffold and three-dimensional printing material due to its low Tm and facile processability into specific shapes [69]. Nevertheless, PCL degrades very slowly, with up to two to three years required for complete degradation under in vivo conditions [70], which strongly limits its applications as drug carrier. The only example of the use of PCL as drug carrier is Capronor®, an implant for contraceptive drug delivery for two years [71]. Various copolymers of PCL with PLA, PGA, PEG, poly(trimethylene carbonate) (PTMC) have been developed for biomedical applications.

PCL-based drug delivery systems have been extensively studied, including degradability, biocompatibility, drug loading capacity, therapeutic effects induced in vivo via targeted and non-targeted drug delivery, application routes, triggered drug release, etc. [72]. PEG-PCL copolymer micelles are able to encapsulate many kinds of hydrophobic drugs such as doxorubicin [73, 74], 5-fluoro uracil [75], curcumin [76], paclitaxel [77], nimodipine [78], *etc.* PCL was also combined with chitosan to produce a cationic graft copolymer. An irinotecan derivative, SN-38 was loaded in PCL-*g*-chitosan micelles with drug loading efficiency (DLE) of up to 8.66% and 84.5%. The drug release was hastened by increasing PCL content [79]. Chitosan-*g*-PCL-*g*-PEG can self-assemble into micelles. After cross-linking by glutaraldehyde, the micelles shrunk

and the drug release slowed down [80]. Curcumin loaded PEG-PCL micelles exhibit cyto-toxicity against in B16-F10, SP-53, Mino and JeKo-1 cell lines [81].

1.2.2.3 Other polyesters

PGA was the first degradable synthetic polymer used for biomedical applications. Since the 1970s, PGA has been used as a degradable suture under the trade name of Dexon® due to its very high mechanical strength and fast degradation. In fact, PGA exhibits a very high tensile strength up to 220 MPa, and a Young's modulus of 6.5 GPa. But PGA is a brittle material due to its very high degree of crystallinity. PGA exhibits a Tg of 35-40 ℃, and a Tm of 220-230 ℃ which is rather close to its decomposition temperature [58]. Because of the high degree of crystallinity, PGA is insoluble in common organic solvents, which greatly restrains its potential biomedical applications. Recent studies focused on PGA as a filler material to prepare composites with other degradable polymers. PGA has been incorporated into scaffolds for tissue engineering applications such as bone, tendon, cartilage, tooth, and spinal regeneration. PGA is also studied for neural regeneration due to its good degradability and FDA approval for nerve grafting [82]. Promising results have been obtained for producing nerve graft structures [83]. PGA has also been utilized in wound healing and adhesives. PGA sheets were used in conjunction with fibrin glue spray as an open wound healing material for soft tissues as well as bone surfaces during oral surgery [84]. As an adhesive, PGA was combined with fibrin sealant to create a very successful tissue adhesive [85]. PGA is not a good drug carrier due to its very high degree of crystallinity and insolubility. But lactide/glycolide copolymers (PLGA) have been largely investigated as drug carrier in the form of injectable microspheres, micelles and hydrogels [86-88].

Polyester degrades in physiological environment by ester bond cleavage via pure hydrolysis, and/or enzyme-catalyzed hydrolysis [89]. The degradation of aliphatic polyesters, and in particular PLA/PGA polymers, has been largely investigated under in vitro or in vivo conditions during the past decades. The process is very complex involving diverse physico-chemical phenomena such as water uptake, ester bond cleavage, property changes, eventual crystallization of degradation by-products, and

loss of soluble oligomers. Degradation of polyesters is catalyzed by carboxyl endgroups generated by chain cleavage, a phenomenon known as autocatalysis. On the other hand, amorphous regions of semi-crystalline polyesters are preferentially degraded as compared to crystalline ones. Long-term systemic investigations showed that degradation proceeds faster inside than at the surface of large-size polymers due to internal autocatalysis. Degradation-induced morphological and compositional changes were also reported [71, 90, 91].

1.2.3 Poloxamers®

Among the polymers displaying micelle-formation ability, it is worth mentioning that PEG-based polymers has a long history due to its resistance to non-specific adsorption in blood, avoiding phagocytes uptake, and prolonged circulation time in vivo. In fact, PEG is the most commonly used hydrophilic component to prepare amphiphilic block copolymers with hydrophobic blocks such as polyesters [72, 88], and poly(amino acids) [92, 93].

Poloxamers®, also known as Pluronics®, are a class of water soluble non-ionic A-B-A and B-A-B triblock copolymers, A and B designating poly(ethylene oxide) (PEO) and poly(propylene oxide) (PPO), respectively. Tetronic® block copolymers are composed of four PPO-PEO chains extending outward from an amine-terminated central molecule. Poloxamers® are not degradable, but can be filtered by the kidney and cleared in urine if the molar mass is below 15 KDa [94, 95].

The chemical structure of A-B-A type Poloxamers® is shown in Fig. 1.12. Poloxamers® exhibit an amphiphilic character as PEO is soluble in water and PPO is insoluble. Poloxamers® are able to self-assemble to various structures driven by different ratios of their constituent PEO and PPO blocks. Some of them are thermos-sensitive. Thus temperature is an important parameter influencing their micellization behaviors.

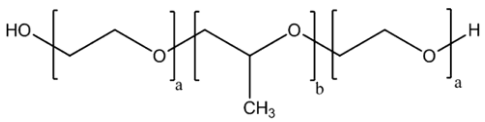

Fig. 1. 12 Chemical structure of Poloxamers® with a = 2-130 and b = 15-67

Table 1.3 shows the physicochemical properties of a number of Pluronics® as a function of molar mass, PPO and PEO block lengths, and temperature. The micellization process starts either by increasing the concentration over the critical micellization concentration (CMC) at a certain temperature or by increasing the temperature to the critical micellization temperature (CMT) at a certain concentration [96]. Pluronics® with higher PPO content are more sensitive to temperature [97]. The CMC generally decreases with increasing hydrophobic PPO content, and with increasing temperature. In fact, increasing temperature leads to higher hydrophobicity of polymers. Thermo-responsive Pluronics® have been extensively investigated in controlled drug delivery.

Table 1. 3 Physicochemical properties of Pluronic® PEO-PPO-PEO block copolymers used in drug formulation. Data obtained from [98]

Pluronic® Notation	MW	PO Units	EO Units	cmc at 25 °C (% *w/v*)	cmc at 30 °C (% *w/v*)	cmc at 35 °C (% *w/v*)
L64	2900	30	26	n/a	1.5	0.4
P65	3400	17	36	n/a	4	1
P84	4200	43	38	2.6	0.6	0.15
P85	4600	40	52	4	0.9	0.2
F88	11,400	39	206	n/a	n/a	1.7
P103	4950	60	34	0.07	0.01	0.002
P104	5900	61	54	0.3	0.04	0.008
P105	6500	56	74	0.3	0.025	0.005
F108	14,600	50	264	4.5	0.8	0.15
P123	5750	69	38	0.03	0.005	0.001
F127	12,600	65	200	0.7	0.1	0.025

Drug delivery systems prepared from Poloxamers® can be obtained by using different methods such as direct solubilization, film rehydration, solvent displacement, and temperature-induced emulsification. By direct solubilization, encapsulation of the drug in micelles is achieved by simple aqueous or aqueous-organic solvent mixture including both drug and polymer. Film hydration method consists in dissolving both drug and polymer in a common solvent, followed by solvent evaporation to obtain a dried film structure which can be rehydrated prior to administration. Solvent

displacement techniques, including dialysis, nanoprecipitation and co-solvent evaporation, rely on the mixture of fully, partially or non-miscible phases in order to achieve formation of drug loaded micelles. In temperature-induced emulsification, emulsions are formed at elevated temperatures and then rapidly cooled. Drug-loaded micelles of one or more Poloxamers® have shown great potential in controlled delivery of anticancer and benzoporphyrin derivatives for photodynamic therapy [96, 99-101]. Mixed micelles and nanoparticles typically combine Poloxamers® of opposing hydrophilic-lipophilic balance (HLB) values so as to achieve enhanced solubilization in the PPO core and steric stabilization due to the PEO corona.

At concentrations around 20 w/w%, certain Poloxamers® undergo a thermo-reversible phase transition around 37 ℃ from micellar solution to a stiff gel. Such hydrogels present great interest for the delivery of hydrophobic drugs as they allow drug administration by subcutaneous injection in the form of a flowing micellar solution which in situ solidifies to yield a stable drug depot [102, 103]. The thermo-reversible gelation of Poloxamers® is also useful to counter constant tear generation of the eye, which will rapidly wash away the drug [104]. Hydrogel formation also allows for targeted subcutaneous drug delivery [105, 106].

1.2.4 Other polymers in drug delivery systems

Zwitterions refer to molecules containing both negatively charged groups and positively charged ones in the same chain, including phosphorylcholine (PC), carboxy betaine (CB), and sulfobetaine (SB). Zwitterions can minimize the interaction with biological components such as proteins and cells due to cell membrane-like surface. This is a very important characteristic of zwitterions, which is also called non-fouling property which is dependent on the hydration ability of materials [107]. It has been reported that each sulfobetaine unit tightly binds 7-8 water molecules, while each ethylene oxide unit only binds one [108]. Many researchers have focused on modification of nanoparticles by zwitterions or utilization of zwitterions as hydrophilic component in drug delivery systems [109, 110].

Poly(N-isopropyl acrylamide) (PNIPAAm) is one of the most extensively

investigated thermo-sensitive polymers that exhibit a LCST in aqueous solution [111]. The LCST of PNIPAAm is around 32 ℃. PNIPAAm exhibits a random coil structure below the LCST, and is thus water soluble. It turns to a collapsed globular structure above the LCST, and becomes water insoluble. Therefore, PNIPAAm can be either the shell-forming segment or the core-forming one. With PNIPAAm as the hydrophilic block, copolymers can form a micelle with a hydrophobic inner core able to encapsulate hydrophobic drugs below the LCST and a PNIPAAm hydrophilic outer shell which ensures aqueous solubilization as well as temperature responsiveness. When the temperature increases above the LCST, PNIPAAm becomes hydrophobic, and thus aggregation of micelles occurs, which could favor drug release from the core.

Thermo-responsive amphiphilic block copolymers composed of PNIPAAm and a hydrophobic block, such as degradable polyesters like PLA and PCL, and non degradable polystyrene (PS), poly(methyl methacrylate) (PMMA), and poly(tert-butyl acrylate) (PtBA), have been reported in literature [111]. PNIPAAm-PLA block copolymers were obtained by ring-opening polymerization (ROP) of lactide initiated by hydroxyl-terminated PNIPAAm precursor [112, 113]. RAFT and ATRP were also employed to synthesize PNIPAAm-PLA copolymers with well controlled molar mass and narrow dispersity [114-116]. Copolymers composed of a central PLLA block and two poly(N-isopropylacrylamide-co-N,N-dimethylacrylamide) (P(NIPAAm-co-DMAAm)) lateral blocks were also obtained to tailor the LCST of copolymers above the body temperature [117].

On the other hand, copolymers consisting of PNIPAAm as hydrophobic block can form a micelle with a hydrophobic PNIPAAm core which ensures encapsulation of hydrophobic drugs and also temperature responsiveness below LCST, and a hydrophilic outer shell which stabilizes the micelle structure in aqueous solution. Below the LCST, the copolymer is soluble in aqueous solution. And above the LCST, the thermo-sensitive PNIPAAm block precipitates, and copolymer chains self-assemble into polymeric micelles. The advantage of thermo-sensitive PNIPAAm core-forming micelles is that micelles can be prepared by simply heating the aqueous solution above

the LCST [111].

1.3 Polymeric nanocarriers

In the past decades, remarkable progress has been made on biomedical applications of polymeric nanocarriers, such as biosensors, optoelectronics, catalysis, energy, biotechnology, and medicine. In particular, polymeric nanostructured materials are wildly used in drug delivery systems including dendrimers, nanoparticles, nanogels, polymersomes, micelles, nanocapsules, nanofibers, *etc*.

Generally, polymeric nanocarriers for biomedical applications should present a number of physico-chemical properties : (a) good dispersibility in aqueous solution, (b) suitable size (10–200 nm) to avoid fast clearance and to achieve preferred biodistribution, (c) biodegradability to minimize side effects (residue with $M_n < 45K$ or hydrodynamic size <10 nm for complete clearance from circulation), (d) functionality to link with drug, targeting component, or imaging element, etc. (e) responsiveness to release therapeutic loading under triggered conditions [118]. Fig. 1.13 summarizes all the nanoscale architectures used for cancer therapy, and their key properties determining biodistribution, drug release profile, targeting, and biological process after administration in the blood stream.

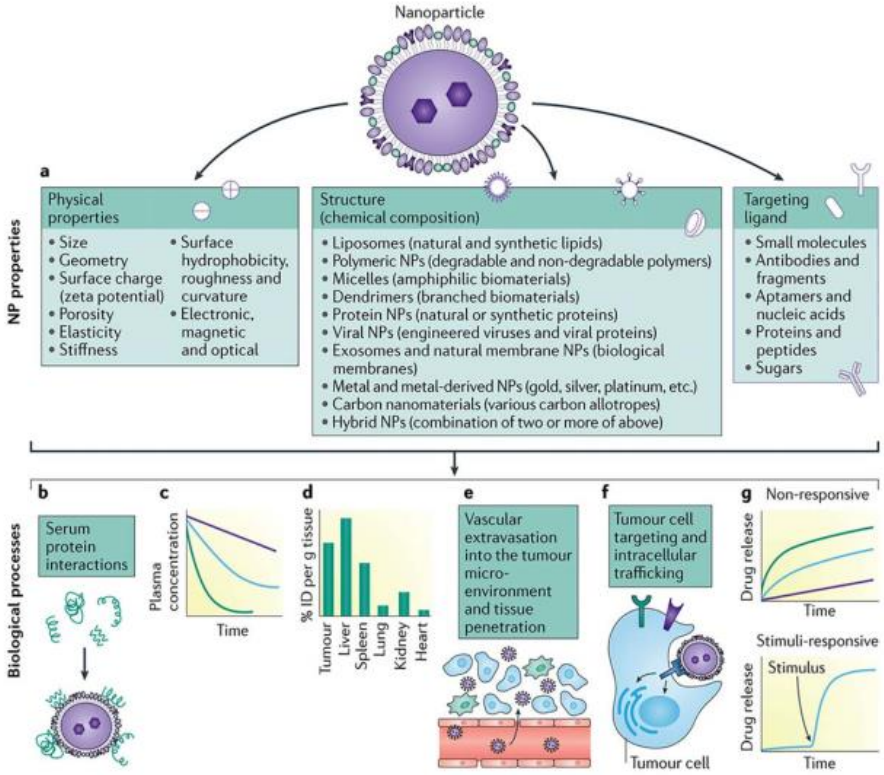

Fig. 1. 13 Nanoparticles for cancer therapy

(a) Nanoparticles for cancer therapy can be made from a variety of materials, be produced to have varied physicochemical properties, and include an array of targeting ligands on the surface. (b,c) The nanoparticle surface properties and targeting ligands greatly affect its interactions with serum proteins and can be modified to increase blood circulation time and slow clearance mechanisms from the body. (c,d,f) Particle properties (such as size, geometry, surface charge, surface hydrophilicity, elasticity, etc.) can be modified to drive preferential biodistribution in tumors by increasing particle extravasation into the tumor microenvironment via the characteristic leaky vasculature in tumor vessels and increasing uptake and intracellular trafficking by tumor cells. (g) Particles can also be designed to control cargo release in response to intracellular biological stimuli [119, 120]

1.3.1 Dendrimers

Dendrimer consists of three dimensional globular macromolecules with one

central core, branches and functional terminal groups. The particle size of dendrimers usually ranges from 1 to 100 nm with monodispersity, and can be controlled by the generation number [121]. Most importantly, dendrimers have well-defined molar mass, size, structure and surface functionality [122]. Drugs can be incorporated in the core, internal cavities or at the surface functional groups by covalent bonding or by electrostatic interaction, as shown in Fig. 1.14 [119, 123]. Dendrimer presents many advantages as drug delivery system, including increased solubility, stability, permeability and half-life of drugs in blood circulation, capability to deliver a variety of drugs including hydrophilic and hydrophobic ones, reduced macrophage uptake, facile passage across biological barriers, targeting ability, rapid cellular entry, improved delivery efficiency, and reduced side effects by targeted delivery [119, 124-127].

Nevertheless, the terminal groups on the surface of dendrimers causes some toxicity. In fact, dendrimers with neutral or anionic surface groups present good biocompatibility, but cationic dendrimers exhibit more or less toxicity [128]. Therefore, dendrimers still have many obstacles to overcome for uses as drug carrier, such as poor biocompatibility, unstable hydrophobic drug loading, and inefficient targeting-drug release [129]. One approach is to exploit dendronized polymers, i.e. linear polymers that contain dendrons on every repeat unit [130]. Another approach is to incorporate a degradable link in dendrimers to improve controlled release [131]. Efforts have also been made to improve the biocompatibility of dendrimers by neutralization of surface cationic charge using PEGlation, acetylation, carbonhydrate, peptide conjugation, *etc*. [132-135].

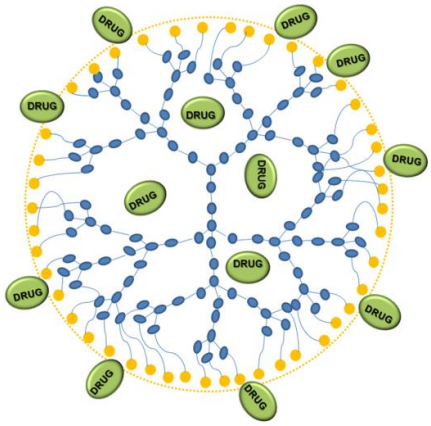

Fig. 1. 14 Scheme of drug loading in dendrimeric structure [119]

1.3.2 Nanoparticles

Nanoparticles refer to particles made of inorganic materials that keep their original shape and size, or to particles made of organic materials that are subject to size and shape changes under specific conditions of temperature, pH, pressure and ionic strength [119, 136]. In general, the suitable size of nanoparticles for biomedical application is below 200 nm. Different from other nanostructures such as micelles or liposomes, nanoparticles can be easily prepared with a stable structure [118]. Drugs are either entrapped inside or adsorbed on the surface of nanoparticles. Drug-loaded nanoparticles can enter human body by subcutaneous or intravenous injection, oral administration and inhalation [136]. Typically, nanoparticles consist of therapeutic molecules, constituent material, and biological surface modifiers which determine their biodistribution or tumor-targeting [137].

Inorganic nanoparticles include gold, silica, titanium, calcium phosphate (CaP), carbon-based, *etc.* As a natural component of human body, CaP nanoparticles have been largely investigated as drug carrier which is able to encapsulate hydrophobic drugs alone or with polymers [138]. Carbon-based nanoparticles include carbon nanotubes (CNTs), and graphene oxides (GOs). Carbon nanotubes are usually functionalized by PEG or other polymers to improve their water-solubility. CNTs and GOs nanoparticles have great drug entrapment capability which is the main potential to be explored in drug delivery [138]. Gold nanoparticles are developed as drug carrier due to their

biocompatibility, surface tenability and stability against oxidation and degradation [139]. Nevertheless, the clinical uses of inorganic nano-systems are still under strong debate due to the lack of data regarding the bio-safety, especially the biodegradation behavior, excretion routes and long-term toxicity assessments.

Polymer-based nanoparticles are colloidal systems in which a therapeutic agent of interest can be embedded or encapsulated inside, adsorbed or conjugated on the surface. They are widely investigated for controlled delivery of a number of biomolecules, drugs, genes and vaccines to the targeted site in vivo. Biodegradable polymeric nanoparticles, in particular those prepared from PLA and PLGA, are most promising drug delivery systems because of their outstanding properties such as biocompatibility and degradability [140]. They can be applied in the form of injectable, oral and implantable formulations encapsulating a wide range of drug molecules, including protein/peptide molecules which should be protected in physiological conditions. Their superiorities over conventional drug delivery systems make them a useful tool for biopharmaceutical industry. Nevertheless, biodegradable nanoparticles also have some disadvantages. Their small size and large surface area could provoke instability or aggregation of the system. Nanoparticle-drug conjugates are exposed to phagocytosis in the body. Low drug loading capacity and low loading efficiency are the other limitations of developing a nanoparticle drug delivery system.

1.3.3 Nanogels

Nanogels consist of a swellable three-dimensional nano-structure formed by chemical or physical crosslinking of hydrophilic or amphiphilic macromolecular chains. Nanogels exhibit fluid-like transport properties due to the fact that they can hold large amount of water and preserve their structure without dissolving [141]. Usually, the size of nanogels is in the range between 1 and 1000 nm [142]. Nanogels can be obtained from both natural and synthetic polymers via physical approaches like hydrogen bonding, stereocomplexation, electrostatic interaction and hydrophobic interaction or by chemical approach, i.e. covalent bonding [143, 144]. The great capacity of absorbing water of nanogels is attributed to the presence of amounts of hydrophilic functional

groups on the polymer chain, for instance –OH, –CONH–, $–NH_2$, -COOH, and $–SO_3H$. Natural polymer derived nanogels include protein polymers, such as collagen, albumin and fibrin, and polysaccharide polymers such as chitosan, HA, heparin, chondroitin sulfate, agarose and alginate. Typical synthetic materials are mainly polyacrylates, polymethacrylates, PEG, PNIPAAm, *etc.*

Nanogels present many advantages as drug delivery systems such as tunable size, relatively high drug loading capacity, encapsulation of diverse drugs, convenient preparation, minimal toxicity, stability in physiological serum, and responsivity to external stimuli [141, 145, 146]. In fact, the particle size and surface properties of nanogels can be tailored to avoid rapid clearance by phagocytic cells, making possible both passive and active drug targeting. Controlled and sustained drug release at the target site allows to improve the therapeutic efficacy and to reduce side effects. Nanogels are able to reach the smallest capillary vessels due to their tiny volume, and to penetrate the tissues either through paracellular or transcellular pathway [147]. All these properties make nanogels most promising drug carrier. Nevertheless, nanogel shows also some limitations, in particular expensive techniques to totally remove the solvents and surfactants after the preparation process as these impurities can impart toxicity [148, 149].

1.3.4 Polymersomes

Polymeric vesicles, also known as polymersomes, are nanoscale hollow spheres with a hydrophilic interior, hydrophobic bilayer and a hydrophilic shell, in contrast to polymeric micelles with a hydrophobic core surrounded by a hydrophilic shell. Amphiphilic copolymers are able to self-assemble in an aqueous medium into diverse nanostructures according to their physico-chemical properties, in particular the packing parameter ρ according to Israelachvili's concept, and the hydrophilic weight fraction *f*. Fig 1.15 shows the various nanostructures obtained by self-assembly of amphiphilic copolymers with different ρ and *f* values. It is well admitted that high curvature ($\rho < 1/3$) and high hydrophilic weight fraction ($f > 50\%$) lead to highly spherical micelles, intermediate curvature ($1/3 \leq \rho \leq 1/2$) and hydrophilic fraction ($35\% < f < 50\%$) lead to

cylindrical or rod-like micelles, low curvature ($1/2 \leq \rho \leq 1$) and low hydrophilic fraction ($10\% < f < 25\%$) lead to bilayer vesicle structure [150-152].

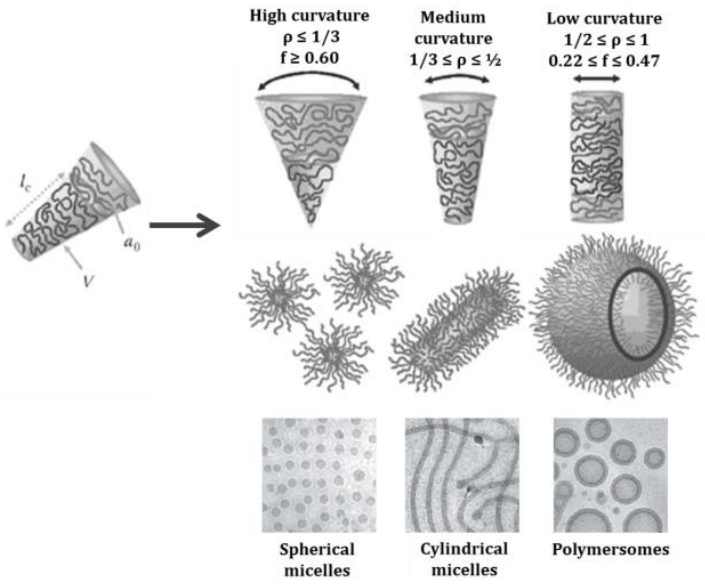

Fig. 1. 15 Interrelations between the self-assembled structures formed by amphiphilic copolymers in aqueous solution with packing parameter ρ and hydrophilic fraction f; Scheme reproduced from Ref [6] and cryo-TEM images extracted from [7]

Polymeric vesicles are able to encapsulate both hydrophilic and lipophilic drugs and deliver drugs to the target site based on their unique hydrophobic membrane and hydrophilic interior structure. Vesicles can be classified in various categories according to their diameter and number of bilayers, i.e. small unilamellar vesicles (20-100 nm), large unilamellar vesicles (100-500 nm), giant unilamellar vesicles (0.5 – 100 μm), and also multilamellar vesicles having a membrane composed of several bilayer shells, and multivesicular vesicles with large or giant vesicles encapsulating smaller vesicles inside [153]. Thus, the main critical properties of vesicles are size, thickness of membrane and surface of membrane. Vesicles present interesting properties such as nanoscale size, high surface-to-volume ratio, and favorable physicochemical characteristics. Hence, they can enhance the therapeutic index, increase the in vivo stability, extend the blood

circulation time, and allow controlled drug release for improved drug biodistribution [154]. In fact, the therapeutic efficacy can be enhanced by optimizing the spatiotemporal distribution of therapeutics, which can be achieved by introducing stimuli-responsive component in the membrane polymers [155].

1.4 Micelles

Micelles consist of a core-shell nanostructure obtained by self-assembly of amphiphilic macromolecules in aqueous medium. The hydrophobic component forms the core which is able to encapsulate hydrophobic drugs, whereas the hydrophilic component constitutes the shell providing desired properties such as stabilization of the system and prolonged circulation by avoiding clearance. Micelles are typical of 10–200 nm in diameter, enabling them to extravasate through the leaky vasculature in tumor tissue [120]. Compared with other long-circulating nanocarriers like nanoparticles or liposomes, polymeric micelles present many advantages, including controlled drug release by introducing stimuli-responsive structure on the polymer chain, increased tissue penetrating ability, and reduced toxicity by introducing functional group on the surface, as shown in Fig.1.16 [156].

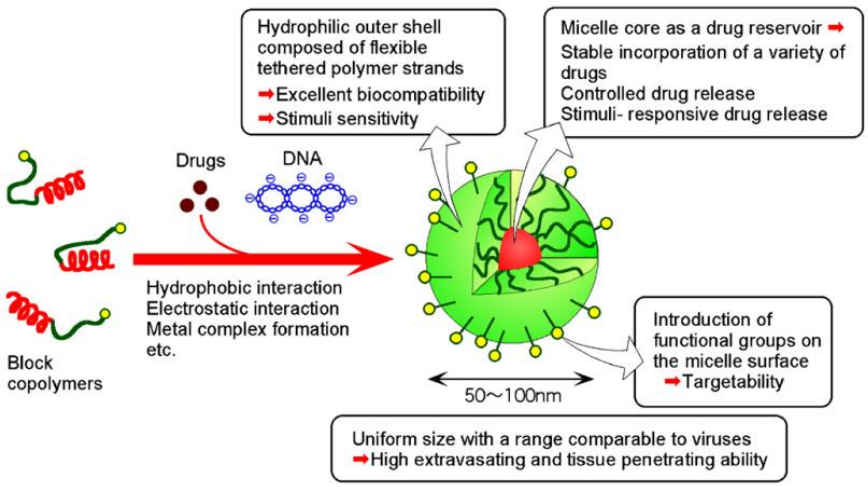

Fig. 1. 16 Polymeric micelles as intelligent nanocarriers for drug and gene delivery [156]

1.4.1 Topology

Amphiphilic copolymers with proper hydrophilic/hydrophobic ratio are able to self-assemble into micelles. In addition to the chemical composition, the topological structure of polymers also determines the self-assembly as well as the drug encapsulation and release properties. Topology, also called architecture, refers to the spatial or geometrical features of molecular chains, such as linear, Y-type, star-shaped (multi-armed), branch, grafted and cyclic structures. In Fig.1.17 are summarized the various geometrical arrangements of chemical bonds in copolymers.

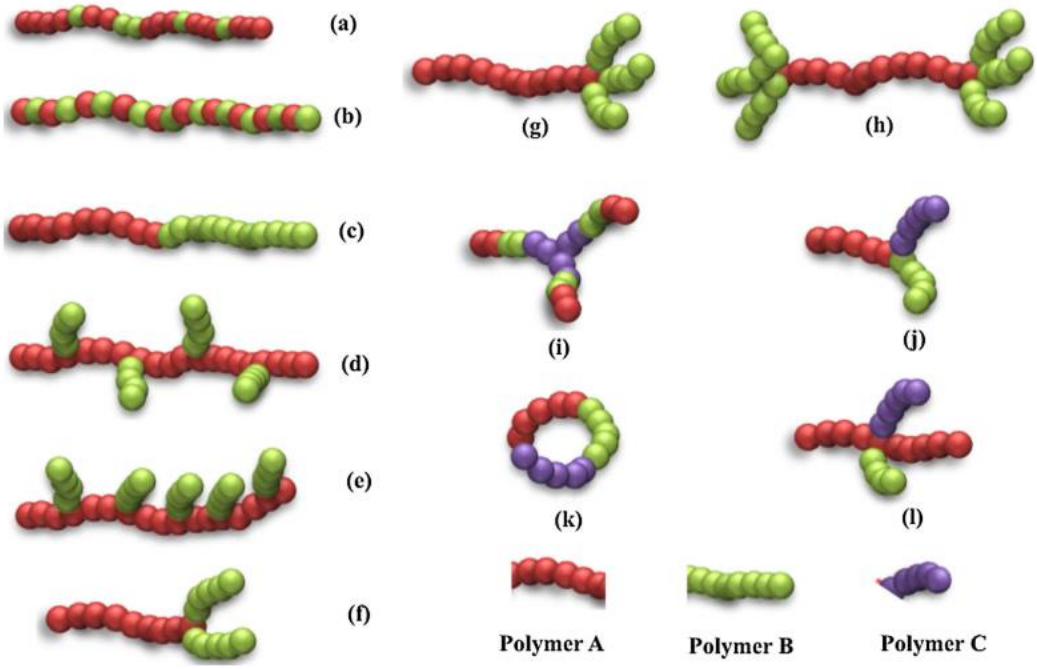

Fig. 1. 17 Various geometrical arrangements of chemical bonds in a copolymer: (a) random, (b) alternate, (c) block, (d) graft, (e) brush type, (f) AB2 type, (g) palm tree shaped, (h) dumbbell shaped, (i) star shaped triblock, (j) Miktoarm triblock, (k) cyclic trib [157]

Amphiphilic linear block copolymers, and in particular copolymers of hydrophilic PEG with a hydrophobic and degradable polyester such as PLA, PLGA and PCL, have been extensively investigated as drug delivery systems because of the possibility of

modulating the chain structure (AB, ABA, BAB), the lengths or molar masses of blocks and the hydrophilic/hydrophobic ratio. The chain conformations of AB diblock, ABA and BAB triblock copolymers in a micellar state are shown in Fig1.18. Diblock copolymers tend to form micelles with a stick-like chain structure. In contrast, ABA and BAB triblock chains have to fold so as to insert the hydrophobic blocks inside micelles.

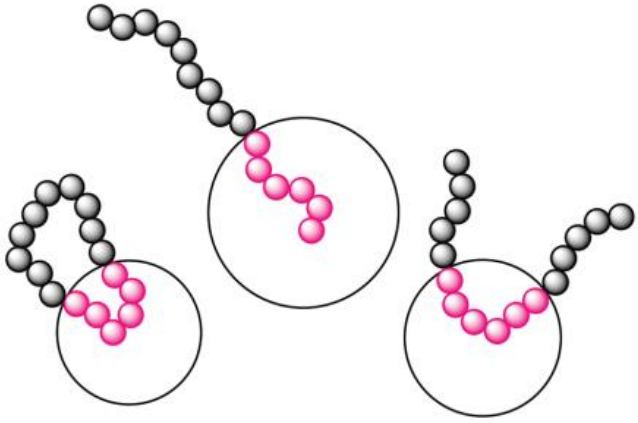

Fig. 1. 18 Chain conformations of AB diblock, ABA and BAB triblock copolymers in a micellar state [158]

Amphiphilic PLA-PEG copolymers have been most widely investigated as potential drug vector [59]. They can self-assemble in aqueous environment to yield aggregates having a variety of structures such as spherical micelles, rod-like micelles, worm-like or filomicelles, polymersomes, and nanotubes [159, 160]. The self-assembled structure mainly depends on the hydrophilic/hydrophobic ratio, chain structure (AB, ABA and BAB) and the regularity of the hydrophobic chain. The effect of the hydrophilic/hydrophobic ratio is mentioned in Fig. 1.15. Spherical micelles, rod-like micelles, worm-like or filomicelles can be obtained from PLA-PEG copolymers with decreasing hydrophilic/hydrophobic ratio. Artificial hollow aggregates, i.e. polymersomes and nanotubes are obtained from asymmetric PEG-PLA-PEG copolymers with appropriate block lengths. Nanotubes have recently attracted much interest as novel drug carriers because they can achieve long circulation time similar to

filomicelles [161]. They also exhibit higher drug encapsulation ability in comparison with spherical micelles because of larger core volume. Moreover, nanotubes are able to encapsulate both hydrophobic and hydrophilic drugs because of the co-existence of internal hydrophilic regions and intermediate hydrophobic regions within the architecture. In fact, drug delivery systems loaded with two or more drugs could present a synergistic therapeutic effect in treating cancers [162, 163].

Interestingly, the hydrophobic chain regularity also affects the self-assembled structure of PLA-PEG copolymers. As shown in Fig.1.19, only spherical micelles are observed for $PDLLA_{80}PEG_{114}$. In contrast, essentially filomicelles are obtained for $PLLA_{85}PEG_{114}$ with similar hydrophilic and hydrophobic block lengths. In fact, stereoregular PLLA blocks are more rigid than PDLLA ones with randomly distributed L- and D-lactide units, and rigid blocks seem to be more inclined to form filomicelles.

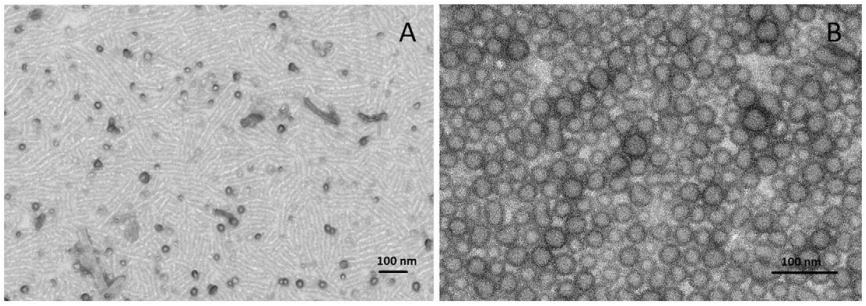

Fig. 1. 19 TEM images of PTX-loaded $PLLA_{85}PEG_{114}$ worm-like micelles (A), and PTX-loaded $PDLLA_{80}PEG_{114}$ spherical micelles (B) [164]

Compared to linear polymers, branch or graft polymers have more parameters for modulation of self-assembly properties such as number and length of arms or grafts, and have more reactive groups which can react with cross-linkers or drugs. Generally, nonlinear polymers present lower critical micelle concentration, smaller size and higher drug loading capacity [165], and longer release time [64]. For crystallizable polymers like polyesters, nonlinear polyester with same molar mass has higher accumulative drug release compared to linear one because of lower crystallinity [166]. Bioactive compounds can be effectively introduced into the polymer matrix via chemical bonding

to form drug-polymer conjugates, including poly(ionic liquid)s with pharmaceutical counterions, or by physical interactions in the self-assemblies. Although graft copolymers are able to carry similar amounts of ionically attached drug as their linear analogs, they are still advantageous systems for delivery due to smaller sizes of nanoparticles.

Cyclic polymers are a class of polymers without chain end and possess small hydrodynamic volume and radius of gyration. Compared to linear triblock copolymer with equivalent composition, cyclic polymer presents similar self-assembly behavior, such as similar hydrodynamic radius and CMC but smaller aggregation number. However, compared with linear diblock copolymer, cyclic polymer has smaller size and aggregation number and higher CMC. It can be explained by the structure of amphiphilic copolymer. In fact, both the cyclic and linear triblock copolymers have two block connections in the core-solvent interface, which is entropically disfavored. As a result, these two copolymers have a higher CMC than linear diblock copolymers. Furthermore, the larger size of linear diblock copolymer micelles may be assigned to the relatively better stretching and packing ability [158]. It has also been reported that cyclic polymers exhibit better thermal stability of micelles than equivalent linear triblock copolymers [167, 168].

1.4.2 Stimuli-responsiveness

Spurred by recent progress in materials chemistry and drug delivery, stimuli-responsive devices that deliver a drug in spatial-, temporal- and dosage-controlled fashions have been made possible [169]. Stimuli-responsive micelles are obtained from polymers with special chemical structure that responds to various intrinsic stimuli, such as low pH, redox potential, elevated temperature due to inflammation and the presence of various over-expressed enzymes, or extrinsic stimuli such as temperature, light (UV, visible, and infra-red), magnetic field and ultrasound that induce controlled drug release, as shown in Fig 1.20. The stimuli-triggered response in the polymers may result in disintegration, destabilization, isomerization, polymerization or aggregation of micelles, thus releasing drugs [170].

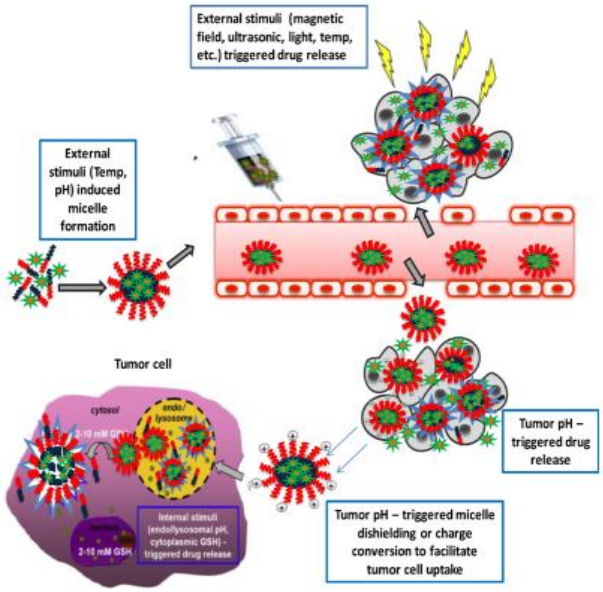

Fig. 1. 20 Stimuli-responsive polymeric micelles as emerging controlled drug release systems. (i) application of an external stimulus such as pH and temperature to facilitate formation of micelles; (ii) application of an external stimulus such as light, magnetic field, ultrasonic, and temperature to trigger drug release; (iii) acidic tumor pH (6.5–7.2) is used to trigger drug release and/or reverse shielding of micelles at tumor site thus enhancing tumor cell uptake of encapsulated drugs; and (iv) intracellular surroundings such as low pH in endo/lysosomal compartments and high redox potential in cytoplasm are employed to enhance intracellular drug release inside tumor cells [170]

1.4.2.1 Thermo-responsive

Thermo-responsive polymers are the most widely investigated stimuli-responsive drug delivery systems. Ideally, thermo-sensitive systems should retain their loaded drugs at body temperature (~37 ℃), and rapidly release them in locally heated tumor site (~40-42 ℃). Thermo-responsive polymers exhibit a LCST or an upper critical solution temperature (UCST) in water. The LCST is the critical temperature below which the polymer is soluble, and above which the polymer becomes insoluble. And the UCST is the opposite. In practice, the LCST (or UCST) is determined from transmittance changes of a polymer solution as a function of temperature, as shown in

Fig. 1.21 [171].

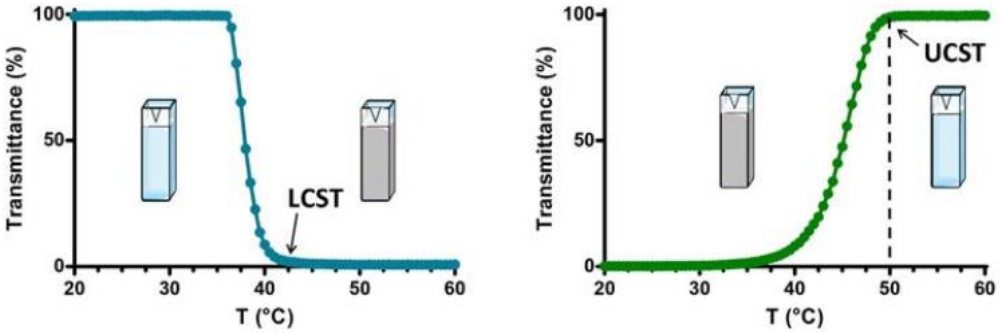

Fig. 1. 21 Model transmittance curves as a function of temperature for LCST (left) and UCST (right) polymers. When transmittance is at 100%, the sample is completely transparent and there are no apparent particles in solution. When transmittance is close to 0%, the sample appears turbid due to the presence of particles [171]

Typical thermo-responsive polymers with a LCST are obtained from N-isopropylacrylamide (NIPAM) [172], N,N-diethylacrylamide (DEAM) [173], methylvinylether (MVE) [174], and N-vinylcaprolactam (NVCL) as monomers [175]. And thermo-responsive polymers with a UCST are based on a combination of acrylamide (AAm) and acrylic acid (AAc) [176]. Some amphiphilic polymers such as Poloxamers [177], also exhibit thermo-responsive behavior.

Polysaccharides such as agarose, carrageenan, and gellan gum naturally possess thermo-responsive characteristics. Water-insoluble cellulose can be made thermo-responsive through chemical modification. In fact, partial or complete derivatisation of the hydroxyl groups of cellulose yields a number of water-soluble and thermo-responsive derivatives. For many biological and biomedical applications, polysaccharides that exhibit an LCST are particularly useful as they afford a free-flowing solution at ambient temperature and transition to a gel when exposed to physiological conditions [178]. This could, for instance, allow the solution to be easily injected into the body with minimal invasion to the patient. Such systems have been

shown to be effective for sustained drug delivery applications, and are also appropriate for cell encapsulation as the cells are not exposed to temperature extremes that might cause cell death [179, 180].

1.4.2.2 pH-responsive

pH-responsive nano-carriers have been largely studied in cancer therapy due to pH changes in the tumor microenvironment. As shown in Fig 1.22, pH in the bloodstream is around 7.4 and decreases to 6.4–6.8 in the tumor regions. In the intracellular environment, pH is 6.5 in the early endosomal compartment, and below pH 5 in the late lysosomal compartment [181]. Nano-carriers respond to pH by changing surface charge, swelling, or disintegration [182]. pH-responsive drug delivery systems can be constructed by three methods: using polymers with ionizable groups, using acid-labile linkages, or using crosslinkers which can either combine charge shifting polymers with non-cleavable linkages to create swellable micelles or acid-labile linkages which lead to pH-responsive disassembly. A schematic diagram of the three methods is shown in Fig. 1.23.

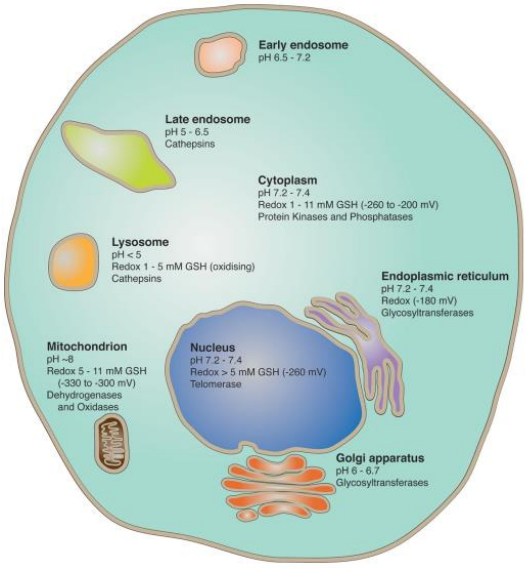

Fig. 1. 22 Schematic representation of diverse cellular microenvironments in terms of pH values, redox potential, and abundance of enzymes [181]

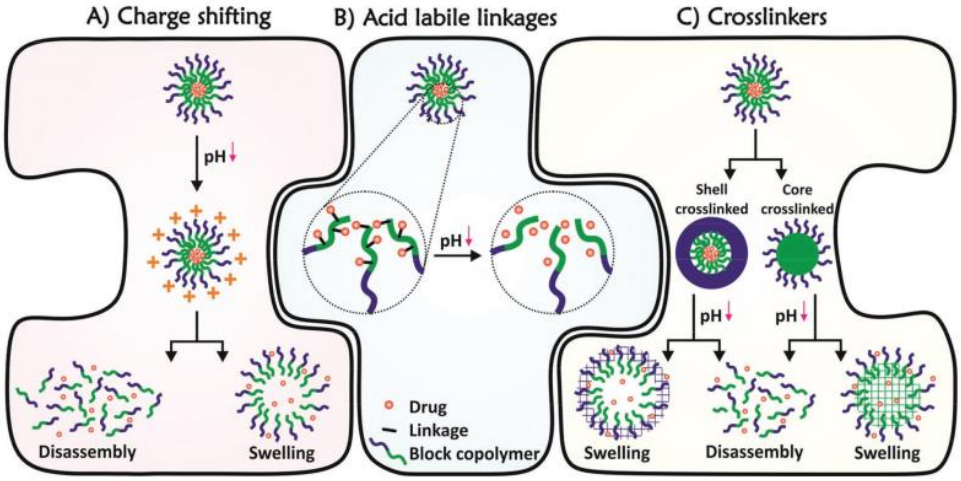

Fig. 1. 23 Strategies to construct pH-responsive nano-carriers, A) use of charge shifting polymers, B) acid labile linkages, and C) crosslinkers that can either combine charge shifting polymers with non-cleavable linkages to create swellable particles or acid labile linkages which lead to pH-responsive disassembly [182]

Charge shifting polymers are based on the reversible protonation and deprotonation of ionizable groups [183]. Generally, ionizable polymers include polybases which are protons acceptor at low pH and polyacids which are protons donor at high pH. In other words, anionic polymers which are negatively charged and hydrophilic at high pH will become hydrophobic with decrease of pH. And the opposite trend is observed for cationic polymers [184]. Polybases contain typical function groups including amines, pyridines, morpholines, piperazines, whereas polyacids contain typical function groups including carboxylic acids, sulfonic acids, phosphoric acids, boronic acids, *etc*. [184, 185]. Among them, polymers containing amino groups are commonly used to synthesize polymers such as poly(2-(diisopropylamine)ethyl methacrylate) (PDPAEMA) [186, 187], poly(4-vinyl pyridine) (P4VP) [188], polyhistidine [189, 190], and poly(β-amino ester) [191]. Natural polymers such as hyaluronic acid [192], chitosan [193], carboxymethyl cellulose [194] and alginate [195] have also been investigated for pH-responsive drug delivery. Polymers with acid-labile or base-labile linkages responding to pH by different mechanisms are summarized in

Table 1.4.

Table 1. 4 Summary of the cleavage of acid-labile or base-labile linkages [184]

Type of Linkages	Structure	Product after Acid Cleavage
Hydrozone	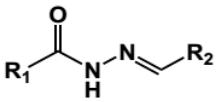	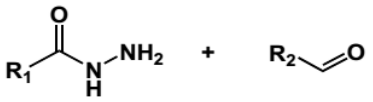
Acetal	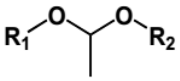	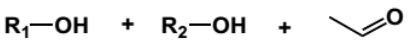
Ketal	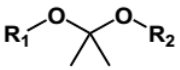	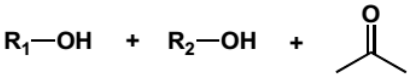
Boronate ester	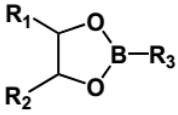	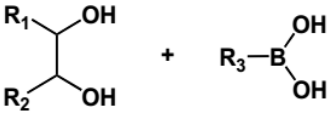

1.4.2.3 Redox-responsive

Redox-responsive systems were proposed due to the different levels of thiol-reduced (GSH) in tumor cell and normal cell: the intracellular concentration of GSH is approximately 2-10 mM, and the extracellular concentration is around 2-20 mM, as shown in Fig.1.22 [196]. Tumor cell has more GSH due to irregular oxidation metabolism. The reducing environment of tumor cells is controlled by two reduction agents GSH and NADPH, both having reduction and oxidation states. In a reducing environment, GSH plays a decisive role in microenvironment regulation on account of its higher concentration compared to that of NADPH [197, 198]. At molecular levels, GSH controls the cellular reducing environment mainly through the formation and cleavage of disulfide bonds and the reaction with excess reactive oxygen species (ROS) [181, 197, 199]. The main chemical structures of redox-responsive polymers are disulfide bonds and diselenide bonds, which can be found in the backbone or side chain, or act as the linkers, as summarized in Fig 1.24. Disulfide bond can be broken by reducing glutathione into two sulfhydryl groups, which leads to degradation of delivery system and release of drugs [200, 201]. Diselenide bond has similar properties but is more sensitive as compared to disulfide bond [202, 203] .

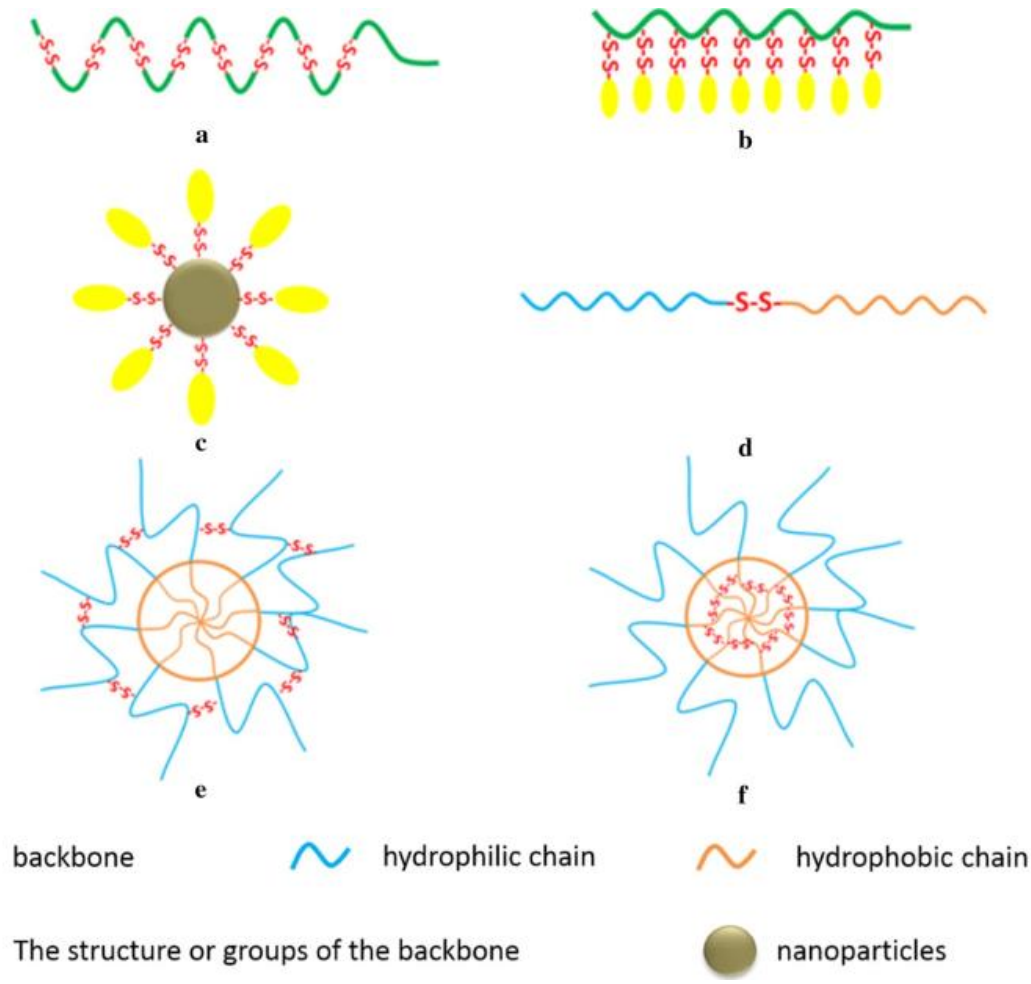

Fig. 1. 24 Schematic presentation of disulfide bonds in redox responsive delivery systems. a) Disulfide bonds present in the backbone; b) Disulfide bonds present in side chains; c) Disulfide bonds attached to the surface of nanoparticles; d) Disulfide bonds linking two moieties; e) Shell crosslinked micelles; f) Core crosslinked micelles [197]

1.4.3 Characterization of micelles

Micelles are generally characterized by the measurements of critical micelle concentration (CMC), size, zeta potential and morphology. The CMC is the lowest concentration at which amphiphilic polymers can aggregate into micelles. It can be determined from different parameters using different techniques, including interfacial tension, conductivity, osmotic pressure, intensity of light scattering [204], elution time from gel permeation chromatography [205], fluorescence spectra of pyrene [206] and

DOSY-NMR [207]. The CMC depends on the chemical structure of polymer, the hydrophilic/hydrophobic ratio and also the molar mass. Normally, higher hydrophobicity leads to lower CMC value. In addition, temperature also has influence on the CMC of thermo-sensitive polymers [208].

The hydrodynamic radius (R_h) of micelles is usually determined by dynamic light scattering (DLS) with resolution limit of 2 nm. DLS measures intensity fluctuations of the scattered laser light with time. The intensity fluctuations are induced by the Brownian motion of particles in solution. The velocity of Brownian motion is related to the particle size. Therefore the particle size can be calculated from the measured intensity fluctuations, using the Stokes-Einstein equation [209].

Static light scattering (SLS) is a technique that measures the intensity of the scattered light to obtain the average molar mass M_w and the aggregation number (N_{agg}) which is the number of polymer chains to compose a micelle. N_{agg} can be obtained from the ratio of the micelles' M_w to that of the polymer. Measurement of the scattering intensity at different angles allows to calculate the root mean square radius, also called the radius of gyration (R_g). By measuring the scattering intensity at various concentrations, the second virial coefficient A_2 can be calculated.

Small-angle X-ray (SAXS) and neutron scattering (SANS), jointly referred to as small-angle scattering (SAS), are conceptually very simple. In fact, the basic principles are similar to those of light scattering. Both techniques provide information at the nanoscale (resolution limit of both: 0.5 nm) and have been largely utilized to investigate blank or drug loaded micelles. SAXS makes it possible to reconstruct the structure of drug carriers in a natural aqueous environment. The dimension, shape and electron density maps can be obtained. SAXS investigations can also help to localize the active guest molecules in the self-assembled nanostructures and therefore study the effect of drug loading on the inner morphology. In addition, SAXS can provide information about the structural arrangement of the loaded drugs, which is strictly related to the pharmacological activity.

Electron microscopy (EM), especially transmission electron microscopy (TEM,

resolution limit: 0.1–0.5 nm) and scanning electron microscopy (SEM, resolution limit: 2–30 nm) are the most frequently used analytical techniques to determine the size as well as the morphology of micelles. TEM image is based on the interaction between electrons and samples. Areas with high electron density in the sample (strong interaction) are black, whereas areas with low electron density (low interaction) are white. For SEM, image is based on the energy of secondary electrons which interact and excite sample atoms [210]. Staining is often used to improve the contrast. Both TEM and SEM operate under vacuum, but soft material may suffer deformation under these conditions. Therefore, cryo-TEM and cryo-SEM are also used to observe frozen samples at -180 ℃.

Atomic force microscopy (AFM, resolution limit: 1 nm) is another technique for size and morphology measurements. AFM uses a sharp tip with radius of curvature on the cantilever to scan the surface of samples. When the tip interacts with the sample, the cantilever deflects according to Hooke's law. This kind of deflection can be measured by a change of the laser reflection on the cantilever, which is subsequently transformed to morphology information. Thus, the resolution of AFM is dependent on the sensitivity of the cantilever tip [209, 211].

Zeta potential is defined as the average electrostatic potential in the interfacial double layer at the hydrodynamic slipping plane. It is an important parameter determining the stability, biodistribution and cell uptake of micelles. A large positive or negative zeta potential indicates good physical stability of nano-suspensions due to electrostatic repulsion. It is generally admitted that zeta potential values below −30 mV or above +30 mV provide sufficient repulsive force to ensure physical colloidal stability. On the other hand, a small zeta potential value between −30 and +30 mV can result in particle aggregation and flocculation due to van der Waals attractive forces, thus leading to physical instability. Zeta potential is obtained from the electrophoretic mobility which is determined by dynamic light scattering based on electrophoretic light scattering [212].

1.4.4 Drug encapsulation methods

The drug encapsulation ability is a key parameter of micelles which are used as nanocarrier of hydrophobic drugs. The encapsulation ability can be expressed by drug loading efficiency which is defined as the ratio of the amount of drug actually encapsulated in micelles to the amount of initially added drug. Another parameter commonly used is drug loading content which is the ratio of encapsulated drug to the total amount of micelles. There are many factors affecting drug loading ability, such as the compatibility between drug and core material [213, 214], block length and crystallinity of the core polymer [215], the concentrations of both the polymer and the drug [215], as well as the preparation method of micelles [216]. Drug-core compatibility indicates the miscibility of drug and core polymer, which is the key factor affecting the drug loading content. The miscibility can be quantified by the Flory-Huggins interaction parameter. Generally, core materials with low Flory-Huggins parameter show high drug loading contents [213, 214].Normally, longer core-forming block length leads to higher drug loading content because it enlarges the core volume [215]. Nevertheless, it has been reported that for crystalline polymers, high crystallinity obstructs the encapsulation of drugs. As crystallization increases with increasing molar mass, the core-forming block length increase could lead to drug loading content decrease for crystalline polymers [217],[215].

Polymer concentration and drug concentration also have influence on drug loading content. According to Monte Carlo simulations, increasing polymer concentration results in increase of drug loading content up to a maximum value, and beyond, no further increase is expected [215, 218]. The location of drug incorporated in the micelles also affects the drug loading content. It is well admitted that drug is located in the core of micelles. However, it has been proposed that drugs may be incorporated either in the core, or shell or at the interface between core and shell [218, 219], as shown in Fig.1.25. This could account for the ‘burst release’ often observed in drug release. The type and concentration of organic solvents used for preparation of micelles also have influence on the drug loading efficiency [220].

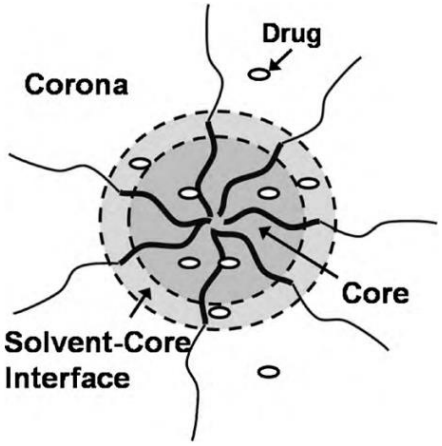

Fig. 1. 25 Illustration of the three regions for drug solubilization in a block copolymer micelle [220]

As mentioned above, micelle preparation method has influence on micelle size, size distribution and drug loading content. The selection of proper method mainly depends on the solubility of polymers. Direct dissolution is the simplest method that just involves addition of a water soluble polymer into an aqueous medium without using organic solvent. Hydrophobic drugs can be incorporated inside micelles with the assistance of ultrasonication and/or stirring [221]. This method also can be used to prepare micelles driven by electrostatic interactions, for instance, poly(2-isopropyl-2-oxazoline)-*b*-poly(L-lysine) [PiPrOxP(Lys)] and poly(2-isopropyl-2-oxazoline)-*b*-poly(aspartic acid) micelles [222], drug loaded carboxyl-containing polymers micelles [223, 224], or metal complexation [225, 226].

Fig. 1.26 illustrates three other methods commonly used for preparation of drug-loaded micelles from water insoluble polymers. In dialysis method, a water-miscible organic solvent is used to dissolve both polymer and drug. Afterwards, the organic solvent is slowly removed by dialysis. It has been reported that adding water to the organic solution before dialysis leads to narrower size distribution of micelles [227]. The organic solvents usually used include ethanol, acetone, DMF, THF, DMSO, and DMAc. The selection for solvent depends on the properties of polymers and drugs, and could have influence on the size of micelles [227]. Film casting method, also named as

film hydration, or membrane hydration method, consists of dissolving the polymer and drug in a volatile organic solvent, followed by removal of the solvent by evaporation to form a thin film. Subsequently, water is added under stirring or sonication to disintegrate the film. In this method, drug and the hydrophobic segment of copolymer are well mixed in the process of solution casting. Then during the hydration process, the hydrophobic block forms the core of micelles encapsulating the drug, while the hydrophilic block forms the shell [220, 228]. Solvent evaporation method first employs a water immiscible organic solvent to dissolve polymers and drugs. Then water is added under stirring to yield an oil-in-water emulsion. The organic solvent is subsequently removed by evaporation. During the evaporation process, the polarity environment gradually changes from organic to aqueous one. As the organic solvent is removed after adding water, and that the change from organic to aqueous environment is gradual; the drug can be encapsulated into the hydrophobic core of micelles rather than precipitate from the solution [220].

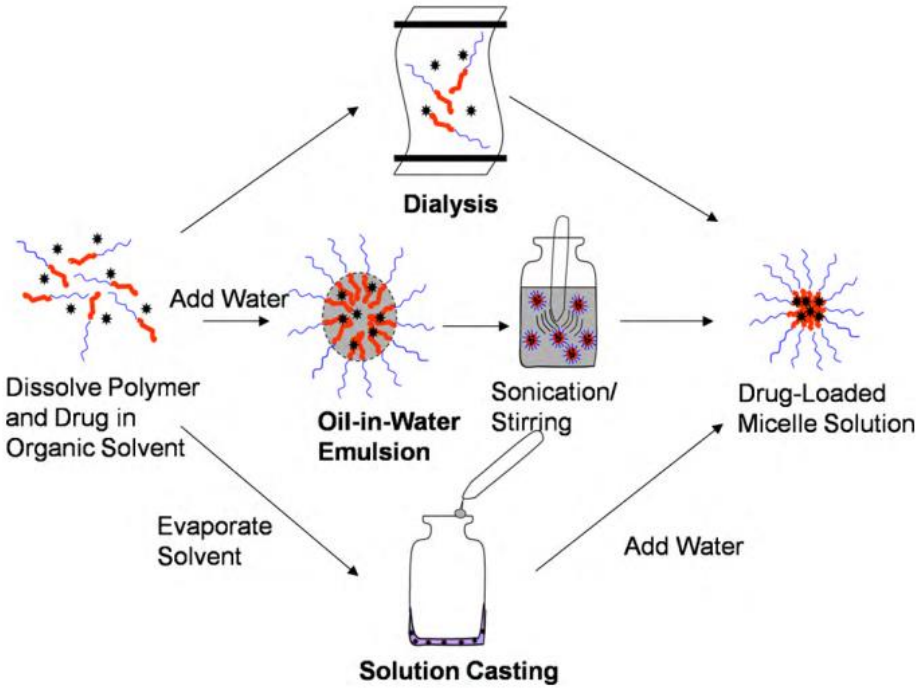

Fig. 1. 26 Illustration of drug loaded micelle preparation methods [220]

1.5 Hydrophobic anticancer drugs

Various hydrophobic anticancer drugs have been studied in controlled drug delivery, including paclitaxel (PTX), curcumine, 5-Fu, doxorubicin, *etc.*

PTX is a natural chemotherapy medication which can efficiently treat a variety of cancers including ovarian cancer, breast cancer, lung cancer, Kaposi's sarcoma, cervical cancer, and pancreatic cancer. The chemical structure of PTX is shown in Fig.1.27. The main mechanism of action of PTX is interference with the normal function of microtubules during cell division. It promotes the formation of microtubules but prevents the decomposition of microtubules to tubulin, which leads to the inability of cell division. PTX is one of the most efficient anti-cancer drugs. But its application is limited by its poor water solubility (0.3-1.0 μg/mL) and high efflux from cells [229]. In clinics, the currently used formulations of PTX are Taxol® and Abraxane®. Taxol® consists of a 50:50 mixture of Cremophor EL and dehydrated alcohol as co-solvent. Nevertheless, Cremophor EL has some toxic effects and also reduces penetration of PTX [230, 231]. Abraxane® is an injectable albumin-bound PTX nanoparticle formulation which was approved by FDA in 2005. But its neurotoxicity has been reported [232]. Therefore, novel nanocarriers improving the therapeutic effect and reducing the side effects of PTX have attracted considerable research interest, including drug-conjugation, nanoparticles, liposome and micelles [229].

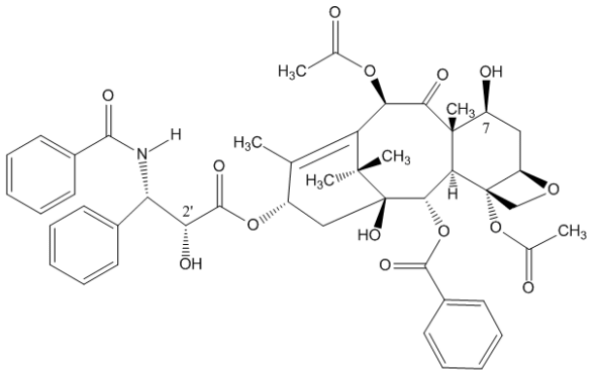

Fig. 1. 27 Chemical structure of paclitaxel (PTX) [229]

Curcumin is a natural phenolic anti-cancer drug which is mainly extracted from Curcuma longa Linn. The commercial product of curcumin is a mixture containing structurally related compounds curcumin, demethoxycurcumin and bisdemethoxycurcumin whose chemical structures are shown in Fig.1.28. Curcumin is used to prevent and treat a variety of cancers, such as gastrointestinal, melanoma, genitourinary, breast, lung, hematological, head and neck, neurological and sarcoma cancers [233]. In addition, curcumin is also an antioxidant, anti-inflammatory, anti-microbial, and anti-Alzheimer drug with high oral administration toleration (12 g/day). Curcumin has a pleiotropic anti-cancer mechanism which makes it more effective than single pathway anticancer chemotherapeutics. At the molecular level, curcumin increases the target locus of drug and regulates the signal transmission of tumor cells, and thereby inhibits the activity of certain enzymes and the expression of tumor-associated proteins and genes. At the cell level, curcumin can inhibit the proliferation, promote the apoptosis, reverse the multi-drug resistance of tumor cells. At the tissue level, curcumin inhibits the growth of vessels in tumor [234, 235]. Curcumin has a very low aqueous solubility (0.6 μg/ml) and is unstable in alkaline conditions. Thus, nanocarriers have been widely investigated to encapsulate curcumin so as to improve its solubility and therapeutic effect, including liposomes, conjugates, nanoparticles and micelles [235].

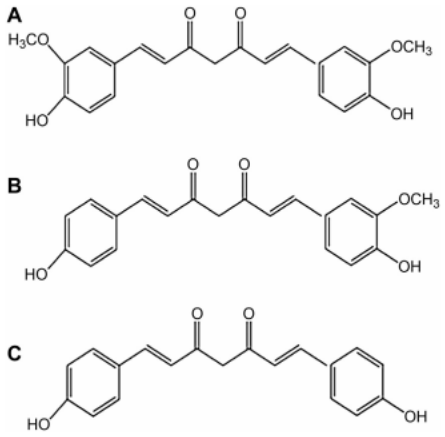

Fig. 1. 28 Chemical structures of curcumin (A), demethoxycurcumin (B) and bisdeme thoxycurcumin (C)

1.6 Summary and work plan

In recent decades, self-assembled polymeric micelles from amphiphilic copolymers have attracted much attention due to their potential advantages as nano drug delivery systems, such as improved drug solubility and bioavailability, prolonged blood circulation, passive targeting to tumor issue and reduced side effects. Polymers that are non-cytotoxic, biocompatible and biodegradable arouse interest since they can be metabolized in or excreted from human body without causing adverse reactions. Great efforts have been made to explore biobased polysaccharides and derivatives in drug delivery due to their non-toxicity, biocompatibility, and easy chemical modification. Hydrophilic cellulose derivatives have been widely explored through grafting with various monomers and polymers. However, few data are available on cellulose derivative based amphiphilic block copolymers as drug delivery systems.

HPMC as a hydrophilic cellulose derivative has been widely used in oral controlled drug delivery devices due to its good biocompatibility and thermo-responsive behavior. The reducing end (hemiacetal group) on the cellulose chain makes it possible to combine with other polymers containing amino groups. Thus, HPMC based amphiphilic block copolymers can be synthesized by reductive amination between the hemiacetal group on the HPMC and amino groups on hydrophobic polymers. Biocompatible and bioresorbable aliphatic polyesters such as PLA and PCL have been commonly used as the hydrophobic block which aggregates into the core of micelles to encapsulate hydrophobic drugs. In addition, PEO/PPO copolymers are the most broadly investigated block copolymers in drug delivery, and have been used in clinics. JEFFAMINE is a family of polyetheramines composed of PPO, PEO, or mixed PPO/PEO blocks with primary amino groups attached to the polyether chain ends. JEFFAMINE is not biodegradable, but it is biocompatible and can be eliminated by kidney filtration if its molar mass is below 15 KDa. Moreover, some of them are thermo-responsive.

This work aims to prepare HPMC based amphiphilic block copolymers by

reductive amination between HPMC and amino terminated hydrophobic polymers. Three kinds of amino terminated hydrophobic polymers were used, including PLA, PCL and JEFFAMINE. The latter was used as received as it contains amino endgroups, whereas amino terminated PLA and PCL were synthesized by ring-opening polymerization of lactide or ε-caprolactone using 3-(Boc-amino)-1-propanol as initiator, followed by removal of the Boc group by using trifluoroacetic acid. Another synthetic route previously used in our group was also applied for the sake of comparison. Thiol-terminated HPMC (HPMC-SH) was obtained by coupling the aldehyde endgroup of HPMC with the amine group of cysteamine, followed by reductive scission of the central disulfide bond. And allyl-terminated PLLA was prepared by ring-opening polymerization of L-lactide in the presence of allyl alcohol. Subsequently UV-initiated thiol-ene click reaction was performed to couple HPMC-SH with allyl-terminated PLLA to yield a HPMC-PLLA block copolymer. The various copolymers were characterized by NMR, DOSY NMR, FT-IR, GPC and DSC. The influence of copolymer composition, molar mass of HPMC and hydrophobic blocks, hydrophilic/hydrophobic ratio and topology on the thermo-responsive and self-assembly properties was determined by UV, NMR, fluorescence spectroscopy, DLS and TEM. Two hydrophobic anti-cancer drugs, PTX and curcumin were encapsulated in micelles to investigate the drug loading and release behaviors of copolymers. MTT assay was performed on blank copolymer micelles to assess their cytocompatibility on L929 cells, and SRB assay was performed on blank and drug loaded copolymer micelles to assess the cytotoxicity against SK-BR-3 cancer cells. The potential of HPMC based amphiphilic block copolymers as nano-carrier of anti-tumor drugs was evaluated.

References

[1] P. Dong, K.P. Rakesh, H.M. Manukumar, Y.H.E. Mohammed, C.S. Karthik, S. Sumathi, P. Mallu, H.L. Qin, Innovative nano-carriers in anticancer drug delivery-a

comprehensive review, Bioorg Chem 85 (2019) 325-336.

[2] L.L. Bu, J. Yan, Z. Wang, H. Ruan, Q. Chen, V. Gunadhi, R.B. Bell, Z. Gu, Advances in drug delivery for post-surgical cancer treatment, Biomaterials 219 (2019) 119182.

[3] A. Wicki, D. Witzigmann, V. Balasubramanian, J. Huwyler, Nanomedicine in cancer therapy: challenges, opportunities, and clinical applications, J Control Release 200 (2015) 138-57.

[4] M. Elsabahy, K.L. Wooley, Design of polymeric nanoparticles for biomedical delivery applications, Chem Soc Rev 41(7) (2012) 2545-61.

[5] I. Wijesekara, R. Pangestuti, S.-K. Kim, Biological activities and potential health benefits of sulfated polysaccharides derived from marine algae, Carbohydrate Polymers 84(1) (2011) 14-21.

[6] T.G. Barclay, C.M. Day, N. Petrovsky, S. Garg, Review of polysaccharide particle-based functional drug delivery, Carbohydrate Polymers 221 (2019) 94-112.

[7] D. Klemm, B. Heublein, H.P. Fink, A. Bohn, Cellulose: fascinating biopolymer and sustainable raw material, Angew Chem Int Ed Engl 44(22) (2005) 3358-93.

[8] D. Trache, M.H. Hussin, C.T. Hui Chuin, S. Sabar, M.R.N. Fazita, O.F.A. Taiwo, T.M. Hassan, M.K.M. Haafiz, Microcrystalline cellulose: Isolation, characterization and bio-composites application—A review, International Journal of Biological Macromolecules 93 (2016) 789-804.

[9] L. Negahdar, I. Delidovich, R. Palkovits, Aqueous-phase hydrolysis of cellulose and hemicelluloses over molecular acidic catalysts: Insights into the kinetics and reaction mechanism, Applied Catalysis B: Environmental 184 (2016) 285-298.

[10] S.J. Horn, G. Vaaje-Kolstad, B. Westereng, V.G. Eijsink, Novel enzymes for the degradation of cellulose, Biotechnol Biofuels 5(1) (2012) 45.

[11] E. Ostmark, D. Nystrom, E. Malmstrom, Unimolecular nanocontainers prepared by ROP and subsequent ATRP from hydroxypropylcellulose, Macromolecules 41(12) (2008) 4405-4415.

[12] M.-F. Hsieh, N. Van Cuong, C.-H. Chen, Y.T. Chen, J.-M. Yeh, Nano-Sized Micelles of Block Copolymers of Methoxy Poly(ethylene glycol)-Poly(ε-

caprolactone)- Graft-2-Hydroxyethyl Cellulose for Doxorubicin Delivery, Journal of Nanoscience and Nanotechnology 8(5) (2008) 2362-2368.

[13] J. Siepmann, N.A. Peppas, Modeling of drug release from delivery systems based on hydroxypropyl methylcellulose (HPMC), Advanced Drug Delivery Reviews 64 (2012) 163-174.

[14] S.M. Silva, F.V. Pinto, F.E. Antunes, M.G. Miguel, J.J. Sousa, A.A. Pais, Aggregation and gelation in hydroxypropylmethyl cellulose aqueous solutions, J Colloid Interface Sci 327(2) (2008) 333-40.

[15] C. Clasen, W.M. Kulicke, Determination of viscoelastic and rheo-optical material functions of water-soluble cellulose derivatives, Prog Polym Sci 26(9) (2001) 1839-1919.

[16] J. Siepmann, N.A. Peppas, Modeling of drug release from delivery systems based on hydroxypropyl methylcellulose (HPMC), Adv Drug Deliv Rev 48(2-3) (2001) 139-57.

[17] S. Kamel, N. Ali, K. Jahangir, S.M. Shah, A.A. El-Gendy, Pharmaceutical significance of cellulose: A review, Express Polymer Letters 2(11) (2008) 758-778.

[18] K. Gong, I.U. Rehman, J.A. Darr, Characterization and drug release investigation of amorphous drug-hydroxypropyl methylcellulose composites made via supercritical carbon dioxide assisted impregnation, J Pharm Biomed Anal 48(4) (2008) 1112-9.

[19] W. Cui, Y. Zhou, J. Chang, Electrospun nanofibrous materials for tissue engineering and drug delivery, Sci Technol Adv Mater 11(1) (2010) 014108.

[20] T.J. Sill, H.A. von Recum, Electrospinning: applications in drug delivery and tissue engineering, Biomaterials 29(13) (2008) 1989-2006.

[21] W. Zhu, J. Wang, S. Wang, Z. Gu, J.L. Aceña, K. Izawa, H. Liu, V.A. Soloshonok, Recent advances in the trifluoromethylation methodology and new CF3-containing drugs, Journal of Fluorine Chemistry 167 (2014) 37-54.

[22] A. Khalf, S.V. Madihally, Recent advances in multiaxial electrospinning for drug delivery, Eur J Pharm Biopharm 112 (2017) 1-17.

[23] S. Gim, Y. Zhu, P.H. Seeberger, M. Delbianco, Carbohydrate-based nanomaterials

for biomedical applications, Wiley Interdiscip Rev Nanomed Nanobiotechnol 11(5) (2019) e1558.

[24] M. Ikechukwu Ugwoke, G. Kaufmann, N. Verbeke, R. Kinget, Intranasal bioavailability of apomorphine from carboxymethylcellulose-based drug delivery systems, Int J Pharm 202(1-2) (2000) 125-31.

[25] M.H. Shakarami, T. Mohammadabadi, H. Motamedi, M. Sari, A. Teimouri Yansari, Isolation and identification of cellulolytic bacteria from gastrointestinal tract of Arabian horse and investigation of their effect on the nutritional value of wheat straw, J Appl Microbiol 127(2) (2019) 344-353.

[26] F. Laffleur, K. Netsomboon, A. Bernkop-Schnürch, D. Westmeier, R.H. Stauber, D. Docter, Comprehensive mucoadhesive study of anionic polymers and their derivate, European Polymer Journal 93 (2017) 314-322.

[27] K.K. Mali, S.C. Dhawale, R.J. Dias, V.S. Ghorpade, N.S. Dhane, Development of Vancomycin-Loaded Polysaccharide-Based Hydrogel Wound Dressings: In Vitro and In Vivo Evaluation, Asian J Pharm 12(2) (2018) 94-105.

[28] D.M. Varma, H.A. Lin, R.G. Long, G.T. Gold, A.C. Hecht, J.C. Iatridis, S.B. Nicoll, Thermoresponsive, redox-polymerized cellulosic hydrogels undergo in situ gelation and restore intervertebral disc biomechanics post discectomy, Eur Cell Mater 35 (2018) 300-317.

[29] C. Chen, H. Li, J. Pan, Z. Yan, Z. Yao, W. Fan, C. Guo, Biodegradable composite scaffolds of bioactive glass/chitosan/carboxymethyl cellulose for hemostatic and bone regeneration, Biotechnology Letters 37(2) (2015) 457-465.

[30] M. Swetha, K. Sahithi, A. Moorthi, N. Srinivasan, K. Ramasamy, N. Selvamurugan, Biocomposites containing natural polymers and hydroxyapatite for bone tissue engineering, Int J Biol Macromol 47(1) (2010) 1-4.

[31] D. Roy, M. Semsarilar, J.T. Guthrie, S. Perrier, Cellulose modification by polymer grafting: a review, Chem Soc Rev 38(7) (2009) 2046-64.

[32] L.I. Atanase, J. Desbrieres, G. Riess, Micellization of synthetic and polysaccharides-based graft copolymers in aqueous media, Prog Polym Sci 73 (2017)

32-60.

[33] H. Lönnberg, Q. Zhou, H. Brumer, T.T. Teeri, E. Malmström, A. Hult, Grafting of Cellulose Fibers with Poly(ε-caprolactone) and Poly(l-lactic acid) via Ring-Opening Polymerization, Biomacromolecules 7(7) (2006) 2178-2185.

[34] D.H. Solomon, Genesis of the CSIRO polymer group and the discovery and significance of nitroxide-mediated living radical polymerization, Journal of Polymer Science Part A: Polymer Chemistry 43(23) (2005) 5748-5764.

[35] F. Joubert, O.M. Musa, D.R. Hodgson, N.R. Cameron, The preparation of graft copolymers of cellulose and cellulose derivatives using ATRP under homogeneous reaction conditions, Chem Soc Rev 43(20) (2014) 7217-35.

[36] J. Glasing, P. Champagne, M.F. Cunningham, Graft modification of chitosan, cellulose and alginate using reversible deactivation radical polymerization (RDRP), Current Opinion in Green and Sustainable Chemistry 2 (2016) 15-21.

[37] C. Schatz, S. Lecommandoux, Polysaccharide-containing block copolymers: synthesis, properties and applications of an emerging family of glycoconjugates, Macromol Rapid Commun 31(19) (2010) 1664-84.

[38] A.B. Lowe, B.S. Sumerlin, C.L. McCormick, The direct polymerization of 2-methacryloxyethyl glucoside via aqueous reversible addition-fragmentation chain transfer (RAFT) polymerization, Polymer 44(22) (2003) 6761-6765.

[39] M. Bodnar, J.F. Hartmann, J. Borbely, Preparation and Characterization of Chitosan-Based Nanoparticles, Biomacromolecules 6(5) (2005) 2521-2527.

[40] J. Liu, H. Pu, S. Liu, J. Kan, C. Jin, Synthesis, characterization, bioactivity and potential application of phenolic acid grafted chitosan: A review, Carbohydr Polym 174 (2017) 999-1017.

[41] A.A. Elzatahry, M.S.M. Eldin, E.A. Soliman, E.A. Hassan, Evaluation of alginate-chitosan bioadhesive beads as a drug delivery system for the controlled release of theophylline, Journal of Applied Polymer Science 111(5) (2009) 2452-2459.

[42] C. Feng, J. Li, M. Kong, Y. Liu, X.J. Cheng, Y. Li, H.J. Park, X.G. Chen, Surface charge effect on mucoadhesion of chitosan based nanogels for local anti-colorectal

cancer drug delivery, Colloids and Surfaces B: Biointerfaces 128 (2015) 439-447.
[43] M.C.G. Pellá, M.K. Lima-Tenório, E.T. Tenório-Neto, M.R. Guilherme, E.C. Muniz, A.F. Rubira, Chitosan-based hydrogels: From preparation to biomedical applications, Carbohydrate Polymers 196 (2018) 233-245.
[44] Z. Liu, Y. Jiao, Y. Wang, C. Zhou, Z. Zhang, Polysaccharides-based nanoparticles as drug delivery systems, Adv Drug Deliv Rev 60(15) (2008) 1650-62.
[45] J. Wang, J.-S. Chen, J.-Y. Zong, D. Zhao, F. Li, R.-X. Zhuo, S.-X. Cheng, Calcium Carbonate/Carboxymethyl Chitosan Hybrid Microspheres and Nanospheres for Drug Delivery, The Journal of Physical Chemistry C 114(44) (2010) 18940-18945.
[46] T. Li, X.W. Shi, Y.M. Du, Y.F. Tang, Quaternized chitosan/alginate nanoparticles for protein delivery, J Biomed Mater Res A 83(2) (2007) 383-90.
[47] Y. Yuan, J. Tan, Y. Wang, C. Qian, M. Zhang, Chitosan nanoparticles as non-viral gene delivery vehicles based on atomic force microscopy study, Acta Biochim Biophys Sin (Shanghai) 41(6) (2009) 515-26.
[48] H.Q. Mao, K. Roy, V.L. Troung-Le, K.A. Janes, K.Y. Lin, Y. Wang, J.T. August, K.W. Leong, Chitosan-DNA nanoparticles as gene carriers: synthesis, characterization and transfection efficiency, Journal of Controlled Release 70(3) (2001) 399-421.
[49] H.T. Ta, C.R. Dass, D.E. Dunstan, Injectable chitosan hydrogels for localised cancer therapy, J Control Release 126(3) (2008) 205-16.
[50] N. Goodarzi, R. Varshochian, G. Kamalinia, F. Atyabi, R. Dinarvand, A review of polysaccharide cytotoxic drug conjugates for cancer therapy, Carbohydr Polym 92(2) (2013) 1280-93.
[51] E. Hachet, H. Van Den Berghe, E. Bayma, M.R. Block, R. Auzély-Velty, Design of Biomimetic Cell-Interactive Substrates Using Hyaluronic Acid Hydrogels with Tunable Mechanical Properties, Biomacromolecules 13(6) (2012) 1818-1827.
[52] G. Tiwari, R. Tiwari, A.K. Rai, Cyclodextrins in delivery systems: Applications, J Pharm Bioallied Sci 2(2) (2010) 72-79.
[53] V. Suvarna, P. Gujar, M. Murahari, Complexation of phytochemicals with cyclodextrin derivatives – An insight, Biomedicine & Pharmacotherapy 88 (2017)

1122-1144.

[54] J.R. Lakkakula, R.W. Maçedo Krause, A vision for cyclodextrin nanoparticles in drug delivery systems and pharmaceutical applications, Nanomedicine 9(6) (2014) 877-894.

[55] R.S. Thombre, P.P. Kanekar, CYCLODEXTRIN GLYCOSYL TRANSFERASE (CGTase): AN OVERVIEW OF THEIR PRODUCTION AND BIOTECHNOLOGICAL APPLICATIONS, Industrial Biotechnology: Sustainable Production and Bioresource Utilization (2017) 141-159.

[56] Y. Yi, G. Lin, S. Chen, J. Liu, H. Zhang, P. Mi, Polyester micelles for drug delivery and cancer theranostics: Current achievements, progresses and future perspectives, Mater Sci Eng C Mater Biol Appl 83 (2018) 218-232.

[57] M. Nofar, D. Sacligil, P.J. Carreau, M.R. Kamal, M.C. Heuzey, Poly (lactic acid) blends: Processing, properties and applications, Int J Biol Macromol 125 (2019) 307-360.

[58] J.C. Middleton, A.J. Tipton, Synthetic biodegradable polymers as orthopedic devices, Biomaterials 21(23) (2000) 2335-2346.

[59] B. Tyler, D. Gullotti, A. Mangraviti, T. Utsuki, H. Brem, Polylactic acid (PLA) controlled delivery carriers for biomedical applications, Adv Drug Deliv Rev 107 (2016) 163-175.

[60] Z. Li, P.L. Chee, C. Owh, R. Lakshminarayanan, X.J. Loh, Safe and efficient membrane permeabilizing polymers based on PLLA for antibacterial applications, RSC Advances 6(34) (2016) 28947-28955.

[61] Z. Li, D. Yuan, G. Jin, B.H. Tan, C. He, Facile Layer-by-Layer Self-Assembly toward Enantiomeric Poly(lactide) Stereocomplex Coated Magnetite Nanocarrier for Highly Tunable Drug Deliveries, ACS Applied Materials & Interfaces 8(3) (2016) 1842-1853.

[62] L. Yang, X. Wu, F. Liu, Y. Duan, S. Li, Novel biodegradable polylactide/poly(ethylene glycol) micelles prepared by direct dissolution method for controlled delivery of anticancer drugs, Pharm Res 26(10) (2009) 2332-42.

[63] H. Cho, J. Gao, G.S. Kwon, PEG-b-PLA micelles and PLGA-b-PEG-b-PLGA sol-gels for drug delivery, J Control Release 240 (2016) 191-201.

[64] P. Jie, S.S. Venkatraman, F. Min, B.Y. Freddy, G.L. Huat, Micelle-like nanoparticles of star-branched PEO-PLA copolymers as chemotherapeutic carrier, J Control Release 110(1) (2005) 20-33.

[65] D. Le Garrec, S. Gori, L. Luo, D. Lessard, D.C. Smith, M.A. Yessine, M. Ranger, J.C. Leroux, Poly(N-vinylpyrrolidone)-block-poly(D,L-lactide) as a new polymeric solubilizer for hydrophobic anticancer drugs: in vitro and in vivo evaluation, J Control Release 99(1) (2004) 83-101.

[66] A. Zajdel, A. Wilczok, K. Jelonek, M. Musial-Kulik, A. Forys, S. Li, J. Kasperczyk, Cytotoxic Effect of Paclitaxel and Lapatinib Co-Delivered in Polylactide-co-Poly(ethylene glycol) Micelles on HER-2-Negative Breast Cancer Cells, Pharmaceutics 11(4) (2019).

[67] W. Shen, J. Luan, L. Cao, J. Sun, L. Yu, J. Ding, Thermogelling Polymer–Platinum(IV) Conjugates for Long-Term Delivery of Cisplatin, Biomacromolecules 16(1) (2015) 105-115.

[68] M.A. Woodruff, D.W. Hutmacher, The return of a forgotten polymer—Polycaprolactone in the 21st century, Prog Polym Sci 35(10) (2010) 1217-1256.

[69] J. Fu, X. Yu, Y. Jin, 3D printing of vaginal rings with personalized shapes for controlled release of progesterone, Int J Pharm 539(1-2) (2018) 75-82.

[70] M. Bartnikowski, T.R. Dargaville, S. Ivanovski, D.W. Hutmacher, Degradation mechanisms of polycaprolactone in the context of chemistry, geometry and environment, Prog Polym Sci 96 (2019) 1-20.

[71] P.D. Darney, Hormonal implants: Contraception for a new century, American Journal of Obstetrics and Gynecology 170(5, Part 2) (1994) 1536-1543.

[72] P. Grossen, D. Witzigmann, S. Sieber, J. Huwyler, PEG-PCL-based nanomedicines: A biodegradable drug delivery system and its application, Journal of Controlled Release 260 (2017) 46-60.

[73] L.Y. Qiu, Y.H. Bae, Self-assembled polyethylenimine-graft-poly(epsilon-

caprolactone) micelles as potential dual carriers of genes and anticancer drugs, Biomaterials 28(28) (2007) 4132-42.

[74] F. Ahmed, D.E. Discher, Self-porating polymersomes of PEG-PLA and PEG-PCL: hydrolysis-triggered controlled release vesicles, J Control Release 96(1) (2004) 37-53.

[75] C. Gu, V. Le, M. Lang, J. Liu, Preparation of polysaccharide derivates chitosan-graft-poly(varepsilon-caprolactone) amphiphilic copolymer micelles for 5-fluorouracil drug delivery, Colloids Surf B Biointerfaces 116 (2014) 745-50.

[76] L. Youssouf, A. Bhaw-Luximon, N. Diotel, A. Catan, P. Giraud, F. Gimie, D. Koshel, S. Casale, S. Benard, V. Meneyrol, L. Lallemand, O. Meilhac, C. Lefebvre D'Hellencourt, D. Jhurry, J. Couprie, Enhanced effects of curcumin encapsulated in polycaprolactone-grafted oligocarrageenan nanomicelles, a novel nanoparticle drug delivery system, Carbohydr Polym 217 (2019) 35-45.

[77] X. Shuai, T. Merdan, A.K. Schaper, F. Xi, T. Kissel, Core-cross-linked polymeric micelles as paclitaxel carriers, Bioconjug Chem 15(3) (2004) 441-8.

[78] H. Ge, Y. Hu, X. Jiang, D. Cheng, Y. Yuan, H. Bi, C. Yang, Preparation, characterization, and drug release behaviors of drug nimodipine-loaded poly(ε-caprolactone)-poly(ethylene oxide)-poly(ε-caprolactone) amphiphilic triblock copolymer micelles, Journal of Pharmaceutical Sciences 91(6) (2002) 1463-1473.

[79] K. Duan, X. Zhang, X. Tang, J. Yu, S. Liu, D. Wang, Y. Li, J. Huang, Fabrication of cationic nanomicelle from chitosan-graft-polycaprolactone as the carrier of 7-ethyl-10-hydroxy-camptothecin, Colloids Surf B Biointerfaces 76(2) (2010) 475-82.

[80] C. Chen, G. Cai, H. Zhang, H. Jiang, L. Wang, Chitosan-poly(epsilon-caprolactone)-poly(ethylene glycol) graft copolymers: synthesis, self-assembly, and drug release behavior, J Biomed Mater Res A 96(1) (2011) 116-24.

[81] T.K. Dash, V.B. Konkimalla, Poly-small je, Ukrainian-caprolactone based formulations for drug delivery and tissue engineering: A review, J Control Release 158(1) (2012) 15-33.

[82] G. Xu, D.-y. Nie, W.-z. Wang, P.-h. Zhang, J. Shen, B.-t. Ang, G.-h. Liu, X.-g. Luo, N.-l. Chen, Z.-c. Xiao, Optic nerve regeneration in polyglycolic acid–chitosan conduits

coated with recombinant L1-Fc, NeuroReport 15(14) (2004) 2167-2172.

[83] H.J. Costa, R.F. Bento, R. Salomone, D. Azzi-Nogueira, D.B. Zanatta, M. Paulino Costa, C.F. da Silva, B.E. Strauss, L.A. Haddad, Mesenchymal bone marrow stem cells within polyglycolic acid tube observed in vivo after six weeks enhance facial nerve regeneration, Brain Res 1510 (2013) 10-21.

[84] Y. Tsuji, M. Fujishiro, S. Kodashima, S. Ono, K. Niimi, S. Mochizuki, I. Asada-Hirayama, R. Matsuda, C. Minatsuki, C. Nakayama, Y. Takahashi, Y. Sakaguchi, N. Yamamichi, K. Koike, Polyglycolic acid sheets and fibrin glue decrease the risk of bleeding after endoscopic submucosal dissection of gastric neoplasms (with video), Gastrointestinal Endoscopy 81(4) (2015) 906-912.

[85] N. Shinya, S. Oka, S. Miyabashira, H. Kaetsu, T. Uchida, M. Sueyoshi, K. Takase, M. Akuzawa, A. Miyamoto, T. Shigaki, Improvement of the Tissue-adhesive and Sealing Effect of Fibrin Sealant Using Polyglycolic Acid Felt, Journal of Investigative Surgery 22(5) (2009) 383-389.

[86] K. Jelonek, J. Kasperczyk, Polyesters and polyestercarbonates for controlled drug delivery, Polimery-W 58(9) (2013) 654-662.

[87] F. Sadat Tabatabaei Mirakabad, K. Nejati-Koshki, A. Akbarzadeh, M.R. Yamchi, M. Milani, N. Zarghami, V. Zeighamian, A. Rahimzadeh, S. Alimohammadi, Y. Hanifehpour, S.W. Joo, PLGA-based nanoparticles as cancer drug delivery systems, Asian Pac J Cancer Prev 15(2) (2014) 517-35.

[88] K. Zhang, X. Tang, J. Zhang, W. Lu, X. Lin, Y. Zhang, B. Tian, H. Yang, H. He, PEG-PLGA copolymers: their structure and structure-influenced drug delivery applications, J Control Release 183 (2014) 77-86.

[89] B.D. Ulery, L.S. Nair, C.T. Laurencin, Biomedical Applications of Biodegradable Polymers, J Polym Sci B Polym Phys 49(12) (2011) 832-864.

[90] T. Wu, Y. He, Z. Fan, J. Wei, S. Li, Investigations on the morphology and melt crystallization of poly(L-lactide)-poly(ethylene glycol) diblock copolymers, Polymer Engineering & Science 48(3) (2008) 425-433.

[91] S. Li, Hydrolytic degradation characteristics of aliphatic polyesters derived from

lactic and glycolic acids, Journal of Biomedical Materials Research 48(3) (1999) 342-353.

[92] A. Lavasanifar, J. Samuel, G.S. Kwon, Poly(ethylene oxide)-block-poly(L-amino acid) micelles for drug delivery, Adv Drug Deliv Rev 54(2) (2002) 169-90.

[93] T. Li, J. Lin, T. Chen, S. Zhang, Polymeric micelles formed by polypeptide graft copolymer and its mixtures with polypeptide block copolymer, Polymer 47(13) (2006) 4485-4489.

[94] D.A. Chiappetta, A. Sosnik, Poly(ethylene oxide)-poly(propylene oxide) block copolymer micelles as drug delivery agents: improved hydrosolubility, stability and bioavailability of drugs, Eur J Pharm Biopharm 66(3) (2007) 303-17.

[95] J. Michael Grindel, T. Jaworski, O. Piraner, R. Martin Emanuele, M. Balasubramanian, Distribution, Metabolism, and Excretion of a Novel Surface-Active Agent, Purified Poloxamer 188, in Rats, Dogs, and Humans, Journal of Pharmaceutical Sciences 91(9) (2002) 1936-1947.

[96] A.M. Bodratti, P. Alexandridis, Formulation of Poloxamers for Drug Delivery, J Funct Biomater 9(1) (2018).

[97] P. Linse, Micellization of poly(ethylene oxide)-poly(propylene oxide) block copolymers in aqueous solution, Macromolecules 26(17) (1993) 4437-4449.

[98] P. Alexandridis, T.A. Hatton, Poly(Ethylene Oxide)-Poly(Propylene Oxide)-Poly(Ethylene Oxide) Block-Copolymer Surfactants in Aqueous-Solutions and at Interfaces - Thermodynamics, Structure, Dynamics, and Modeling, Colloid Surface A 96(1-2) (1995) 1-46.

[99] D.S. Pellosi, A.L. Tessaro, F. Moret, E. Gaio, E. Reddi, W. Caetano, F. Quaglia, N. Hioka, Pluronic® mixed micelles as efficient nanocarriers for benzoporphyrin derivatives applied to photodynamic therapy in cancer cells, Journal of Photochemistry and Photobiology A: Chemistry 314 (2016) 143-154.

[100] D.S. Pellosi, I.R. Calori, L.B. de Paula, N. Hioka, F. Quaglia, A.C. Tedesco, Multifunctional theranostic Pluronic mixed micelles improve targeted photoactivity of Verteporfin in cancer cells, Materials Science and Engineering: C 71 (2017) 1-9.

[101] S.S. Kulthe, N.N. Inamdar, Y.M. Choudhari, S.M. Shirolikar, L.C. Borde, V.K. Mourya, Mixed micelle formation with hydrophobic and hydrophilic Pluronic block copolymers: implications for controlled and targeted drug delivery, Colloids Surf B Biointerfaces 88(2) (2011) 691-6.

[102] A.C.S. Akkari, J.Z.B. Papini, G.K. Garcia, M. Franco, L.P. Cavalcanti, A. Gasperini, M.I. Alkschbirs, F. Yokaichyia, E. de Paula, G.R. Tofoli, D.R. de Araujo, Poloxamer 407/188 binary thermosensitive hydrogels as delivery systems for infiltrative local anesthesia: Physico-chemical characterization and pharmacological evaluation, Mater Sci Eng C Mater Biol Appl 68 (2016) 299-307.

[103] M.A.F. Z, A. Vangala, M. Longman, K.A. Khaled, A.K. Hussein, O.H. El-Garhy, R.G. Alany, Poloxamer-based thermoresponsive ketorolac tromethamine in situ gel preparations: Design, characterisation, toxicity and transcorneal permeation studies, Eur J Pharm Biopharm 114 (2017) 119-134.

[104] R. Barse, C. Kokare, A. Tagalpallewar, Influence of hydroxypropylmethylcellulose and poloxamer composite on developed ophthalmic in situ gel: Ex vivo and in vivo characterization, Journal of Drug Delivery Science and Technology 33 (2016) 66-74.

[105] F. Nasir, Z. Iqbal, J.A. Khan, A. Khan, F. Khuda, L. Ahmad, A. Khan, A. Khan, A. Dayoo, Roohullah, Development and evaluation of diclofenac sodium thermorevesible subcutaneous drug delivery system, Int J Pharm 439(1-2) (2012) 120-6.

[106] M. Gao, H. Xu, C. Zhang, K. Liu, X. Bao, Q. Chu, Y. He, Y. Tian, Preparation and characterization of curcumin thermosensitive hydrogels for intratumoral injection treatment, Drug Development and Industrial Pharmacy 40(11) (2014) 1557-1564.

[107] Q. Jin, Y. Chen, Y. Wang, J. Ji, Zwitterionic drug nanocarriers: a biomimetic strategy for drug delivery, Colloids Surf B Biointerfaces 124 (2014) 80-6.

[108] J. Wu, W. Lin, Z. Wang, S. Chen, Y. Chang, Investigation of the Hydration of Nonfouling Material Poly(sulfobetaine methacrylate) by Low-Field Nuclear Magnetic Resonance, Langmuir 28(19) (2012) 7436-7441.

[109] Z. Cao, S. Jiang, Super-hydrophilic zwitterionic poly(carboxybetaine) and amphiphilic non-ionic poly(ethylene glycol) for stealth nanoparticles, Nano Today 7(5) (2012) 404-413.

[110] X. Liu, Q. Jin, Y. Ji, J. Ji, Minimizing nonspecific phagocytic uptake of biocompatible gold nanoparticles with mixed charged zwitterionic surface modification, J. Mater. Chem. 22(5) (2012) 1916-1927.

[111] H. Wei, S.-X. Cheng, X.-Z. Zhang, R.-X. Zhuo, Thermo-sensitive polymeric micelles based on poly(N-isopropylacrylamide) as drug carriers, Prog Polym Sci 34(9) (2009) 893-910.

[112] P. Li, Z. Zhang, Z. Su, G. Wei, Thermosensitive polymeric micelles based on the triblock copolymer poly(d,l-lactide)-b-poly(N-isopropyl acrylamide)-b-poly(d,l-lactide) for controllable drug delivery, Journal of Applied Polymer Science 134(37) (2017) 45304.

[113] Y. Hu, V. Darcos, S. Monge, S. Li, Synthesis and self-assembling of poly(N-isopropylacrylamide-block-poly(L-lactide)-block-poly(N-isopropylacrylamide) triblock copolymers prepared by combination of ring-opening polymerization and atom transfer radical polymerization, Journal of Polymer Science Part A: Polymer Chemistry 51(15) (2013) 3274-3283.

[114] K. Matyjaszewski, J. Xia, Atom Transfer Radical Polymerization, Chemical Reviews 101(9) (2001) 2921-2990.

[115] T.E. Patten, J. Xia, T. Abernathy, K. Matyjaszewski, Polymers with Very Low Polydispersities from Atom Transfer Radical Polymerization, Science 272(5263) (1996) 866.

[116] F. Su, X. Shen, Y. Hu, V. Darcos, S. Li, Biocompatibility of thermo-responsive PNIPAAm-PLLA-PNIPAAm triblock copolymer as potential drug carrier, Polymers for Advanced Technologies 26(12) (2015) 1567-1574.

[117] Y. Hu, V. Darcos, S. Monge, S. Li, Y. Zhou, F. Su, Thermo-responsive release of curcumin from micelles prepared by self-assembly of amphiphilic P(NIPAAm-co-DMAAm)-b-PLLA-b-P(NIPAAm-co-DMAAm) triblock copolymers, Int J Pharm

476(1-2) (2014) 31-40.

[118] Z. Tang, C. He, H. Tian, J. Ding, B.S. Hsiao, B. Chu, X. Chen, Polymeric nanostructured materials for biomedical applications, Prog Polym Sci 60 (2016) 86-128.

[119] I. Venditti, Morphologies and functionalities of polymeric nanocarriers as chemical tools for drug delivery: A review, Journal of King Saud University - Science 31(3) (2019) 398-411.

[120] A.M. Wagner, D.S. Spencer, N.A. Peppas, Advanced architectures in the design of responsive polymers for cancer nanomedicine, J Appl Polym Sci 135(24) (2018).

[121] S. Sadekar, H. Ghandehari, Transepithelial transport and toxicity of PAMAM dendrimers: implications for oral drug delivery, Adv Drug Deliv Rev 64(6) (2012) 571-88.

[122] U. Gupta, H.B. Agashe, A. Asthana, N.K. Jain, A review of in vitro-in vivo investigations on dendrimers: the novel nanoscopic drug carriers, Nanomedicine 2(2) (2006) 66-73.

[123] P. Kesharwani, K. Jain, N.K. Jain, Dendrimer as nanocarrier for drug delivery, Prog Polym Sci 39(2) (2014) 268-307.

[124] M. Najlah, A. D'Emanuele, Crossing cellular barriers using dendrimer nanotechnologies, Curr Opin Pharmacol 6(5) (2006) 522-7.

[125] M. Najlah, S. Freeman, D. Attwood, A. D'Emanuele, In vitro evaluation of dendrimer prodrugs for oral drug delivery, Int J Pharm 336(1) (2007) 183-90.

[126] H.L. Wong, X.Y. Wu, R. Bendayan, Nanotechnological advances for the delivery of CNS therapeutics, Adv Drug Deliv Rev 64(7) (2012) 686-700.

[127] A.R. Menjoge, R.M. Kannan, D.A. Tomalia, Dendrimer-based drug and imaging conjugates: design considerations for nanomedical applications, Drug Discov Today 15(5-6) (2010) 171-85.

[128] N. Malik, R. Wiwattanapatapee, R. Klopsch, K. Lorenz, H. Frey, J.W. Weener, E.W. Meijer, W. Paulus, R. Duncan, Dendrimers:: Relationship between structure and biocompatibility in vitro, and preliminary studies on the biodistribution of 125I-labelled polyamidoamine dendrimers in vivo, Journal of Controlled Release 65(1) (2000) 133-

148.

[129] J. Bugno, H.J. Hsu, S. Hong, Tweaking dendrimers and dendritic nanoparticles for controlled nano-bio interactions: potential nanocarriers for improved cancer targeting, J Drug Target 23(7-8) (2015) 642-50.

[130] D.A.T.J.B.C.U. Boas, Dendrimers, Dendrons, and Dendritic Polymers Discovery, Applications, and the Future, Cambridge University Press, Cambridge, UK, 2012.

[131] Y. Chang, N. Liu, L. Chen, X. Meng, Y. Liu, Y. Li, J. Wang, Synthesis and characterization of DOX-conjugated dendrimer-modified magnetic iron oxide conjugates for magnetic resonance imaging, targeting, and drug delivery, Journal of Materials Chemistry 22(19) (2012) 9594.

[132] K. Jain, P. Kesharwani, U. Gupta, N.K. Jain, Dendrimer toxicity: Let's meet the challenge, Int J Pharm 394(1-2) (2010) 122-142.

[133] A. Janaszewska, M. Ciolkowski, D. Wrobel, J.F. Petersen, M. Ficker, J.B. Christensen, M. Bryszewska, B. Klajnert, Modified PAMAM dendrimer with 4-carbomethoxypyrrolidone surface groups reveals negligible toxicity against three rodent cell-lines, Nanomedicine 9(4) (2013) 461-4.

[134] P. Kesharwani, S. Banerjee, U. Gupta, M.C.I. Mohd Amin, S. Padhye, F.H. Sarkar, A.K. Iyer, PAMAM dendrimers as promising nanocarriers for RNAi therapeutics, Materials Today 18(10) (2015) 565-572.

[135] A.-M. Caminade, S. Fruchon, C.-O. Turrin, M. Poupot, A. Ouali, A. Maraval, M. Garzoni, M. Maly, V. Furer, V. Kovalenko, J.-P. Majoral, G.M. Pavan, R. Poupot, The key role of the scaffold on the efficiency of dendrimer nanodrugs, Nature Communications 6(1) (2015).

[136] S.A.A. Rizvi, A.M. Saleh, Applications of nanoparticle systems in drug delivery technology, Saudi Pharm J 26(1) (2018) 64-70.

[137] M. Ferrari, Cancer nanotechnology: opportunities and challenges, Nature Reviews Cancer 5(3) (2005) 161-171.

[138] M. Mabrouk, R. Rajendran, I.E. Soliman, M.M. Ashour, H.H. Beherei, K.M. Tohamy, S. Thomas, N. Kalarikkal, G. Arthanareeswaran, D.B. Das, Nanoparticle- and

Nanoporous-Membrane-Mediated Delivery of Therapeutics, Pharmaceutics 11(6) (2019).

[139] I. Mohammad, Gold nanoparticle: An efficient carrier for MCP I of Carica papaya seeds extract as an innovative male contraceptive in albino rats, Journal of Drug Delivery Science and Technology 52 (2019) 942-956.

[140] F. Qi, J. Wu, H. Li, G. Ma, Recent research and development of PLGA/PLA microspheres/nanoparticles: A review in scientific and industrial aspects, Frontiers of Chemical Science and Engineering 13(1) (2019) 14-27.

[141] I. Neamtu, A.G. Rusu, A. Diaconu, L.E. Nita, A.P. Chiriac, Basic concepts and recent advances in nanogels as carriers for medical applications, Drug Deliv 24(1) (2017) 539-557.

[142] E. Akiyama, N. Morimoto, P. Kujawa, Y. Ozawa, F.M. Winnik, K. Akiyoshi, Self-Assembled Nanogels of Cholesteryl-Modified Polysaccharides: Effect of the Polysaccharide Structure on Their Association Characteristics in the Dilute and Semidilute Regimes, Biomacromolecules 8(8) (2007) 2366-2373.

[143] T.R. Hoare, D.S. Kohane, Hydrogels in drug delivery: Progress and challenges, Polymer 49(8) (2008) 1993-2007.

[144] R. Censi, T. Vermonden, H. Deschout, K. Braeckmans, P. di Martino, S.C. De Smedt, C.F. van Nostrum, W.E. Hennink, Photopolymerized Thermosensitive Poly(HPMAlactate)-PEG-Based Hydrogels: Effect of Network Design on Mechanical Properties, Degradation, and Release Behavior, Biomacromolecules 11(8) (2010) 2143-2151.

[145] J.K. Oh, R. Drumright, D.J. Siegwart, K. Matyjaszewski, The development of microgels/nanogels for drug delivery applications, Prog Polym Sci 33(4) (2008) 448-477.

[146] R.T. Chacko, J. Ventura, J. Zhuang, S. Thayumanavan, Polymer nanogels: a versatile nanoscopic drug delivery platform, Adv Drug Deliv Rev 64(9) (2012) 836-51.

[147] V. Carvalho, P. Castanheira, T.Q. Faria, C. Goncalves, P. Madureira, C. Faro, L. Domingues, R.M. Brito, M. Vilanova, M. Gama, Biological activity of heterologous

murine interleukin-10 and preliminary studies on the use of a dextrin nanogel as a delivery system, Int J Pharm 400(1-2) (2010) 234-42.

[148] G.H. Rossetti, E.D. Albizzati, O.M. Alfano, Decomposition of Formic Acid in a Water Solution Employing the Photo-Fenton Reaction, Industrial & Engineering Chemistry Research 41(6) (2002) 1436-1444.

[149] D. Xu, J. Hong, K. Sheng, L. Dong, S. Yao, Preparation of polyethyleneimine nanogels via photo-Fenton reaction, Radiation Physics and Chemistry 76(10) (2007) 1606-1611.

[150] D.E. Discher, A. Eisenberg, Polymer Vesicles, Science 297(5583) (2002) 967.

[151] J.L. Wang, M. Caceres, S.M. Li, A. Deratani, Synthesis and Self-Assembly of Amphiphilic Block Copolymers from Biobased Hydroxypropyl Methyl Cellulose and Poly(L-lactide), Macromol Chem Phys 218(10) (2017).

[152] A. Blanazs, S.P. Armes, A.J. Ryan, Self-Assembled Block Copolymer Aggregates: From Micelles to Vesicles and their Biological Applications, Macromol Rapid Commun 30(4-5) (2009) 267-77.

[153] <DAO_THI_PHUONG_TUYEN_2016.pdf>.

[154] C. Marianecci, S. Petralito, F. Rinaldi, P.N. Hanieh, M. Carafa, Some recent advances on liposomal and niosomal vesicular carriers, Journal of Drug Delivery Science and Technology 32 (2016) 256-269.

[155] U. Kauscher, M.N. Holme, M. Bjornmalm, M.M. Stevens, Physical stimuli-responsive vesicles in drug delivery: Beyond liposomes and polymersomes, Adv Drug Deliv Rev 138 (2019) 259-275.

[156] N. Nishiyama, K. Kataoka, Current state, achievements, and future prospects of polymeric micelles as nanocarriers for drug and gene delivery, Pharmacol Ther 112(3) (2006) 630-48.

[157] A.S. Deshmukh, P.N. Chauhan, M.N. Noolvi, K. Chaturvedi, K. Ganguly, S.S. Shukla, M.N. Nadagouda, T.M. Aminabhavi, Polymeric micelles: Basic research to clinical practice, Int J Pharm 532(1) (2017) 249-268.

[158] R.J. Williams, A.P. Dove, R.K. O'Reilly, Self-assembly of cyclic polymers,

Polymer Chemistry 6(16) (2015) 2998-3008.

[159] A.C. Wauters, I.A.B. Pijpers, A.F. Mason, D.S. Williams, J. Tel, L.K.E.A. Abdelmohsen, J.C.M. van Hest, Development of Morphologically Discrete PEG–PDLLA Nanotubes for Precision Nanomedicine, Biomacromolecules 20(1) (2019) 177-183.

[160] K. Jelonek, S. Li, X. Wu, J. Kasperczyk, A. Marcinkowski, Self-assembled filomicelles prepared from polylactide/poly(ethylene glycol) block copolymers for anticancer drug delivery, Int J Pharm 485(1-2) (2015) 357-64.

[161] S.M. Loverde, D.A. Pantano, D.A. Christian, A. Mahmud, M.L. Klein, D.E. Discher, Curvature, rigidity, and pattern formation in functional polymer micelles and vesicles – From dynamic visualization to molecular simulation, Current Opinion in Solid State and Materials Science 15(6) (2011) 277-284.

[162] F. Ahmed, R.I. Pakunlu, A. Brannan, F. Bates, T. Minko, D.E. Discher, Biodegradable polymersomes loaded with both paclitaxel and doxorubicin permeate and shrink tumors, inducing apoptosis in proportion to accumulated drug, J Control Release 116(2) (2006) 150-8.

[163] X. Shen, X. Liu, R. Li, P. Yun, C. Li, F. Su, S. Li, Biocompatibility of filomicelles prepared from poly(ethylene glycol)-polylactide diblock copolymers as potential drug carrier, Journal of Biomaterials Science, Polymer Edition 28(15) (2017) 1677-1694.

[164] K. Jelonek, S. Li, J. Kasperczyk, X. Wu, A. Orchel, Effect of polymer degradation on prolonged release of paclitaxel from filomicelles of polylactide/poly(ethylene glycol) block copolymers, Mater Sci Eng C Mater Biol Appl 75 (2017) 918-925.

[165] J.-Z. Du, L.-Y. Tang, W.-J. Song, Y. Shi, J. Wang, Evaluation of Polymeric Micelles from Brush Polymer with Poly(ε-caprolactone)-b-Poly(ethylene glycol) Side Chains as Drug Carrier, Biomacromolecules 10(8) (2009) 2169-2174.

[166] L.Y. Qiu, Y.H. Bae, Polymer architecture and drug delivery, Pharm Res 23(1) (2006) 1-30.

[167] T. Yamamoto, Synthesis of cyclic polymers and topology effects on their diffusion and thermal properties, Polymer Journal 45(7) (2012) 711-717.

[168] S. Honda, T. Yamamoto, Y. Tezuka, Topology-Directed Control on Thermal Stability: Micelles Formed from Linear and Cyclized Amphiphilic Block Copolymers, J Am Chem Soc 132(30) (2010) 10251-10253.

[169] S. Mura, J. Nicolas, P. Couvreur, Stimuli-responsive nanocarriers for drug delivery, Nat Mater 12(11) (2013) 991-1003.

[170] S. Biswas, P. Kumari, P.M. Lakhani, B. Ghosh, Recent advances in polymeric micelles for anti-cancer drug delivery, Eur J Pharm Sci 83 (2016) 184-202.

[171] A. Bordat, T. Boissenot, J. Nicolas, N. Tsapis, Thermoresponsive polymer nanocarriers for biomedical applications, Adv Drug Deliv Rev 138 (2019) 167-192.

[172] H.G. Schild, Poly(N-isopropylacrylamide): experiment, theory and application, Prog Polym Sci 17(2) (1992) 163-249.

[173] I. Idziak, D. Avoce, D. Lessard, D. Gravel, X.X. Zhu, Thermosensitivity of Aqueous Solutions of Poly(N,N-diethylacrylamide), Macromolecules 32(4) (1999) 1260-1263.

[174] L.M. Mikheeva, N.V. Grinberg, A.Y. Mashkevich, V.Y. Grinberg, L.T.M. Thanh, E.E. Makhaeva, A.R. Khokhlov, Microcalorimetric Study of Thermal Cooperative Transitions in Poly(N-vinylcaprolactam) Hydrogels, Macromolecules 30(9) (1997) 2693-2699.

[175] K. Van Durme, S. Verbrugghe, F.E. Du Prez, B. Van Mele, Influence of Poly(ethylene oxide) Grafts on Kinetics of LCST Behavior in Aqueous Poly(N-vinylcaprolactam) Solutions and Networks Studied by Modulated Temperature DSC, Macromolecules 37(3) (2004) 1054-1061.

[176] T. Aoki, M. Kawashima, H. Katono, K. Sanui, N. Ogata, T. Okano, Y. Sakurai, Temperature-Responsive Interpenetrating Polymer Networks Constructed with Poly(acrylic acid) and Poly(N,N-dimethylacrylamide), Macromolecules 27(4) (1994) 947-952.

[177] O. Klep, Y. Bandera, S.H. Foulger, Temperature responsive nanoparticles: poloxamers as a modulator of Forster resonance energy transfer (FRET), Nanoscale 10(19) (2018) 9401-9409.

[178] Y.B. Schuetz, R. Gurny, O. Jordan, A novel thermoresponsive hydrogel based on chitosan, European Journal of Pharmaceutics and Biopharmaceutics 68(1) (2008) 19-25.

[179] W. Wei, J. Li, X. Qi, Y. Zhong, G. Zuo, X. Pan, T. Su, J. Zhang, W. Dong, Synthesis and characterization of a multi-sensitive polysaccharide hydrogel for drug delivery, Carbohydrate Polymers 177 (2017) 275-283.

[180] P.M. Niang, Z. Huang, V. Dulong, Z. Souguir, D. Le Cerf, L. Picton, Thermo-controlled rheology of electro-assembled polyanionic polysaccharide (alginate) and polycationic thermo-sensitive polymers, Carbohydr Polym 139 (2016) 67-74.

[181] G.K. Such, Y. Yan, A.P. Johnston, S.T. Gunawan, F. Caruso, Interfacing materials science and biology for drug carrier design, Adv Mater 27(14) (2015) 2278-97.

[182] N. Deirram, C. Zhang, S.S. Kermaniyan, A.P.R. Johnston, G.K. Such, pH-Responsive Polymer Nanoparticles for Drug Delivery, Macromol Rapid Commun 40(10) (2019).

[183] S. Bazban-Shotorbani, M.M. Hasani-Sadrabadi, A. Karkhaneh, V. Serpooshan, K.I. Jacob, A. Moshaverinia, M. Mahmoudi, Revisiting structure-property relationship of pH-responsive polymers for drug delivery applications, J Control Release 253 (2017) 46-63.

[184] H. Tang, W. Zhao, J. Yu, Y. Li, C. Zhao, Recent Development of pH-Responsive Polymers for Cancer Nanomedicine, Molecules 24(1) (2018).

[185] G. Kocak, C. Tuncer, V. Bütün, pH-Responsive polymers, Polymer Chemistry 8(1) (2017) 144-176.

[186] C.H. Lee, S.K. Kang, J.A. Lim, H.S. Lim, J.H. Cho, Electrospun smart fabrics that display pH-responsive tunable wettability, Soft Matter 8(40) (2012) 10238.

[187] S.T. Gunawan, K. Liang, G.K. Such, A.P. Johnston, M.K. Leung, J. Cui, F. Caruso, Engineering enzyme-cleavable hybrid click capsules with a pH-sheddable coating for intracellular degradation, Small 10(20) (2014) 4080-6.

[188] W.Q. Zhang, L.Q. Shi, R.J. Ma, Y.L. An, Y.L. Xu, K. Wu, Micellization of thermo- and pH-responsive triblock copolymer of poly(ethylene glycol)-b-poly(4-

vinylpyridine)-b-poly(N-isopropylacrylamide), Macromolecules 38(21) (2005) 8850-8852.

[189] P. Bilalis, L.-A. Tziveleka, S. Varlas, H. Iatrou, pH-Sensitive nanogates based on poly(l-histidine) for controlled drug release from mesoporous silica nanoparticles, Polymer Chemistry 7(7) (2016) 1475-1485.

[190] H. Wu, L. Zhu, V.P. Torchilin, pH-sensitive poly(histidine)-PEG/DSPE-PEG co-polymer micelles for cytosolic drug delivery, Biomaterials 34(4) (2013) 1213-22.

[191] A.S. Wong, S.K. Mann, E. Czuba, A. Sahut, H. Liu, T.C. Suekama, T. Bickerton, A.P. Johnston, G.K. Such, Self-assembling dual component nanoparticles with endosomal escape capability, Soft Matter 11(15) (2015) 2993-3002.

[192] Y.-M. Lim, H.-J. Gwon, J.-S. Park, Y.-C. Nho, J.-W. Shim, I.K. Kwon, S.-E. Kim, S.-H. Baik, Synthesis and properties of hyaluronic acid containing copolymers crosslinked by γ-ray irradiation, Macromolecular Research 19(5) (2011) 436-441.

[193] A. Basu, K.R. Kunduru, E. Abtew, A.J. Domb, Polysaccharide-Based Conjugates for Biomedical Applications, Bioconjugate Chemistry 26(8) (2015) 1396-1412.

[194] A. Lohani, G. Singh, S.S. Bhattacharya, R. Rama Hegde, A. Verma, Tailored-interpenetrating polymer network beads of κ-carrageenan and sodium carboxymethyl cellulose for controlled drug delivery, Journal of Drug Delivery Science and Technology 31 (2016) 53-64.

[195] R. Guo, L. Zhang, Z. Jiang, Y. Cao, Y. Ding, X. Jiang, Synthesis of Alginic Acid−Poly[2-(diethylamino)ethyl methacrylate] Monodispersed Nanoparticles by a Polymer−Monomer Pair Reaction System, Biomacromolecules 8(3) (2007) 843-850.

[196] A. Raza, U. Hayat, T. Rasheed, M. Bilal, H.M.N. Iqbal, Redox-responsive nano-carriers as tumor-targeted drug delivery systems, Eur J Med Chem 157 (2018) 705-715.

[197] X. Guo, Y. Cheng, X. Zhao, Y. Luo, J. Chen, W.E. Yuan, Advances in redox-responsive drug delivery systems of tumor microenvironment, J Nanobiotechnology 16(1) (2018) 74.

[198] G. Wu, Y.Z. Fang, S. Yang, J.R. Lupton, N.D. Turner, Glutathione metabolism and its implications for health, J Nutr 134(3) (2004) 489-92.

[199] M.A. Aon, S. Cortassa, B. O'Rourke, Redox-optimized ROS balance: a unifying hypothesis, Biochim Biophys Acta 1797(6-7) (2010) 865-77.

[200] C. Gong, M. Shan, B. Li, G. Wu, A pH and redox dual stimuli-responsive poly(amino acid) derivative for controlled drug release, Colloids and Surfaces B: Biointerfaces 146 (2016) 396-405.

[201] Y.W. Hu, N. Liu, B.L. Cheng, Y.N. Tan, L.J. Wen, H. Yuan, F.Q. Hu, Sequential delivery of therapeutic agents using a rationally designed disulfide-linked glycolipid-like nanocarrier, Oncotarget 7(50) (2016) 83258-83269.

[202] S. Zhai, X. Hu, Y. Hu, B. Wu, D. Xing, Visible light-induced crosslinking and physiological stabilization of diselenide-rich nanoparticles for redox-responsive drug release and combination chemotherapy, Biomaterials 121 (2017) 41-54.

[203] S. Ji, W. Cao, Y. Yu, H. Xu, Dynamic diselenide bonds: exchange reaction induced by visible light without catalysis, Angew Chem Int Ed Engl 53(26) (2014) 6781-5.

[204] I. Astafieva, X.F. Zhong, A. Eisenberg, Critical micellization phenomena in block polyelectrolyte solutions, Macromolecules 26(26) (1993) 7339-7352.

[205] M. Yokoyama, T. Sugiyama, T. Okano, Y. Sakurai, M. Naito, K. Kataoka, Analysis of Micelle Formation of an Adriamycin-Conjugated Poly(Ethylene Glycol)–Poly(Aspartic Acid) Block Copolymer by Gel Permeation Chromatography, Pharmaceutical Research 10(6) (1993) 895-899.

[206] G. Kwon, M. Naito, M. Yokoyama, T. Okano, Y. Sakurai, K. Kataoka, Micelles based on AB block copolymers of poly(ethylene oxide) and poly(.beta.-benzyl L-aspartate), Langmuir 9(4) (1993) 945-949.

[207] Y. Bakkour, V. Darcos, S. Li, J. Coudane, Diffusion ordered spectroscopy (DOSY) as a powerful tool for amphiphilic block copolymer characterization and for critical micelle concentration (CMC) determination, Polymer Chemistry 3(8) (2012) 2006.

[208] J.E. Chung, M. Yokoyama, M. Yamato, T. Aoyagi, Y. Sakurai, T. Okano, Thermo-responsive drug delivery from polymeric micelles constructed using block copolymers of poly(N-isopropylacrylamide) and poly(butylmethacrylate), Journal of Controlled

Release 62(1-2) (1999) 115-127.

[209] J. Habel, A. Ogbonna, N. Larsen, S. Cherré, S. Kynde, S.R. Midtgaard, K. Kinoshita, S. Krabbe, G.V. Jensen, J.S. Hansen, K. Almdal, C. Hélix-Nielsen, Selecting analytical tools for characterization of polymersomes in aqueous solution, RSC Advances 5(97) (2015) 79924-79946.

[210] V. Klang, C. Valenta, N.B. Matsko, Electron microscopy of pharmaceutical systems, Micron 44 (2013) 45-74.

[211] F.J. Giessibl, Advances in atomic force microscopy, Reviews of Modern Physics 75(3) (2003) 949-983.

[212] S. Honary, F. Zahir, Effect of Zeta Potential on the Properties of Nano-Drug Delivery Systems - A Review (Part 1), Tropical Journal of Pharmaceutical Research 12(2) (2013).

[213] F. Gadelle, W.J. Koros, R.S. Schechter, Solubilization of Aromatic Solutes in Block Copolymers, Macromolecules 28(14) (1995) 4883-4892.

[214] R. Nagarajan, M. Barry, E. Ruckenstein, Unusual selectivity in solubilization by block copolymer micelles, Langmuir 2(2) (1986) 210-215.

[215] L. Xing, W.L. Mattice, Strong Solubilization of Small Molecules by Triblock-Copolymer Micelles in Selective Solvents, Macromolecules 30(6) (1997) 1711-1717.

[216] H.M. Aliabadi, S. Elhasi, A. Mahmud, R. Gulamhusein, P. Mahdipoor, A. Lavasanifar, Encapsulation of hydrophobic drugs in polymeric micelles through co-solvent evaporation: the effect of solvent composition on micellar properties and drug loading, Int J Pharm 329(1-2) (2007) 158-65.

[217] H. Kang, J.D. Kim, S.H. Han, I.S. Chang, Self-aggregates of poly(2-hydroxyethyl aspartamide) copolymers loaded with methotrexate by physical and chemical entrapments, J Control Release 81(1-2) (2002) 135-44.

[218] J.H. Collett, E.A. Tobin, Relationships between poloxamer structure and the solubilization of some para-substituted acetanilides, Journal of Pharmacy and Pharmacology 31(1) (1979) 174-177.

[219] Y. Shen, Y. Zhan, J. Tang, P. Xu, P.A. Johnson, M. Radosz, E.A. Van Kirk, W.J.

Murdoch, Multifunctioning pH-responsive nanoparticles from hierarchical self-assembly of polymer brush for cancer drug delivery, AIChE Journal 54(11) (2008) 2979-2989.

[220] Z.L. Tyrrell, Y. Shen, M. Radosz, Fabrication of micellar nanoparticles for drug delivery through the self-assembly of block copolymers, Prog Polym Sci 35(9) (2010) 1128-1143.

[221] C. Gong, S. Shi, X. Wang, Y. Wang, S. Fu, P. Dong, L. Chen, X. Zhao, Y. Wei, Z. Qian, Novel Composite Drug Delivery System for Honokiol Delivery: Self-Assembled Poly(ethylene glycol)−Poly(ε-caprolactone)−Poly(ethylene glycol) Micelles in Thermosensitive Poly(ethylene glycol)−Poly(ε-caprolactone)−Poly(ethylene glycol) Hydrogel, The Journal of Physical Chemistry B 113(30) (2009) 10183-10188.

[222] J.S. Park, Y. Akiyama, Y. Yamasaki, K. Kataoka, Preparation and characterization of polyion complex micelles with a novel thermosensitive poly(2-isopropyl-2-oxazoline) shell via the complexation of oppositely charged block ionomers, Langmuir 23(1) (2007) 138-46.

[223] M. Li, W. Song, Z. Tang, S. Lv, L. Lin, H. Sun, Q. Li, Y. Yang, H. Hong, X. Chen, Nanoscaled Poly(l-glutamic acid)/Doxorubicin-Amphiphile Complex as pH-responsive Drug Delivery System for Effective Treatment of Nonsmall Cell Lung Cancer, ACS Applied Materials & Interfaces 5(5) (2013) 1781-1792.

[224] S. Lv, M. Li, Z. Tang, W. Song, H. Sun, H. Liu, X. Chen, Doxorubicin-loaded amphiphilic polypeptide-based nanoparticles as an efficient drug delivery system for cancer therapy, Acta Biomater 9(12) (2013) 9330-42.

[225] N. Nishiyama, S. Okazaki, H. Cabral, M. Miyamoto, Y. Kato, Y. Sugiyama, K. Nishio, Y. Matsumura, K. Kataoka, Novel cisplatin-incorporated polymeric micelles can eradicate solid tumors in mice, Cancer Res 63(24) (2003) 8977-8983.

[226] Y. Huang, Z. Tang, X. Zhang, H. Yu, H. Sun, X. Pang, X. Chen, pH-Triggered Charge-Reversal Polypeptide Nanoparticles for Cisplatin Delivery: Preparation and In Vitro Evaluation, Biomacromolecules 14(6) (2013) 2023-2032.

[227] P. Vangeyte, S. Gautier, R. Jérôme, About the methods of preparation of

poly(ethylene oxide)-b-poly(ε-caprolactone) nanoparticles in water, Colloids and Surfaces A: Physicochemical and Engineering Aspects 242(1-3) (2004) 203-211.

[228] K. Letchford, H. Burt, A review of the formation and classification of amphiphilic block copolymer nanoparticulate structures: micelles, nanospheres, nanocapsules and polymersomes, Eur J Pharm Biopharm 65(3) (2007) 259-69.

[229] Y. Liu, B. Zhang, B. Yan, Enabling anticancer therapeutics by nanoparticle carriers: the delivery of Paclitaxel, Int J Mol Sci 12(7) (2011) 4395-413.

[230] I. Knemeyer, M.G. Wientjes, J.L.S. Au, Cremophor reduces paclitaxel penetration into bladder wall during intravesical treatment, Cancer Chemotherapy and Pharmacology 44(3) (1999) 241-248.

[231] A.K. Singla, A. Garg, D. Aggarwal, Paclitaxel and its formulations, Int J Pharm 235(1) (2002) 179-192.

[232] V.A. de Weger, J.H. Beijnen, J.H.M. Schellens, Cellular and clinical pharmacology of the taxanes docetaxel and paclitaxel – a review, Anti-Cancer Drugs 25(5) (2014) 488-494.

[233] A. Duvoix, R. Blasius, S. Delhalle, M. Schnekenburger, F. Morceau, E. Henry, M. Dicato, M. Diederich, Chemopreventive and therapeutic effects of curcumin, Cancer Lett 223(2) (2005) 181-90.

[234] A.M. Kamat, G. Sethi, B.B. Aggarwal, Curcumin potentiates the apoptotic effects of chemotherapeutic agents and cytokines through down-regulation of nuclear factor-kappaB and nuclear factor-kappaB-regulated gene products in IFN-alpha-sensitive and IFN-alpha-resistant human bladder cancer cells, Mol Cancer Ther 6(3) (2007) 1022-30.

[235] O. Naksuriya, S. Okonogi, R.M. Schiffelers, W.E. Hennink, Curcumin nanoformulations: a review of pharmaceutical properties and preclinical studies and clinical data related to cancer treatment, Biomaterials 35(10) (2014) 3365-83.

Chapter 2 Synthesis and Self-Assembly of AB_2-type Amphiphilic Copolymers from Biobased Hydroxypropyl Methyl Cellulose and Poly(L-lactide)

Abstract: AB_2-type amphiphilic $(HPMC)_2$-PLA copolymers with various hydrophilic block lengths were synthesized using a three step procedure: ring-opening polymerization of L-lactide initiated by propynol, amination reduction of the aldehyde endgroup of HPMC, and thiol-click reaction. The resulted copolymers were characterized by NMR, DOSY-NMR, SEC and FT-IR. The cloud point (CP) was determined by UV–visible spectrometer. Data show that the HPMC block length has little effect on the Cp of the copolymers which is lower than that of HPMC. The self-assembly behavior of the copolymers was investigated from DLS, TEM, and critical micelle concentration (CMC) measurements. Spherical micelles are obtained by self-assembly of copolymers in aqueous solution. The micelle size and the CMC of copolymers increase with increasing HPMC block length. It is concluded that biobased and biodegradable $(HPMC)_2$-PLA copolymers could be promising as nano-carrier of hydrophobic drugs.

Keywords: Hydroxypropyl methyl cellulose; Poly(L-lactide); Topology; Self-assembly; Micelles

2.1. Introduction

Micelles based on amphiphilic block copolymers have been extensively investigated as drug carrier due to their favorable advantages in molecular design, long circulation, enhanced drug loading and therapeutic effect, and biocompatibility (Kataoka, Harada, & Nagasaki, 2001). Thus, biocompatible and bioresorbable aliphatic

polyesters such as polylactide (PLA), polyglycolide (PGA), poly(lactide-co-glycolide) (PLGA), and poly(ε-caprolactone) (PCL) have been commonly used as the hydrophobic block, whereas poly(ethylene glycol) (PEG), poly(N-vinyl-2-pyrrolidone) (PVP), poly(N-isopropylacrylamide) (PNIPAAm), poly(vinyl alcohol) (PVA), poly(amino acid), and more recently polysaccharides as the hydrophilic block to construct amphiphilic block copolymers (Elsabahy & Wooley, 2012; Guo, Wang, Shen, Shu, & Sun, 2013; Mi, Wang, Nishiyama, & Cabral, 2017; Yi et al., 2018). PLA, as an FDA-approved biobased polyester, is widely used in biomedical and pharmaceutical fields in the form of drug carrier, tissue engineering scaffolds, bone fracture internal fixation devices, orthopedic screws and plates, etc, due to its good degradability, processability, and mechanical strength (Lassalle & Ferreira, 2007; Rajendra P. Pawara & Abraham J. Dombb, 2014; Ramzi A. Abd Alsaheb, 2015; Rancan et al., 2009; Saini, Arora, & Kumar, 2016; Tsuji, 2005). Interestingly, PLA stereocomplex has been used to construct colloidal systems such as mixed micelles and hydrogels for pharmaceutical applications (L. Yang, Wu, Liu, Duan, & Li, 2009).

PEG is also an FDA-approved polymer widely used for biomedical and pharmaceutical applications. Nevertheless, PEG as a polyether is prone to peroxidation, which could adversely affect cells (Barz, Luxenhofer, Zentel, & Vicent, 2011; Ishida & Kiwada, 2008). Therefore, great effort has been made to search for hydrophilic alternatives of PEG. Polysaccharides have attracted increasing attention in recent years for uses as biomaterials to solve problems related to immunogenicity and toxicity associated with synthetic polymers because of their biodegradability, biocompatibility and bio-based nature (Aminabhavi, Nadagouda, Joshi, & More, 2014; Ganguly, Chaturvedi, More, Nadagouda, & Aminabhavi, 2014). Certain polysaccharides present inherent bioactivity that can help in mucoadhesion, thus improving drug targeting and diminishing inflammatory response. Recent years have witnessed a rapid growth on polysaccharide based micelles as drug delivery system (Aminabhavi et al., 2014; Rudzinski & Aminabhavi, 2010), such as pullulan (Jeong et al., 2006), cellulose (Guo, Wang, Shu, Shen, & Sun, 2012), dextran (Jeong et al., 2011; Sun et al., 2009), chitosan

(Huo et al., 2012), heparin (Tian et al., 2010), and hyaluronan (Y. L. Yang, Kataoka, & Winnik, 2005). Among them, cellulose is of great importance because of its outstanding properties, but its applications are restrained due to its poor solubility. Thus, soluble cellulose derivatives have been studied as a hydrophilic building block to prepare amphiphilic copolymers which can self-assemble in micelles, such as ethyl cellulose, hydroxyl propyl cellulose (Ostmark, Nystrom, & Malmstrom, 2008), hydroxyl propyl methyl cellulose (HPMC) (Ostmark et al., 2008), hydroxyl ethyl cellulose (Hsieh, Van Cuong, Chen, Chen, & Yeh, 2008) etc. Graft copolymerization of PLA onto cellulose and cellulose derivatives have been reported (Chen & Sun, 2000; Teramoto & Nishio, 2003; Yuan, Yuan, Zhang, & Xie, 2007). However, the grafting of PLA on the side chain hydroxyl group results in complex chain structure and the reaction is poorly controllable.

In our previous work (Wang, Caceres, Li, & Deratani, 2017), linear HPMC-*b*-PLA diblock copolymers with various HPMC block lengths were synthesized by combination of ring-opening polymerization, amination reduction and thiol-click reaction. The resulted amphiphilic copolymers are susceptible to self-assemble into spherical micelles with a diameter of 60-120 nm. It has been shown that the geometrical structure of copolymers affect the morphology, stability and size of micelles because the hydrophobic and hydrophilic segments lead to complex spatial arrangements during the micellization process (Cao et al., 2013; Li, Kesselman, Talmon, Hillmyer, & Lodge, 2004). In this work, amphiphilic AB_2-type PLA-$(HPMC)_2$ copolymers with various HPMC molar masses were synthesized and characterized. The self-assembly properties of the copolymers were investigated from the morphology, size and size distribution, cloud point (Cp) and critical micelle concentration (CMC) measurements.

2.2. Materials and Methods

2.2.1 Materials

L-lactide was purchased from Purac Biochem (Goerinchem, Netherlands) and purified by recrystallization from ethyl acetate. HPMC (K4M) was kindly provided by

Colorcon-Dow chemical (Bougival, *France*). Propynol, stannous octoate ($Sn(Oct)_2$), cysteamine, sodium cyanoborohydride ($NaBH_3CN$), 1,4-dithiothreito (DTT), 2,2-dimethoxy-2-phenylacetophenone (DMPA), diethyl ether and dimethyl sulfoxide were purchased from Sigma-Aldrich, and used as received. Toluene was purchased from Sigma-Aldrich, dried over by calcium chloride ($CaCl_2$) and distilled prior to use.

2.2.2 Synthesis of alkynyl terminated PLLA

Alkynyl terminated PLLA was synthesis by ring-open polymerization, of L-lactide using propynol as initiator and $Sn(Oct)_2$ as catalyst. Typically, L-lactide (7.2 g), propynol (0.112 g), and $Sn(Oct)_2$ (0.2 g) were introduced into a dried Schlenk tube, and 30 mL anhydrous toluene was added under stirring. The solution was degassed by performing five freeze–pump–thaw cycles. The reaction then proceeded 24 h at 80℃. Finally the product was obtained by precipitation in methanol, followed by vacuum drying.

2.2.3 Enzymatic degradation of HPMC and determination of substitution degree

HPMC was depolymerized to yield HPMC oligomers as reported in a previous work (Wang et al., 2017). Briefly, 1 g HPMC was added in 100 mL citrate phosphate buffer (pH = 5), and stirred overnight at 47 ℃ to ensure complete dissolution. Cellulase was added to the solution, and enzymatic depolymerization proceeded for various time periods. The reaction was stopped by heating the solution to 85 ℃, and the suspension was hot filtrated. The collected solution was purified by dialysis for 3 days using a membrane of MWCO=3500 g mol^{-1}, followed by freeze drying.

HPMC is a cellulose derivative whose hydroxyl groups are substituted by methyl and hydroxypropyl groups. The average number of substituents per repeat unit is characterized by the molar substitution or hydroxypropylaction (MS_{HP}) and the degree of substitution or methylation (DS_{Me}). The former can be higher than 3 and the latter varies between 0 and 3. HPMC with a DS_{Me} between 0.1 and 2.0 is water soluble as the substitution groups allow to decrease the intra- and inter-chain hydrogen bonding. In contrast, when the DS is above 2, HPMC becomes insoluble in water due to the presence of many hydrophobic methyl groups. (Claes, 2006). The ^1H NMR spectra of

acetylated HPMC oligomers were acquired in $CDCl_3$ at 50 ℃. The DS_{Me} and MS_{HP} values were then calculated according to the method reported by Fitzpatrik (Fitzpatrick et al., 2006).

2.2.4 Synthesis of thiol terminated HPMC

Thiol terminated HPMC was obtained by reductive amination connecting the aldehyde end group of HPMC molecules and the amine group of cysteamine in the presence of sodium cyanoborohydride. Briefly, HPMC with DS_{Me} of 1.43 and average molar mass of 7000 g mol^{-1} (1 g) and $NaBH_3CN$ (0.2 g) were solubilized in a mixture (3/1 v/v) of 50 mL dimethyl sulfoxide (DMSO) and 0.01 M NaCl at 60 ℃. Cysteamine (0.1 g) was added, and the solution was stirred at 60 ℃ for 6 days under reflux. The solution was then dialyzed against deionized water for 3 days (MWCO 3500 g mol^{-1}), followed by freeze drying. Afterwards, the product was dissolved in water, and stirred overnight in the presence of excess DTT under nitrogen atmosphere. Finally, the solution was dialyzed against deionized water and freeze dried. Ellman assay was performed to determine the content of thiol group using 5,5'-dithio-bis-(2-nitrobenzoic acid) (DTNB) as Ellman's reagent. DTNB is a versatile water soluble compound for quantitating free sulfhydryl groups as a measurable yellow-colored product is formed when DTNB reacts with sulfhydryl in solution.

2.2.5 Synthesis of $(HPMC)_2$-PLLA

Amphiphilic block copolymers were synthesized by thiol-yne click reaction connecting thiol terminated HPMC and alkynyl terminated PLLA. The reaction was initiated in a Dinics M3 UV chamber equipped with a PL-L 36 W/01/4P Hg Lamp. Typically, thiol terminated HPMC (1.0 g), alkynyl terminated PLLA (0.15 g), and DMPA (0.013 g) were dissolved in 10 mL DMSO. The solution was degassed for 30 min using purified argon, and then subjected to UV irradiation for 5 h. The crude product was collected by precipitation in acetonitrile, followed by centrifugation at 4500 rpm for 15 min. The above dissolution–precipitation cycle was repeated twice. Finally, $(HPMC)_2$-PLLA copolymers were obtained as a white solid after vacuum drying.

2.2.6 Characterization

^{1}H NMR spectra were recorded on Bruker spectrometer operating at 300 MHz (AMX300) using $CDCl_3$ and DMSO-d_6 as solvent. Diffusion ordered spectroscopy (DOSY) NMR was performed on Bruker Avance (AQS600) NMR spectrometer, operating at 600 MHz and equipped with a Bruker multinuclear z-gradient inverse probe head which is able to produce gradients in the z direction with the strength of 55 Gcm^{-1}. The DOSY spectra were acquired from Bruker topspin software (version 2.1) with the ledbpgp2s pulse program. The strength of the pulsed field gradients with respect to maximum 32 increments on a quadratic scale was logarithmically incremented from 2 to 95%. The diffusion sensitive period (Δ) of 200 ms and the gradient duration (δ) of 5 ms were optimized to allow the signals of interest to decrease by a factor of 10–20, in order to keep the relaxation contribution to the signal attenuation constant and ensure full signal attenuation for all samples. Data were processed using the MestRe Nova software.

Size exclusion chromatography (SEC), equipped with MALLS in combination with refractive index (RI) detection allows to determine the absolute molar mass of polymers. 5 mg of samples were added in the mobile phase (0.01 M NaCl containing 0.02% NaN_3), and stirred for 24 h at room temperature. The solution was filtered using 0.45 μm polytetrafluoroethylene (PTFE) filter (Millipore). The filtrate was injected through a 100 μL loop (Rheodyne injector 7725), and eluted on a TSK-GEL GMPWXL 7.8×300 mm column (TosoHaas Bioseparation Specialists, Stuttgart, Germany) at a flow rate of 0.5 mL min^{-1} (Waters pump 515). MALS detector (Dawn DSP, Wyatt Technology Co, Santa Barbara, CA, USA) and RI detector (Optilab Wyatt Technology Co) were used to online determine the absolute molar mass for each elution fraction of 0.01 mL, which enables to calculate the weight average molar mass (M_w) and the dispersity ($Đ=M_w/M_n$). The refractive index increment (dn/dc) for calculation was 0.137 mL g^{-1}. Data analysis was realized using Astra 4 (Wyatt Technology Co).

Fourier transform infrared (FT-IR) spectra were recorded on a Nicolet NEXUS spectrometer with a DTGS detector at 4 cm^{-1} resolution. 64 scans were taken per

sample in the frequency range from 400 to 4000 cm^{-1}. Sample pellets were prepared by mixing 2–2.5 mg of polymer with 200 mg of spectral grade potassium bromide, followed by compression using a press.

The cloud point (Cp) of the copolymers was estimated from transmittance changes of copolymer solutions in the temperature range from 30 to 90°C. The solution at 3.0 mg mL^{-1} was stirred for 24 h and kept at 5 ℃ overnight before analysis. Measurements were made at a wavelength of 600 nm with a Perkin Elmer Lambda 35 UV–visible spectrometer equipped with a Peltier temperature programmer PTP-1+1. The temperature ramp was 0.1 ℃ min^{-1}. Temp Lab software was used for data treatment.

Dynamic light scattering (DLS) was performed at 25 ℃ with 173 °scattering angle using Nano-ZS (Malvern Instrument) equipped with a He–Ne laser (λ =632.8 nm). The aqueous solutions of copolymers at 1.0 mg mL^{-1} were filtered through a 0.45 μm PTFE microfilter before measurements. The correlogram was analyzed via NNLS in order to extract the distribution of diffusion coefficient. The apparent equivalent hydrodynamic radius (R_H) was obtained using the cumulate method from the Stoke–Einstein equation.

The critical micelle concentration (CMC) of copolymers was determined using an autocorrelation function according to the methodology proposed by Muller et al (Muller et al., 2015). Aqueous solutions of copolymers were prepared in deionized water at concentrations ranging from 0.006 to 1.0 g L^{-1}, and were incubated overnight. The scattering intensity of the solutions was measured at 25 ℃ with a Malvern Instrument Nano-ZS. The scattering intensity depend on the 6th power of size and number of objects present in the solution was recorded. The CMC was taken as the intersection of regression lines from the plots of the scattering intensity against the polymer concentration.

Transmission electron microscopy (TEM) was performed on JEOL 1200 EXII instrument, operating at an acceleration voltage of 120 kV. 5 μL of micellar solution at 1.0 mg mL^{-1} were dropped onto a carbon coated copper grid, and air dried before measurements.

2.3. Results and Discussion

2.3.1 Synthesis of amphiphilic block copolymers

HPMC was depolymerized by using cellulase to yield oligomers with various molar masses. The weight average molar mass (M_w) of the resulted HPMC oligomers was 5000, 7000 and 10000 Daltons, respectively, as determined by SEC. The NMR spectra of acetylated HPMC were recorded in $CDCl_3$ (Fig. 2. 1). The DS_{Me} and MS_{HP} were calculated according to the method reported by Fitzpatrik (Table 2.1). The DS_{Me} varies from 1.17 to 1.43, indicating that HPMC samples are water soluble.

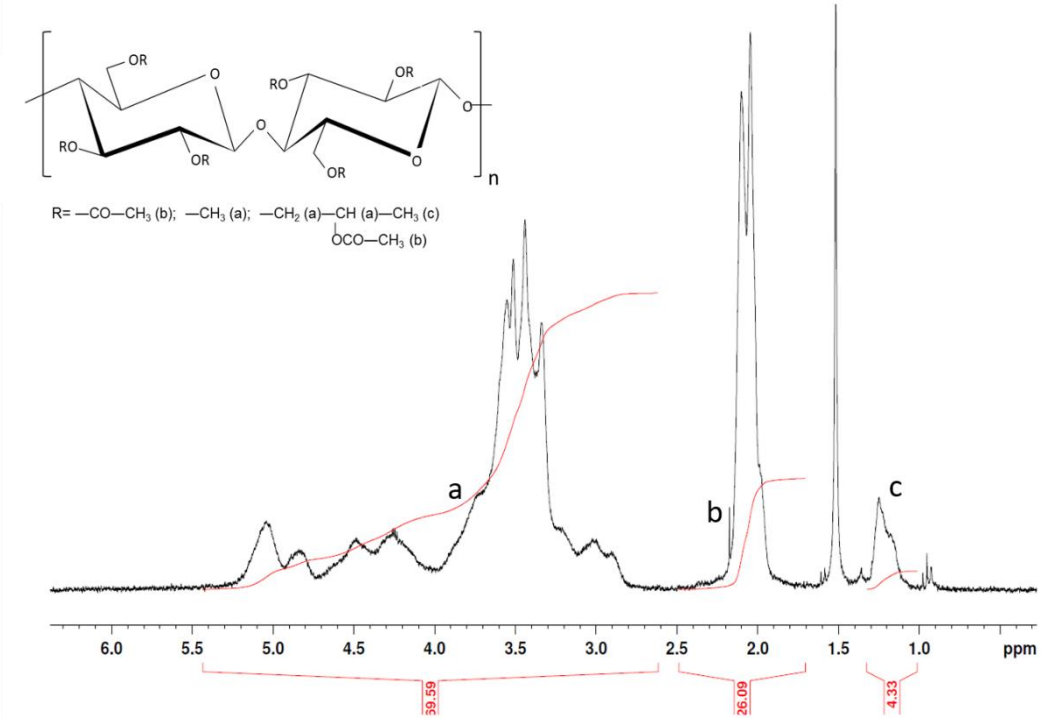

Fig. 2. 1 NMR spectrum in $CDCl_3$ of acetylated K4M. Signal (a) is assigned to protons on the glucose ring, the methyl substituents and the protonson isopropyl substituents, signal (b) to protons on the acetyl groups and signal (c) to methyl protons on isopropyl substituents.

The sum of the integrations (a) + (b) was normalized to 16 protons (7 coming from the glucose ring and 9 coming from the substituents).

$$x = \frac{16}{(a+b)}$$

The degree of methylation was calculated by:

$$DS_{Me} = \frac{(xa - xb - 7)}{3}$$

The hydroxypropyl substitution degree was obtained from:

$$MS_{HP} = \frac{xc}{3}$$

The degree of substitution is also expressed as weight percent, MeO % and HPO %.

Table 2. 1. Chemical composition of the starting HPMC and the oligomers

Samples	M_W(g/mol)	DS_{Me}	MS_{HP}	MeO%	HPO%
K4M	230000	1.30	0.24	20.8	9.3
HPMC10K	10000	1.17	0.28	18.7	10.8
HPMC7K	7000	1.43	0.26	22.5	9.9
HPMC5K	5000	-	-	-	-

The synthesis of $(HPMC)_2$- PLA copolymers was achieved in three steps (Scheme 2.1): a) synthesis of alkynyl terminated PLLA, b) thiolation of HPMC, and c) UV-initiated thiol-yne click reaction between thiolated HPMC and alkynyl terminated PLLA.

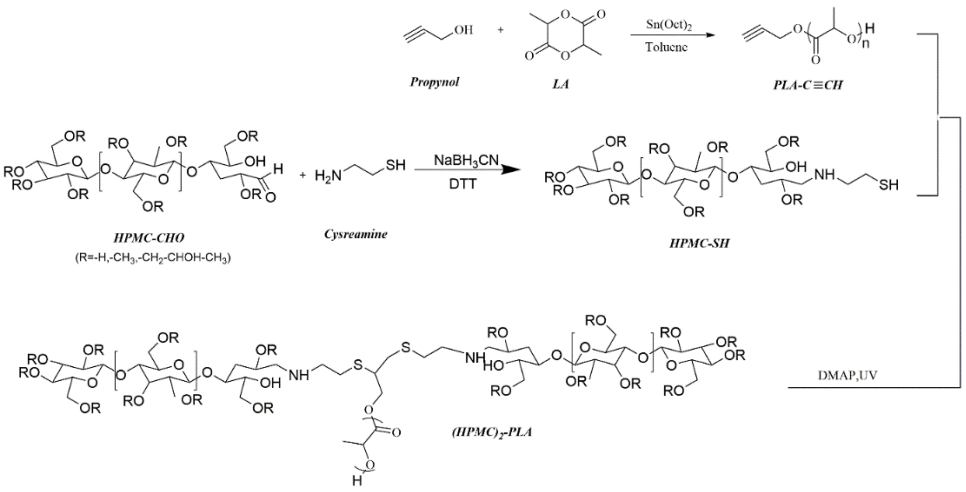

Scheme 2. 1. Synthesis route of $(HPMC)_2$-PLA block copolymers

Alkynyl terminated PLLA was synthesized by ring-opening polymerization of L-lactide using propynol as initiator with a monomer/initiator molar ratio of 25/1. Fig. 2.2 shows the 1H NMR spectrum of the resulting alkynyl terminated PLLA. The signals at 2.4 (a) and 4.75 (b) ppm are assigned to the alkynyl group and the methylene groups adjacent to the alkynyl group, respectively. The signals at 1.62 (d) and 5.25 (c) ppm are assigned to the methyl and methyne protons of PLA main chain, and the signals at 1.50 (f) and 4.42 (e) ppm to methyl and methyne protons of the hydroxyl terminal unit. The polymerization degree (DP) of PLA calculated from the integration ratio of signals c to e was 28, corresponding to a number average molar mass (Mn, NMR) of about 2000 g/mol.

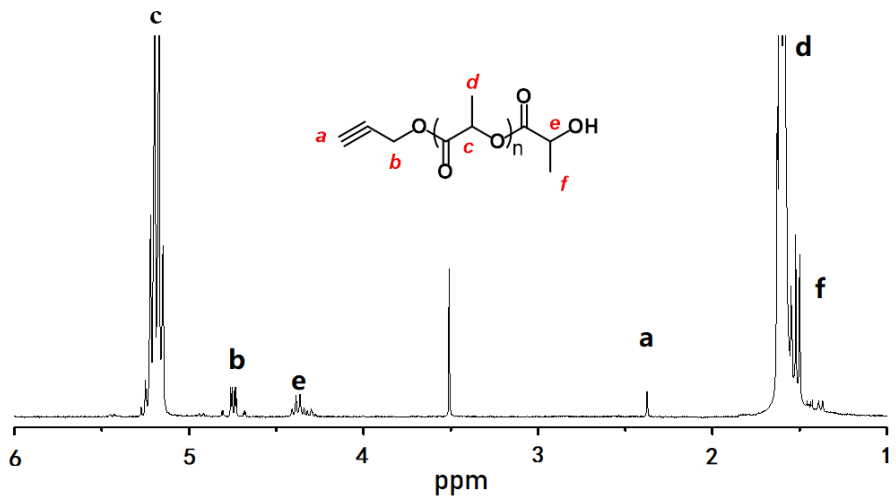

Fig. 2. 2 NMR spectrum of alkynyl–terminated PLA in $CDCl_3$

Thiol terminated HPMC was obtained by reductive amination of HPMC with cysteamine. The molecular chain of cellulose has a non reducing group at one end, and a hemiacetal group at the other end. The latter is a reducing group which can be easily converted to aldehyde group (Schatz & Lecommandoux, 2010). The amine functional group of cysteamine reacted with the unique aldehyde endgroup of HPMC through reductive amination to yield HPMC-S-S-HPMC together with small amounts of unreacted HPMC, HPMC-SH, and HPMC-S-S-$(CH_2)_6$-NH_2. HPMC-S-S-HPMC was then reduced using DTT to yield HPMC-SH (Wang et al., 2017). The final product was characterized by using Ellman assay and SEC measurement. Ellman's assay showed that the content of thiol terminated HPMC in the final product was 88%. SEC confirmed that the final product is predominantly composed of HPMC-SH because its M_w is almost the same as that of the initial HPMC. These findings showed that thiol terminated HPMC was successful synthesized.

Finally amphiphilic block copolymers were obtained by UV-initiated thiol-yne click reaction between thiol terminated HPMC and alkynyl terminated PLLA. Three copolymers, namely $(HPMC5K)_2$-PLA2K, $(HPMC7K)_2$-PLA2K and $(HPMC10K)_2$-PLA2K were synthesized using the same hydrophobic PLA block with M_n of 2000 g mol^{-1} and different hydrophilic HPMC-SH blocks with M_w of 5000, 7000, and 10000 g mol^{-1}, respectively. Fig. 3.2 shows the ^1H NMR spectra of $(HPMC7K)_2$-PLA2K copolymer in D_2O and DMSO-d_6. The spectrum in DMSO-d_6 shows the signal at 1.05 ppm (a) corresponding to the methyl protons in the hydroxypropyl group, and those in the range of 2.75–4.75 ppm (b) to the methyl protons adjacent to the oxygen moieties of the ether linkages, inner methylene and methine protons and HPMC backbone protons (Fig. 2.3A). The signals at 1.49 (d) and 5.24 ppm (c) belong to the methyl and methine protons of PLLA blocks. Moreover, the signal detected at 2.3 ppm is assigned to the methylene group of the connecting unit. These results confirm the successful synthesis of copolymers by thiol-yne click reaction.

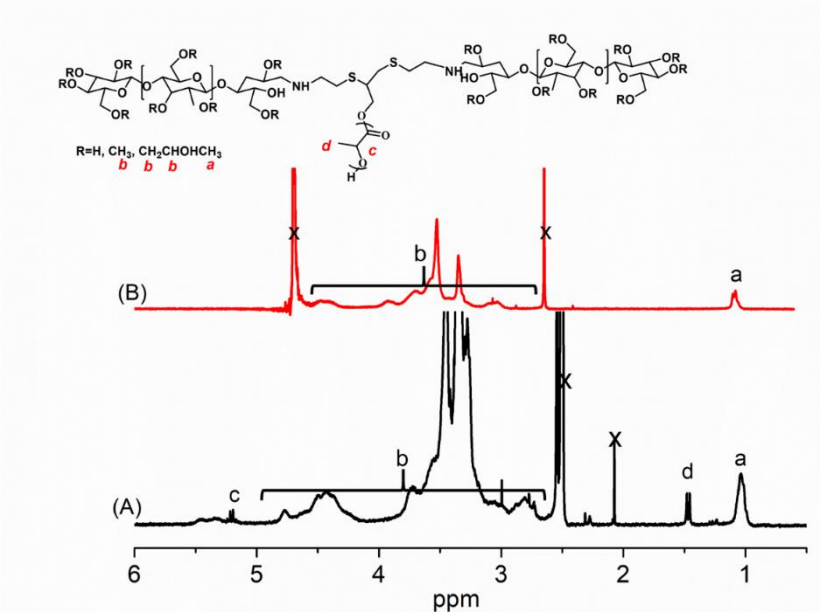

Fig. 2. 3 ^{1}H NMR spectra of $(HPMC)_2$-PLA in DMSO-d_6 (A) and in D_2O (B)

The structure of block copolymers was also confirmed by DOSY-NMR. DOSY is an excellent tool commonly used for the analysis of complex mixtures as it allows virtual separation of multicomponent systems. DOSY-NMR data are presented in a two-dimensional (2D) pattern: one dimension is related to the chemical shift information, and the other represents the diffusion coefficient which reflects the molecular effective sizes (Pages, Gilard, Martino, & Malet-Martino, 2017). As shown in Fig.2.4, the signals of both PLA and HPMC components present the same diffusion coefficient, which indicates that the two blocks are attached in one molecule. In other words, the copolymer was effectively synthesized.

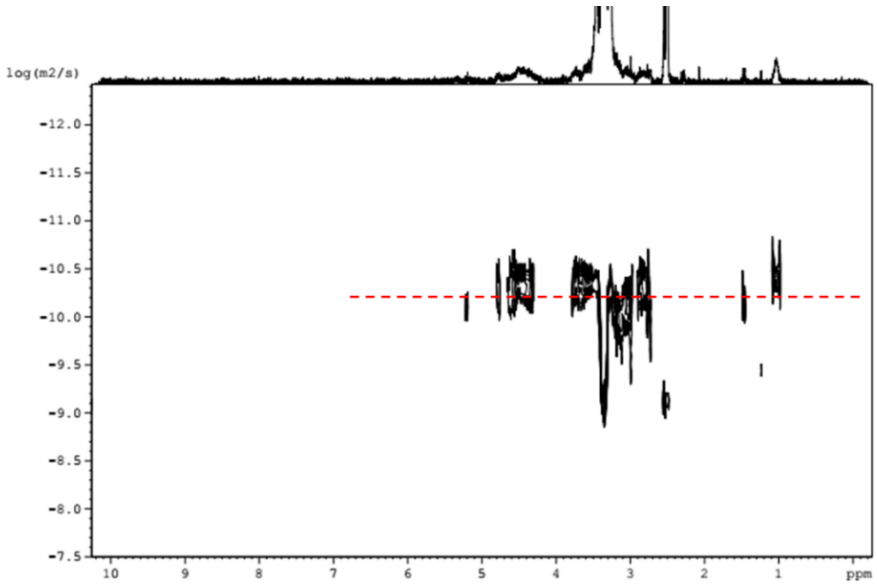

Fig. 2. 4 DOSY NMR spectrum of $(HPMC7K)_2$-PLA2K copolymer in DMSO-d_6 at 25 ℃

FT-IR is also used to examine the structure of copolymers. Fig. 2.5 presents the FT-IR spectra of alkynyl terminated PLLA, thiol terminated HPMC, and $(HPMC7K)_2$-PLA2K copolymer. Alkynyl terminated PLLA presents characteristic absorption bands at 1760, 2130 and 3300 cm^{-1} belonging to the carbonyl group, and alkynyl group, respectively. Thiol terminated HPMC presents an amide adsorption band at 1652 cm^{-1}, a strong C-O absorption band at 1047 cm^{-1}, and a broad O-H stretching vibration band at 3480 cm^{-1}. $(HPMC)_2$-PLA shows the characteristic bands from both components, in agreement with the successful coupling of PLLA and HPMC blocks.

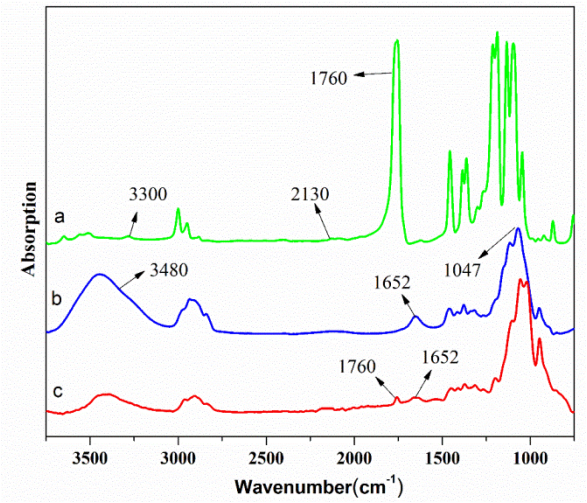

Fig. 2. 5 FT-IR spectra of (a) alkynyl terminated PLLA, (b) thiol terminated HPMC, and (c) $(HPMC7K)_2$-PLA2K copolymer

The molar mass of the copolymers was determined by SEC in conjunction with online light scattering and refractive index (RI) detectors, as shown in Fig. 2.6. RI detector is most commonly used as concentration detector whose response is proportional to the total solute concentration in the detector cell. Meanwhile, the response of multi-angle laser light scattering (MALLS) detector depends on the molar mass of a polymer in the detector cell (Kostanski, Keller, & Hamielec, 2004). Combination of the two curves allows to determine the weight average molar mass of copolymers.

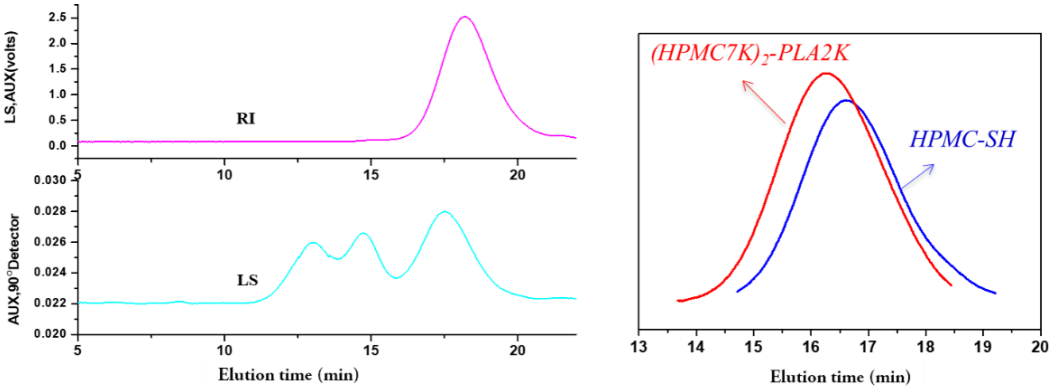

Fig. 2. 6 Refractive index and light scattering curves of $(HPMC7K)_2$-PLA2K (left), and SEC curves of HPMC-SH and $(HPMC7K)_2$-PLA2K in water

The M_w and dispersity data of the three copolymers are summarized in Table 2.2. The M_w ranges from 12000 for $(HPMC5K)_2$-PLA2K to 22 0000 g mol^{-1} for $(HPMC10K)_2$ -PLA2K. It is noted that the M_w of the copolymers well agrees with the sum of the molar masses of both components although the value of M_n is used for PLA. Meanwhile, the dispersity ($Đ=M_w/M_n$) ranges from 1.13 to 1.26, in agreement with narrow molar mass distribution of copolymers.

Table 2. 2 Characterization of $(HPMC)_2$-PLA copolymers

Sample	$M_{w, SEC}$ (g/mol)	Đ	Cp (℃)	CMC (mg/mL)	R_h (nm)	PDI
$(HPMC10K)_2$-PLA2K	22000	1.26	65.2	0.16	120	0.21
$(HPMC7K)_2$-PLA2K	16000	1.24	64.8	0.15	90	0.12
$(HPMC5K)_2$-PLA2K	12000	1.13	64.1	0.14	66	0.19

[a] Determined from SEC/MALS/RI measurement in water at 5.0 mg mL^{-1}

[b] Determined from turbidimetry measurement in water at 20.0 mg mL^{-1}

[c] Determined at 25 ℃ by dynamic light scattering

[d] Determined at 25 ℃ by dynamic light scattering at 1.0 mg mL^{-1}

2.3.2. Cloud point of $(HPMC)_2$-PLA copolymers

The cloud point (Cp), also named lower critical solution temperature (LCST), is considered as the solubility limit of amphiphiles due to phase-separation as the temperature increases. In fact, the hydrogen bonding between polymer chains and surrounding water molecules weakens when the temperature approaches the cloud point, leading to decrease of the polymer solubility and phase separation. Thus the polymer precipitates out of solution as a consequence of equal chemical potentials between the two phases: one is rich in polymer, and the other rich in solvent (Sardar, Kamil, Kabir

ud, & Sajid Ali, 2011).

Fig.2.7 shows the transmittance changes of $(HPMC7K)_2$-PLA2K solutions at 3.0 mg/mL, in comparison with HPMC7K homopolymer. The two solutions initially exhibit a transmittance close to 100%. With increasing temperature, the transmittance of HPMC7K remained almost unchanged till 90 ℃. This indicates that HPMC oligomers are not thermo-responsive in this temperature range, in contrast to high molar mass HPMC (Sardar et al., 2011). Interestingly, $(HPMC7K)_2$-PLA2K exhibits a decrease of light transmittance to nearly 20% from about 60 ℃ up to 90 ℃. The clouding at a given temperature results from the destruction of hydrogen bonding between water and HPMC molecules leading to phase separation (Khan, Anjum, Koya, Qadeer, & Kabir ud, 2014). The Cp value was determined by extrapolation of the linear region of 100% of transmittance and tangent line of the inflexion point. A Cp value of 64.8 ℃ is obtained for $(HPMC7K)_2$-PLA2K. Similarly, Cp values of 65.2 and 64.1 ℃ are obtained for $(HPMC10K)_2$-PLA2K and $(HPMC5K)_2$-PLA2K (Table 2.2). Therefore, the length of HPMC blocks has little effect on the Cp value of the copolymers. Similar results have been previously reported in literature for poly(lactide-*b*-*N*-isopropylacrylamide-*b*-lactide) (PLA-*b*-PNIPAAm- *b*-PLA) triblock copolymers (You, Hong, Wang, Lu, & Pan, 2004). In fact, a Cp value of about 31 ℃ was obtained for copolymers with PLA/PNIPAAm ratios of 1.0/1.9, 1.0/3.0 and 1.0/3.6.

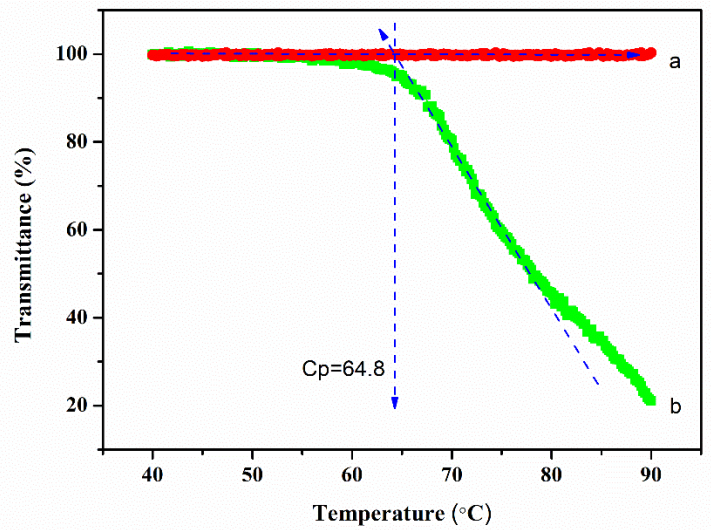

Fig. 2. 7 Transmittance changes of HPMC7K (a) and $(HPMC7K)_2$-PLA2K (b) solutions at 3.0 mg/mL as a function of temperature

In our previous work, the phase separation behavior of linear HPMC-*b*-PLA diblock copolymers with different HPMC block lengths (HPMC5K-PLA2K, HPMC8K-PLA2K, and HPMC10K-PLA2K) was investigated (Wang et al., 2017). All copolymers exhibit a slow decrease of light transmittance from 55 to 80 ℃. Beyond, a sharper decrease of transmittance down to 78% is detected. The three diblock copolymers exhibit almost the same Cp values of *c.a.* 80 ℃. Therefore, the length of HPMC blocks has little effect on the Cp, but the copolymer topology seems to significantly affect the phase separation behavior of HPMC-*b*-PLA copolymers. It has been reported that the cloud point was elevated by more than 40 ℃ through the linear-to-cyclic topological conversion of the polymer amphiphiles (Honda, Yamamoto, & Tezuka, 2010).

2.3.3. Self-assembly of $(HPMC)_2$-PLA copolymers

The self-assembly properties of $(HPMC)_2$-PLA copolymers were investigated to evaluate their potential as drug carrier. NMR provides a means to analyze the self-assembly behavior of amphiphilic block copolymers in solvents which can dissolve one of the two blocks only. Fig 2.3(B) shows the ^{1}H NMR spectrum of $(HPMC7K)_2$-PLA2K copolymer in deuterated water (D_2O). Different from DMSO-d_6 which is a good solvent for both HPMC and PLLA, D_2O only solubilizes hydrophilic HPMC segments. Therefore, only signals belonging to HPMC block are detected. Signals corresponding to PLLA block are not detected because of the limited molecular motion in aqueous medium, which is consistent with the formation of micelles with a hydrophilic HPMC shell and a hydrophobic PLLA core.

Similar to low molar mass surfactants, the self-assembly of the amphiphilic copolymers occurs when the concentration reaches the CMC. The latter is an important parameter of amphiphilic copolymers as it determines the stability of micelles. In the case of drug delivery systems, drug loaded micelles should remain stable with dilution

after intravenous injection. In this work, the CMC was determined from scattering intensity changes of copolymer solutions as a function of concentration. At low concentrations, the scattered intensity is very low because of the absence of nano-objects. With increasing concentration, the intensity strongly increases due to the formation of nano-micelles. The CMC value is obtained from the crossover point of the two regression lines. As shown in Table 2.2, the CMC of $(HPMC10K)_2$-PLA2K, $(HPMC7K)_2$-PLA2K, and $(HPMC5K)_2$-PLA2K copolymers is 0.16, 0.15, and 0.14 g L^{-1}, respectively. These values well agree with the reported CMC value 0.13 mg/mL for cellulose-*g*-polylactide (Guo et al., 2012). Obviously the CMC increases with the hydrophilic ratio or the HPMC block length as the self-assembly of neutral block copolymers is mainly determined by the hydrophilic/hydrophobic balance (Larue et al., 2008).

The self-assembled $(HPMC)_2$-PLA micelles are composed of a PLA core surrounded by a HPMC corona. The average diameter of $(HPMC5K)_2$-PLA2K, $(HPMC7K)_2$-PLA2K, $(HPMC10K)_2$-PLA2K micelles was 66, 90 and 120 nm as determined by DLS, as shown in Table 2.2. All the micelles exhibited a unimodal size distribution, and the PDI was in the range of 0.12 to 0.21. Thus, the micelle size of copolymers increases with the increase of hydrophilic HPMC chain length, in agreement with literature. In our previous work, the average micelle size of HPMC5K-PLA2K, HPMC8K-PLA2K, HPMC10K-PLA2K diblock copolymers was 62, 96, 120 nm, respectively (Wang et al., 2017). Thus, micelles of $(HPMC5K)_2$-PLA2K had a smaller size compared to HPMC10K-PLA2K with the same hydrophilic/hydrophobic balance but a Y-type topology. It has been reported that the chain architecture affects the micellization properties, including the aggregation number, size, polydispersity, and micelle density (Liu et al., 2007). Generally, the micelle size of multiple-arm copolymers is smaller than that of linear ones. Meanwhile, micelles with the same HPMC block length but different topologies had almost the same size. This finding could be attributed to the fact that the core is composed of the same PLA blocks, and the corona of similar HPMC chains although the chain density should be higher for Y-

type copolymers.

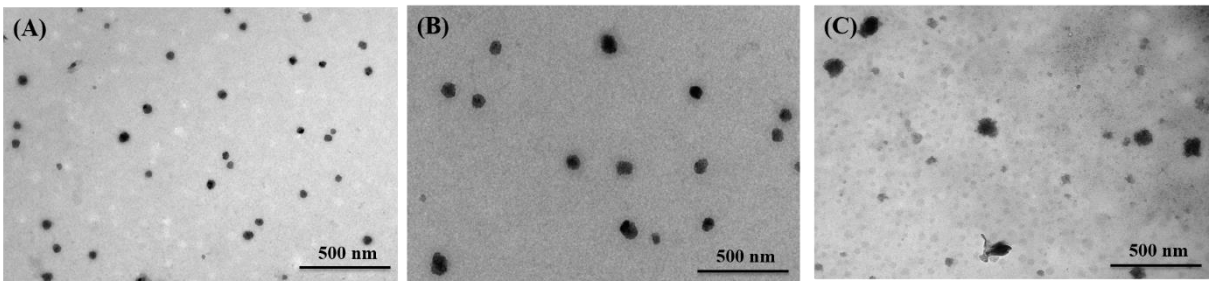

Fig. 2. 8 TEM images of $(HPMC)_2$-PLA micelles in water: (A) $(HPMC5K)_2$-PLA2K; (B) $(HPMC7K)_2$-PLA2K; (C) (HPMC10K)2-PLA2K

The morphology of $(HPMC)_2$-PLA micelles was characterized by using TEM. Fig. 2.8 shows that the micelles were spherical in shape and uniformly distributed. The observed micelle size increased with the increasing of the HPMC chain length, which well agreed with the results obtained by DLS.

2.4. Conclusion

AB_2-type amphiphilic block copolymers $(HPMC)_2$-PLA with three different HPMC block lengths were synthesized by ring opening polymerization, reductive amination and click reaction. The copolymers were characterized by using various methods, including NMR, DOSY-NMR, SEC and FT-IR. The cloud point of AB_2-type $(HPMC)_2$-PLA are nearly 64 ℃, which is obviously lower than HPMC oligomers and linear HPMC-b-PLA diblock copolymers. The HPMC block length has little effect the Cp value. $(HPMC)_2$-PLA copolymers can self-assemble to form spherical micelles with narrow distribution. The size of copolymer micelles increases with the increase of HPMC fraction. So does the CMC of $(HPMC)_2$-PLA. It is thus concluded that biobased and biodegradable HPMC-PLA copolymers could be promising as nano-carrier of hydrophobic drugs.

References

Aminabhavi, T. M., Nadagouda, M. N., Joshi, S. D., & More, U. A. (2014). Guar gum as platform for the oral controlled release of therapeutics. *Expert Opin Drug Deliv,* 11(5), 753-766.

Barz, M., Luxenhofer, R., Zentel, R., & Vicent, M. J. (2011). Overcoming the PEG-addiction: well-defined alternatives to PEG, from structure–property relationships to better defined therapeutics. *Polymer Chemistry,* 2(9), 1900.

Cao, J., Lu, A., Li, C., Cai, M., Chen, Y., Li, S., & Luo, X. (2013). Effect of architecture on the micellar properties of poly (varepsilon-caprolactone) containing sulfobetaines. *Colloids Surf B Biointerfaces,* 112, 35-41.

Chen, D., & Sun, B. (2000). New tissue engineering material copolymers of derivatives of cellulose and lactide: their synthesis and characterization. *Materials Science and Engineering: C,* 11(1), 57-60.

Claes, M. (2006). New Methods for Enzyme Hydrolysis,Analysis, and Characterization of Modified Cellulose. *Analytical Chemistry* (Vol. Ph.D, p. 180). Lund: Lund University.

Elsabahy, M., & Wooley, K. L. (2012). Design of polymeric nanoparticles for biomedical delivery applications. *Chem Soc Rev,* 41(7), 2545-2561.

Fitzpatrick, F., Schagerlöf, H., Andersson, T., Richardson, S., Tjerneld, F., Wahlund, K.-G., & Wittgren, B. (2006). NMR, Cloud-Point Measurements and Enzymatic Depolymerization: Complementary Tools to Investigate Substituent Patterns in Modified Celluloses. *Biomacromolecules,* 7(10), 2909-2917.

Ganguly, K., Chaturvedi, K., More, U. A., Nadagouda, M. N., & Aminabhavi, T. M. (2014). Polysaccharide-based micro/nanohydrogels for delivering macromolecular therapeutics. *J Control Release,* 193, 162-173.

Guo, Y., Wang, X., Shen, Z., Shu, X., & Sun, R. (2013). Preparation of cellulose-graft-poly(varepsilon-caprolactone) nanomicelles by homogeneous ROP in ionic liquid. *Carbohydr Polym,* 92(1), 77-83.

Guo, Y., Wang, X., Shu, X., Shen, Z., & Sun, R. C. (2012). Self-assembly and paclitaxel loading capacity of cellulose-graft-poly(lactide) nanomicelles. *J Agric Food Chem,* 60(15), 3900-3908.

Honda, S., Yamamoto, T., & Tezuka, Y. (2010). Topology-directed control on thermal stability: micelles formed from linear and cyclized amphiphilic block copolymers. *J Am Chem Soc,* 132(30), 10251-10253.

Hsieh, M.-F., Van Cuong, N., Chen, C.-H., Chen, Y. T., & Yeh, J.-M. (2008). Nano-Sized Micelles of Block Copolymers of Methoxy Poly(ethylene glycol)-Poly(ε-caprolactone)- Graft-2-Hydroxyethyl Cellulose for Doxorubicin Delivery. *Journal of Nanoscience and Nanotechnology,* 8(5), 2362-2368.

Huo, M., Zou, A., Yao, C., Zhang, Y., Zhou, J., Wang, J., Zhang, Q. (2012). Somatostatin receptor-mediated tumor-targeting drug delivery using octreotide-PEG-deoxycholic acid conjugate-modified N-deoxycholic acid-O, N-hydroxyethylation chitosan micelles. *Biomaterials,* 33(27), 6393-6407.

Ishida, T., & Kiwada, H. (2008). Accelerated blood clearance (ABC) phenomenon upon repeated injection of PEGylated liposomes. *Int J Pharm,* 354(1-2), 56-62.

Jeong, Y. I., Kim, D. H., Chung, C. W., Yoo, J. J., Choi, K. H., Kim, C. H., Kang, D. H. (2011). Doxorubicin-incorporated polymeric micelles composed of dextran-b-poly(DL-lactide-co-glycolide) copolymer. *Int J Nanomedicine,* 6, 1415-1427.

Jeong, Y. I., Na, H. S., Oh, J. S., Choi, K. C., Song, C. E., & Lee, H. C. (2006). Adriamycin release from self-assembling nanospheres of poly(DL-lactide-co-glycolide)-grafted pullulan. *Int J Pharm,* 322(1-2), 154-160.

Kataoka, K., Harada, A., & Nagasaki, Y. (2001). Block copolymer micelles for drug delivery: design, characterization and biological significance. *Adv Drug Deliv Rev,* 47(1), 113-131.

Khan, I. A., Anjum, K., Koya, P. A., Qadeer, A., & Kabir ud, D. (2014). Cloud point, fluorimetric and 1H NMR studies of ibuprofen-polymer systems. *Journal of Molecular Structure,* 1056-1057, 254-261.

Kostanski, L. K., Keller, D. M., & Hamielec, A. E. (2004). Size-exclusion

chromatography-a review of calibration methodologies. *J Biochem Biophys Methods,* 58(2), 159-186.

Larue, I., Adam, M., Zhulina, E. B., Rubinstein, M., Pitsikalis, M., Hadjichristidis, N., Sheiko, S. S. (2008). Effect of the soluble block size on spherical diblock copolymer micelles. *Macromolecules,* 41(17), 6555-6563.

Lassalle, V., & Ferreira, M. L. (2007). PLA nano- and microparticles for drug delivery: an overview of the methods of preparation. *Macromol Biosci,* 7(6), 767-783.

Li, Z., Kesselman, E., Talmon, Y., Hillmyer, M. A., & Lodge, T. P. (2004). Multicompartment micelles from ABC miktoarm stars in water. *Science,* 306(5693), 98-101.

Liu, H., Xu, J., Jiang, J., Yin, J., Narain, R., Cai, Y., & Liu, S. (2007). Syntheses and micellar properties of well-defined amphiphilic AB2 and A2B Y-shaped miktoarm star copolymers of ε-caprolactone and 2-(dimethylamino)ethyl methacrylate. *Journal of Polymer Science Part A: Polymer Chemistry,* 45(8), 1446-1462.

Mi, P., Wang, F., Nishiyama, N., & Cabral, H. (2017). Molecular Cancer Imaging with Polymeric Nanoassemblies: From Tumor Detection to Theranostics. *Macromol Biosci,* 17(1).

Muller, J., Marchandeau, F., Prelot, B., Zajac, J., Robin, J.-J., & Monge, S. (2015). Self-organization in water of well-defined amphiphilic poly(vinyl acetate)-b-poly(vinyl alcohol) diblock copolymers. *Polymer Chemistry,* 6(16), 3063-3073.

Ostmark, E., Nystrom, D., & Malmstrom, E. (2008). Unimolecular nanocontainers prepared by ROP and subsequent ATRP from hydroxypropylcellulose. *Macromolecules,* 41(12), 4405-4415.

Pages, G., Gilard, V., Martino, R., & Malet-Martino, M. (2017). Pulsed-field gradient nuclear magnetic resonance measurements (PFG NMR) for diffusion ordered spectroscopy (DOSY) mapping. *Analyst,* 142(20), 3771-3796.

Rajendra P. Pawara, S. U. T., Suresh U. Shisodiaa, Jalinder T. Totrea and, & Abraham J. Dombb. (2014). Biomedical Applications of Poly(Lactic Acid). *Recent Patents on Regenerative Medicine,* 4, 40-51.

Ramzi A. Abd Alsaheb, A. A., Nor Zalina Othman, Roslinda Abd Malek,Ong Mei Leng, Ramlan Aziz1 and Hesham A. El Enshasy. (2015). Recent applications of polylactic acid in pharmaceutical and medical industries. *Journal of Chemical and Pharmaceutical Research,* 7(12), 51-63.

Rancan, F., Papakostas, D., Hadam, S., Hackbarth, S., Delair, T., Primard, C., Vogt, A. (2009). Investigation of Polylactic Acid (PLA) Nanoparticles as Drug Delivery Systems for Local Dermatotherapy. *Pharmaceutical Research,* 26(8), 2027-2036.

Rudzinski, W. E., & Aminabhavi, T. M. (2010). Chitosan as a carrier for targeted delivery of small interfering RNA. *Int J Pharm,* 399(1-2), 1-11.

Saini, P., Arora, M., & Kumar, M. (2016). Poly(lactic acid) blends in biomedical applications. *Adv Drug Deliv Rev,* 107, 47-59.

Sardar, N., Kamil, M., Kabir ud, D., & Sajid Ali, M. (2011). Solution Behavior of Nonionic Polymer Hydroxypropylmethyl Cellulose: Effect of Salts on the Energetics at the Cloud Point. *Journal of Chemical & Engineering Data,* 56(4), 984-987.

Schatz, C., & Lecommandoux, S. (2010). Polysaccharide-Containing Block Copolymers: Synthesis, Properties and Applications of an Emerging Family of Glycoconjugates. *Macromolecular Rapid Communications,* 31(19), 1664-1684.

Sun, H., Guo, B., Cheng, R., Meng, F., Liu, H., & Zhong, Z. (2009). Biodegradable micelles with sheddable poly(ethylene glycol) shells for triggered intracellular release of doxorubicin. *Biomaterials,* 30(31), 6358-6366.

Teramoto, Y., & Nishio, Y. (2003). Cellulose diacetate-graft-poly(lactic acid)s: synthesis of wide-ranging compositions and their thermal and mechanical properties. *Polymer,* 44(9), 2701-2709.

Tian, J. L., Zhao, Y. Z., Jin, Z., Lu, C. T., Tang, Q. Q., Xiang, Q., Zhang, Y. (2010). Synthesis and characterization of Poloxamer 188-grafted heparin copolymer. *Drug Dev Ind Pharm,* 36(7), 832-838.

Tsuji, H. (2005). Poly(lactide) stereocomplexes: formation, structure, properties, degradation, and applications. *Macromol Biosci,* 5(7), 569-597.

Wang, J., Caceres, M., Li, S., & Deratani, A. (2017). Synthesis and Self-Assembly of

Amphiphilic Block Copolymers from Biobased Hydroxypropyl Methyl Cellulose and Poly(l-lactide). *Macromolecular Chemistry and Physics,* 218(10), 1600558.

Yang, L., Wu, X., Liu, F., Duan, Y., & Li, S. (2009). Novel biodegradable polylactide/poly(ethylene glycol) micelles prepared by direct dissolution method for controlled delivery of anticancer drugs. *Pharm Res,* 26(10), 2332-2342.

Yang, Y. L., Kataoka, K., & Winnik, F. M. (2005). Synthesis of diblock copolymers consisting of hyaluronan and poly(2-ethyl-2-oxazoline). *Macromolecules,* 38(6), 2043-2046.

Yi, Y., Lin, G., Chen, S., Liu, J., Zhang, H., & Mi, P. (2018). Polyester micelles for drug delivery and cancer theranostics: Current achievements, progresses and future perspectives. *Mater Sci Eng C Mater Biol Appl,* 83, 218-232.

You, Y. Z., Hong, C. Y., Wang, W. P., Lu, W. Q., & Pan, C. Y. (2004). Preparation and characterization of thermally responsive and biodegradable block copolymer comprised of PNIPAAM and PLA by combination of ROP and RAFT methods. *Macromolecules,* 37(26), 9761-9767.

Yuan, W., Yuan, J., Zhang, F., & Xie, X. (2007). Syntheses, characterization, and in vitro degradation of ethyl cellulose-graft-poly(epsilon-caprolactone)-block-poly(L-lactide) copolymers by sequential ring-opening polymerization. *Biomacromolecules,* 8(4), 1101-1108.

Chapter 3 Self-Assembled Micelles Prepared from Bio-Based Hydroxypropyl Methyl Cellulose and Polylactide Amphiphilic Block Copolymers for Anti-Tumor Drug Release

Abstract: Fully bio-based amphiphilic diblock copolymers were synthesized from hydroxypropyl methyl cellulose (HPMC) and amino-terminated poly(L-lactide) (PLLA) or poly(L-lactide-co-DL-lactide) (PLA) by reductive amination. The resulting HPMC-PLLA and HPMC-PLA copolymers with various hydrophobic block lengths were characterized by NMR, DOSY-NMR and FT-IR. Micelles were obtained by self-assembly of copolymers in aqueous medium. The micelles are spherical in shape, and the micelle size ranges from 150 to 180 nm with narrow distribution. The critical micelle concentration decreases with increasing PLA block length. Paclitaxel was loaded in micelles. Enhanced drug loading is obtained with increase of PLA block length. A biphasic release profile is observed with a burst of 40% followed by slower release up to 80%. MTT assay indicates the good cytocompatibility of HPMC-PLA micelles. SRB assay shows a significant cytotoxicity of paclitaxel-loaded micelles against SK-BR-3cells. It is thus concluded that bio-based HPMC-PLA block copolymers could be promising nano-carrier of anti-tumor drugs.

Key words: hydroxypropyl methyl cellulose; polylactide; self-assembly; paclitaxel; micelle; drug release; cytotoxicity

3.1 Introduction

Amphiphilic block copolymers are able to self-assemble in aqueous medium, yielding a variety of ordered structures, including micelles, cylinders, lamellae, vesicles, etc. These aggregates present great interests for applications such as drug and gene

delivery, nanoreactor, diagnostic imaging, etc [1]. Among them, micelles with a core-shell structure have been largely studied as nano-carrier of hydrophobic drugs due to their outstanding properties, e.g. prolonged blood circulation, enhanced drug bioavailability and reduced side effects [2]. The hydrophobic core of micelles generally consists of a biodegradable polymer such as polylactide (PLA), polyglycolide (PGA), or poly(ε-caprolacone) (PCL), and serves as reservoir for poorly soluble drugs. On the other hand, the hydrophilic shell is usually composed of hydrophilic polymers such as poly(ethylene glycol) (PEG), poly(N-isopropyl acrylamide) (PNIPAAm), or poly(2-ethyl-2-oxazoline) (PEOz), which assures micelle stabilization and interactions with plasmatic proteins and cell membranes. The biodistribution of micelles is mainly dependent on the nature of the hydrophilic shell [3].

Aliphatic polyesters, and in particular PLA, PGA and PCL have been widely used in the biomedical field for drug delivery, tissue regeneration and tissue engineering in the form of scaffolds, sutures, drug carriers, and bone fracture internal fixation devices due to their biocompatibility, degradability and good processability [4]. PLA is generally obtained by ring-opening polymerization (ROP) of lactide, the cyclic dimer of lactic acid. As lactic acid is a chiral molecule which has two enantiomers, L- and D-lactic acids, various PLA polymers are available, including isotactic poly(L-lactide) (PLLA), poly(DL-lactide) (PDLLA), and poly(D-lactide-co-L-lactide) stereocopolymers with different L/D ratios [5]. The stereochemistry of PLA is a most important parameter determining its physico-chemical properties such as morphology, mechanical strength, degradation rate, etc. Interestingly, Jelonek et al. reported that the PLA chain stereoregularity greatly affects the self-assembled architecture of PLA/PEG micelles [6]. Worm-like micelles are obtained for PLLA-PEG diblock copolymers, whereas PDLLA-PEG copolymers with similar compositions yield spherical micelles. PDLLA-PEG micelles entrapping an anti-tumor drug, paclitaxel (PTX), have been approved under the trademark of Genexol-PM in South Korea for treating breast cancer and non-small cell lung cancer [7].

Polysaccharides have attracted growing attention as a hydrophilic building block

for construction of amphiphilic block copolymers because of their bio-based origin, biodegradability, biocompatibility non-toxicity and inherent bioactivity which allows to improve drug bioavailability and to reduce inflammation [2, 8]. Various polysaccharides have been considered, including chitosan, dextran, starch, cyclodextrin and cellulose. Cellulose chains are composed of β (1 → 4) linked D-glucose units which endow cellulose with unique physical and chemical properties [9]. Nevertheless, the poor solubility of cellulose greatly restricts its potential applications. Thus, chemical modification of cellulose is performed to obtain soluble derivatives for uses as a hydrophilic building block, such as ethyl cellulose [10], hydroxylpropyl cellulose [11], hydroxylpropylmethyl cellulose (HPMC) [12], etc. Actually, various cellulose-based amphiphilic copolymers have been designed via grafting hydrophilic polymers onto the main chain of cellulose [9]. However, such reactions are poorly controllable and may lead to complex structures. And it is difficult to achieve cellulose-based graft copolymers with high purity, low dispersity and good reproducibility which strongly influence their micellization characteristics [9]. In contrast, the reducing hemiacetal end group of cellulose which is in equilibrium with an aldehyde one allows to synthesize amphiphilic block copolymers via reductive amination [8, 12].

In a previous work, we reported for the first time the synthesis of linear HPMC-PLA and AB_2-type PLA-$(HPMC)_2$ block copolymers by combination of ROP, amination reduction and UV initiated thiol-ene or thiol-yne click reaction. The copolymers exhibit interesting thermo-responsive and self-assembly properties, but the overall yield of the reaction is low [12, 13]. In this work, a more efficient and simpler procedure was proposed to synthesize HPMC-PLA block copolymers by reductive amination. Amino-terminated PLA (NH_2-PLA) was first synthesized by tert-butyl-N-(3-hydroxypropyl) carbamate initiated ROP of lactide, followed by deprotection of the N-tert-butoxycarbonyl (Boc) group. HPMC-PLA copolymers with various PLA chain lengths were then synthesized by reductive amination between NH_2-PLA's amino group and HPMC's hemiacetal end group. The self-assembly of copolymers including morphology, micelle size and size distribution, zeta potential and critical micelle

concentration (CMC) was investigated. Drug loading and drug release, MTT and SRB assays were performed to evaluate the potential of HPMC-PLA copolymers as nano-carrier of hydrophobic drugs.

3.2 Materials and Methods

3.2.1 Materials

L-lactide and DL-lactide were purchased from Purac Biochem (Goerinchem, Netherlands) and Alfa-Aesar, respectively, and purified by recrystallization in ethyl acetate. HPMC was kindly supplied by Dow Colorcon Limited France. HPMC oligomers with Mw of 7000 were obtained by enzymatic depolymerization as previously reported [12, 13]. Tert-butyl-*N*-(3-hydroxypropyl) carbamate (3-(Boc-amino)-1-propanol), tin (II) 2-ethyl hexanoate ($Sn(Oct)_2$) and sodium triacetoxyborohydride ($NaBH(OAc)_3$) were obtained from Sigma-Aldrich and used as received. Trifluoroacetic acid (TFA) was purchased from Merck KGaA. Toluene and dichloromethane were obtained from Sigma-Aldrich, dried over by calcium chloride ($CaCl_2$) and distilled prior to use.

SK-BR-3cell line was provided by American Type Culture Collection (ATCC-LGC Standard). Fetal bovine serum (FBS) was purchased from Thermo Fisher Scientific. All other organic solvents were of analytic grade from Sigma-Aldrich and used as received.

3.2.2 Synthesis of amino-terminated PLA

Amino-terminated PLA was synthesized by ROP of lactide using 3-(Boc-amino)-1-propanol as initiator and $Sn(Oct)_2$ as catalyst, followed by deprotection of the BOC group using TFA . Typically, L-lactide (27 mmol, 3.888g), DL-lactide (3 mmol, 0.432g), 3-(Boc-amino)-1-propanol (2 mmol, 0.35g) and $Sn(Oct)_2$ (2.3 mmol, 0.0932g) were added into a dried Schlenk tube. 20 mL anhydrous toluene was added under nitrogen atmosphere with stirring. The solution was degassed by performing five freeze–pump-thaw cycles. The reaction proceeded 24 h at 80℃. Finally, the crude product Boc-NH-PLA was purified by precipitation in ethanol, and drying in vacuo.

1.0 g Boc-NH-PLA was introduced in a nitrogen purged flask. 5 mL freshly distilled dichloromethane was then added, followed by addition of 5 mL anhydrous TFA. The reaction proceed at room temperature for 1 h, and terminated by evaporating all the liquid. The crude product was dissolved in dichloromethane, successively washed with 5% $NaHCO_3$ aqueous solution and water, and finally dried over $MgSO_4$. After filtration, the solution was precipitated in cold ethanol, and the product dried in vacuum at room temperature up to constant weight.

3.2.3 Synthesis of HPMC-PLA block copolymers

HPMC-PLA copolymers were synthesized by reductive amination according to the method reported in literature [14, 15]. Typically, under nitrogen atmosphere, 1.0 g HPMC (1.0 g, 0.14 mmol), NH_2-PLA (0.154 mmol, 0.23g) and $NaBH(OAc)_3$ (0.042 g, 0.2 mmol) were dissolved in 20 mL anhydrous DMSO. The reaction was allowed to proceed under nitrogen atmosphere at 35 ℃ for 72 h. The reaction mixture was dialyzed against distilled water for 72 h, followed by 48 h freeze-drying to yield the final product.

3.2.4 Characterization

^1H NMR spectra were obtained using Bruker AVANCE 300 spectrometer with $CDCl_3$, DMSO-d_6 or D_2O as solvent. Data were analyzed by using MestRe Nova software. DOSY NMR was performed on Bruker Avance 400 spectrometer equipped with a Bruker multinuclear z-gradient which can produce gradients in the z-direction with a strength of 55 Gcm^{-1}. The spectra were proceeded using Bruker topspin software (version 3.5) with the ledbpgp2s pulse program.

GPC was performed on a Viscotek TDA 305 multidetector GPC/SEC system. All samples were prepared at a concentration of 10 g/L and filtered through 0.22 μm PTFE filter. THF was used as eluent at a flow rate of 1.0 mL/min. Calibration was realized by using polystyrene standards (Polysciences, Warrington, PA).

FT-IR spectra were recorded on a Nicolet NEXUS spectrometer with attenuated total reflectance (ATR) accessory in the frequency range from 400 to 4000 cm^{-1}. 32 scans were performed for each analysis at at 4 cm^{-1} resolution.

DSC was performed on TA DSC Q20 system in the temperature range of 0 ℃-

160 ℃ under dry nitrogen atmosphere. Samples of *c.a.* 5 mg were put into an aluminum pan and sealed. Measurements were made using the following procedure: 1) heating from 0℃ to 160 ℃ at 10 ℃/min to erase the thermal history of samples, 2) cooling down to 0℃, 3) heating to 160 ℃ at 10 ℃/min. The glass transition temperature (Tg), melting temperature (Tm) and melting enthalpy (ΔHm) were determined from the second heating scan.

A Zetasizer Nano-ZS from Malvern Instrument equipped with a He–Ne laser (λ =632.8 nm) was used to determined the hydrodynamic size and zeta potential of copolymer micelles. Dynamic light scattering (DLS) was performed at 25 ℃ at a scattering angle of 173 °. Copolymer solutions at 1.0 mg mL^{-1} were filtered through a 0.45 μm cellulose acetate (CA) membrane filters before measurements.

The CMC of copolymers was determined by fluorescence spectroscopy using pyrene as fluorescent probe. The copolymers solutions were prepared with concentrations varying from 1.0×10^{-3} to 2.0 mg/mL, whereas the concentration of pyrene was fixed at 6×10^{-7}g/L. The excitation spectra of the above solutions were recorded on PerkinElmer LS55 fluorescence spectrometer at an excitation wavenumber of 395 nm. The CMC value was estimated from the intersection of regression lines of intensity ratios at 336 nm and 334 nm *versus* the logarithm of concentration plots.

TEM images were obtained by using JEOL 1400 plus instrument, operating at an acceleration voltage of 120 kV. Samples were prepared by dropping 1.0 mg mL^{-1} micelle solution onto a carbon coated copper grid and exposed to ruthenium oxide vapor for 7 min before measurements.

3.2.5 In vitro drug release

Drug-loaded micelles were prepared in two steps. 20 mg copolymer was first dissolved in distilled water to yield blank micelles. 2 mg paclitaxel dissolved in 50 μL ethanol was then added to the micellar solution under vigorous stirring. Drug-loaded micelles were obtained after evaporation of the solvent overnight. Unloaded drug was eliminated by filtration using 0.8 μm CA filter. Finally the solution was lyophilized and stored at 4 ℃.

HPLC-MS measurements were performed to determine the concentration of PTX in solution. The mobile phase was a 50/50 (v/v) mixture of acetonitrile and pH 7.4 phosphate buffered saline (PBS). A calibration curve was previously established from standard PTX solutions at concentrations ranging from 0.128 to 5 ppm (R2 =0.999). The following equations [16] were used to determine the drug loading content (DLC) and drug loading efficiency (DLE):

$$\mathrm{DLC} = \frac{\text{weight of loaded drug}}{\text{weight of polymeric micelles}} \times 100\% \quad (1)$$

$$\mathrm{DLE} = \frac{\text{weight of drug in micelles}}{\text{theoretical drug loading}} \times 100\% \quad (2)$$

In vitro drug release from PTX-loaded micelles was carried out using dialysis method. Lyophilized drug-loaded micelles were dispersed in pH 7.4 PBS at 2.0 mg/mL. 1 mL micelle solution was introduced into a Float-A-Lyzer G2 dialysis device with a MWCO of 3 500 Da which was immerged in 40 mL PBS. Drug release experiments were realized at 37 ℃ under constant shaking. At preset time intervals up to 120 h, an aliquot of 25 μL solution was withdrawn from each device and replaced by the same volume of fresh PBS. The whole release medium was removed and replaced regularly to keep sink conditions. The amount of residual PTX in collected samples was measured by HPLC.

3.2.6 MTT assay

L-929 cells in logarithmic growth phase were added in 96-well plates (Corning Costar, U.S.A.) at 1×10^4 cells/mL in DMEM medium (10% calf serum, 100 μg/mL Penicillin, 100 μg/mL streptomycin), 100 μL per well. The plates were placed in an NU-4850 incubator (NuAire, U.S.A.) at 37 ℃ under humidified atmosphere with 5% CO_2. After 24 h, the medium was removed and replaced with 100 μL fresh medium or HPMC-PLA micellar solution at concentrations from 0.25 to 5.0 mg/mL containing 10.0 % calf serum. 100 μL fresh medium was used as the negative control, and 100 μL phenol solution as the positive control [17]. After 24, 48 and 72 h, 20 μL MTT solution at 5 mg/mL was added. The medium was removed after 6 h incubation. 150 μL DMSO was added, and the plates were shaken for 10 min. The optical density (OD) was

measured by using a microplate reader (Elx800; BioTek, U.S.A.) at 570 nm. All experiments were carried out in triplicate. The cell viability was calculated from the OD values of the test sample and negative control using the following equation:

$$\text{Relative activity (\%)} = (OD_{\text{test sample}} / OD_{\text{negative control}}) \times 100 \qquad (3)$$

3.2.7 Sulforhodamine B (SRB) assay

SK-BR-3cells in growth phase were suspended in 96-well plates at a density of 3 $\times 10^4$ cells, 100 μL per well in McCoy's 5A (Modified) Medium supplemented with 10 % FBS, 100 U/mL penicillin, and 100 μg/mL streptomycin. The cells were incubated 24 h at 37 ℃ in a humidified atmosphere containing 5 % CO_2 to allow cell adhesion. Subsequently, the medium was replaced by blank micelles, drug-loaded micelles, or free drug solution. Blank micelles and drug-loaded micelles were dissolved directly in culture medium. Free PTX was dissolved in 0.125 % DMSO/medium. Untreated cells were used as negative control. PTX concentration of both free drug and drug-loaded micelles ranged from 0.025 to 25 μg/mL. Blank micelles were prepared at concentrations used for drug-loaded micelles (18-48 μg/mL). Each concentration was carried out in quadruplicate, and each experiment repeated three times. After 72 h incubation, the cells were fixed with 100 μL 10 % trichloroacetic acid for 1 h at 4 ℃, and washed twice with deionized water. Then the cells were stained with 0.4 % SRB dissolved in 1.0 % acetic acid for 30 min at room temperature and rinsed three times using 1.0 % acetic acid. Finally, 200 μL of 10 mM Tris base solution were used to dissolve the incorporated dye. Absorbance at 570 and 690 nm was measured using MRX Revelation plate reader (Dynex Technologies). One-way ANOVA and Tukey post-hoc test in SPSS software were used for statistical analysis. The relative activity of cells was calculated from the following equation:

$$\text{Relative activity (\%)} = (OD_{\text{test sample}} / OD_{\text{negative control}}) \times 100 \qquad (4)$$

3.3 Results and discussion

3.3.1 Synthesis of amphiphilic block copolymers

The synthesis of HPMC-PLA copolymers is realized in 3 steps as illustrated in Scheme 3.1. At first, 3-(Boc-amino)-1-propanol was used to initiate the ROP of lactide, yielding Boc-NH-PLA. Then, the protective Boc group at the chain end was removed by treatment using trifluoroacetic acid to obtain amino terminated PLA. Finally, the hemiacetal end group of hydrophilic HPMC block and the amino group of hydrophobic PLA block were coupled by reductive amination in the presence of $NaBH(OAc)_3$, yielding amphiphilic HPMC-PLA block copolymers. To the best of our knowledge, this is the first time that such copolymers are synthesized by reductive amination.

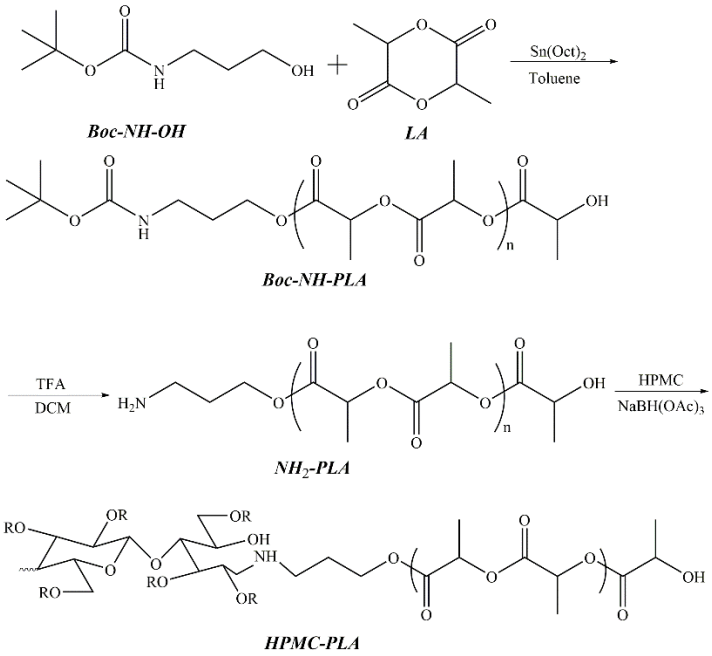

Scheme 3. 1 Synthesis route of HPMC-PLA block copolymers by reductive amination

Amino terminated NH_2-PLA was synthesized according to the method reported by Gotsche et al. [18] and Ju et al. [19]. Boc group was used as the protective group since it is stable during lactide polymerization and could be easily removed. Boc-NH-PLA was synthesized by ROP of L-lactide or a mixture of L- and DL-lactides using 3-(Boc-

amino)-1-propanol as initiator with various monomer/initiator molar ratios ranging from 10/1 to 40/1. In fact, PLLA with a degree of polymerization (DP) above 20 is poorly soluble in DMSO, solvent used for reductive amination in the last step. A mixture of L- and DL-lactides at L/DL ratio of 90/10 was thus used for the synthesis of PLA with higher DP to ensure full solubility of PLA in DMSO. For the sake of clarity, PLLA and PLA refer to poly(L-lactide) and poly(L-lactide-co-DL-lactide), respectively. Five polymers were synthesized in this work, namely $PLLA_{10}$, $PLLA_{20}$, PLA20, PLA_{30} and PLA_{40}. In these abbreviations, the number refers to the DP of PLLA or PLA.

Fig. 3.1(A) shows the ^1H NMR spectrum of Boc-NH-PLA. The characteristic signals of Boc are detected at 1.42 ((C*H*$_3$)$_3$-O-, **a**), 4.18 (-CH_2-C*H*$_2$-O-, **e**), 1.84 (-NH-CH_2-C*H*$_2$-, **d**) and 3.20 (-NH-C*H*$_2$-CH_2-,**c**) ppm. The signals at 1.62 (-CO-CH (C*H*$_3$)-O-,-**f**) and 5.25 (-CO-C*H* (CH_3)-O,-**g**) ppm are attributed to protons of PLA main chain, and those at 1.50 (-CO-CH (C*H*$_3$)-OH, **j**) and 4.42 (-CO-C*H* (CH_3)-OH **h**) ppm corresponding to the hydroxyl terminated unit. The DP of PLA is determined from the integration ratio of signals **e** to **g**. As summarized in Table 3.1, the DP determined by NMR is very close to the feed ratio, in agreement with the successful ring opening polymerization of lactide initiated by Boc-NH-OH. The Mn calculated from the DP of PLA and the molar mass of the protecting group varies from 950 to 3040 (Table 3.1).

Table 3. 1 Characterization of Boc-NH-PLA polymers

Sample	L-/DL-lactide ratio	DP [a]	Mn_{NMR} [a]	Mn_{GPC} [b]	$Đ$ [b]	Tg [c] (℃)	Tm [c] (℃)	ΔHm [c] (J/g)
$PLLA_{10}$	100/0	11	950	1670	1.59	23.8	112.4	25.6
$PLLA_{20}$	100/0	19	1530	2190	1.30	43.7	136.5	62.2
PLA_{20}	90/10	20	1600	2170	1.55	38.5	115.6	18.7
PLA_{30}	90/10	31	2390	2450	1.29	39.7	123.6	27.7
PLA_{40}	90/10	40	3040	3130	1.46	43.6	131.6	38.1

[a] Determined from NMR

[b] Determined from GPC

[c] Determined from DSC

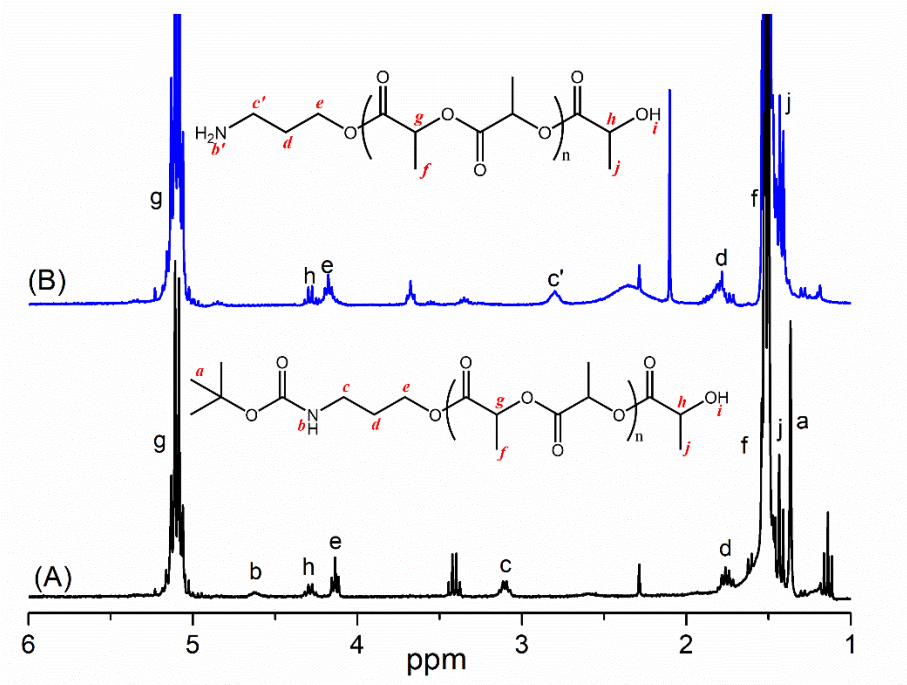

Fig. 3. 1 NMR spectra of Boc-NH-PLA_{20} (A) and NH_2-PLA_{20} (B) in $CDCl_3$

The molar masses of the various Boc-NH-PLA polymers are also measured by GPC. In all cases, the GPC curve exhibits a symmetric molar mass distribution, as shown in Fig. 3.2. The Mn obtained by GPC varies from 1670 to 3130, which is slightly higher than that calculated from NMR. The dispersity of polymers ranges from 1.29 to 1.59, indicating narrow distribution of molar mass.

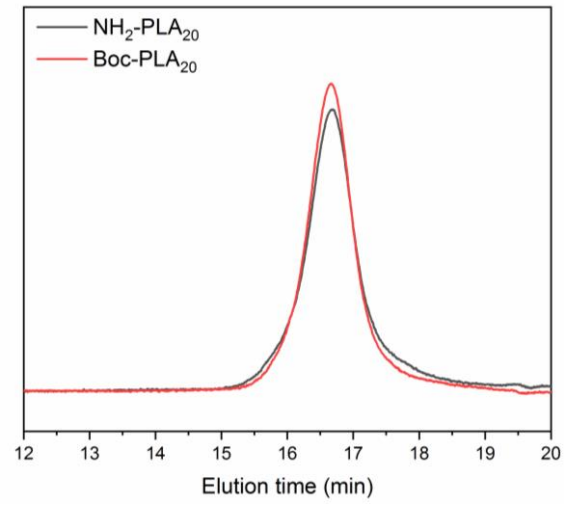

Fig. 3. 2 GPC curves of Boc-NH-PLA_{20} and NH_2-PLA_{20} in THF

The thermal properties of Boc-NH-PLA polymers were determined by DSC as shown in Table 3.1. $PLLA_{10}$ and $PLLA_{20}$ exhibit a Tg at 23.8 and 43.7℃, respectively, indicating that the Tg of PLLA oligomers increases with increasing molar mass or DP according to the free volume theory of glass transition. In fact, the chain ends present higher mobility than the main chain. In a given polymeric matrix, the free volume increases with increase of the number of chain ends or with decrease of DP, thus leading to lower Tg. Similarly, the Tg of PLA_{20}, PLA_{30} and PLA_{40} is detected at 38.5, 39.7 and 43.6 ℃, respectively. It is of interest to note that $PLLA_{20}$ exhibits higher Tg than PLA_{20} because the former presents higher chain stereoregularity. On the other hand, $PLLA_{10}$ and $PLLA_{20}$ exhibit a Tm at 112.4 and 136.5℃ with corresponding ΔHm of 25.6 and 62.2 J/g, respectively, suggesting higher crystallinity with increasing DP of PLLA oligomers. The same trend is observed for PLA_{20}, PLA_{30} and PLA_{40}. It is also noteworthy that $PLLA_{20}$ exhibits higher Tm and ΔHm than PLA_{30} and PLA_{40} in spite of its lower DP, which means that the chain stereoregularity has stronger influence on the crystallinity than the DP of PLA oligomers.

Amino terminated PLA was obtained by removal of the Boc group from Boc-NH-PLA in the presence of TFA. As shown in Fig. 3.1(B), the characteristic signal ((C*H*$_3$)$_3$-O-, **a**) at 1.42 ppm attributed to the terminal Boc group totally disappears, whereas the signal **c** at 3.20 ppm shifts to 2.75 ppm (**c'**) since the adjacent amide group is converted to amino group. These findings indicate full deprotection of all primary amino groups. The integration ratio between signal **c'** and signal **g** or **f** of lactyl units remains constant after removal of the Boc group, indicating that deprotection did not provoke PLA degradation. This is proved by GPC analysis (Fig. 3.2). The GPC curves of Boc-NH-PLA_{20} and NH-PLA_{20} almost overlap, in agreement with the same molar mass.

Finally, reductive amination was carried out between the hemiacetal group of HPMC and the amine group of PLA using $NaBH(OAc)_3$ as reducing agent, yielding HPMC-PLA block copolymers. The ^{1}H NMR spectra of HPMC-PLA in DMSO-*d*$_6$ and D_2O are shown in Fig. 3.3. The characteristics signals of HMPC are observed on the spectrum in DMSO-*d*$_6$ (Fig. 3.3A), including signals at 1.05 ppm (-CH_2-CHOHC*H*$_3$ of

substituent groups, **n**), 2.75–4.75 ppm (C-H of the glucose units and substituent groups, **m**) and those of PLA at 1.49 (-CO-CH (CH_3)-O-, **f**) and 5.24 (-CO-C*H* (CH_3)-O, **g**). These results suggest the successful synthesis of HPMC-PLA copolymers by reductive amination between HPMC and amino terminated PLA. Compared to the synthesis of HPMC-PLA and $(HPMC)_2$-PLA copolymers by thiol-ene or thiol-yne click reaction in our previous work [12,13], the synthesis of HPMC-PLA by reductive amination is simpler and more efficient as it allows to shorten the synthesis route. In fact, the previous method involves a three step procedure: ring-opening polymerization of L-lactide initiated by allyl alcohol or propynol, amination reduction of the aldehyde endgroup of HPMC, and UV-initiated thiol-click reaction. Reaction of cysteamine with the aldehyde endgroup of HPMC yields a mixture of HPMC-S-S-HPMC together with small amounts of unreacted HPMC, HPMC-SH, and HPMC-S-S-$(CH_2)_6$-NH_2. A supplementary step was needed to reduce HPMC-S-S-HPMC to HPMC-SH using 1,4-dithiothreitol (DTT) [12,13].

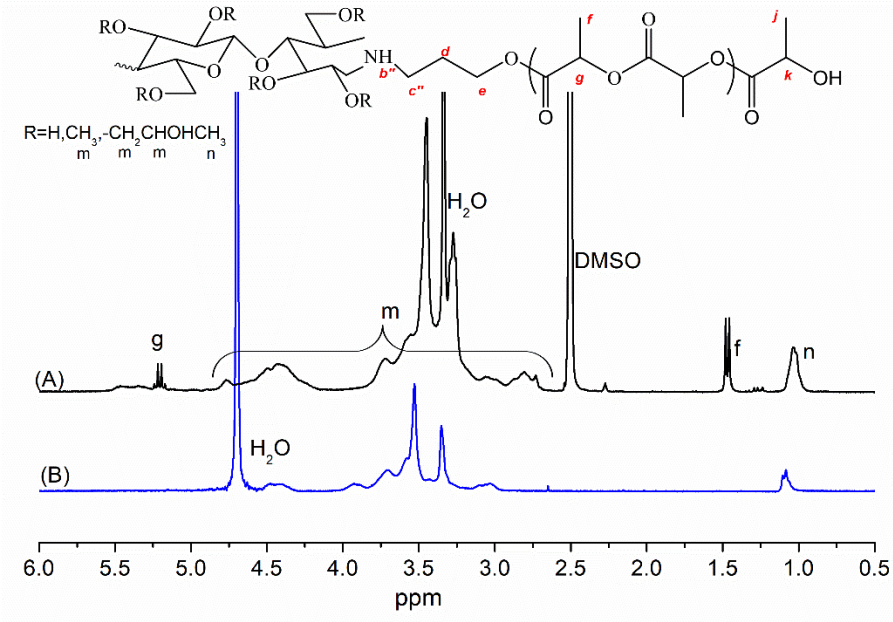

Fig. 3. 3 ^{1}H NMR spectra of HPMC-PLA_{20} in DMSO-d_6 (A) and D_2O (B)

NMR is also a means to evidence the core-shell structure of micelles self-

assembled from amphiphilic block copolymers. In selective solvents, only the characteristic signals of soluble block can be detected, while those of insoluble block are invisible because of the limited movement. Thus, on the spectrum in D_2O as solvent, only the signals corresponding to hydrophilic HPMC block are detected as shown in Fig. 3.3(B).

DOSY-NMR is a technique of choice to characterize block copolymers, which allows the separation of NMR signals of different species according to their diffusion coefficients related to the hydrodynamic radius of molecules [20]. As shown in Fig. 3.4, the signals corresponding to both PLA and HPMC blocks present the same diffusion coefficient of 3.16×10^{-11} m^2/s. It also should be noted that the diffusion coefficient of PLA_{10} and HPMC homopolymers is 1.0×10^{-10} and 5.62×10^{-11} m^2/s, respectively. Thus, DOSY-NMR clearly indicates the effective combination of the two blocks in a copolymer without residual homopolymers.

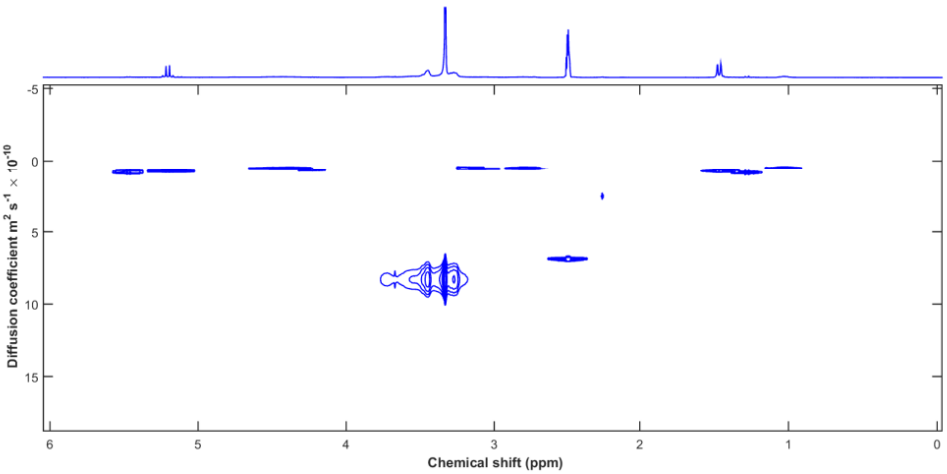

Fig. 3. 4 DOSY- NMR spectrum of HPMC-PLA_{10} in DMSO-d_6

FT-IR spectra confirmed the chemical structure of copolymers. Fig. 3.5 shows the FT-IR spectra of Boc-OH, Boc-NH-PLA, NH_2-PLA, HPMC-PLA and HPMC. Boc-OH presents a large band around 3260 cm^{-1} of O-H bond, and characteristic bands at 1689, 1527, 1366 and 1392 cm^{-1} assigned to CO-NH, C=O and C-H (methyl) bonds, respectively. These characteristic bands become much weaker in Boc-PLA, and aren't

visible in NH_2-PLA due to removal of the Boc group. On the spectrum of HPMC-PLA, characteristic bands at 3480, 2890, and 1047 cm^{-1} corresponding to O-H, C-H and C-O from HPMC and at 1760 cm^{-1} of PLA are detected, thus confirming the presence of both blocks.

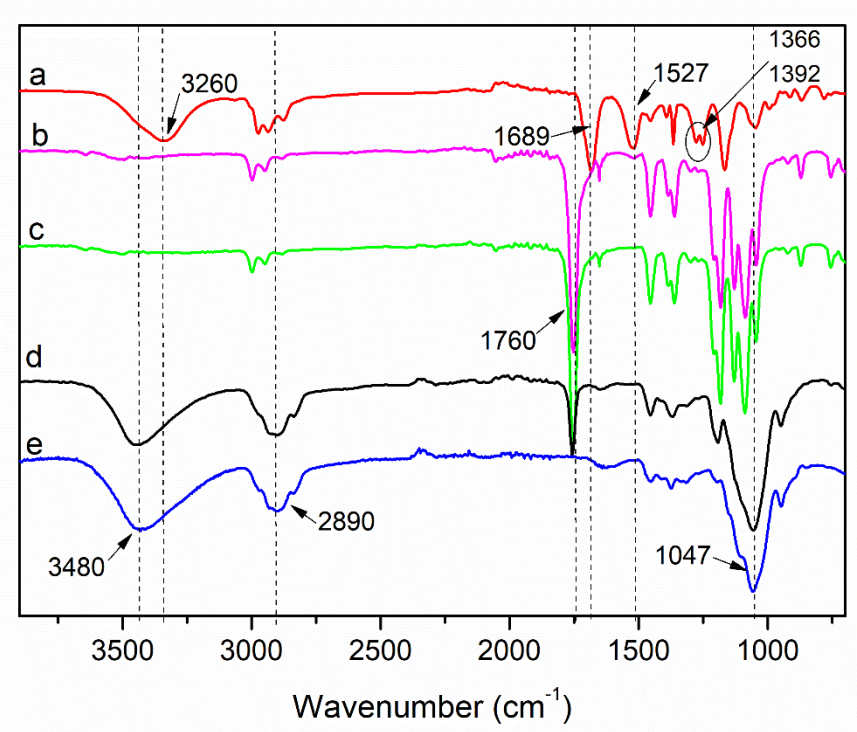

Fig. 3. 5 FT-IR spectra of Boc-OH (a), Boc-NH-PLA_{30} (b), NH_2-PLA_{30} (c), HPMC-PLA_{30} (d) and HPMC (e)

3.3.2 Self-assembly of copolymers

The self-assembly of water soluble HPMC-PLA copolymers is achieved by dissolution in Milli-Q water. The CMC of block copolymers was determined by fluorescence spectroscopy using pyrene as probe due to its characteristic dependence of the vibrational fine structure [21]. As shown in Fig. 3.6(A), the absorption at 334 nm of the fluorescence excitation spectra corresponds to a polar environment of pyrene, and the absorption at 336 nm corresponds to a nonpolar environment of pyrene because of the migration of pyrene into the hydrophobic core of micelles. Thus, the onset of micellization is evidenced by a red shift of the fluorescence excitation spectra due to

the variation of polar environment of pyrene. The intensity ratio I_{336}/I_{334} *versus* copolymer concentration is plotted as shown in Fig. 3.6(B), and the CMC is obtained from the intersection point of regression lines.

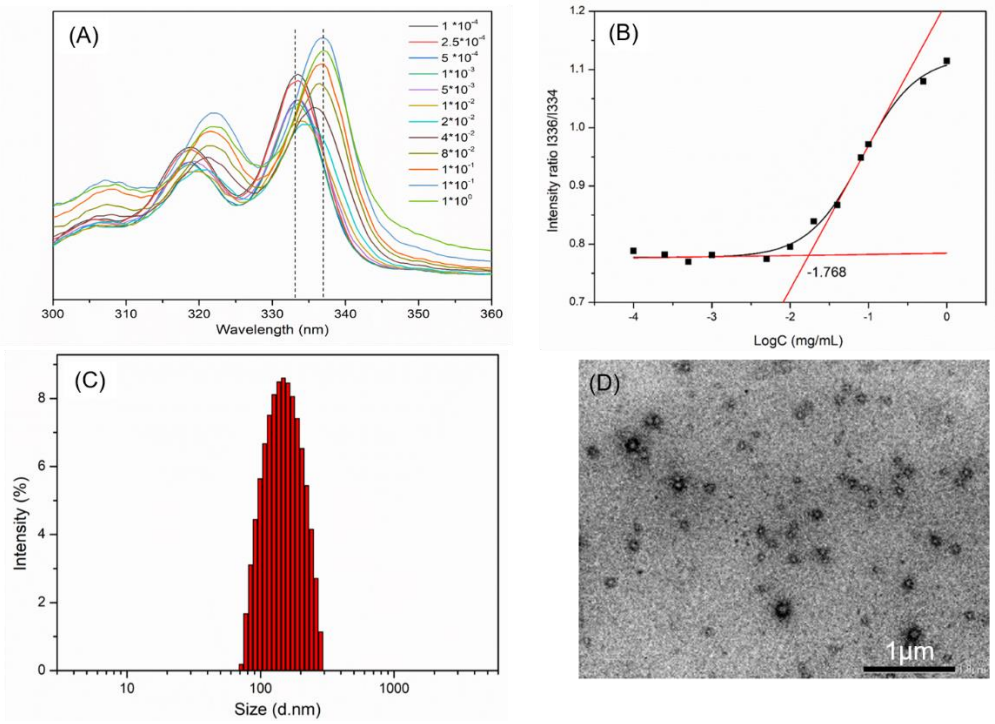

Fig. 3. 6 Fluorescence excitation spectra (A), and I_{336}/I_{334} *vs.* LogC plot (B) of HPMC-PLA_{20} solutions at different concentrations, size distribution (C) and TEM image (D) of HPMC-PLA_{20} micelles

In Table 3.2 are listed the CMC values of HPMC-PLA copolymers. $PLLA_{10}$-HPMC exhibits a CMC of 0.15 g/L, which is the highest among the 5 copolymers. The CMC of $PLLA_{20}$-HPMC and PLA_{20}-HPMC is 0.017 and 0.016 g/L, respectively. With longer PLA block length, PLA_{30}-HPMC and PLA_{40}-HPMC exhibit a CMC of 0.011 and 0.009 g/L, respectively. Therefore, longer hydrophobic block length facilitates micelle formation, thus leading to lower CMC [22, 23]. On the other hand, the stereochemistry of PLA block seems not to affect the CMC of HPMC-PLA copolymers.

Table 3. 2 Self-assembly and drug loading properties of HPMC-PLA block copolymers

Sample	Blank micelles				PTX-loaded micelles			
	Size (nm)	PDI	Zeta (mV)	CMC (mg/mL)	Size (nm)	PDI	DLC (%)	DLE (%)
$PLLA_{10}$-HPMC	159±1.2	0.25	-3.3	0.15	184.9±1.2	0.23	4.8	45.6
$PLLA_{20}$-HPMC	153.8±3.0	0.15	-2.1	0.017	186.6±1.2	0.20	3.6	26.3
PLA_{20}-HPMC	169.7±1.6	0.16	-1.9	0.016	175.2±1.2	0.15	5.3	50.2
PLA_{30}-HPMC	171.5±1.2	0.23	-2.0	0.011	180.4±1.2	0.27	6.2	58.2
PLA_{40}-HPMC	178.3±2.1	0.28	-6.9	0.009	216.3±1.2	0.16	6.4	59.8

The size and polydispersity index (PDI) of micelles were determined by DLS, and the morphology visualized by TEM as shown in Fig. 3.6(C, D). The average micelle size of copolymers ranges from 153.8 to 178.3 nm, and the PDI from 0.15 to 0.28 (Table 3.2). These findings suggest that the micelle size of HPMC-PLA copolymers is hardly affected by the PLA block length. On the other hand, Fig. 3.6(D) shows that micelles are uniformly distributed with well-defined spherical structure. The zeta potential of the micelles is close to zero, which corroborates with the fact that the micelle surface is almost neutral.

3.3.3 In vitro drug release

The hydrophobic core of micelles can encapsulate poorly soluble drugs. Many factors affect the encapsulation capacity of micelles, such as compatibility between drugs and core polymers, core block length and crystallinity, *etc.* PLA has good compatibility with PTX since PTX contains OH and NH groups which can interact with carbonyl groups of PLA [24]. Thus PTX was selected to investigate the drug encapsulation and release properties of HPMC-PLA copolymer micelles.

PTX-loaded micelles were prepared by adding a PTX solution in ethanol to pre-formed micellar solution under vigorous stirring. The solution of $PLLA_{10}$-HPMC appears transparent, whereas that of other copolymers are whitish. This difference could

be assigned to the fact that HPMC-$PLLA_{10}$ presents the highest hydrophilic/ hydrophobic ratio. The size of PTX-loaded micelles is slightly larger than that of blank micelles, as shown in Table 3.2. This increase of micelles size could be caused by PTX encapsulation in the micelle core [25]. The DLC and DLE data are also summarized in Table 3.2. $PLLA_{10}$-HPMC presents a DLE of 45.6% and a DLC of 4.8%. Higher DLE and DLC are obtained for PLA_{20}-HPMC, PLA_{30}-HPMC and PLA_{40}-HPMC. The latter presents the highest DLE and DLC of 59.8% and 6.4%, respectively. HPMC-PLA_{40} presents the highest DLE and DLC of 59.8% and 6.4%, respectively. Surprisingly, lower DLE and DLC are obtained for $PLLA_{20}$-HPMC. This discrepancy could be attributed to the higher crystallinity of $PLLA_{20}$ as mentioned above since higher crystallinity disfavors drug loading [26]. Increasing DLC and DLE are obtained with increase of PLA block length from PLA_{20}-HPMC to PLA_{40}-HPMC, in agreement with literature. It has been reported that the DLC of PCL-PEG-PCL micelles encapsulating nimodipine increases from 3.03 to 4.96% with increasing PCL block length [23]. Similar results are obtained for PEG-PCL micelles encapsulating amiodarone [27]. It is also noteworthy that the drug loading capacity of HPMC-PLA is comparable with those of PLA-PEG copolymer micelles which present a DLC from 4.7% to 6.5% [6].

HPMC-PLA micelles were selected for drug release studies as they exhibit better drug loading capacity as compared to HPMC-PLLA ones. Fig. 3.7 shows the release profiles of PTX from copolymers micelles. A biphasic pattern is observed. All micelles exhibit a large burst release of *c.a.* 40% at 6 h, followed by a slower release to reach 80.4%, 73.8%, and 66.7% at 120 h for PLA_{20}-HPMC, PLA_{30}-HPMC and PLA_{40}-HPMC, respectively. The burst release could be assigned to the fact that drug is partly located at the core-shell interface [26]. PLA_{40}-HPMC exhibits the lowest release ratio at the later stages. Nevertheless, the amount of cumulative released drug is very close for the 3 copolymers. Similar results has been reported for PCL-PEG-PCL micelles which exhibit a decrease of drug release rate with increase of PCL block length [23].

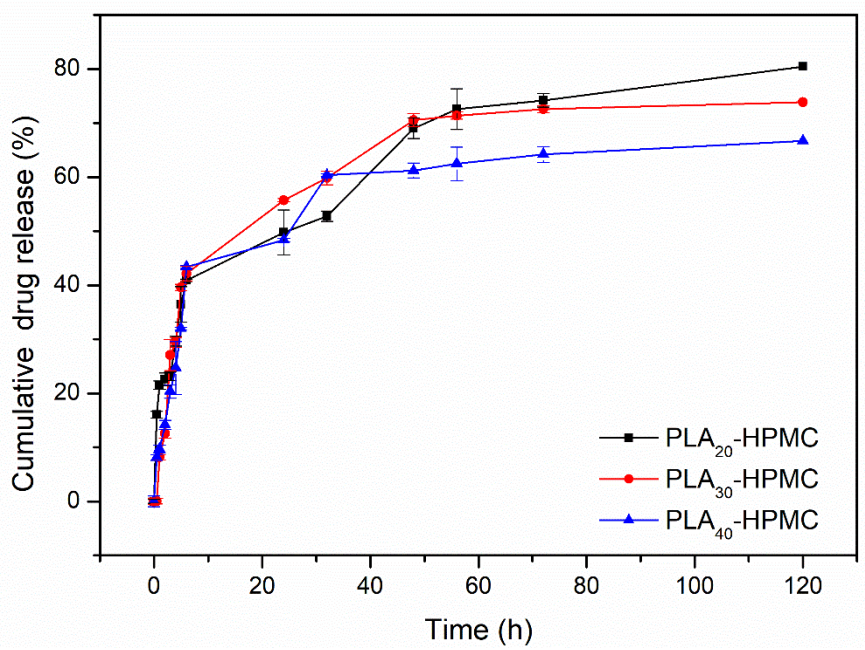

Fig. 3. 7 In vitro release curves of PTX from HPMC-PLA copolymer micelles. Each point represents mean ± SD for three samples. Error bars represent the standard deviation (n = 3)

3.3.4 Biocompatibility of HPMC-PLA copolymer micelles

In vitro cytotoxicity of blank micelles is evaluated by MTT assay using murine fibroblasts L-929 cells [28]. The effect of HPMC-PLLA$_{10}$ and HPMC-PLLA$_{20}$ micelle solutions on the growth of L-929 cells is shown in Fig. 3.8(A, B). The cell viability of cells remains above 95% when the micelle concentration increases from 0.25 to 5.0 mg/mL, and after incubation up to 72h. In contrast to the positive control, HPMC-PLLA micelles are not toxic to L-929 cells according to the US Pharmacopeia Standards.

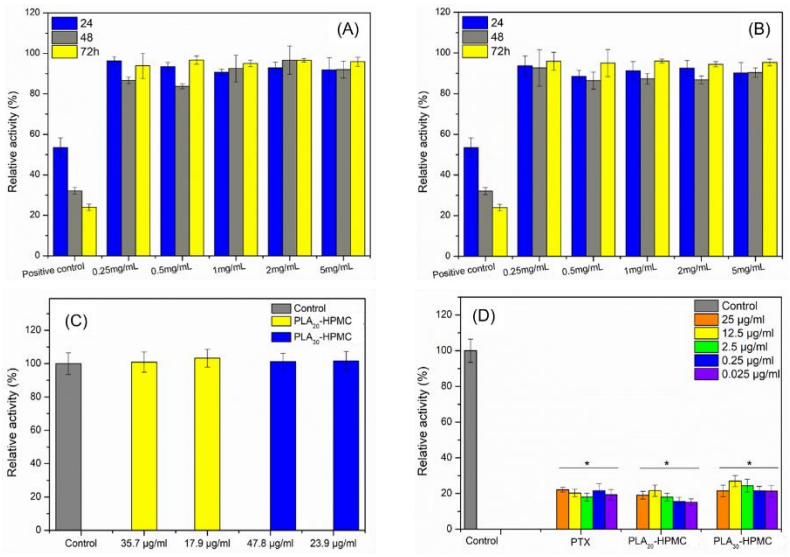

Fig. 3. 8 Relative activity of L-929 cells after 24, 48 and 72 h culture with $PLLA_{10}$-HPMC (A) and $PLLA_{20}$-HPMC (B) micelle solutions at different concentrations compared to the positive control. Data are presented as the mean ± sd (n = 3). Relative activity of SK-BR-3cells after 72 h culture with blank micelles of PLA_{20}-HPMC and PLA_{30}-HPMC at different concentrations (C), free PTX and drug-loaded micelles at different PTX concentrations (D) compared to the positive control. Data are presented as the mean ± sd (n = 12) (*P < 0.05 *versus* the control)

3.3.5 Cytotoxic activity of drug-loaded micelles

In vitro cytotoxicity of drug-loaded micelles was evaluated by SRB assay using a human breast cancer cell line, SK-BR-3 cells. SRB assay was used by Skehan et al. [29] to determine cell density by measuring cellular protein content. SRB is a water-soluble protein dye that can bind with residues basic amino acids of protein in cells under mild acidic conditions, and can be dissolved under mild basic conditions. The amount of SRB bound in cells reflects the total protein amount and thus the number of cells. A linearity is observed over a 20-fold range with high reproducibility [30].

The effect of HPMC-PLA_{20} and HPMC-PLA_{30} blank micelles on the growth of SK-BR-3 cells is shown in Fig. 3.8 C. Blank micelles were tested at concentrations corresponding to those of drug-loaded micelles (18 – 48 μg/mL). The viability of cells cultured with blank micelles is comparable to that of the control. Even the highest

micelle concentration did not affect the cell viability.

The effect of free PTX and PTX-loaded micelles on the proliferation of SK-BR-3cells was examined in the PTX concentration range of 0.025–25 μg/mL as shown in Fig. 3.8(D). For both free PTX and drug-loaded micelles, even the lowest concentration (0.025 μg/mL) significantly reduced cell proliferation. The cytotoxic effect was comparable in the whole PTX concentration range. Similar cytotoxicity on SKBR3 cells was observed after treatment with 0.3-30 nM PTX or Tripalm-NPs-PTX [31].

3.4 Conclusion

Amphiphilic HPMC-PLLA and HPMC-PLA diblock copolymers with different hydrophobic block lengths were synthesized by using combination of ROP and reductive amination. NMR, DOSY-NMR, and FT-IR analyses showed that block copolymers were successfully obtained. All copolymers can self-assemble in aqueous medium into spherical micelles with narrow distribution. The CMC decreases with increase of hydrophobic block length. The DLC and DLE of copolymers increase with increasing PLA block length. HPMC-PLA micelles exhibit biphasic drug release. Both MTT and SRB assays demonstrate the outstanding cytocompatibility of HPMC-PLA copolymers. Last but not least, PTX-loaded micelles exhibit significant cytotoxicity to SK-BR-3cells, thus showing that HPMC-PLA copolymer micelles could be most promising as nano-carrier of antitumor drugs.

References

[1] Y. Mai, A. Eisenberg, Self-assembly of block copolymers, Chem Soc Rev 41(18) (2012) 5969-85.

[2] Z. Liu, M. Chen, Y. Guo, X. Wang, L. Zhang, J. Zhou, H. Li, Q. Shi, Self-assembly of cationic amphiphilic cellulose-g-poly (p-dioxanone) copolymers, Carbohydr Polym 204 (2019) 214-222.

[3] M.-C. Jones, J.-C. Leroux, Polymeric micelles – a new generation of colloidal

drug carriers, European Journal of Pharmaceutics and Biopharmaceutics 48(2) (1999) 101-111.
[4] P. Saini, M. Arora, M. Kumar, Poly(lactic acid) blends in biomedical applications, Adv Drug Deliv Rev 107 (2016) 47-59.
[5] H. Tsuji, Poly(lactide) Stereocomplexes: Formation, Structure, Properties, Degradation, and Applications, Macromolecular Bioscience 5(7) (2005) 569-597.
[6] K. Jelonek, S. Li, X. Wu, J. Kasperczyk, A. Marcinkowski, Self-assembled filomicelles prepared from polylactide/poly(ethylene glycol) block copolymers for anticancer drug delivery, Int J Pharm 485(1-2) (2015) 357-64.
[7] Y. Yi, G. Lin, S. Chen, J. Liu, H. Zhang, P. Mi, Polyester micelles for drug delivery and cancer theranostics: Current achievements, progresses and future perspectives, Mater Sci Eng C Mater Biol Appl 83 (2018) 218-232.
[8] A. Lu, E. Petit, S. Li, Y. Wang, F. Su, S. Monge, Novel thermo-responsive micelles prepared from amphiphilic hydroxypropyl methyl cellulose-block-JEFFAMINE copolymers, Int J Biol Macromol 135 (2019) 38-45.
[9] L.I. Atanase, J. Desbrieres, G. Riess, Micellization of synthetic and polysaccharides-based graft copolymers in aqueous media, Prog Polym Sci 73 (2017) 32-60.
[10] W. Yuan, J. Zhang, H. Zou, T. Shen, J. Ren, Amphiphilic ethyl cellulose brush polymers with mono and dual side chains: Facile synthesis, self-assembly, and tunable temperature-pH responsivities, Polymer 53(4) (2012) 956-966.
[11] E. Ostmark, D. Nystrom, E. Malmstrom, Unimolecular nanocontainers prepared by ROP and subsequent ATRP from hydroxypropylcellulose, Macromolecules 41(12) (2008) 4405-4415.
[12] J. Wang, M. Caceres, S. Li, A. Deratani, Synthesis and Self-Assembly of Amphiphilic Block Copolymers from Biobased Hydroxypropyl Methyl Cellulose and Poly(l
-lactide), Macromol Chem Phys 218(10) (2017) 1600558.
[13] A. Lu, J. Wang, M.C. Najarro, S. Li, A. Deratani, Synthesis and self-assembly of

AB2-type amphiphilic copolymers from biobased hydroxypropyl methyl cellulose and poly(L-lactide), Carbohydrate Polymers 211 (2019) 133-140.

[14] A. Moussa, A. Crepet, C. Ladaviere, S. Trombotto, Reducing-end "clickable" functionalizations of chitosan oligomers for the synthesis of chitosan-based diblock copolymers, Carbohydr Polym 219 (2019) 387-394.

[15] A.F. Abdel-Magid, S.J. Mehrman, A review on the use of sodium triacetoxyborohydride in the reductive amination of ketones and aldehydes, Org Process Res Dev 10(5) (2006) 971-1031.

[16] Y. Hu, V. Darcos, S. Monge, S. Li, Thermo-responsive drug release from self-assembled micelles of brush-like PLA/PEG analogues block copolymers, Int J Pharm 491(1-2) (2015) 152-61.

[17] W. Zhang, M. Torabinejad, Y. Li, Evaluation of Cytotoxicity of MTAD Using the MTT-Tetrazolium Method, Journal of Endodontics 29(10) (2003) 654-657.

[18] M. Gotsche, H. Keul, H. Höcker, Amino-termined poly(L-lactide)s as initiators for the polymerization of N-carboxyanhydrides: synthesis of poly(L-lactide)-block-poly(α-amino acid)s, Macromol Chem Phys 196(12) (1995) 3891-3903.

[19] M. Ju, F. Gong, S. Cheng, Y. Gao, Fast and Convenient Synthesis of Amine-Terminated Polylactide as a Macroinitiator forω-Benzyloxycarbonyl-L-Lysine-N-Carboxyanhydrides, International Journal of Polymer Science 2011 (2011) 1-7.

[20] G. Pages, V. Gilard, R. Martino, M. Malet-Martino, Pulsed-field gradient nuclear magnetic resonance measurements (PFG NMR) for diffusion ordered spectroscopy (DOSY) mapping, Analyst 142(20) (2017) 3771-3796.

[21] J. Aguiar, P. Carpena, J.A. Molina-Bolívar, C. Carnero Ruiz, On the determination of the critical micelle concentration by the pyrene 1:3 ratio method, Journal of Colloid and Interface Science 258(1) (2003) 116-122.

[22] Y. Hu, X. Jiang, Y. Ding, L. Zhang, C. Yang, J. Zhang, J. Chen, Y. Yang, Preparation and drug release behaviors of nimodipine-loaded poly(caprolactone)–poly(ethylene oxide)–polylactide amphiphilic copolymer nanoparticles, Biomaterials 24(13) (2003) 2395-2404.

[23] H. Ge, Y. Hu, X. Jiang, D. Cheng, Y. Yuan, H. Bi, C. Yang, Preparation, characterization, and drug release behaviors of drug nimodipine-loaded poly(ε-caprolactone)-poly(ethylene oxide)-poly(ε-caprolactone) amphiphilic triblock copolymer micelles, Journal of Pharmaceutical Sciences 91(6) (2002) 1463-1473.

[24] K. Jelonek, S. Li, B. Kaczmarczyk, A. Marcinkowski, A. Orchel, M. Musial-Kulik, J. Kasperczyk, Multidrug PLA-PEG filomicelles for concurrent delivery of anticancer drugs-The influence of drug-drug and drug-polymer interactions on drug loading and release properties, Int J Pharm 510(1) (2016) 365-74.

[25] C. Wang, Y. Wang, Y. Wang, M. Fan, F. Luo, Z. Qian, Characterization, pharmacokinetics and disposition of novel nanoscale preparations of paclitaxel, Int J Pharm 414(1-2) (2011) 251-9.

[26] Z.L. Tyrrell, Y. Shen, M. Radosz, Fabrication of micellar nanoparticles for drug delivery through the self-assembly of block copolymers, Prog Polym Sci 35(9) (2010) 1128-1143.

[27] S. Elhasi, R. Astaneh, A. Lavasanifar, Solubilization of an amphiphilic drug by poly(ethylene oxide)-block-poly(ester) micelles, Eur J Pharm Biopharm 65(3) (2007) 406-13.

[28] H. Li, S. Tao, Y. Yan, G. Lv, Y. Gu, X. Luo, L. Yang, J. Wei, Degradability and cytocompatibility of tricalcium phosphate/poly(amino acid) composite as bone tissue implants in orthopaedic surgery, Journal of Biomaterials Science, Polymer Edition 25(11) (2014) 1194-1210.

[29] P. Skehan, R. Storeng, D. Scudiero, A. Monks, J. McMahon, D. Vistica, J.T. Warren, H. Bokesch, S. Kenney, M.R. Boyd, New Colorimetric Cytotoxicity Assay for Anticancer-Drug Screening, JNCI: Journal of the National Cancer Institute 82(13) (1990) 1107-1112.

[30] W. Voigt, Sulforhodamine B assay and chemosensitivity, Methods Mol Med 110 (2005) 39-48.

[31] M.C. Leiva, R. Ortiz, R. Contreras-Caceres, G. Perazzoli, I. Mayevych, J.M. Lopez-Romero, F. Sarabia, J.M. Baeyens, C. Melguizo, J. Prados, Tripalmitin

nanoparticle formulations significantly enhance paclitaxel antitumor activity against breast and lung cancer cells in vitro, Sci Rep 7(1) (2017) 13506.

Chapter 4. Synthesis and Self-Assembly of Amphiphilic Block Copolymers from Hydroxypropyl Methyl Cellulose and Poly(ε-caprolactone)

Abstract: A serious of amphiphilic diblock copolymers with different hydrophilic and hydrophobic block lengths were synthesized from hydroxypropyl methyl cellulose (HPMC) and amino-terminated poly(ε-caprolactone) (NH_2-PCL) by reductive amination. NH_2-PCL was synthesized by ring-opening polymerization of ε-caprolactone using 3-(Boc-amino)-1-propanol as initiator, followed by removal of the Boc group with trifluoroacetic acid treatment. NMR, DOSY-NMR, FT-IR, and Kaiser test confirmed the successful synthesis of block copolymers. Self-assembly of copolymers yielded spherical micelles of *c.a.* 200 nm with narrow size distribution, as evidenced by dynamic light scattering and transmission electron microscopy. Larger micelle size was obtained for copolymers with longer hydrophilic HPMC blocks. The critical micelle concentration determined by fluorescence spectroscopy decreases with increase of the hydrophobic PCL block length. Curcumin was loaded in copolymer micelles. A biphasic release profile is observed, including an initial burst followed by slower release. Faster drug release is observed for copolymers with shorter PCL block length and lower drug load. HPMC-PCL copolymer micelles present outstanding cytocompatibility, as shown by MTT test using L929 cells. Therefore, biobased and biodegradable HPMC-PCL block copolymers could be promising as nano-carrier of hydrophobic anticancer drugs.

Key words: hydroxypropyl methyl cellulose; poly(ε-caprolactone); block copolymer; reductive amination; micelle; self-assembly; drug release

4.1 Introduction

In the past decades, polymeric micelles have attracted increasing attention as drug delivery systems due to their unique advantages including enhanced drug solubility, prolonged blood circulation, passive targeting to tumor issue by enhanced permeability and retention (EPR) effect, enhanced drug bioavailability and reduced side effects [1]. Micelles are generally obtained by self-assembly of amphiphilic block copolymers. The hydrophobic component aggregates into the core which is able to encapsulate hydrophobic drugs, whereas the hydrophilic component forms the shell to stabilize the micelle structure in aqueous medium. Generally, amphiphilic copolymers used in drug delivery should be biocompatible, bioresorbable, and non-toxic as they should be metabolized in or excreted from the human body without causing adverse reactions. Poly(ε-caprolactone) (PCL) is a FDA-approved biocompatible and biodegradable polyester which is extensively studied as drug carriers, medical implants and tissue engineering scaffolds [2]. In drug delivery, PCL has been widely used in many formulations such as nanoparticles, nanofibers, hydrogels, polymersomes, micelles, polyplexes and drug-conjugates [3]. In fact, PCL can be used as a degradable and hydrophobic block to combine with various hydrophilic polymers, including both natural biopolymers like starch [4], and chitosan [5, 6], and synthetic polymers such as poly(ethylene glycol) (PEG) [3], polyurethane (PU) [7], *etc*. Importantly, PCL is compatible with a wide range of drugs [8, 9]. It has been reported that PCL-based micelles can encapsulate doxorubicin [10, 11], 5-fluoro uracil [12], curcumin [6], paclitaxel [13], nimodipine [14], *etc.*

As a hydrophilic polymer, polysaccharides including cellulose, chitosan, alginate, dextran, cyclodexitrin, *etc*. have attracted widespread interest due to their biocompatibility, biodegradabibility, non-toxicity and the presence of numerous hydroxyl groups allowing chemical modification [15]. Among them, cellulose is the most abundant polysaccharide which is a linear β-1,4-glucan molecule with an acetal linkage between C1 and C4 carbon atoms [16]. Due to the presence of hydroxyl groups,

there exists strong intermolecular and intramolecular hydrogen bonding which leads to insolubility of cellulose in either organic solvents or aqueous media [17]. This insolubility greatly restrains the potential applications of cellulose for the synthesis of amphiphilic copolymers. To overcome this limitation, substitution derivatives of cellulose are synthesized, including hydroxyethyl cellulose (HEC), carboxymethyl cellulose (CMC), ethyl cellulose (EC), hydroxypropyl cellulose (HPC), and hydroxyl propylmethyl cellulose (HPMC) [18]. Controlled radical polymerization processes based on the hydroxyl groups have been used to synthesize well-defined graft copolymers. Eduardo et al. synthesized a series of oxidized carboxymethyl cellulose-graft-poly(ethylene glycol)-dodecylamine (OCMC-g-PEG-DDA) with different contents of DDA [19]. The copolymers are able to form micelles with narrow size distribution. Wang et al. synthesized ethyl cellulose-graft-poly(2-(diethylamino) ethyl methacrylate) (EC-g-PDEAEMA) [20]. pH-responsive micelles are obtained from the copolymers which can efficiently encapsulate rifampicin. Das et al. evaluated hydroxypropyl methyl cellulose-graft-polyacrylamide (HPMC-g-PAM) as a potential carrier of 5-amino salicylic acid [21]. However, grafting polymerization is poorly controllable due to the large number of hydroxyl groups on the polymer backbone. In contrast, water soluble cellulose derivatives can be used as a hydrophilic component for the preparation of amhiphilic block copolymers since the reducing end (hemiacetal group) of cellulose is easily converted to an aldehyde group. Reductive amination between aldehyde and amino groups is well established, but is rarely used to synthesize cellulose based block copolymers because of the lack of common solvent for the two blocks, the side reactions induced by lateral hydroxyl groups, and the limited availability of the hemiacetal group at the chain end.

In our previous work, linear amphiphilic and thermo-responsive HPMC-polylactide (HPMC-PLA) and AB_2-type $(HPMC)_2$-PLA block copolymers were synthesized for the first time by combination of ring-opening polymerization (ROP), amination reduction and UV initiated thiol-yne or thiol-ene click reaction [22, 23]. More recently, diblock, triblock and three-armed copolymers were synthesized by

reductive amination between the aldehyde endgroup of HPMC and the amine group of monoamine, diamine, or triamine JEFFAMINE. These various amphiphilic and thermo-responsive copolymers are able to self-assemble in micelles and serve as nanocarrier of hydrophobic drugs. In this work, amino-terminated PCL (NH_2-PCL) was synthesized by tertbutyl-N-(3-hydroxypropyl) carbamate initiated ROP of ε-caprolactone, followed by removal of the N-tert-butoxycarbonyl (Boc) group. HPMC-PCL block copolymers with various PCL and HPMC block lengths were then obtained by reductive amination between the amine group of NH_2-PCL and the hemiacetal end group of HPMC. The self-assembly, drug loading and drug release behaviors, and the biocompatibility of HPMC-PCL copolymers were investigated to evaluate their potential in controlled delivery of hydrophobic antitumor drugs.

4.2 Materies and Methods

4.2.1 Materials

ε-caprolactone was purchased from Aldrich and purified by distillation under reduced pressure. HPMC was provided by Dow Colorcon Limited France, and HPMC oligomers with Mw of 7000 and 18000 Daltons were obtained by enzymatic depolymerization as reported in our previous work [22, 23]. Tert-butyl-*N*-(3-hydroxypropyl) carbamate (3-(Boc-amino)-1-propanol), tin(II) 2-ethylhexanoate ($Sn(Oct)_2$), sodium triacetoxyborohydride ($NaBH(OAc)_3$) and curcumin (CUR) were purchased from Sigma-Aldrich, and used as received. Trifluoroacetic acid (TFA) was purchased from Merck KGaA. Dichloromethane was purchased from Sigma-Aldrich, dried by anhydrous calcium chloride ($CaCl_2$) and distilled before use.

4.2.2 Synthesis of amino terminated PCL

Amino terminated PCL was synthesized by ROP of ε-carprolactone using 3-(Boc-amino)-1-propanol as initiator and $Sn(Oct)_2$ as catalyst, followed by deprotection with TFA [24, 25]. Typically, ε-caprolactone (40 mmol, 4.56 g), 3-(Boc-amino)-1-propanol (2 mmol, 0.35 g) and $Sn(Oct)_2$ (2.3 mmol, 0.0932 g) were introduced into a dried Schlenk tube. The mixture was degassed by performing three freeze-pump-thaw cycles.

Polymerization then proceeded in an oil bath at 120 ℃ for 24 h. The crude product was dissolved in dichloromethane, precipitated in cold methanol, and vacuum dried up to constant weight to yield Boc-NH-PCL as a white powder.

Subsequently, the Boc group of Boc-NH-PCL was removed with TFA. Typically, 1 g Boc-NH-PCL was dissolved in 5 mL freshly distilled dichloromethane in a dried flask. The setup was purged with nitrogen, and 5 mL anhydrous TFA was added. The solution was stirred at room temperature for 1 h. Then the solvent and residual TFA were removed by using rotary evaporator. The crude product was dissolved in dichloromethane, successively washed with aqueous $NaHCO_3$ (5%) and water, and finally dried over $MgSO_4$. After filtration, the solution was precipitated in cold methanol, and vacuum dried at room temperature up to constant weight.

4.2.3 Synthesis of HPMC-PCL block copolymers

HPMC-PCL block copolymers were synthesized by reductive amination according to literature [26, 27]. Briefly, NH_2-PCL (0.154 mmol, 0.16 g), HPMC (0.14 mmol, 1.0 g) with Mw=7000, and $NaBH(OAc)_3$ (0.2 mmol, 0.042 g) were dissolved in 20 mL anhydrous DMSO under stirring. The reaction proceeded 72 h under nitrogen atmosphere at 35 ℃. The crude product was purified by dialysis in deionized water for 72 h, followed by 48 h freeze-drying.

4.2.4 Characterization

^1H NMR was performed on 300 MHz Bruker spectrometer (AMX300), and diffusion ordered spectroscopy (DOSY) NMR was performed on a 400 MHz Bruker Avance spectrometer (AQS400) equipped with a Bruker multinuclear z-gradient inverse probe head. $CDCl_3$, DMSO-d_6 and D_2O were used as solvent. NMR spectra were processed by using MestRe Nova software, and DOSY NMR spectra by using Bruker topspin software.

Kaiser test was performed using Kaiser test kit from Sigma-Aldrich containing KCN in H_2O/pyridine (Reagent A), 6% Ninhydrin in ethanol (Reagent B), and 80% phenol in ethanol (Reagent C). A small amount of polymer was added into a test tube, followed by successive addition of 2 or 3 drops of Reagent A, B, and C. Then, the tube

was heated at 110 ℃ for 5 minutes. The solution color was finally compared to that of the control without addition of polymer. The tests were performed in triplicate.

Gel permeation chromatography (GPC) was performed on a Viscotek TDA 305 multidetector GPC/SEC system. All samples were dissolved in THF at a concentration of 10 g/L, and filtered through 0.22 μm Millipore filters before injection. Calibration was realized with polystyrene standards (Polysciences, Warrington, PA).

Fourier transform infrared (FT-IR) spectra were recorded on a Nicolet NEXUS spectrometer using attenuated total reflectance (ATR) mode at 4 cm^{-1} resolution. Each sample was scanned 32 times in the range from 600 to 4000 cm^{-1}.

Dynamic light scattering (DLS) was carried out on Anton Parr Litesizer 500. Samples were prepared at a concentration of 1.0 mg mL^{-1}, and filtered through a 0.45 μm cellulose acetate (CA) filter. Measurements were performed at 25 ℃ and at a scattering angle of 90 °.

The critical micelle concentration (CMC) of copolymers was determined by fluorescence spectroscopy using pyrene as hydrophobic fluorescent probe. An aqueous pyrene solution (6×10^{-7} g/L) was used to prepare copolymer solutions at concentrations ranging from 1.0×10^{-4} to 2.0 mg/mL. The excitation spectra of the pyrene solutions were registered in the 300 to 360 nm range at an excitation wavenumber of 395. The CMC value was derived from the intensity ratio at 336 nm and 334 nm *versus* copolymer concentration plots.

Transmission electron microscopy (TEM) images were obtained using JEOL 1400 plus instrument at an acceleration voltage of 120 kV. Micelle solution at 1.0 mg mL^{-1} was dropped on a carbon coated copper grid, and exposed to ruthenium oxide vapor for 7 min at room temperature before measurements. Ruthenium(VIII) oxide solution was prepared as follows: sodium periodate (2.0 g) was added in water (50 g), and then ruthenium(IV) oxide (0.30 g) was added in the solution under stirring at room temperature, yielding a yellow solution of ruthenium(VIII) oxide [28, 29].

4.2.5 In vitro drug release

Drug loaded micelles were prepared in two steps. Blank micelles were first

prepared by dissolution of copolymers in distilled water. Predetermined amount of curcumin in ethanol was then added to the micellar solution under vigorous stirring. The solvent was evaporated overnight, yielding drug loaded micelle solution. Unloaded drug was eliminated by filtration using 0.8 μm cellulose acetate filter. Finally the solution was lyophilized and stored at 4 ℃ for further analysis.

HPLC-MS measurements were performed to determine the concentration of curcumin in solution. The mobile phase was a 50/50 v/v mixture of acetonitrile and pH 7.4 phosphate buffered saline (PBS). A calibration curve was previously established from a series of standard curcumin solutions at concentrations ranging from 0.2 to 16 ppm (R^2 =0.999). Drug loading content (DLC) and drug loading efficiency (DLE) of drug loaded micelles were determined from the following equations [30]:

$$\mathrm{DLC} = \frac{\text{weight of loaded drug}}{\text{weight of polymeric micelles}} \times 100\% \quad (1)$$

$$\mathrm{DLE} = \frac{\text{weight of drug in micelles}}{\text{theoretical drug loading}} \times 100\% \quad (2)$$

In vitro release was realized by using dialysis method. Lyophilized drug-loaded micelles were dispersed in pH 7.4 PBS at a concentration of 2.0 mg/mL. 1 mL micelle solution was introduced into a Float-A-Lyzer G2 dialysis device with MWCO of 3 500 Da. Each dialysis device was placed in 40 mL PBS which was renewed regularly to ensure sink conditions. Drug release experiments were realized at 37 ℃ in a water bath under constant shaking. An aliquot of 25 μL was withdrawn from each device at various time intervals up to 120 h, and replaced by the same volume of fresh PBS. The amount of released drug was determined by HPLC.

4.2.6 MTT assay

L-929 cells in logarithmic growth phase were added in 96-well plates (Corning Costar, U.S.A.) at 1 × 10^4 cells/mL in DMEM medium (10% calf serum, 100 μg/mL Penicillin, 100 μg/mL streptomycin), 100 μL per well. The plates were placed in an NU-4850 incubator (NuAire, U.S.A.) at 37 ℃ under humidified atmosphere with 5% CO_2. After 24 h culture, the medium was removed and replaced by 100 μL fresh medium (negative control), phenol solution (positive control), or HPMC-PCL micellar

solution at various concentrations (0.25, 0.5, 1.0, 2.0, 2.5 and 5.0 mg/mL) [31]. After 24, 48 and 72 h, 20 μL MTT solution at 5 mg/mL was added. The medium was removed after 6 h incubation, and 150 μL DMSO was added. The plates were shaken for 10 min. The optical density (OD) was measured by using a microplate reader (Elx800; BioTek, U.S.A.) at 570 nm. The cell viability was calculated from the OD values of the test sample and negative control using the following equation:

$$\text{Relative activity (\%)} = (OD_{\text{test sample}} / OD_{\text{negative control}}) \times 100 \quad (3)$$

All experiments were performed in triplicate, and the data were expressed as the mean ± SD.

4.3 Results and discussion

4.3.1 Synthesis and characterization of amphiphilic copolymers

Amphiphilic HPMC-PCL block copolymers were synthesized in three steps, as shown in Scheme 4.1. Boc-NH_2-PCL was first synthesized by ROP of ε-caprolactone initiated by 3-(Boc-amino)-1-propanol which has a protected amine group and a hydroxyl endgroup. The Boc group was then removed with trifluoroacetic acid to obtain amino terminated PCL. Finally, the hemiacetal end group of HPMC and the amino group of PCL were coupled through reductive amination in the presence of $NaBH(OAc)_3$ [32], yielding an amphiphilic HPMC-PCL block copolymer.

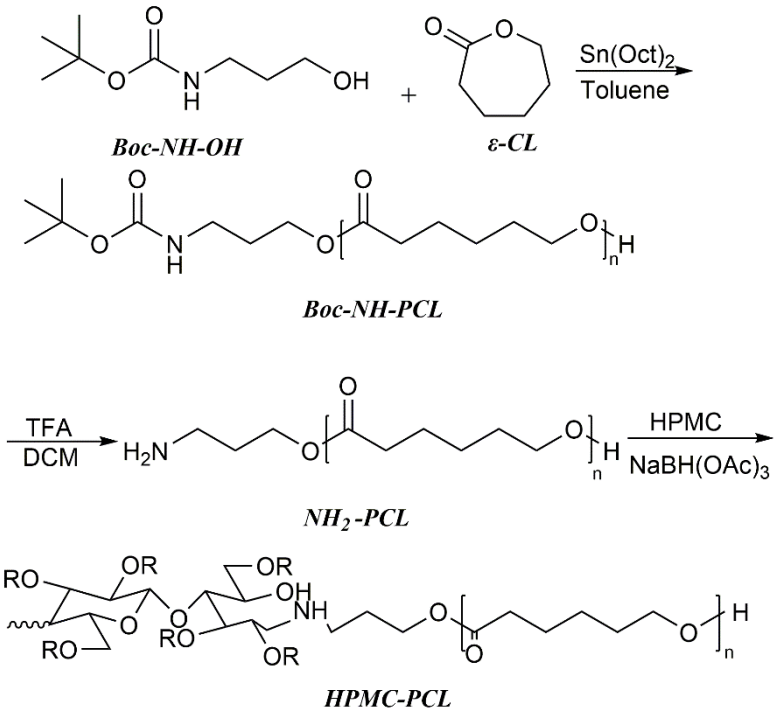

Scheme 4. 1 Synthesis route of HPMC-PCL block copolymers

The synthesis of amino terminated NH_2-PCL was based on the method reported by Gotsche et al. [33, 34]. Boc group was chosen as the protective group because it is stable under the polymerization condition of ε-caprolactone, and can be easily removed under mild conditions [33]. Boc-NH-PCL was synthesized by ROP of ε-caprolactone using 3-(Boc-amino)-1-propanol as initiator with a predetermined monomer/initiator (M/I) molar ratio of 10, 20 or 30. The obtained polymers was characterized by ^{1}H NMR, FT-IR and GPC. As shown in Fig. 4.1A, the signals at 1.42 (**a**), 4.18 (**e**), 1.84 (**d**) and 3.20 (**c**) ppm correspond to the methyl and the methylene groups of the terminal Boc group, respectively. And the signals at 1.30 (**h**), 1.62 (**j**), 2.75 (**f**) and 4.0 (**i**) ppm belong to the methyne protons of PCL backbone. The degree of polymerization (DP) of PCL was estimated from the integration ratio of signals **f** to **c**. The obtained DP of PCL polymers is 10.8, 22.4 and 30.5, respectively, which is very close to the feed ratio. The number average molar mass (Mn_{NMR}) was calculated from the DP values. It varied from 1320 to 3600 as summarized in Table 4.1.

Table 4. 1 Characterization of Boc-NH-PCL polymers by NMR and GPC

Sample	M/I feed ratio	DP_{PCL} a)	Mn_{NMR} a)	Mn_{GPC} b)	$Đ$ b)
PCL_{10}	10	10.8	1320	3180	1.29
PCL_{20}	20	22.4	2680	4200	1.41
PCL_{30}	30	30.5	3600	5140	1.34

a) Determined from NMR

b) Determined from GPC

The molar mass and dispersity ($Đ$ = Mw/Mn) of polymers were also confirmed by GPC, as shown in Fig. 4.2A. A symmetric molar mass distribution is observed. The Mn_{GPC} increases from 3180 to 5140 with increase of DP_{PCL} from 10 to 30, whereas the dispersity ranges from 1.29 to 1.41 (Table 4.1). The Mn_{GPC} values are larger than those from NMR. The difference can be assigned to the fact that Mn_{GPC} is obtained on the basis of the hydrodynamic volume of polymer chains in the solvent compared to polystyrene standards, in contrast to Mn_{NMR} values which are calculated from the integrations of NMR signals.

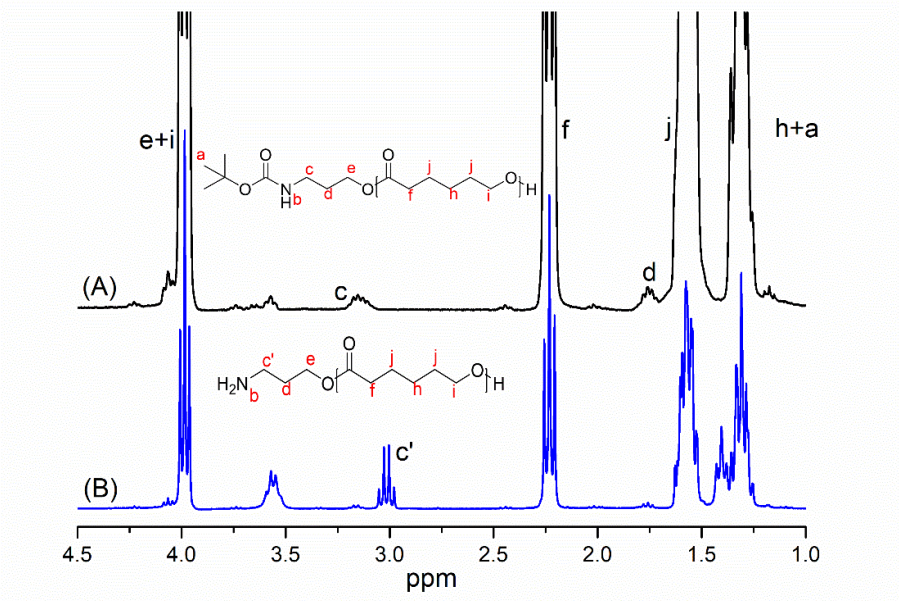

Fig. 4. 1 NMR spectra of Boc-NH-PCL_{10} (A) and NH_2-PCL_{10} (B) in $CDCl_3$

NH_2-PCL was obtained by treating Boc-NH-PCL with TFA to remove the Boc group. As shown in Fig. 4.2, the two GPC curves of Boc-NH-PCL_{30} and NH_2-PCL_{30}

almost overlap. In other words, deprotection by TFA treatment didn't cleave PCL chains. ^{1}H NMR was performed to evidence the effective removal of the Boc group. The methyl peak (**a**) at 1.42 ppm corresponding to the methyl of terminal Boc group totally disappears, and the signal (**c**) at 3.20 ppm shifts from 3.20 to 2.75 ppm (**c'**) due to the conversion of the adjacent acylamino group to amino group. The intensity ratio between signals **c** and **f** remains constant after deprotection, which means that deprotection does not provoke polymer degradation.

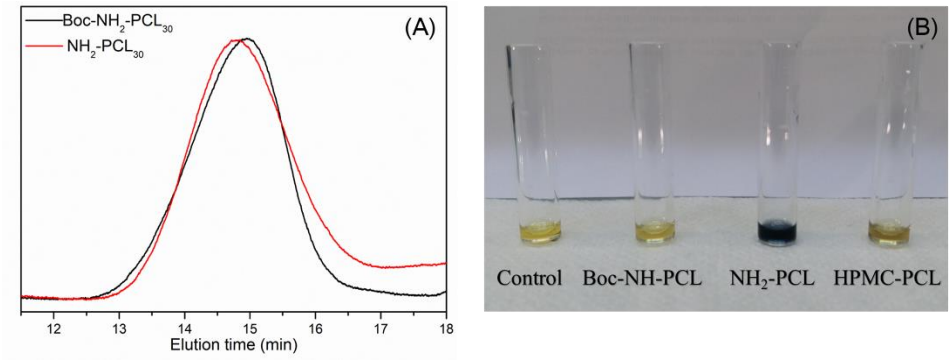

Fig. 4. 2 GPC curves of Boc-NH-PCL$_{30}$ and NH$_2$-PCL$_{30}$ in THF (A), Kaiser test of Boc-NH-PCL$_{30}$, NH$_2$-PCL$_{30}$ and HPMC7K-PCL$_{30}$ (B)

Kaiser test is commonly utilized to evidence the presence of primary amines. The main effective constituent of the Kit, ninhydrin reacts with amine groups to produce an intense blue color. As shown in Fig. 4.2B, Boc-NH-PCL presents almost the same color as the control, while NH$_2$-PCL solution is dark blue. This finding demonstrates the presence of primary amino groups in NH$_2$-PCL, but not in Boc-NH-PCL.

Finally, amphiphilic HPMC-PCL block copolymers were synthesized by reductive amination of the amine group of PCL and the hemiacetal end group of HPMC in the presence of a reducing agent, NaBH(OAc)$_3$. Six HPMC-PCL copolymers were obtained in this work, namely HPMC7K-PCL$_{10}$, HPMC7K-PCL$_{20}$, HPMC7K-PCL$_{30}$, HPMC18K-PCL$_{10}$, HPMC18K-PCL$_{20}$, HPMC18K-PCL$_{30}$ (Table 4.2). The ^{1}H NMR spectra of HPMC-PCL in DMSO-d_6 and D$_2$O are shown in Fig. 4.3. Signals at 1.05 ppm (**q**) belongs to the methyl protons of hydroxypropyl substitution group, and signals in

the range of 2.75–4.75 ppm (**p**) correspond to the methylene and methine protons of the substitution group, methyl protons adjacent to the oxygen moieties of ether linkage, and the protons of glucose units (Fig. 4.3A). The signals at 1.30 (**h**), 1.62 (**j**), 2.75 (**f**) and 4.0 (**i**) ppm belong to the methylene protons of PCL blocks. Kaiser test also corroborates with the effective reductive amination (Fig. 4.2B). In fact, HPMC-PCL almost shows the same color as the control, indicating the absence of primary amines. In other words, all the terminal amino groups of NH_2-PCL_{30} have reacted with aldehyde groups of HPMC.

Table 4. 2 Self-assembly and drug loading properties of HPMC-PCL block copolymers

Sample	Size (nm)	PDI	ZETA (mV)	CMC (mg/mL)	DLC (%)	DLE (%)
HPMC7K-PCL_{10}	179.0±2.1	0.16	-4.5±0.3	0.012	4.3	41.5
HPMC7K-PCL_{20}	182.8±1.2	0.17	-2.3±0.4	0.0058	5.1	48.2
HPMC7K-PCL_{30}	195.9±2.5	0.12	-6.7±0.2	0.0009	8.2	75.8
HPMC18K-PCL_{10}	205.1±3.4	0.19	-6.8±0.2	0.009	3.8	36.4
HPMC18K-PCL_{20}	216.9±1.3	0.16	-8.9±0.4	0.005	4.4	41.7
HPMC18K-PCL_{30}	222.0±3.0	0.11	-5.4±0.2	0.003	7.2	67.0

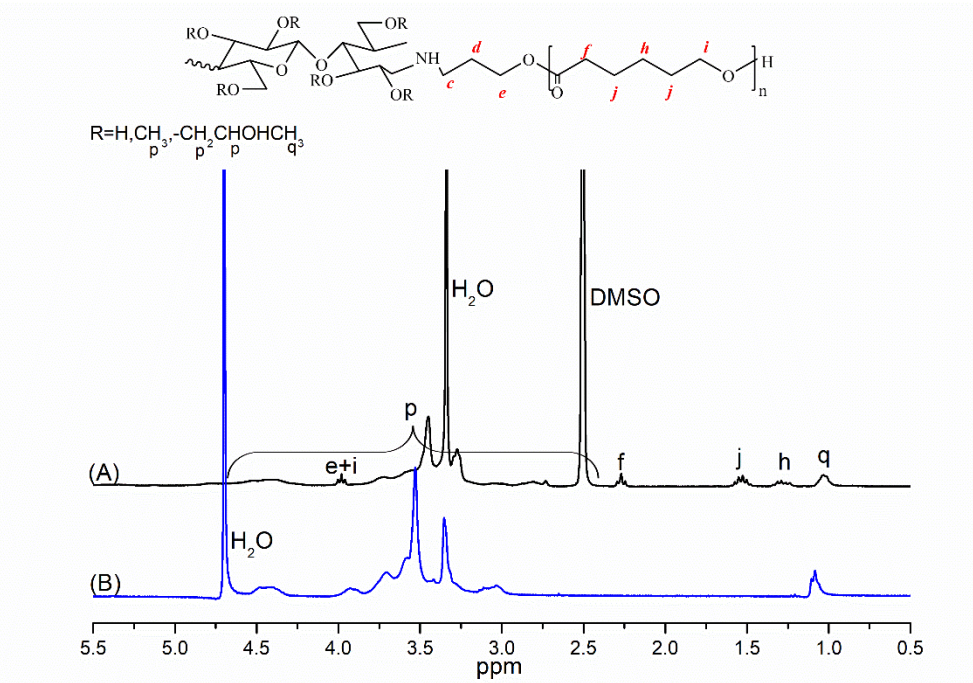

Fig. 4. 3 ^{1}H NMR spectra of HPMC-PCL$_{10}$ in DMSO-d_6 (A) and D_2O (B)

DOSY-NMR was also used to evidence the synthesis of HPMC-PCL block copolymers. DOSY-NMR spectrum is a two-dimensional diagram: one dimension shows the chemical shift, and the other dimension provides separation on the basis of differences in self diffusion coefficients of the dissolved molecules [35, 36]. As shown in Fig. 4.4, the resonance signals corresponding to PCL and HPMC present the same diffusion coefficient. This finding indicates that the two components are combined in the same polymer chain, thus confirming the successful synthesis of HPMC-PCL block copolymer.

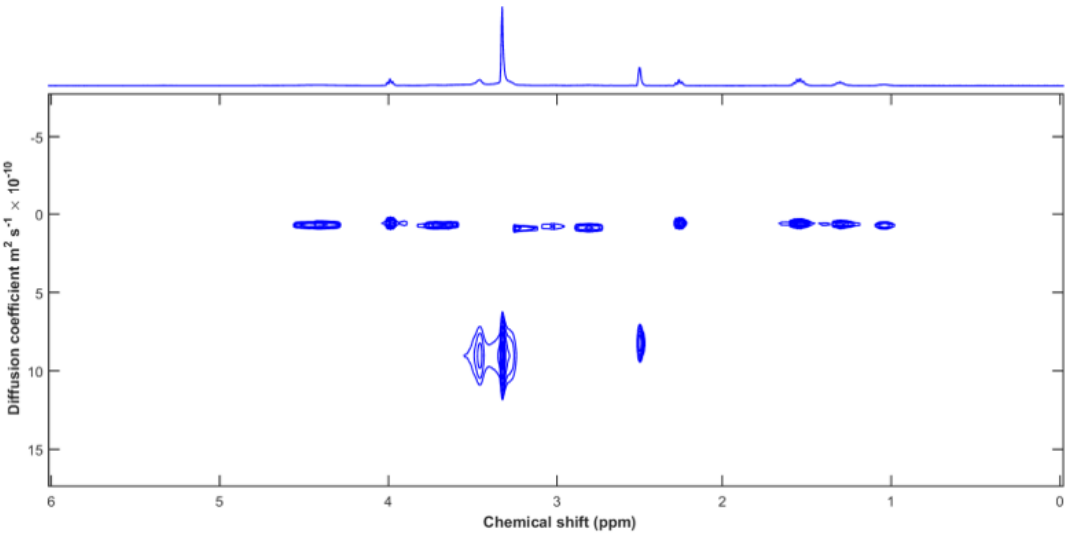

Fig. 4. 4 DOSY- NMR spectrum of HPMC7K-PCL_{30} in DMSO-d_6

As shown in Fig. 4.5, FT-IR was also used to analyze the chemical structure of HPMC copolymers and precursors. Boc-OH presents characteristic bands at 3260, 1689, 1527, 1392 and 1366 cm^{-1} which are assigned to O-H, C=O, CO-NH, and C-H (methyl) groups, respectively. These characteristic bands become much weaker on the spectrum of Boc-NH-PCL, and aren't visible for NH_2-PCL due to removal of the Boc group. The carbonyl band of PCL is detected at 1760 cm^{-1}. On the spectrum of HPMC, absorption bands of O-H, C-H and C-O bonds are detected at 3480, 2890, and 1047 cm^{-1} . Signals corresponding to both HPMC and PCL are observed on the spectrum of HPMC7K-PCL_{30}, which corroborates with the presence of both blocks in the copolymer.

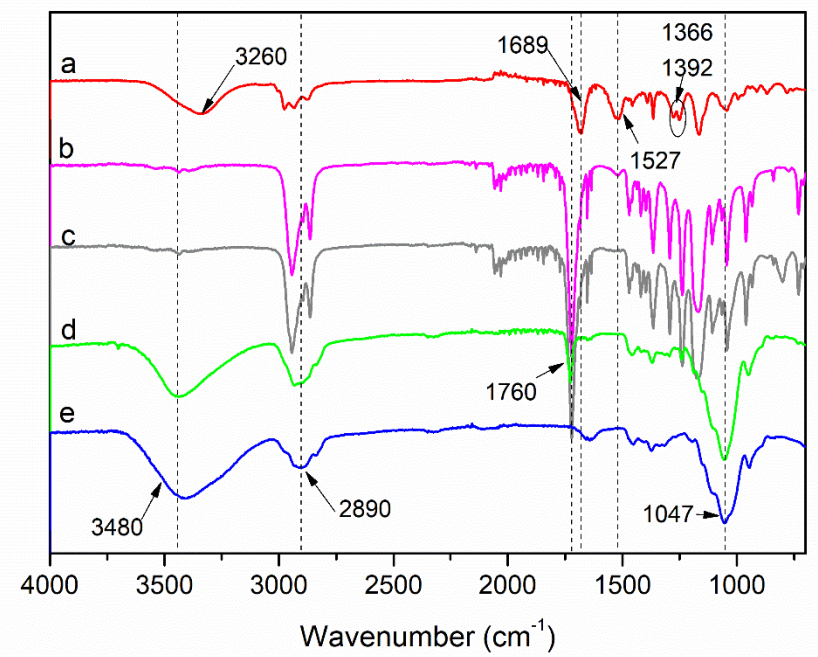

Fig. 4. 5 FT-IR spectra of Boc-OH (a), Boc-NH-PCL_{30} (b), NH_2-PCL_{30} (c), HPMC7K-PCL_{30} (d) and HPMC7K (e)

4.3.2 Self-assembly of amiphiphilic block copolymers

HPMC-PCL amphiphilic block copolymers are able to self-assemble into micelles with shell-core structure by direct dissolution in water. The self-assembly properties of copolymers were investigated by means of NMR, DLS, TEM and fluorescence spectroscopy.

NMR provides a means of choice to examine the core-shell structure of micelles by using selective solvent of the amphiphilic copolymer. Water is able to dissolve the hydrophilic block, *i.e.* the shell block of micelles, but not the hydrophobic block. Thus only the signals corresponding to HPMC are visible on the NMR spectrum in deuterated water, as shown in Fig. 4.3B. Signals belonging to PCL blocks are not detected due to their limited movement. This finding well corroborates with the formation of micelles with a hydrophilic HPMC shell and a hydrophobic PCL core.

The critical micelle concentration (CMC) is an important parameter of self-assembled polymeric micelles. In this work, the CMC was determined by using fluorescence spectroscopy with pyrene as fluorescent probe. Once hydrophobic

association of copolymers occurs in aqueous medium, pyrene significantly migrates into hydrophobic regions, resulting in changes of its photo-physical properties [37]. As shown in Fig. 4.6A, the red shift of the fluorescence excitation spectra signifies the polar environment change of pyrene, indicating pyrene migration into the nonpolar core of micelles and formation of micelles. The CMC is obtained from the two tangent lines of the intensity ratio of I_{336}/I_{334} *versus* polymer concentration plots (Fig. 4.6B). As shown in Table 4.2, the CMC value of HPMC7K-PCL copolymers ranges from 0.012 to 0.0009 g/L, and that of HPMC18K-PCL is in the range of 0.003 to 0.009 g/L. The CMC value decreases with increase of the hydrophobic block length since longer hydrophobic segment favors formation of micelles, which is in agreement with literature data [38-40].

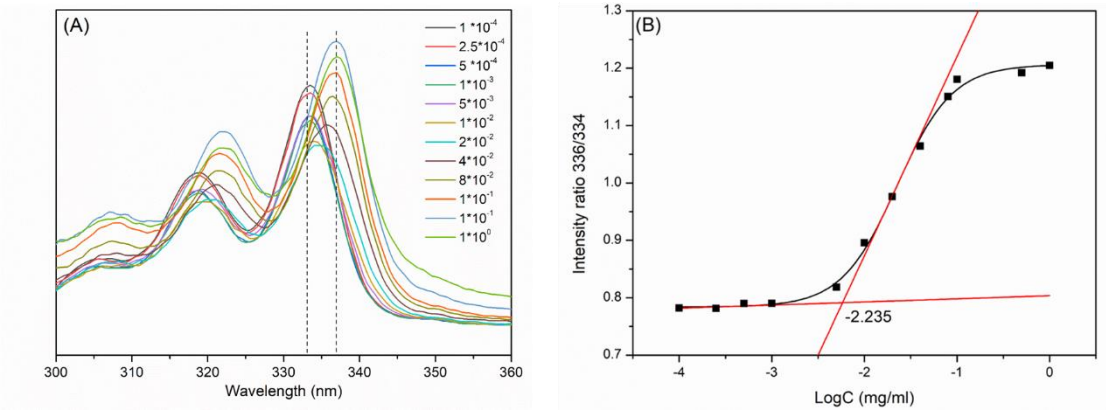

Fig. 4. 6 Fluorescence excitation spectra (A), and I_{336}/I_{334} *vs.* LogC plots (B) of HPMC7K-PCL_{20} diblock copolymer solutions at different concentrations

The micelle size, size distribution and zeta potential of micelles are determined by DLS. The diameter of HPMC7K-PCL micelles is in the range of 179.0-195.9 nm with a narrow polydispersity index (PDI) in the range from 0.12 to 0.17, as shown in Table 4.2. The size of HPMC18K-PCL micelles ranges from 205.1 to 222.0 nm, *i.e.* slightly larger than that of HPMC7K-PCL ones due to the longer hydrophilic block length of the former. In contrast, the micelle size only slightly increases with increase of the PCL block length. The zeta potential of micelles is slightly negative since there are no

charged groups at the surface of the HPMC shell (Table 4.2). The morphology of micelles was visualized by TEM, as shown in Fig. 4.7B. All the HPMC-PCL micelles are uniformly distributed with well defined spherical structure. The size of micelles by TEM ranges from 50 to 100 nm, *i.e.* smaller than that determined by DLS. This difference could be attributed to dehydration of micelles during TEM observation [19].

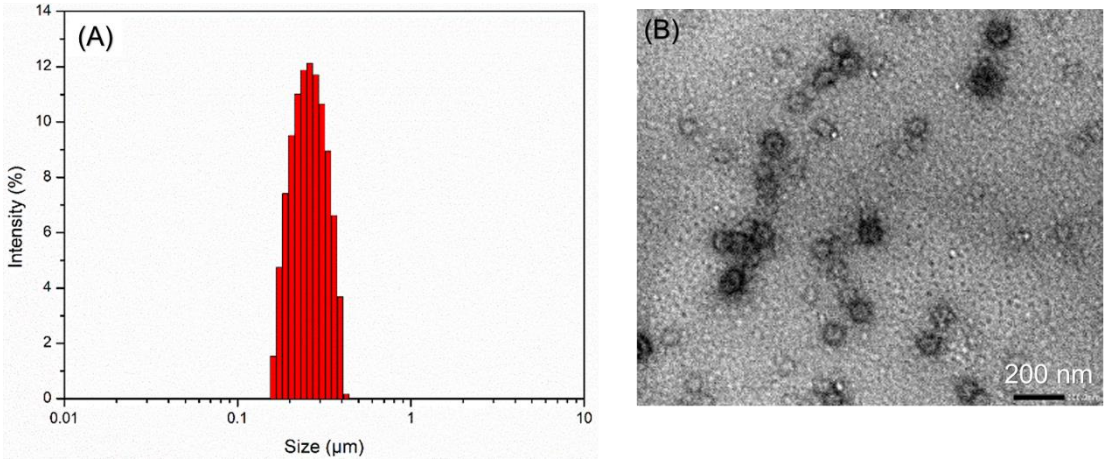

Fig. 4. 7 Size distribution by DLS (A) and TEM image (B) of HPMC7K-PCL_{20} copolymer micelles

4.3.3 Drug loading and in vitro drug release

Curcumin was chosen as the hydrophobic model drug to evaluate the drug loading and release behaviors of HPMC-PCL copolymer micelles. Curcumin is a wide spectrum chemotherapeutic drug with outstanding anti-proliferative and pro-apoptotic activities. In addition, it has been demonstrated that curcumin is able to regulate the intracellular levels of ATP-binding cassette drug transporters which is important for multidrug resistance.

Drug loaded micelles were prepared in two steps, direct dissolution of block copolymers in water to form micelles, and addition of a curcumin solution in methanol to the micellar solution under vigorous stirring. As shown in Table 4.2, higher DLC and DLE are obtained with increase of hydrophobic PCL block length. In the case of the HPMC7K-PCL series, the DLC increases from 4.3% for HPMC7K-PCL_{10} to 8.2% for HPMC7K-PCL_{30}, whereas the DLE increases from 41.5% for HPMC7K-PCL_{10} to 75.8%

for HPMC7K-PCL_{30}. Similar phenomena are observed for HPMC18K-PCL copolymer micelles. Nevertheless, HPMC7K-PCL presents higher DLC and DLE than HPMC18K-PCL with the same PCL block length. In other words, micelles with higher hydrophobic/hydrophilic ratio present stronger encapsulation ability. Danafar et al. reported that DLC and DLE of curcumin encapsulated in PCL-PEG micelles increase from 15.9 to 20.6% and from 65.4 to 82.3, respectively, with the increase of CL/EG ratio from 2 to 5 [41]. It has been reported that the DLC of nimodipine loaded PCL-PEG-PCL micelles increases from 3.0 to 4.9% with increasing PCL/PEG ratio [39]. And similar results are obtained for amiodarone loaded PEG-PCL micelles, the DLC increasing from 2.4 to 7.8% with increase of PCL molar mass from 5000 to 24000 [42].

In vitro drug release was performed by using dialysis method in pH 7.4 PBS at 37 °C. Fig. 4.8 shows the release profiles of curcumin from the various copolymer micelles. A similar biphasic pattern is observed, including a rapid initial release within the first 6 h and a slower release up to 120 h. The burst release could be assigned to the fact that part of drug is located at the core-shell interface [43]. HPMC18K-PCL_{10} presents the largest burst release of over 80% in the first 6 h, whereas HPMC7K-PCL_{30} presents a burst of 15% only. The total release at 120 h is 99.8%, 97.4%, 94.9% and 96.5% for HPMC18K-PCL_{10}, HPMC18K-PCL_{20}, HPMC7K-PCL_{10}, and HPMC7K-PCL_{20}, respectively. In contrast, the total release at 120 h is 74.4% for HPMC7K-PCL_{30} and 76.1% for HPMC18K-PCL_{30}, which is much lower than that of copolymers with shorter PCL block length. Therefore, the release rate and release percentage from HPMC-PCL copolymer micelles is dependent on the hydrophobic block length and the hydrophobic/hydrophilic ratio. The longer hydrophobic block, the larger the hydrophobic/hydrophilic ratio, the lower the release rate. It should also be noted that micelles with longer hydrophobic block have higher drug load. Hu et al. reported that curcumin loaded P(NIPAAm-co-DMAAm)-b-PLLA copolymer micelles with higher drug load present slower release rate compared to those with lower drug load [44]. Therefore, drug release rate is also dependent on the drug loading. In fact, the solubility of curcumin in the release medium should be a limiting factor. Ge et al. also observed

a decrease of drug release rate with increase of PCL block length in the case of nimodipine-loaded PCL-PEO-PCL micelles [39]. Similarly, Danafar et al. reported that curcumin release from PCL-PEG micelles in 120 h increases from 57.1% to 80.2% with CL/EG ratio increase from 2 to 5 [41].

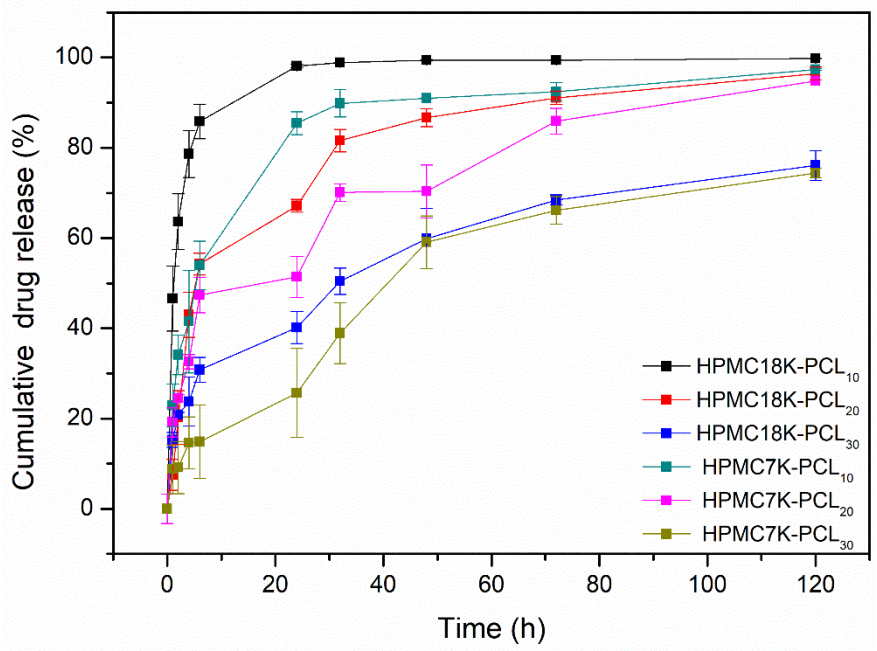

Fig. 4. 8 In vitro release of curcumin from HPMC-PCL micelles. Each point represents mean ± SD for three samples.

Error bars represent the standard deviation (n = 3)

4.3.4 Biocompatibility of micelles

MTT test was applied to assess the cytocompatibility of HPMC-PCL micelles on L929 cells. MTT can react with succinate mitochondrial dehydrogenases in living cells to yield formazan, a purple dye. The latter is insoluble in water but soluble in DMSO. Thus the absorbance of formazan in DMSO solution is measured to assess the number of living cells.

L-929 cells are a commonly used murine fibroblast cell line for cytocompatibility evaluation. The effect of HPMC7K-PCL_{10} and HPMC7K-PCL_{20} micelle solutions on the growth of L-929 cells is shown in Fig. 4.9. The viability of cells is well above 80%

with the concentration varying from 0.25 to 5.0 mg/mL. After 72 h incubation, the cell viability is around 90% in all cases. These results indicate that, in contrast to the positive control, HPMC-PCL micelles are not toxic to L-929 cells.

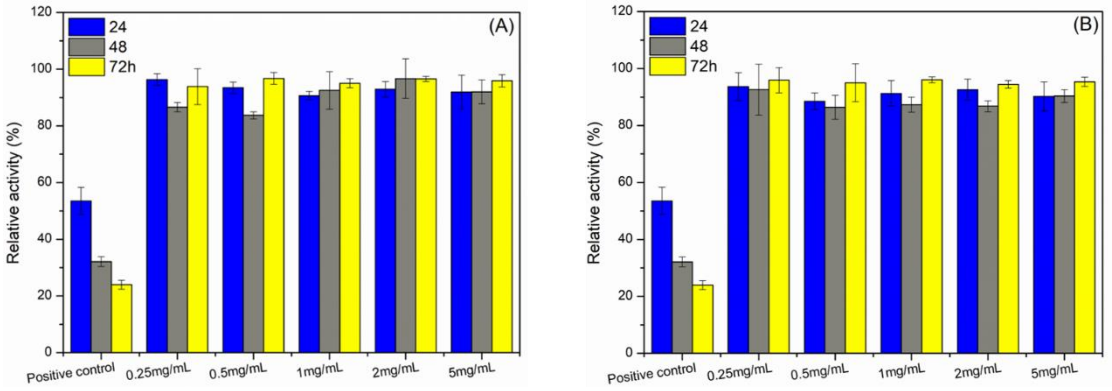

Fig. 4. 9 Relative activity of L-929 cells after 24, 48 and 72 h culture with micelle solutions of HPMC7K-PCL_{10} (A) and HPMC7K-PCL_{20} (B) at different concentrations in comparison with the positive control. Data are presented as the mean ± sd (n = 3)

4.4 Conclusion

In this work, amphiphilic HPMC-PCL diblock copolymers with various HPMC and PCL block lengths were synthesized by combination of ring opening polymerization, deprotection of the Boc group, and reductive amination. The copolymers and precursors were characterized by NMR, DOSY-NMR, FT-IR, GPC and Kaiser test. The self-assembly of copolymers were evidenced by fluorescence spectroscopy, DLS and TEM measurements. All the copolymers are able to self-assemble in aqueous medium into spherical micelles with narrow distribution. Longer hydrophilic HPMC block leads to larger micelle size. The CMC of copolymers decreases with increasing hydrophobic PCL block length. Curcumin was successfully loaded in the core of micelles as a hydrophobic anticancer drug. Higher drug loading was obtained for copolymers with longer PCL block length. The drug release rate is dependent on the PCL block length and the drug load. Larger PCL block length or higher drug load leads to slower drug release. MTT test shows that HPMC-PCL micelles present outstanding cytocompatibility. It is thus concluded that biobased and

biodegradable HPMC-PCL block copolymers could be promising as potential nano-carrier of hydrophobic drugs.

References

[1] H. Cabral, K. Miyata, K. Osada, K. Kataoka, Block Copolymer Micelles in Nanomedicine Applications, Chem Rev 118(14) (2018) 6844-6892.

[2] T.K. Dash, V.B. Konkimalla, Poly-small je, Ukrainian-caprolactone based formulations for drug delivery and tissue engineering: A review, J Control Release 158(1) (2012) 15-33.

[3] P. Grossen, D. Witzigmann, S. Sieber, J. Huwyler, PEG-PCL-based nanomedicines: A biodegradable drug delivery system and its application, Journal of Controlled Release 260 (2017) 46-60.

[4] Z. Karami Ghaleseiedi, A. Dadkhah Tehrani, M. Parsamanesh, Starch-based dual amphiphilic graft copolymer as a new pH-sensitive maltidrug co-delivery system, Int J Biol Macromol 118(Pt A) (2018) 913-920.

[5] L. Liu, Y. Wang, X. Shen, Y. Fang, Preparation of chitosan-g-polycaprolactone copolymers through ring-opening polymerization of epsilon-caprolactone onto phthaloyl-protected chitosan, Biopolymers 78(4) (2005) 163-70.

[6] L. Youssouf, A. Bhaw-Luximon, N. Diotel, A. Catan, P. Giraud, F. Gimie, D. Koshel, S. Casale, S. Benard, V. Meneyrol, L. Lallemand, O. Meilhac, C. Lefebvre D'Hellencourt, D. Jhurry, J. Couprie, Enhanced effects of curcumin encapsulated in polycaprolactone-grafted oligocarrageenan nanomicelles, a novel nanoparticle drug delivery system, Carbohydr Polym 217 (2019) 35-45.

[7] M. Irani, G. Mir Mohamad Sadeghi, I. Haririan, Gold coated poly (epsilon-caprolactonediol) based polyurethane nanofibers for controlled release of temozolomide, Biomed Pharmacother 88 (2017) 667-676.

[8] V.R. Sinha, K. Bansal, R. Kaushik, R. Kumria, A. Trehan, Poly-epsilon-caprolactone microspheres and nanospheres: an overview, Int J Pharm 278(1) (2004) 1-

23.

[9] M. Hakkarainen, A.-C. Albertsson, Heterogeneous biodegradation of polycaprolactone – low molecular weight products and surface changes, Macromol Chem Phys 203(10-11) (2002) 1357-1363.

[10] L.Y. Qiu, Y.H. Bae, Self-assembled polyethylenimine-graft-poly(epsilon-caprolactone) micelles as potential dual carriers of genes and anticancer drugs, Biomaterials 28(28) (2007) 4132-42.

[11] F. Ahmed, D.E. Discher, Self-porating polymersomes of PEG-PLA and PEG-PCL: hydrolysis-triggered controlled release vesicles, J Control Release 96(1) (2004) 37-53.

[12] C. Gu, V. Le, M. Lang, J. Liu, Preparation of polysaccharide derivates chitosan-graft-poly(varepsilon-caprolactone) amphiphilic copolymer micelles for 5-fluorouracil drug delivery, Colloids Surf B Biointerfaces 116 (2014) 745-50.

[13] X. Shuai, T. Merdan, A.K. Schaper, F. Xi, T. Kissel, Core-cross-linked polymeric micelles as paclitaxel carriers, Bioconjug Chem 15(3) (2004) 441-8.

[14] H. Ge, Y. Hu, X. Jiang, D. Cheng, Y. Yuan, H. Bi, C. Yang, Preparation, characterization, and drug release behaviors of drug nimodipine-loaded poly(ε-caprolactone)-poly(ethylene oxide)-poly(ε-caprolactone) amphiphilic triblock copolymer micelles, Journal of Pharmaceutical Sciences 91(6) (2002) 1463-1473.

[15] Z. Liu, Y. Jiao, Y. Wang, C. Zhou, Z. Zhang, Polysaccharides-based nanoparticles as drug delivery systems, Adv Drug Deliv Rev 60(15) (2008) 1650-62.

[16] D. Klemm, B. Heublein, H.P. Fink, A. Bohn, Cellulose: fascinating biopolymer and sustainable raw material, Angew Chem Int Ed Engl 44(22) (2005) 3358-93.

[17] D. Trache, M.H. Hussin, C.T. Hui Chuin, S. Sabar, M.R.N. Fazita, O.F.A. Taiwo, T.M. Hassan, M.K.M. Haafiz, Microcrystalline cellulose: Isolation, characterization and bio-composites application—A review, International Journal of Biological Macromolecules 93 (2016) 789-804.

[18] J. Yang, J. Li, Self-assembled cellulose materials for biomedicine: A review, Carbohydr Polym 181 (2018) 264-274.

[19] E. Bordallo, J. Rieumont, M.J. Tiera, M. Gomez, M. Lazzari, Self-assembly in

aqueous solution of amphiphilic graft copolymers from oxidized carboxymethylcellulose, Carbohydr Polym 124 (2015) 43-9.

[20] D. Wang, J. Tan, H. Kang, L. Ma, X. Jin, R. Liu, Y. Huang, Synthesis, self-assembly and drug release behaviors of pH-responsive copolymers ethyl cellulose-graft-PDEAEMA through ATRP, Carbohydrate Polymers 84(1) (2011) 195-202.

[21] R. Das, S. Pal, Hydroxypropyl methyl cellulose grafted with polyacrylamide: application in controlled release of 5-amino salicylic acid, Colloids Surf B Biointerfaces 110 (2013) 236-41.

[22] A. Lu, J. Wang, M.C. Najarro, S. Li, A. Deratani, Synthesis and self-assembly of AB2-type amphiphilic copolymers from biobased hydroxypropyl methyl cellulose and poly(L-lactide), Carbohydrate Polymers 211 (2019) 133-140.

[23] J. Wang, M. Caceres, S. Li, A. Deratani, Synthesis and Self-Assembly of Amphiphilic Block Copolymers from Biobased Hydroxypropyl Methyl Cellulose and Poly(l

-lactide), Macromol Chem Phys 218(10) (2017) 1600558.

[24] M.R. ten Breteler, J. Feijen, P.J. Dijkstra, F. Signori, Synthesis and thermal properties of hetero-bifunctional PLA oligomers and their stereocomplexes, Reactive and Functional Polymers 73(1) (2013) 30-38.

[25] M. Le Hellaye, N. Fortin, J. Guilloteau, A. Soum, S. Lecommandoux, S.M. Guillaume, Biodegradable polycarbonate-b-polypeptide and polyester-b-polypeptide block copolymers: synthesis and nanoparticle formation towards biomaterials, Biomacromolecules 9(7) (2008) 1924-33.

[26] A. Moussa, A. Crepet, C. Ladaviere, S. Trombotto, Reducing-end "clickable" functionalizations of chitosan oligomers for the synthesis of chitosan-based diblock copolymers, Carbohydr Polym 219 (2019) 387-394.

[27] A.F. Abdel-Magid, S.J. Mehrman, A review on the use of sodium triacetoxyborohydride in the reductive amination of ketones and aldehydes, Org Process Res Dev 10(5) (2006) 971-1031.

[28] J.S. Trent, Ruthenium Tetraoxide Staining of Polymers - New Preparative Methods

for Electron-Microscopy, Macromolecules 17(12) (1984) 2930-2931.

[29] L.A. Fielding, M.J. Derry, V. Ladmiral, J. Rosselgong, A.M. Rodrigues, L.P.D. Ratcliffe, S. Sugihara, S.P. Armes, RAFT dispersion polymerization in non-polar solvents: facile production of block copolymer spheres, worms and vesicles in n-alkanes, Chemical Science 4(5) (2013) 2081.

[30] Y. Hu, V. Darcos, S. Monge, S. Li, Thermo-responsive drug release from self-assembled micelles of brush-like PLA/PEG analogues block copolymers, Int J Pharm 491(1-2) (2015) 152-61.

[31] W. Zhang, M. Torabinejad, Y. Li, Evaluation of Cytotoxicity of MTAD Using the MTT-Tetrazolium Method, Journal of Endodontics 29(10) (2003) 654-657.

[32] D. Trache, M.H. Hussin, C.T. Hui Chuin, S. Sabar, M.R. Fazita, O.F. Taiwo, T.M. Hassan, M.K. Haafiz, Microcrystalline cellulose: Isolation, characterization and bio-composites application-A review, Int J Biol Macromol 93(Pt A) (2016) 789-804.

[33] M. Ju, F. Gong, S. Cheng, Y. Gao, Fast and Convenient Synthesis of Amine-Terminated Polylactide as a Macroinitiator forω-Benzyloxycarbonyl-L-Lysine-N-Carboxyanhydrides, International Journal of Polymer Science 2011 (2011) 1-7.

[34] M. Gotsche, H. Keul, H. Höcker, Amino-termined poly(L-lactide)s as initiators for the polymerization of N-carboxyanhydrides: synthesis of poly(L-lactide)-block-poly(α-amino acid)s, Macromol Chem Phys 196(12) (1995) 3891-3903.

[35] G. Pages, V. Gilard, R. Martino, M. Malet-Martino, Pulsed-field gradient nuclear magnetic resonance measurements (PFG NMR) for diffusion ordered spectroscopy (DOSY) mapping, Analyst 142(20) (2017) 3771-3796.

[36] Z. Jiang, I. Blakey, A.K. Whittaker, Aqueous solution behaviour of novel water-soluble amphiphilic copolymers with elevated hydrophobic unit content, Polymer Chemistry 8(28) (2017) 4114-4123.

[37] J. Li, J. Yang, Synthesis of folate mediated carboxymethyl cellulose fatty acid ester and application in drug controlled release, Carbohydr Polym 220 (2019) 126-131.

[38] Y. Hu, X. Jiang, Y. Ding, L. Zhang, C. Yang, J. Zhang, J. Chen, Y. Yang, Preparation and drug release behaviors of nimodipine-loaded poly(caprolactone)–

poly(ethylene oxide)–polylactide amphiphilic copolymer nanoparticles, Biomaterials 24(13) (2003) 2395-2404.

[39] H. Ge, Y. Hu, X. Jiang, D. Cheng, Y. Yuan, H. Bi, C. Yang, Preparation, characterization, and drug release behaviors of drug nimodipine-loaded poly(ε-caprolactone)-poly(ethylene oxide)-poly(ε-caprolactone) amphiphilic triblock copolymer micelles, Journal of Pharmaceutical Sciences 91(6) (2002) 1463-1473.

[40] H. Yang, N. Wang, L. Mo, M. Wu, R. Yang, X. Xu, Y. Huang, J. Lin, L.M. Zhang, X. Jiang, Reduction sensitive hyaluronan-SS-poly(epsilon-caprolactone) block copolymers as theranostic nanocarriers for tumor diagnosis and treatment, Mater Sci Eng C Mater Biol Appl 98 (2019) 9-18.

[41] H. Kheiri Manjili, P. Ghasemi, H. Malvandi, M.S. Mousavi, E. Attari, H. Danafar, Pharmacokinetics and in vivo delivery of curcumin by copolymeric mPEG-PCL micelles, Eur J Pharm Biopharm 116 (2017) 17-30.

[42] S. Elhasi, R. Astaneh, A. Lavasanifar, Solubilization of an amphiphilic drug by poly(ethylene oxide)-block-poly(ester) micelles, Eur J Pharm Biopharm 65(3) (2007) 406-13.

[43] Z.L. Tyrrell, Y. Shen, M. Radosz, Fabrication of micellar nanoparticles for drug delivery through the self-assembly of block copolymers, Prog Polym Sci 35(9) (2010) 1128-1143.

[44] Y. Hu, V. Darcos, S. Monge, S. Li, Y. Zhou, F. Su, Thermo-responsive release of curcumin from micelles prepared by self-assembly of amphiphilic P(NIPAAm-co-DMAAm)-b-PLLA-b-P(NIPAAm-co-DMAAm) triblock copolymers, Int J Pharm 476(1-2) (2014) 31-40.

[45] X. Shen, X. Liu, R. Li, P. Yun, C. Li, F. Su, S. Li, Biocompatibility of filomicelles prepared from poly(ethylene glycol)-polylactide diblock copolymers as potential drug carrier, J Biomater Sci Polym Ed 28(15) (2017) 1677-1694.

[46] H. Li, S. Tao, Y. Yan, G. Lv, Y. Gu, X. Luo, L. Yang, J. Wei, Degradability and cytocompatibility of tricalcium phosphate/poly(amino acid) composite as bone tissue implants in orthopaedic surgery, Journal of Biomaterials Science, Polymer Edition

25(11) (2014) 1194-1210.

Chapter 5 Novel Thermo-responsive Micelles Prepared from Amphiphilic Hydroxypropyl Methyl Cellulose-*block*-JEFFAMINE Copolymers

Abstract: A series of amphiphilic and thermo-responsive block copolymers were synthesized by reductive amination between the aldehyde endgroup of hydrophilic HPMC and the amine group of monoamine, diamine, or triamine JEFFAMINE as hydrophobic block. The resulting diblock, triblock and three-armed copolymers with different hydrophilic/hydrophobic ratios and block lengths were characterized by NMR, FT-IR, DOSY-NMR and SEC. The cloud point (CP) of copolymers was determined by UV–visible spectrometer. Data show that both the geometrical structure and the molar mass of HPMC affect the CP of HPMC-JEF copolymers. The higher the hydrophilic/hydrophobic ratio, the higher the CP of copolymers which is lower than that of HPMC homopolymers. The self-assembly behavior of the copolymers was investigated from dynamic light scattering, transmission electron microscope, and critical micelle concentration (CMC) measurements. Spherical nano-micelles are obtained by self-assembly of copolymers in aqueous solution, and the micelle size can be tailored by varying the block length of HPMC and the geometrical structure. Three-armed HPMC-JEF copolymers present lower CMC and smaller micelle size as compared to linear diblock and triblock ones. MTT assay evidenced the cytocompatibility of HPMC-JEF copolymers, indicating that they could be promising as drug carrier in drug delivery systems.

Key words: Hydroxypropyl methyl cellulose; JEFFAMINE; Block copolymer; Micelles; Topology; Self-assembly; Thermo-responsive

5.1 Introduction

Amphiphilic block copolymers are able to self-assemble in aqueous solution yielding various aggregates such as spherical micelles, rod-like micelles, filomicells, polymersomes, nanotubes, etc. These aggregates have received ever-increasing interest for biomedical and pharmacological applications in drug delivery [1], imaging [2], sensing [3], *etc*. Micelles constitute a dynamic system with permanent exchanges between micelle-forming molecules and free molecules in solution, continuously breaking and re-forming. Some of the micellar systems are responsive to external stimuli such as pH, temperature, ionic strength and light irradiation [4-9]. Thermo-responsivity is one of the most interesting properties of stimuli-responsive polymers. Poly(N-isopropylacrylamide) (PNIPAAm) and poly(*N*-vinyl caprolactam) (PVCL) are most extensively investigated thermo-responsive polymers which exhibit a lower critical solution temperature (LCST) of approximately 32 ℃ in aqueous solution [10]. Interestingly, PNIPAAm can be used as hydrophilic shell-forming segments below the LCST and as hydrophobic core-forming segments above the LCST [11].

Polysaccharides such as cellulose, pullulan, dextran, chitosan, and hyaluronan have attracted growing attention in recent years for uses as biomaterials because of their biodegradability, biocompatibility and inherent bioactivity which can help in improving drug targeting and diminishing inflammatory response. Cellulose is the most abundant biopolymer consisting of linear chains of numerous β(1→4) linked D-glucose units. It has been widely used for applications in fiber, paper, painting and pharmaceutical industries. Nevertheless, cellulose is poorly soluble in water due to strong hydrogen bonding between hydroxyl groups on the glucose from one chain with oxygen atoms on the same or on a neighbor chain [12]. Thus, soluble cellulose derivatives have been obtained by chemical modification and used as a hydrophilic building block to prepare amphiphilic copolymers, such as ethyl cellulose [13-15], hydroxyl propyl cellulose (HPC) [16], hydroxyl propyl methyl cellulose (HPMC) [16], hydroxyl ethyl cellulose [17], etc. Some derivatives such as HPC and HPMC exhibit thermo-responsive

behaviors. Most modifications exploit the hydroxyl groups on the glucose moieties to prepare graft copolymers. But such reactions are hardly controllable because of the presence of numerous hydroxyl groups along polymer chains. On the other hand, each cellulose chain has a hemiacetal end group which is easily transformed to aldehyde. The latter can serve as a reducing endgroup to build amphiphilic block copolymers by coupling or initiating polymerization. Nevertheless, such reactions have not been widely exploited despite their potential interest due to the limited availability of the reducing-end, the difficulty of finding a common solvent for both blocks, and the eventual necessity to protect the lateral hydroxyl groups [18]. Meanwhile, HPMC oligomers with molar masses between 5K and 20K have been rarely employed as hydrophilic segment to synthesize amphiphilic block copolymers. In our previous work, HPMC-polylactide (HPMC-PLA) block copolymers were synthesized by using a three step procedure: ring-opening polymerization of L-lactide initiated by allyl alcohol, amination reduction of the aldehyde endgroup of low molar mass HPMC, and UV-initiated thiol-ene click reaction [19].

JEFFAMINE is a family of polyetheramine composed of poly(propylene oxide) (PPO), poly(ethylene oxide) (PEO), or mixed PPO/PEO blocks with primary amino groups attached to the polyether chain ends. JEFFAMINE M2005 with a PPO/PEO ratio of 29/6 exhibits a LCST of around 30 ℃ in water [20]. JEFFAMINE exists in the form of monoamines, diamines, and triamines. Thus, amphiphilic block copolymers with different geometrical structures can be obtained combining JEFFAMINE and a hydrophilic block. It has been shown that the geometrical structure of copolymers affects the morphology, stability and size of self-assembled micelles because the hydrophobic and hydrophilic segments lead to complex spatial arrangements during the micellization process [21, 22]. In this work, HPMC-JEF amphiphilic block copolymers were synthesized from HPMC with different molar masses and JEFFAMINE monoamine, diamine, and triamine by reductive amination. The self-assembly properties of the resulting diblock, triblock and tri-armed copolymers were investigated from the morphology, size and size distribution, cloud point (CP) and critical micelle

concentration (CMC) measurements. MTT assay was performed to evaluate the biocompatibility of HPMC-JEF copolymers as potential drug carrier.

5.2 Materials and Methods

5.2.1 Materials

HPMC was kindly provided by Dow Colorcon Limited France, and depolymerized to yield HPMC oligomers with weight average molar mass (Mw) of 7000 (Đ=2.3) and 18000 ((Đ=3.3) Daltons, as reported in a previous work [19]. JEFFAMINE monoamine M-2005, diamine D-2000, and triamine T-5000 were purchased from Huntsman. Sodium triacetoxyborohydride ($NaBH(OAc)_3$) and dimethyl sulfoxide (DMSO) were purchased from Sigma-Aldrich, and used as received.

5.2.2 Synthesis of HPMC-JEF copolymers

HPMC-JEF copolymers were synthesized by reductive amination as reported in literature. Typically, 0.314 g (0.157 mmol) JEFFAMINE M-2005, 1.0 g (0.143 mmol) HPMC with Mw=7000, and 0.042 g (0.198 mmol) $NaBH(OAc)_3$ were dissolved in 20 mL DMSO under stirring. The reaction proceeded at room temperature for 24 h. The product was obtained by dialysis against deionized water for 72 h, changing water every 12h, followed by freeze-drying to obtain white flocculent solid. Yield 69.4%.

5.2.3 Characterization

1H NMR spectra were record on Bruker spectrometer operating at 300 MHz (AMX300) using D_2O and DMSO-d_6 as solvent. Diffusion ordered spectroscopy (DOSY) NMR was performed on Bruker Avance (AQS600) NMR spectrometer, operating at 600 MHz and equipped with a Bruker multinuclear z-gradient inverse probe head which is able to produce gradients in the z direction with a strength of 55 Gcm^{-1}. The DOSY NMR spectra were acquired from Bruker topspin software with the ledbpgp2s pulse program. The strength of the pulsed field gradients with respect to maximum 32 increments on a quadratic scale was logarithmically incremented from 2 to 95%. The diffusion sensitive period (Δ) of 200 ms and the gradient duration (δ) of 5 ms were optimized to allow the signals of interest to decrease by a factor of 10-20, in

order to keep the relaxation contribution to the signal attenuation constant and ensure full signal attenuation for all samples. MestRe Nova software was used for the treatment of all NMR spectra.

Fourier transform infrared (FT-IR) spectra were recorded on a Nicolet NEXUS spectrometer with a DTGS detector at 4 cm^{-1} resolution. Sixty-four scans were taken for each analysis in the frequency range from 400 to 4000 cm^{-1}. Sample pellets were prepared by mixing 2-2.5 mg of polymer with 200 mg of spectral grade potassium bromide, followed by compression using a press.

The molar mass and polydispersity of polymers were determined by size exclusion chromatography (SEC), equipped with multi-angle laser light scattering (MALLS) in combination with refractive index (RI) detector. 5 mg sample was added in the mobile phase (10×10^{-3} M $NaNO_3$ containing 0.02% NaN_3), and stirred for 24 h at room temperature. The solution was filtered using 0.45 μm polytetrafluoroethylene (PTFE) filter (Millipore). The filtrate was injected through a 100 μL loop (Rheodyne injector 7725), and eluted in a TSK-GEL GMPWXL 7.8×300 mm column (TosoHaas Bioseparation Specialists, Stuttgart, Germany) at a flow rate of 0.5 mL min^{-1} (Waters pump 515). MALLS detector (Dawn DSP, Wyatt Technology Co, Santa Barbara, CA, USA) and RI detector (Optilab Wyatt Technology Co) were used to online determine the absolute molar mass for each elution fraction of 0.01 mL, which enables to calculate the Mw and dispersity (*Đ*). The refractive index increment (dn/dc) used for calculation was 0.129 mL g^{-1} for HPMC-JEF copolymers, and 0.137 for HPMC homopolymers. Data analysis was realized using Astra 4 (Wyatt Technology Co.).

The cloud point (CP) of the copolymers was estimated from transmittance changes of 5.0 mg mL^{-1} solution in the temperature range from 30 to 90 ℃. The solution was stirred for 24 h and kept at 4 ℃ overnight before analysis. Measurements were made at a wavelength of 500 nm with a Perkin Elmer Lambda 35 UV–visible spectrometer equipped with a Peltier temperature programmer PTP-1+1. The temperature ramp was 0.2 ℃ min^{-1}. Temp Lab software was used for data treatment. The critical micelle concentration (CMC) was determined by fluorescence spectroscopy using pyrene as

fluorescent probe. The concentration of polymers varied from 1.0×10^{-3} to 2.0 mg/ml, and the concentration of pyrene was fixed at 6×10^{-7}g/L. The excitation spectra of the micellar solutions were recorded between 300 to 360 nm at an excitation wavenumber of 395. The intensity ratio at 336 nm and 334 nm was plotted *versus* copolymer concentration. The CMC value was obtained from the cross-over point of the two regression lines.

The size and zeta potential of micelles were determined by dynamic light scattering (DLS) using Anton Paar Litesizer 500 at 25°C. The aqueous solutions of copolymers at 1.0 mg mL^{-1} were filtered through a 0.45 μm PTFE microfilter. Micelle size changes as a function of temperature from 4 to 60 ℃ were followed using Zano-ZS (Malvern Instrument) equipped with a He–Ne laser (λ=632.8 nm). Measurements were made after 60 min equilibrium of copolymer solutions at 1.0 mg mL^{-1}.

Transmission electron microscopy (TEM) was performed on JEOL 1200 EXII instrument, operating at an acceleration voltage of 120 kV. 5 μL micellar solution at 1.0 mg mL^{-1} was dropped onto a copper grid, stained with phosphotungstic acid, and air dried before measurement.

5.2.4 MTT assay

L-929 cells in logarithmic growth phase were seeded in 96-well plates (Corning Costar, U.S.A.) with a density of 1×10^4 cells/mL per well in 100 μL DMEM medium (10% calf serum, 100 μg/mL Penicillin, 100 μg/mL streptomycin). The cells were then placed in a CO_2 incubator (NU-4850; NuAire, U.S.A.) at 37 ℃ under humidified atmosphere containing 5% CO_2. After 24 h, the medium was replaced by 100 μL of fresh medium or HPMC-JEF micellar solution at various concentrations (0.25, 0.5, 1.0, 2.0, 2.5 and 5.0 mg/mL) containing 10.0 % calf serum. 100 μL fresh medium was used as the negative control, and 100 μL solution of phenol in water as the positive control [23]. After 24, 48 and 72 h, 20 μL 3-(4, 5-dimethylthiazol-2-yl)-2, 5-diphenyltetrazolium bromide (MTT, 5 mg/mL) was added. The medium was removed after 6 h incubation, and then 150 μL dimethylsulfoxide (DMSO) was added. The plates were shaken for 10 min. The optical density (OD) was measured by using microplate

reader (Elx800; BioTek, U.S.A.) at 570 nm. All experiments were carried out in triplicate. The cell viability was calculated from the OD values of the test sample and the negative control using the following equation.

$$\text{Relative activity (\%)} = (OD_{\text{test sample}} / OD_{\text{negative control}}) \times 100$$

The data were expressed as the mean ± SD.

5.3 Results and discussion

5.3.1 Synthesis of HPMC-JEF

HPMC-JEF amphiphilic block polymers were synthesized by reductive amination of amine groups of JEFFAMINE with the reducing end group of HPMC using $NaBH(OAc)_3$ as reducing agent, as shown in Scheme 5.1. HPMC samples with Mw of 7000 and 18 000 and JEFFAMINE samples M-2005 (monoamine), D-2000 (diamine), and T-5000 (triamine) were used to synthesize diblock, triblock and three-armed amphiphilic copolymers, respectively. The PO/EO molar ratios and molar masses of the three JEFFAMINE samples are shown in Table 5.1.

Table 5. 1 PO/EO molar ratios and molar masses of JEFFAMINE

JEFFAMINE®	**PO/EO mol ratio**	**MW***
M-2005	29/6	2000
D-2000	33/0	2000
T-5000	85/0	5000

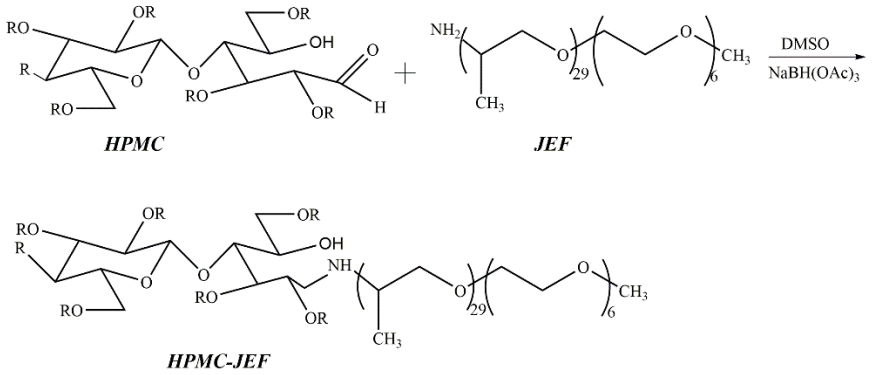

Scheme 5. 1 Synthesis of HPMC-JEF M2K diblock copolymer by reductive amination

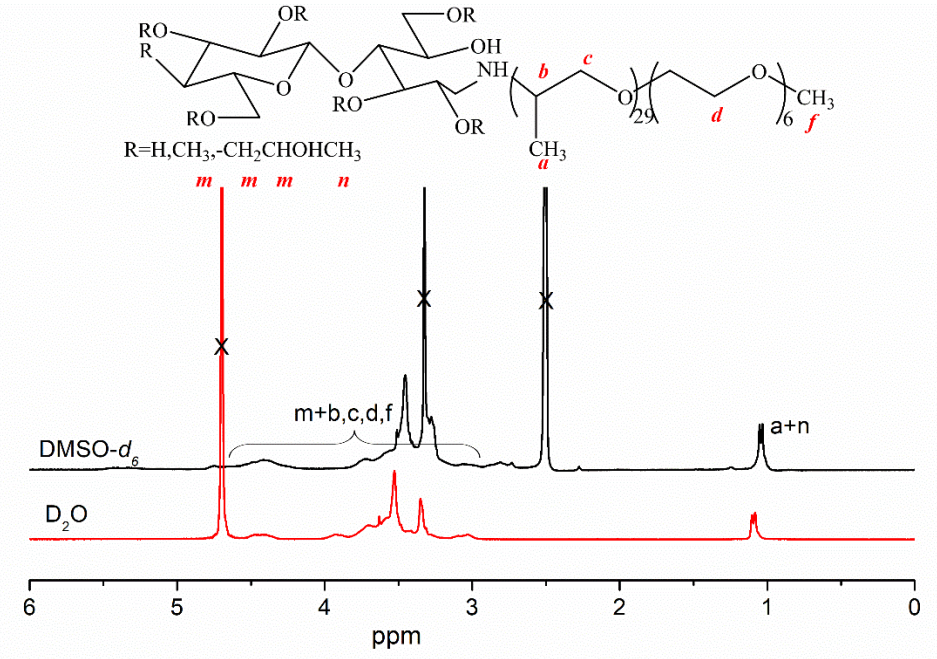

Fig. 5. 1 ^{1}H NMR spectra of HPMC7K-JEF M2K in different solvents

The ^{1}H NMR spectra of HPMC7K-JEF M2K are shown in Fig. 5.1. Signals of both HPMC (δ=2.75–4.75 and 1.05) and JEFFAMINE (δ=3.40–3.90, 2.93 and 1.11) are observed. However, the various signals of both blocks are overlapped in almost the whole range. DOSY-NMR was performed to further confirm the block copolymer structure. In fact, DOSY is an excellent tool allowing virtual separation in multicomponent systems, and thus to evidence if the NMR signals belong to a same molecule or a mixture. DOSY-NMR data are presented in the form of a two-

dimensional (2D) pattern: one dimension is related to the chemical shift information, while the other represents the diffusion coefficient which reflects the molecular effective sizes [24]. As shown in Fig. 5.2, the signals of both JEFFAMINE and HPMC present the same diffusion coefficient, which indicates that the two components are combined in one molecule. In other words, a block copolymer was effectively synthesized.

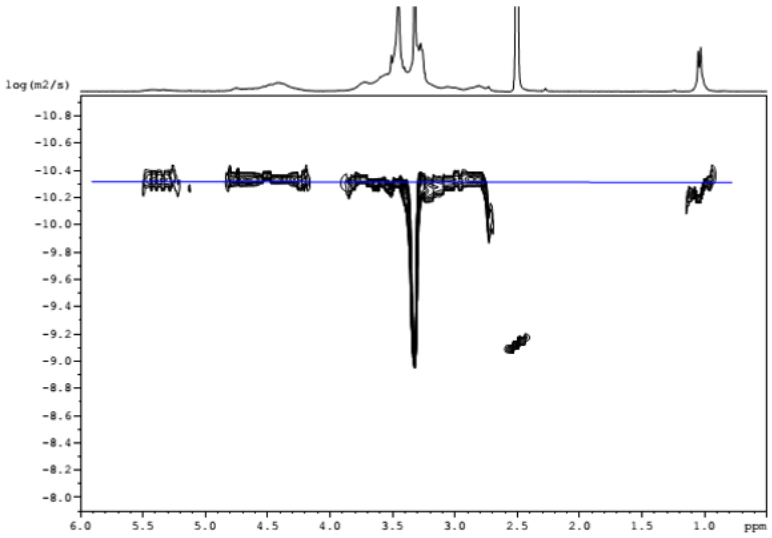

Fig. 5. 2 DOSY NMR spectrum of HPMC7K-JEF M2K copolymer in DMSO-d_6

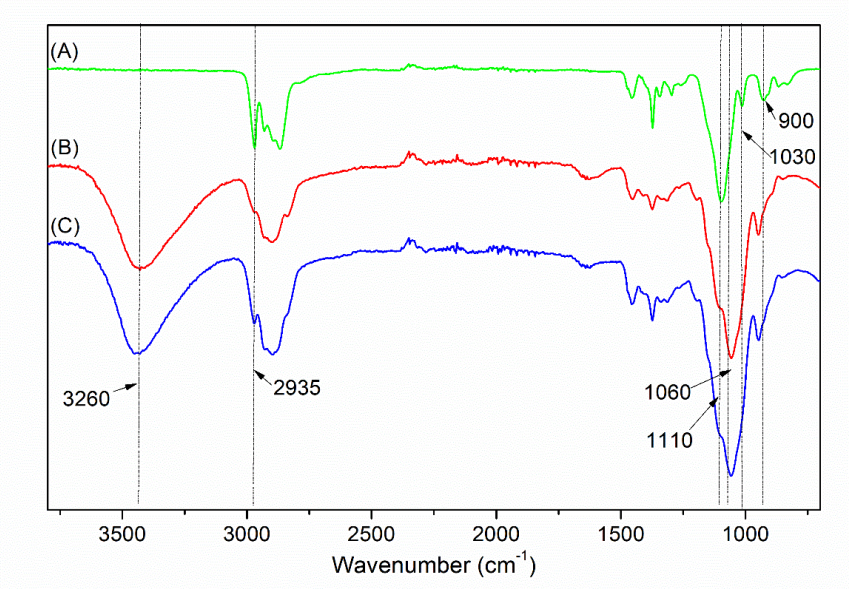

Fig. 5. 3 FT-IR spectra of JEFFAMINE (A), HPMC (B) and HPMC-JEF M2K copolymer (C)

FT-IR was also employed to analyze the chemical structure of polymers. As shown in Fig. 5.3, JEFFAMINE presents characteristic absorption bands at 2935, 1100, 1030 and 900 cm^{-1} belonging to aliphatic C-H stretching, C-O stretching, C-N stretching, and N-H external deformation, respectively. On the other hand, HPMC presents characteristic absorption bands at 3460, 2890, and 1060 cm^{-1} assigned to O-H, C-H and C-O bonds, respectively. In the case of the HPMC-JEF copolymer, all the characteristic bands from the two components are observed, in agreement with the successful coupling of JEFFAMINE and HPMC blocks.

Table 5. 2 Characterization of HPMC-JEF block copolymers

Sample	Mw[a]	*Đ*[a]	CP[b] (℃)	Size[c] (nm)	PDI[c]	Zeta[c] （mV）	CMC[d] (g/L)
HPMC7K-JEF M2K	6500	1.73	42.1/69.0	231.9	0.22	-1.8±0.1	0.24
$(HPMC7K)_2$-JEF D2K	14000	1.95	78.5	261.1	0.19	-4.21±0.3	0.24
$(HPMC7K)_3$-JEF T5K	19000	2.00	82.9	183.7	0.24	-3.7±0.2	0.03
HPMC18K-JEF M2K	25000	1.38	35.1/60.1	298.4	0.18	-7.0±0.3	0.13
$(HPMC18K)_2$-JEF D2K	43000	2.01	55.7	328.2	0.25	-2.0±0.2	0.24
$(HPMC18K)_3$-JEF T5K	56000	2.30	-	270.7	0.18	-6.7±0.3	0.07

a) Determined from SEC/MALS/RI measurement in water at 5.0mg mL^{-1}

b) Determined from turbidimetry measurement in water at 5.0 mg mL^{-1}

c) Determined at 25 ℃ by dynamic light scattering at 1.0 mg mL^{-1}

d) Determined at 25 ℃ by fluorescence spectrometer

The molar mass of copolymers was determined by using aqueous SEC in conjunction with online MALLS and RI detectors. RI detector is most commonly used as concentration detector whose response is proportional to the total solute concentration in the detector cell, whereas the response of MALLS detector depends

on the molar mass of the solute [25]. The molar mass of copolymers was calculated combining with the MALLS and RI curves. When an RI detector is combined with light scattering, the exact concentration of the sample at each data slice needs to be determined in order to calculate the absolute molecular weight. The key parameter to get exact concentration of a sample at each data slice is the refractive index increment (dn/dc). This value is unique for a sample-solvent combination, as it represents the difference in refractive index between the sample and the solvent. The refractive index increment (dn/dc) used for calculation was 0.129 mL g^{-1} for HPMC-JEF copolymers, and 0.137 for HPMC homopolymers. Table 5.2 presents the Mw and dispersity (Đ=Mw/Mn) data of the various copolymers obtained by reaction of HPMC7K and HPMC18K with JEFFAMINE samples M2K, D2K and T5K. The Mw of HPMC7K derived copolymers increases from 6 500 for the diblock copolymer HPMC7K-JEF M2K, to 14 000 for the triblock copolymer (HPMC7K)2-JEF D2K, and to 19 000 for the three-armed copolymer $(HPMC7K)_3$-JEF T5K. Similarly, the Mw of HPMC18K derived copolymers increases from 25 000 for HPMC18K-JEF M2K, to 43 000 and 56 000 for $(HPMC18K)_2$-JEF D2K and $(HPMC18K)_3$-JEF T5K, respectively. These results well corroborate with the initially designed structure of copolymers, indicating the successful synthesis of copolymers by reductive amination. However, there are some errors between the SEC result and the theoretical calculation. SEC is a chromatographic method in which molecules in solution are separated by their size. Thus, the architecture is important to the SEC analysis. HPMC-JEF copolymers with different architecture have some error during the analysis. Meanwhile, copolymers with different architecture and different molar mass may have slight difference on dn/dc, thereby have some errors on SEC results. In addition, HPMC oligomers which were used to synthsize copolymers were degraded from high molecular weight HPMC. Therefore, they have a wide molecular weight distribution, Đ for HPMC 18K is 3.3 and for HPMC 7K is 2.3. Certainly, the HPMC-JEF copolymers have a wide molecular weight distribution. Meanwhile, high-molar-mass species particularly influence the value of Mw [26]. Therefore, the Mw analysis by SEC may has some error. It is also

noted that the dispersity varies from 1.38 for HPMC18K-JEF M2K to 2.30 for $(HPMC18K)_3$-JEF T5K, in agreement with more or less narrow molar mass distribution.

5.3.2 Cloud point

HPMC is a thermo-responsive polymer which precipitates out of the solution when the temperature reaches the cloud point due to loss of water or dehydration [27]. The phase separation leads to a polymer rich phase and a polymer depleted phase. Thus the cloud point can be determined as the polymer rich phase is capable of scattering light [28].

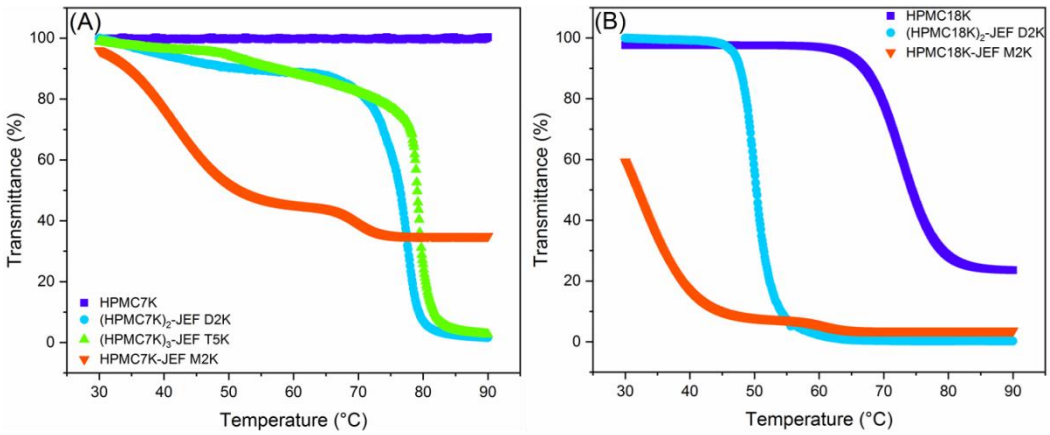

Fig. 5. 4 Plots of light transmittance as a function of temperature for aqueous solutions of HPMC7K-JEF (A) and HPMC18K-JEF (B) copolymers

The CP of the HPMC-JEF aqueous solutions was determined by transmittance measurements at 500 nm, as shown in Fig 5.4. HPMC18K exhibits a CP around 78.0 ℃, whereas HPMC7K has no obvious change in the tested temperature range. Thus, the CP of HPMC homopolymers decreases with the increase of molecule weight. Similar result has been reported in literature in the case of narrow-disperse PNIPAMs. As the $M_{n,NMR}$ increases from 2.8 to 26.5 KDa, the CP drops from 43.0 to 33.3 ℃ [29].

The CP of HPMC-JEF copolymers is lower than that of HPMC homopolymers in all cases. Meanwhile, the CP of linear diblock and triblock HPMC18K-JEF copolymers was higher than that of HPMC7K-JEF ones. Therefore, the CP of linear JEF-HPMC copolymers is strongly dependent on the hydrophilic/hydrophobic ratio. The higher the hydrophilic/hydrophobic ratio, the higher the CP of copolymers. Similar finding has

been reported for P(EO_2MA-*co*-OEGMA) copolymers whose CP could be tuned from 28 ℃ to 90℃ by adjusting the copolymer composition [30-32]. It also has been reported that PLLA-PNIPAAm copolymers exhibit a CP between 32.1 and 32.8 ℃ with the [NIPAAm]/[LA] ratio varying from 2.4 to 6.9 [33].

The situation of the three-armed $(HPMC)_3$-JEF T5K copolymers is more complicated. Compared with the linear copolymers, the three-armed $(HPMC7K)_3$-JEF T5K copolymer presents a higher CP (82.9 ℃) in spite of its higher JEFFAMINE fraction. This finding could be assigned to the topological structures which make the interactions between polymer and solvent different from those of linear copolymers. Honda et al. reported that the CP of amphiphilic poly(butyl acrylate)-*block*-poly(ethylene oxide) copolymers is strongly affected by the topological structure[34]. An increase by more than 40 ℃ was observed through the linear-to-cyclic topological conversion. Data for $(HPMC18K)_3$-JEF T5K are not available because it is not fully soluble at 5 g/L. It should be noted that different from the JEFFAMINE D2K and JEFFAMINE T5K composed of propylene oxide units only, JEFFAMINE M2005 is a thermos-responsive block possessing a CP of 22.6 ℃ at the concentration of 5 g/L (shown in Fig. 5.5) in water due to its different chemical structure (shown is Table 5.1, PO/EO molar ratio of 29/6). Two transitions of transmittance corresponding to both components are observed for the diblock copolymers HPMC7K-JEF M2K and HPMC18K-JEF M2K (Fig. 5.4, Table 5.2).

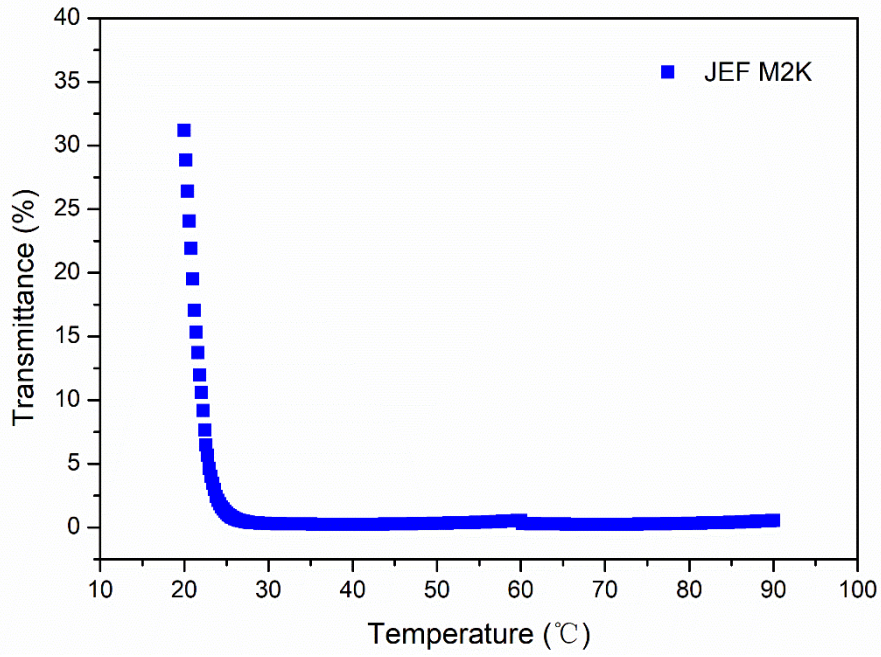

Fig. 5. 5 Plots of light transmittance as a function of temperature for aqueous solutions of JEF M2K at 5 g/L.

5.3.3 Self-assembly of HPMC-JEF copolymers

Micelles of HPMC-JEF copolymers were prepared by direct dissolution method. 10 mg copolymer was dissolved in 10 mL deionized water under stirring overnight. The self-assembled HPMC-JEF micelles consisted of a JEF core surrounded by a HPMC corona.

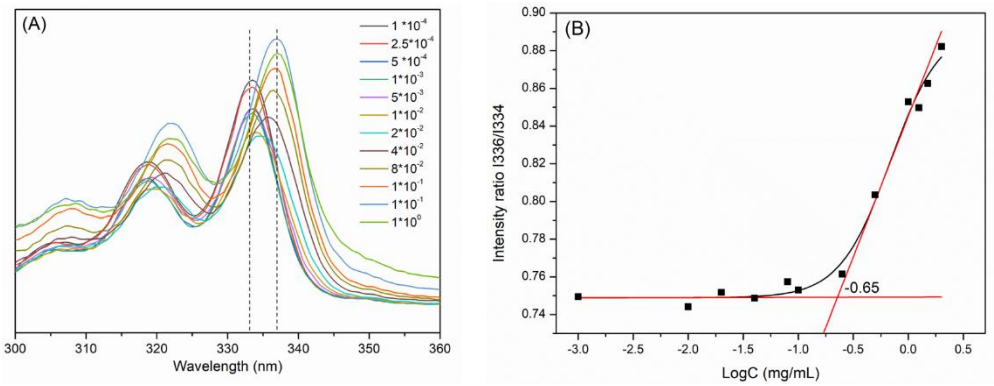

Fig. 5. 6 Fluorescence excitation spectra (A) and I336/I334 *vs.* LogC plots (B) of HPMC7K-JEF M2K diblock copolymer solutions at different concentrations

The critical micelle concentration was determined by fluorescence excitation spectroscopy using pyrene as fluorescence probe. Pyrene is highly hydrophobic and tends to migrate into the lipophilic micellar core in the aqueous solution. As shown in Fig. 5.6, the shift of the fluorescence excitation spectra indicates the process of micellar forming. The CMC value was determined from the two regression lines of the curves of the intensity ratio of I336/334 *versus* polymer concentration. As shown in Table 5.2, no major difference is observed between the CMC values of the diblock and triblock copolymers which are in the range of 0.13 to 0.24 g/L. In contrast, the CMC of the three-armed copolymers is much lower. $(HPMC7K)_3$-JEF T5K and $(HPMC18K)_3$-JEF T5K exhibit a CMC of 0.03 and 0.07 g/L, respectively. In other words, the CMC of three-armed copolymers increases with increasing hydrophilic HPMC block length, which is consistent with literature data [35]. In fact, Guo et al. reported that cellulose-g-PCL graft copolymers with higher degree of substitution (DS) of PCL present lower CMC value than those with lower DS. The fact that three-armed copolymers exhibit lower CMC than linear diblock and triblock copolymers could be assigned to the difference of the topological structures since star-shaped block copolymers facilitate micellization. Similar results have been found for star-shaped PEG-*b*-PCL copolymers [36] and PCL-*b*-PDEAS copolymers [21].

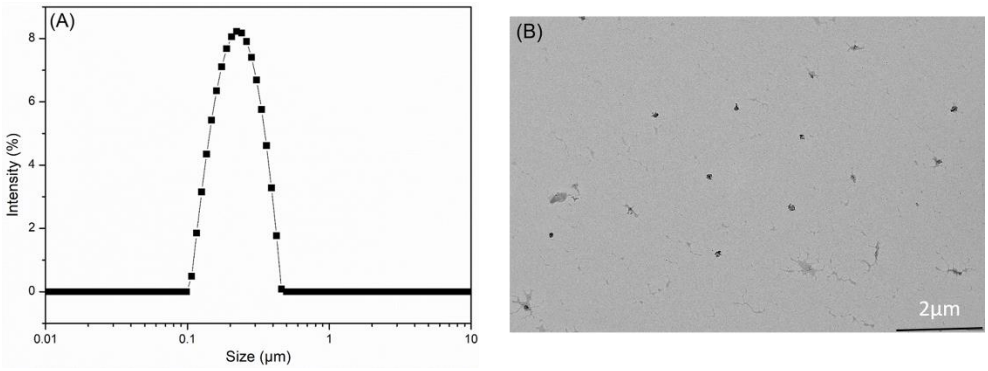

Fig. 5. 7 Size distribution (A) and TEM image (B) of HPMC7K-JEF M2K diblock copolymer micelles

The size, size distribution, zeta potential and morphology of the micelle were determined by DLS and TEM, and the results are displayed in Table 5.2 and in Fig 5.7.

The average size of the micelle with different HPMC and JEF block lengths are in the range from 180 to 320 nm. The three armed copolymers exhibited the smallest micelle size, whereas the triblock ones exhibited the largest micelle size. These findings could be assigned to the difference of topological structures. It has been reported that linear and star-shaped block copolymers with 3, 4 or 6 arms have significant difference in micelle size [21, 36]. On the other hand, HPMC18K derived copolymers exhibit larger micelle size than HPMC7K derived ones, indicating that the micelle size increases with increasing hydrophilic block length [35]. The polydispersity ranges from 0.18 to 0.25, in agreement with narrow distribution of micelle sizes. The morphology of micelles is shown in Fig. 5.7B. Spherical micelles are observed in all cases. It is also noted that the zeta potential of all micelles is close to zero, in agreement with the neutral nature of copolymers (Table 5.2).

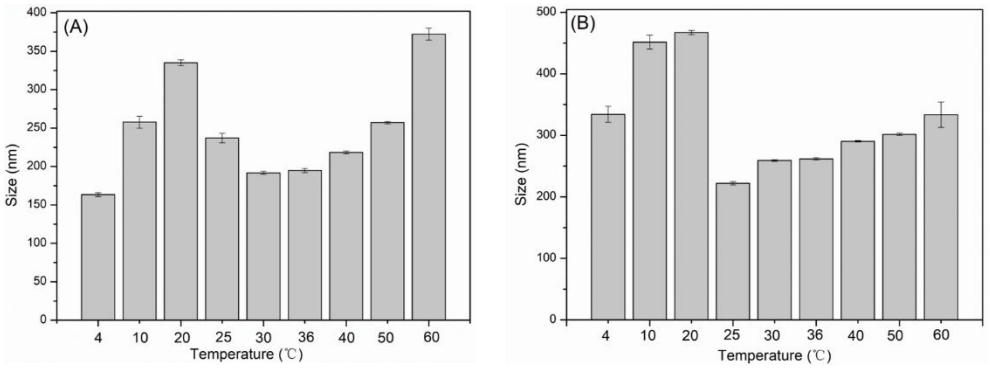

Fig. 5. 8 Micelle size changes of HPMC7K-JEF M2K (A) and HPMC18K-JEF M2K (B) as a function of temperature

It is also of interest to follow the micelle size changes of doubly thermo-responsive diblock copolymers at different temperatures. As shown in Fig. 5.8, three phases of micelle size changes are distinguished for HPMC7K-JEF M2K and HPMC18K-JEF M2K diblock copolymers. In the first phase, the micelle size of HPMC7K-JEF M2K increases from 162 nm at 4℃ to 340 nm at 20℃. In the second phase, the micelle size decreases to reach 190 nm at 30 ℃. Beyond, the micelle size increases again to reach 380 nm at 60℃. Similar changes are observed for HPMC18K-JEF M2K. The micelle

size increase observed in the first and third phases can be assigned to the chain extension of HPMC blocks as the temperature increases. Similar result has been reported in literature. Yang et al. observed a micelle size increase for PLA-PEG copolymers with increasing temperature from 15℃ to 35℃.[37]. In the second phase from 20 to 30℃, the size deceases because of the phase transition of JEF M2Kblocks. It has been reported that the JEF core size of JEF M2K-*b*-poly(L-glutamic acid) copolymer micelles decreases with increasing temperature as a result of dehydration [20]. Above 60℃, the micelles become unstable and aggregated as both blocks become hydrophobic.

5.3.3 MTT assay

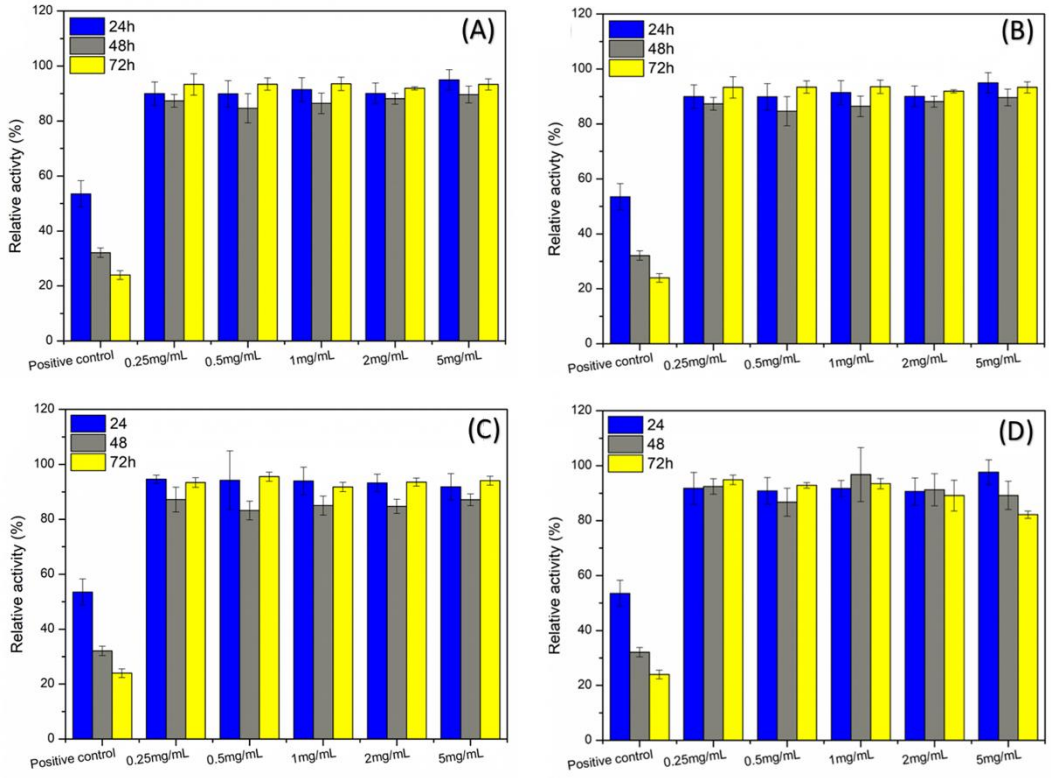

Fig. 5. 9 Relative activity of L-929 cells after 24, 48 and 72 h culture with micelle solutions of HPMC7K-JEF M2K (A), HPMC18K-JEF M2K (B), (HPMC7K)2-JEF D2K (C), and (HPMC7K)3-JEF T5K (D) at different concentrations in comparison with the positive control. Data are presented as the mean ± sd (n = 3)

In vitro cytotoxicity of biomaterials is generally evaluated by MTT assay. This method is based on the reaction between MTT and mitochondrial succinate dehydrogenases in living cells to form a purple formazan which is soluble in DMSO but insoluble in water. The OD value of formazan-DMSO solution is considered to be proportional to the number of living cells [38, 39]. L-929 cells are a commonly used standard cell line in cyto-compatibility evaluation. The effect of micelle solutions on the growth of L-929 cells is shown in Fig. 5.9. The viability of cells is very high in micelle solutions, the relative activity being well above 80% for all samples. With the increase of micelle concentration from 0.25 to 5.0 mg/mL, the cell viability remained almost unchanged. Meanwhile, incubation up to 72 h does not affect the cell viability for all groups. According to the US Pharmacopeia Standards, it can be concluded that HPMC-JEF micelles are not toxic to L-929 cells. It is also noticed that the viability is very low in the positive control.

5.4 Conclusion

Amphiphilic and thermo-responsive block copolymers were synthesized by reductive amination between the aldehyde group of hydrophilic HPMC and the amine group of monoamine, diamine, or triamine JEFFAMINE as hydrophobic block. The resulting diblock, triblock and three-armed copolymers were characterized by NMR, FT-IR, DOSY-NMR and SEC. The various copolymers with different hydrophilic/hydrophobic ratios and block lengths self-assembled in water to yield spherical micelles. The geometrical structure of copolymers strongly affects the micelle size of micelles as well as the cloud point. Compared to the diblock and triblock copolymers, three-armed copolymers exhibit lower CMC, smaller size and lower cloud point. Interestingly, HPMC-JEF M2K diblock copolymers present two CP since both components are thermo-responsive. Moreover, the micelle size significantly changes with increasing temperature due to chain extension and/or dehydration. Last but not least, MTT assay showed that the HPMC-JEF micelles present outstanding cytocompatibility, suggesting that these novel copolymers can be safely used as

potential drug carrier.

References

[1] P. Singh, N. Verma, A Review on Impact of Nanomicelle for Ocular Drug Delivery System, International Journal of Pharmaceutical Sciences and Research 9(4) (2018) 1397-1404.

[2] S.R. Mane, I.L. Hsiao, M. Takamiya, D. Le, U. Straehle, C. Barner-Kowollik, C. Weiss, G. Delaittre, Intrinsically Fluorescent, Stealth Polypyrazoline Nanoparticles with Large Stokes Shift for In Vivo Imaging, Small 14(36) (2018) e1801571.

[3] M. Saleem, L. Wang, H. Yu, A. Zain ul, M. Akram, R.S. Ullah, Synthesis of amphiphilic block copolymers containing ferrocene–boronic acid and their micellization, redox-responsive properties and glucose sensing, Colloid and Polymer Science 295(6) (2017) 995-1006.

[4] Z. Ge, S. Liu, Supramolecular self-assembly of nonlinear amphiphilic and double hydrophilic block copolymers in aqueous solutions, Macromol Rapid Commun 30(18) (2009) 1523-32.

[5] J. Xu, S. Liu, Polymeric nanocarriers possessing thermoresponsive coronas, Soft Matter 4(9) (2008) 1745.

[6] H. Co¨lfen, Double-Hydrophilic Block Copolymers: Synthesis and Application as Novel Surfactants and Crystal Growth Modifiers, Macromolecular Rapid Communication 22 (2001) 219-225.

[7] H.-i. Lee, W. Wu, J.K. Oh, L. Mueller, G. Sherwood, L. Peteanu, T. Kowalewski, K. Matyjaszewski, Light-Induced Reversible Formation of Polymeric Micelles, Angewandte Chemie International Edition 46(14) (2007) 2453-2457.

[8] Y. Zhao, Rational design of light-controllable polymer micelles, Chem Rec 7(5) (2007) 286-94.

[9] D. Wang, T. Wu, X. Wan, X. Wang, S. Liu, Purely Salt-Responsive Micelle Formation and Inversion Based on a Novel Schizophrenic Sulfobetaine Block

Copolymer: Structure and Kinetics of Micellization, Langmuir 23(23) (2007) 11866-11874.

[10] J. Ramos, A. Imaz, J. Forcada, Temperature-sensitive nanogels: poly(N-vinylcaprolactam) versus poly(N-isopropylacrylamide), Polym. Chem. 3(4) (2012) 852-856.

[11] H. Wei, S.-X. Cheng, X.-Z. Zhang, R.-X. Zhuo, Thermo-sensitive polymeric micelles based on poly(N-isopropylacrylamide) as drug carriers, Prog Polym Sci 34(9) (2009) 893-910.

[12] V.L. Finkenstadt, R.P. Millane, Crystal Structure of Valonia Cellulose Iβ, Macromolecules 31(22) (1998) 7776-7783.

[13] H. Dou, M. Jiang, H. Peng, D. Chen, Y. Hong, pH-dependent self-assembly: micellization and micelle-hollow-sphere transition of cellulose-based copolymers, Angew Chem Int Ed Engl 42(13) (2003) 1516-9.

[14] Y. Uraki, T. Imura, T. Kishimoto, M. Ubukata, Body temperature-responsive gels derived from hydroxypropylcellulose bearing lignin, Carbohydrate Polymers 58(2) (2004) 123-130.

[15] W. Yuan, J. Zhang, H. Zou, T. Shen, J. Ren, Amphiphilic ethyl cellulose brush polymers with mono and dual side chains: Facile synthesis, self-assembly, and tunable temperature-pH responsivities, Polymer 53(4) (2012) 956-966.

[16] E. Ostmark, D. Nystrom, E. Malmstrom, Unimolecular nanocontainers prepared by ROP and subsequent ATRP from hydroxypropylcellulose, Macromolecules 41(12) (2008) 4405-4415.

[17] M.-F. Hsieh, N. Van Cuong, C.-H. Chen, Y.T. Chen, J.-M. Yeh, Nano-Sized Micelles of Block Copolymers of Methoxy Poly(ethylene glycol)-Poly(ε-caprolactone)- Graft-2-Hydroxyethyl Cellulose for Doxorubicin Delivery, Journal of Nanoscience and Nanotechnology 8(5) (2008) 2362-2368.

[18] C. Schatz, S. Lecommandoux, Polysaccharide-containing block copolymers: synthesis, properties and applications of an emerging family of glycoconjugates, Macromol Rapid Commun 31(19) (2010) 1664-84.

[19] J. Wang, M. Caceres, S. Li, A. Deratani, Synthesis and Self-Assembly of Amphiphilic Block Copolymers from Biobased Hydroxypropyl Methyl Cellulose and Poly(l
-lactide), Macromol Chem Phys 218(10) (2017) 1600558.
[20] W. Agut, A. Brulet, D. Taton, S. Lecommandoux, Thermoresponsive micelles from Jeffamine-b-poly(L-glutamic acid) double hydrophilic block copolymers, Langmuir 23(23) (2007) 11526-33.
[21] J. Cao, A. Lu, C. Li, M. Cai, Y. Chen, S. Li, X. Luo, Effect of architecture on the micellar properties of poly (varepsilon-caprolactone) containing sulfobetaines, Colloids Surf B Biointerfaces 112 (2013) 35-41.
[22] Z. Li, E. Kesselman, Y. Talmon, M.A. Hillmyer, T.P. Lodge, Multicompartment micelles from ABC miktoarm stars in water, Science 306(5693) (2004) 98-101.
[23] W. Zhang, M. Torabinejad, Y. Li, Evaluation of Cytotoxicity of MTAD Using the MTT-Tetrazolium Method, Journal of Endodontics 29(10) (2003) 654-657.
[24] G. Pages, V. Gilard, R. Martino, M. Malet-Martino, Pulsed-field gradient nuclear magnetic resonance measurements (PFG NMR) for diffusion ordered spectroscopy (DOSY) mapping, Analyst 142(20) (2017) 3771-3796.
[25] L.K. Kostanski, D.M. Keller, A.E. Hamielec, Size-exclusion chromatography-a review of calibration methodologies, J Biochem Biophys Methods 58(2) (2004) 159-86.
[26] W.W.Y. Andre M.Striegel , Joseph J. Kirkland , donale D.Bly, Modern size exclusion chromatography, 2009.
[27] K. Mitchell, J.L. Ford, D.J. Armstrong, P.N.C. Elliott, C. Rostron, J.E. Hogan, The Influence of Additives on the Cloud Point, Disintegration and Dissolution of Hydroxypropylmethylcellulose Gels and Matrix Tablets, Int J Pharm 66(1-3) (1990) 233-242.
[28] M.K. Mohammadpour, Brian; Crowley, Mary Ellen; Walker, Gavin; Crean, Abina M., HPMC CLOUD POINT: EXPLORING HYDROXYPROPYLMETHYL CELLULOSE BEHAVIOR IN PHARMACEUTICAL FORMULATIONS.

[29] Y. Xia, X.C. Yin, N.A.D. Burke, H.D.H. Stover, Thermal response of narrow-disperse poly(N-isopropylacrylamide) prepared by atom transfer radical polymerization, Macromolecules 38(14) (2005) 5937-5943.

[30] J.L. Zhang, R.S. Srivastava, R.D. Misra, Core-shell magnetite nanoparticles surface encapsulated with smart stimuli-responsive polymer: synthesis, characterization, and LCST of viable drug-targeting delivery system, Langmuir 23(11) (2007) 6342-51.

[31] J.F. Lutz, O. Akdemir, A. Hoth, Point by point comparison of two thermosensitive polymers exhibiting a similar LCST: Is the age of poly(NIPAM) over?, J Am Chem Soc 128(40) (2006) 13046-13047.

[32] J.-F. Lutz, A. Hoth, Preparation of Ideal PEG Analogues with a Tunable Thermosensitivity by Controlled Radical Copolymerization of 2-(2-Methoxyethoxy)ethyl Methacrylate and Oligo(ethylene glycol) Methacrylate, Macromolecules 39(2) (2006) 893-896.

[33] Y. Hu, V. Darcos, S. Monge, S. Li, Synthesis and self-assembling of poly(N-isopropylacrylamide-block-poly(L-lactide)-block-poly(N-isopropylacrylamide) triblock copolymers prepared by combination of ring-opening polymerization and atom transfer radical polymerization, Journal of Polymer Science Part A: Polymer Chemistry 51(15) (2013) 3274-3283.

[34] S. Honda, T. Yamamoto, Y. Tezuka, Topology-directed control on thermal stability: micelles formed from linear and cyclized amphiphilic block copolymers, J Am Chem Soc 132(30) (2010) 10251-3.

[35] Y. Guo, X. Wang, Z. Shen, X. Shu, R. Sun, Preparation of cellulose-graft-poly(varepsilon-caprolactone) nanomicelles by homogeneous ROP in ionic liquid, Carbohydr Polym 92(1) (2013) 77-83.

[36] K.H. Kim, G.H. Cui, H.J. Lim, J. Huh, C.-H. Ahn, W.H. Jo, Synthesis and Micellization of Star-Shaped Poly(ethylene glycol)-block-Poly(ε-caprolactone), Macromol Chem Phys 205(12) (2004) 1684-1692.

[37] L. Yang, X. Qi, P. Liu, A. El Ghzaoui, S. Li, Aggregation behavior of self-

assembling polylactide/poly(ethylene glycol) micelles for sustained drug delivery, Int J Pharm 394(1-2) (2010) 43-9.
[38] X. Shen, X. Liu, R. Li, P. Yun, C. Li, F. Su, S. Li, Biocompatibility of filomicelles prepared from poly(ethylene glycol)-polylactide diblock copolymers as potential drug carrier, J Biomater Sci Polym Ed 28(15) (2017) 1677-1694.
[39] H. Li, S. Tao, Y. Yan, G. Lv, Y. Gu, X. Luo, L. Yang, J. Wei, Degradability and cytocompatibility of tricalcium phosphate/poly(amino acid) composite as bone tissue implants in orthopaedic surgery, Journal of Biomaterials Science, Polymer Edition 25(11) (2014) 1194-1210.

Conclusion

In this work, amphiphilic block copolymers containing a hydrophilic block hydroxypropyl methyl cellulose (HPMC), and one of the three hydrophobic blocks polylactide (PLA), poly(ε-caprolactone) (PCL) and JEFFAMINE were synthesized via reductive amination reaction. The resulting copolymers were characterized by various methods, including NMR, DOSY NMR, FT-IR, etc. The influence of copolymer composition, hydrophilic/hydrophobic ratio and topology on the self-assembly, phase transition, drug loading and release properties of copolymers was investigated. The potential of these copolymer micelles as nano-carrier of hydrophobic anti-tumor drugs was furtherly evaluated. The following conclusions can be drawn from this work:

(1) AB_2-type thermo-responsive amphiphilic $(HPMC)_2$-PLA copolymers with three different hydrophilic block lengths were synthesized by ring-opening polymerization, reductive amination and click reaction. HPMC blocks with molar masses of 5K, 7K and 10K were obtained by enzymatic degradation of HPMC for different time periods. The molar mass dispersity of the resulted copolymers is around 1.2. The amphiphilic copolymers self-assembled in spherical micelles in all cases. The micelle size increases from 66 to 120 nm as the hydrophilic HPMC molar mass varying from 5K to 10K. The CMC of copolymers is in the range of 0.14-0.16 mg/mL and the CP is in the range of 64.1-65.2 ℃. Compared to the CP of around 80 ℃ reported for linear HPMC-PLA with the same hydrophilic and hydrophobic block lengths, the CP of AB_2-type $(HPMC)_2$-PLA copolymers is much lower. This finding indicates that the length of HPMC blocks has little effect on the Cp, while the copolymer topology seems to significantly affect the phase separation behavior of HPMC-PLA copolymers.

(2) Amphiphilic HPMC-PLLA and HPMC-PLA diblock copolymers with different hydrophobic block lengths were synthesized from hydroxypropyl methyl cellulose (HPMC) and amino-terminated poly(L-lactide) (PLLA) or poly(L-lactide-co-DL-lactide) (PLA) by reductive amination. HPMC-PLLA and HPMC-PLA copolymers self-assembled to yield spherical micelle in aqueous medium. The micelle size varied

from 153.8 to 178.3 nm. The zeta potential of micelles is close to zero. The CMC value of HPMC-PLA copolymers decreases with the increasing of hydrophobic PLA block length in the range of 0.15-0.009. Besides, the stereochemistry of PLA block seems not to affect the CMC of HPMC-PLA copolymers. HPMC-PLA and HPMC-PLLA copolymers can encapsulate paclitaxel (PTX), a hydrophobic anti-cancer drug, by adding drug solution to pre-formed micelle solution under vigorous stirring. Increasing DLC and DLE are obtained with increase of PLA block length from HPMC-PLA_{20} to HPMC-PLA_{40}. The highest DLE and DLC of 59.8% and 6.4% are obtained for HPMC-PLA_{40}. HPMC-$PLLA_{20}$ shows the lowest DLE and DLC probably due to the higher crystallinity of $PLLA_{20}$. In vitro drug release performed at 37 ℃ in PBS consists in two phases: an initial burst release, followed by a slower release to reach 80.4%, 73.8%, and 66.7% at 120 h for HPMC-PLA_{20}, HPMC-PLA_{30} and HPMC-PLA_{40}. Moreover, MTT and SRB assays demonstrate the outstanding cytocompatibility of HPMC-PLA copolymers. In addition, PTX-loaded micelles exhibit significant cytotoxicity to SKBR 3 cells.

(3) Amphiphilic HPMC-PCL diblock copolymers with different hydrophilic and hydrophobic block lengths were synthesized using the same method mentioned above. All the copolymers self-assemble into spherical micelles with narrow distribution in aqueous medium. The micelle size of copolymers increases with increase of hydrophilic HPMC block length, but the hydrophobic block length has little influence on micelle size. On the other hand, increase of the hydrophobic PCL block length or hydrophobic/hydrophilic ratio leads to CMC decrease from 0.0009 to 0.012 g/L. The zeta potential of micelles is slightly negative. Another hydrophobic anti-cancer drug, curcumin is encapsulated in micelles by adding drug solution into pre-formed micelle solution under vigorous stirring. The DLC and DLE of copolymers increase with increase of PCL block length, High DLC and DLE up to 8.2% and 75.8% are obtained for HPMC-PCL with the longest PCL block length. All the drug release profiles show a biphasic pattern, including a rapid initial release within the first 6 h and a slower release up to 114 h. The drug release rate decreases with increase of PCL block length.

The HPMC-PCL copolymers present outstanding biocompatibility as evidenced by MTT assay.

(4) Amphiphilic and thermo-responsive block copolymers were synthesized by reductive amination between of HPMC and JEFFAMINE. Monoamine, diamine and triamine JEFFAMINE, and HPMC with Mw of 7K and 18K were used, leading to HPMC-JEF copolymers of different topologies, namely diblock, triblock and three-armed copolymers.. Both topology and hydrophilic/hydrophobic ratio have significant influence on the CP and self-assembly properties of copolymers. The CP of all the HPMC-JEF copolymers is lower than that of HPMC homopolymers with the same molar mass of HPMC. Diblock and triblock copolymers with longer HPMC block exhibit lower CP. However, three-armed $(HPMC7K)_3$-JEF T5K presents a higher CP even though it has higher JEFFAMINE fraction. On the other hand, HPMC-JEF M2K diblock copolymers present two CP values since both components are thermo-responsive. All copolymers are able to self-assemble into spherical micelles in aqueous medium at room temperature. The micelle size increases with increase of hydrophilic HPMC molar mass. Three-armed copolymer micelles present lower size. The micelle size of HPMC-JEF M2K significantly changes with increasing temperature due to chain extension and/or dehydration.

In conclusion, this work presents the synthesis and characterization of HPMC based amphiphilic block copolymers, the self-assembly of copolymers into spherical micelles and the applications of these micelles in drug delivery system. The main innovatives point are as follows: (1) The synthesis route of HPMC block copolymers through reductive amination reaction of the hemiacetal group on HPMC chain end was brought forward. Thus it is possible to construct HPMC based block copolymers by this method with various amino-terminated polymers. (2) HPMC based copolymers are thermo-responsive, and the CP of these copolymers is affected by their composition and topology. Thus it should have potential for uses in thermo-responsive controlled drug delivery field. (3) Controlled drug release rate could be realized by varying copolymer composition, molar mass, *etc.* Therefore, HPMC based amphiphilic block copolymers

could be promising as nano-carrier of hydrophobic antitumor drugs.

Publications

1. **Aijing Lu,** Jielin Wang, Marleny Caceres Najarro, Suming Li, Andre Deratani, Synthesis and self-assembly of AB_2-type amphiphilic copolymers from biobased hydroxypropyl methyl cellulose and poly(L-lactide), *Carbohydrate Polymers, 211 (2019), 133–140*

2. **Aijing Lu**, Eddy Petit, Suming Li, Yuandou Wang, Feng Su, Sophie Monge, Novel thermo-responsive micelles prepared from amphiphilic hydroxypropyl methyl cellulose-block-JEFFAMINE copolymers, *International Journal of Biological Macromolecules, 135(2019), 38-45*

3. **Aijing Lu**, Zhengzhong Wu, Xianglin Luo, Suming Li, Protein adsorption and macrophage uptake of zwitterionic sulfobetaine containing micelles, *Colloid and Surfaces B: Biointerface, 167(2018), 252-259*

4. **Aijing Lu**, Eddy Petit, Katarzyna Jelonek, Arkadiusz Orchel, Janusz Kasperczyk, Yuandou Wang, Feng Su, Suming Li, Self-assembled micelles prepared from bio-based hydroxypropyl methyl cellulose and polylactide amphiphilic block copolymers for anti-tumor drug release, *International Journal of Biological Macromolecules,* Accepted.

5. **Aijing Lu**, Eddy Petit, Yuandou Wang, Feng Su, Suming Li, Synthesis and Self-Assembly of Amphiphilic Block Copolymers from Hydroxypropyl Methyl Cellulose and Poly(ε-caprolactone), *ACS Applied Nano Materials,* Submitted.

Communications

1. **Aijing Lu,** Suming Li, Synthesis and Self-Assembly of Amphiphilic Block Copolymers from Bio-based Hydroxypropyl Methyl Cellulose and Poly(L-lactide). 4th International Conference on Biomedical Polymers & Polymeric Biomaterials, July 15-18, 2018, Kraków, Poland.

2. **Aijing Lu,** Suming Li, Synthesis and characterization of amphiphilic copolymers prepared from hydroxypropyl methyl cellulose and poly(L-lactide), Balard Chemistry Conferences, June 18, 2018, Montpellier, France.

Acknowledgements

The first time I saw the university's rainbow-colored hallways, it was right in front of me. After three and a half years, I have now finished my doctoral study and my thesis. I would like to express my gratitude to all those who helped me during these years.

My deepest gratitude goes first and foremost to Dr. Suming Li, my supervisor, for his constant encouragement and guidance. He gave me detailed and comprehensive guidance on the design of experiments, the improvement of the details in experiments, and the process of drafting and revising the thesis. I have learnt a lot from him including his rigorous research attitude, contraction and effective work， gentle and polite way of doing things. He not only help me with my work and also help me to use French and get used to the life in France.

I would like to express my heartfelt gratitude to Dr. Katarzyna Jelonek, Dr. Arkadiusz Orchel, Dr. Janusz Kasperczyk and their group for their support on my experiments. Katarzyna gave me a lot guidance on the professional experiment skills and processing data in cell experiments. I would also appreciate to Dr. Feng Su and Yuandou Wang for their assistance in my cell tests. I want to thank Dr. Sophie Monge and her student Xianyu Ding for their support on UV-Vis spectrometer, and Dr. Mihai BARBOIU for his support on fluorescence spectrometer. I am also greatly indebted to Dr. Eddy Petit for his assistance in measurement and data processing, Dr. Andre Deratani for his gudience on aqueous SEC, and Dr. Mona Semsarilar and Dr. Thi Phuong Tuyen Dao for their assistance in TEM. Many thanks to Dr. Jielin Wang, Dr. Thomas Babut, Dr. Enrique Forlgado, Dr. Etega Cao and all the members worked in our Lab for their help and friendship.

My thanks would go to my parents for their love and great confidence in me. I also owe my sincere gratitude to my friends who spent a lot time on dining and talking with me. These happy moments make me relaxed and remain optimistic.

I also thank China Scholarship Council (CSC) under the Grant CSC N°201606240124 and the Programme “International scholarship exchange of PhD

candidates and academic staff' of the Medical University of Silesia in Katowice (A. Lu) who gave me finicial support to complete this study.

Copolymères à blocs amphiphiles et thermosensibles à base d'hydroxypropyl méthyl cellulose comme nano-vecteurs de principes actifs hydrophobes

Des copolymères à blocs thermosensibles et amphiphiles contenant l'hydroxypropyl méthyl cellulose (HPMC) comme bloc hydrophile et l'un des trois blocs hydrophobes - polylactide, poly(ε-caprolactone) et JEFFAMINE ayant des groupements amine terminaux ont été synthétisés par amination réductrice de l'extrémité de chaîne hémiacétale de l'HPMC. Les copolymères résultants ont été caractérisés par RMN, DOSY-RMN, GPC et FT-IR. Ils sont capables de s'auto-assembler en micelles sphériques en milieu aqueux. La taille des micelles augmente avec l'augmentation de la longueur du bloc hydrophile, tandis que la concentration micellaire critique diminue avec l'augmentation de la longueur du bloc hydrophobe. La topologie des copolymères affecte fortement leurs propriétés d'auto-assemblage. Le point de trouble de la solution de copolymère dépend du rapport hydrophile/hydrophobe et de la topologie. Deux principes actifs hydrophobes, le paclitaxel et la curcumine ont été chargés dans des micelles de copolymère pour évaluer leurs propriétés d'encapsulation et de libération. Les copolymères présentent une très bonne cytocompatibilité aux cellules L929, et les micelles chargées de principes actifs présentent une cytotoxicité sur les cellules SK-BR-3, montrant ainsi leur potentiel en tant que nano-vecteur de principes actifs antitumoraux.

Mots-clés: hydroxypropyl méthyl cellulose, polylactide, poly(ε-caprolactone), JEFFAMINE, amination réductrice, copolymère à blocs, auto-assemblage, thermosensible, administration de principes actifs

Amphiphilic and thermoresponsive block copolymers based on hydroxypropyl methyl cellulose as nano-carrier of hydrophobic drugs

A family of thermo-responsive and amphiphilic block copolymers containing hydroxypropyl methyl cellulose (HPMC) as hydrophilic block and one of the three hydrophobic blocks – amino terminated polylactide, poly(ε-caprolactone) and JEFFAMINE were synthesized through reductive amination of the hemiacetal chain end of HPMC. The resulting copolymers were characterized by NMR, DOSY-NMR, GPC and FT-IR. They are able to self-assemble into spherical micelles in aqueous medium. The micelle size increases with increase of the hydrophilic block length, whereas the critical micelle concentration decreases with increase of the hydrophobic block length. The topology of copolymers strongly affects their self-assembly properties. The cloud point of copolymer solution is dependent on the hydrophilic/hydrophobic ratio and topology. Two hydrophobic drugs, paclitaxel and curcumin were loaded in copolymer micelles to evaluate their drug loading and release properties. The copolymers present outstanding cytocompatibility to L929 cells, and drug loaded micelles exhibit cytotoxicity to SK-BR-3 cells, thus showing their potential as nano-carrier of antitumor drugs.

Key words: hydroxypropyl methyl cellulose, polylactide, poly(ε-caprolactone), JEFFAMINE, reductive amination, block copolymer, self-assembly, thermo-responsive, drug delivery